

# Local Calibration of the Pavement ME for Missouri



June 2020  
Final Report

Project number TR201609  
MoDOT Research Report number cmr 20-007

## PREPARED BY:

Leslie Titus-Glover

Chetana Rao, Ph.D.

Suriyanarayanan Sadasivam, Ph.D.

Rao Research and Consulting, LLC

## PREPARED FOR:

Missouri Department of Transportation

Construction and Materials Division, Research Section

## TECHNICAL REPORT DOCUMENTATION PAGE

<b>1. Report No.</b> cmr 20-007	<b>2. Government Accession No.</b>	<b>3. Recipient's Catalog No.</b>	
<b>4. Title and Subtitle</b> Local Calibration of the Pavement ME for Missouri		<b>5. Report Date</b> May 2020 Published: June 2020	
		<b>6. Performing Organization Code</b>	
<b>7. Author(s)</b> Leslie Titus-Glover; Chetana Rao, Ph.D.; Suriyanarayanan Sadasivam, Ph.D.		<b>8. Performing Organization Report No.</b>	
<b>9. Performing Organization Name and Address</b> Rao Research and Consulting, LLC 1775 Tysons Blvd., 5 <sup>th</sup> Fl Tysons, VA 22102		<b>10. Work Unit No.</b>	
		<b>11. Contract or Grant No.</b> MoDOT project # TR201609	
<b>12. Sponsoring Agency Name and Address</b> Missouri Department of Transportation (SPR-B) Construction and Materials Division P.O. Box 270 Jefferson City, MO 65102		<b>13. Type of Report and Period Covered</b> Final Report (March 2016-June 2019)	
		<b>14. Sponsoring Agency Code</b>	
<b>15. Supplementary Notes</b> Conducted in cooperation with the U.S. Department of Transportation, Federal Highway Administration. Project name: DDI Evaluation. MoDOT research reports are available in the Innovation Library at <a href="https://www.modot.org/research-publications">https://www.modot.org/research-publications</a> .			
<b>16. Abstract</b> Missouri Department of Transportation (MoDOT) was one of the early adopters of the Mechanistic-Empirical Pavement Design Guide procedure and completed the local calibration using the research grade software in 2009. The emphasis in 2009 was on establishing testing and field data collection programs, and calibrating for new designs as adequate performance data were not available for rehabilitation sections. Since adoption by American Association of State Highway and Transportation Officials (AASHTO) and its support for the AASHTOWare Pavement Design ME, several enhancements were made. MoDOT has made changes to the materials program by increasing use of recycled materials and adding advanced testing capabilities to develop Level 1 materials inputs to the Pavement ME Design procedure. These factors bring to fore the need for recalibration of Pavement ME Design distress and IRI prediction models for Missouri. This study aimed to recalibrate distress models for new and rehabilitated flexible and rigid pavements using Version 2.5.5 of the AASHTOWare Pavement ME program. This study included calibration sections in Missouri from MoDOT's pavement management system (PMS) and from the Long-Term Pavement Performance (LTPP) database. Sections covered the range of subgrades, layer material types, thicknesses, climate, traffic, designs, and rehabilitation practices typical for MoDOT. For flexible pavements, New AC, AC over AC, and AC over JPCP designs, and for rigid pavements, New JPCP and Unbonded overlays were considered. Distress models calibrated were Alligator Cracking, Alligator Reflection Cracking, AC Thermal Cracking, Transverse Reflection Cracking, AC Rutting, Total Rutting and Smoothness/ International Roughness Index (IRI) for flexible pavements and Transverse Cracking, Transverse Joint Fault, and IRI for rigid pavements. Level 1 laboratory and field data were used for most design inputs. The predictions showed a deviation from global models and therefore we calibrated to reduce error and eliminate bias in all flexible pavement models considered. Sensitivity analyses were used to study the impact of critical parameters. The rigid pavement sections did not exhibit adequate distress development to warrant a recalibration. Until further distress data are collected, the global models are recommended for rigid pavement designs. The study recommends the use of Level 1 field data for future design.			
<b>17. Key Words</b> Before and after studies; Crash rates; Crash severity; Diamond interchanges; Evaluation; Fatalities; Ramps (Interchanges); Traffic safety; Diverging diamond; Alternative designs; DDI		<b>18. Distribution Statement</b> No restrictions. This document is available through the National Technical Information Service, Springfield, VA 22161.	
<b>19. Security Classif. (of this report)</b> Unclassified.	<b>20. Security Classif. (of this page)</b> Unclassified.	<b>21. No. of Pages</b> 239	<b>22. Price</b>

**FINAL REPORT**  
**MISSOURI DEPARTMENT OF TRANSPORTATION PROJECT 201609**

**LOCAL CALIBRATION OF THE PAVEMENT ME DESIGN  
FOR MISSOURI**

**Prepared by:**  
Leslie Titus-Glover  
Chetana Rao, Ph.D.  
Suriyanarayanan Sadasivam, Ph.D.

**Rao Research & Consulting**  
**1775 Tysons Blvd., 5th Fl**  
**Tysons, VA 22102**

## **COPYRIGHT**

Authors herein are responsible for the authenticity of their materials and for obtaining written permissions from publishers or individuals who own the copyright to any previously published or copyrighted material used herein.

## **DISCLAIMER**

The opinions, findings, and conclusions expressed in this document are those of the investigators. They are not necessarily those of the Missouri Department of Transportation, U.S. Department of Transportation, or Federal Highway Administration. This information does not constitute a standard or specification.

## **ACKNOWLEDGEMENTS**

The authors thank the Missouri Department of Transportation (MoDOT) for supporting this study. The support of MoDOT staff during the conduct of this study is also much appreciated. Mr. John Donahue, P.E. provided the oversight for this project and engaged in several technical discussions. The authors also extend their thanks to Jennifer Harper, P.E. for managing the project and for reviewing of all deliverables. Jason Blomberg, P.E. supported the research team in all aspects of the project. His assistance with assembling inventory, design, laboratory, and field test data are much appreciated. He was the main point of contact for all research data. The authors thank James Whaley for providing pavement condition data, Michael Teel for providing traffic data, and Yvonne Wilbers for providing remote access to digital data. The study also used results of laboratory tests performed by Steven Michael Lusher, Ph.D., P.E., at Missouri University of Science & Technology.

The authors also thank other team members. Dr. Jagannath Mallela provided insights into the calibration effort from 2009. Dr. Charles A. Schwartz reviewed the research results and the documentation. His feedback was extremely valuable. Matthew Bandyk assisted with the assembly of LTPP data and the initial evaluation of the impact of climate database. Finally, the overall project coordination performed by Mr. DeArmond, P.E. is much appreciated.

## EXECUTIVE SUMMARY

Missouri was one of the early adopters of the research grade pavement design procedure and software program developed under NCHRP 1-37A and 1-40D (Mallela, et al., 2009). With ongoing enhancements to the design procedure, calibration models, and the software program, MoDOT recognized the need to reevaluate the applicability of the global calibration models to Missouri's local conditions. Concurrently, MoDOT has been making changes to the HMA materials program, including increasing RAP additions to the HMA and adding advanced testing capabilities to develop Level 1 materials inputs to the Pavement ME Design procedure. MoDOT project 201609 was initiated to recalibrate all Pavement ME Design distress and IRI prediction models. One of the goals of this study was to incorporate current and future materials into the calibration process to ensure the models can be used for future designs. Thus, distress prediction models and the IRI prediction models in the globally calibrated Pavement ME Design were verified and recalibrated to represent Missouri site and pavement design/construction conditions. The verification and local calibration effort involved several major tasks. A summary of key tasks and outcomes are discussed in this chapter.

### Selection of Pavement Design Types of Interest

One of the goals of this study was to include pavement types that are used in current designs and will be used in future MoDOT pavement designs. Based on discussions with MoDOT, pavement types selected were for the verification and calibration of distress models were:

- a. New AC pavement
- b. AC over AC pavement
- c. AC over JPCP
- d. New JPCP
- e. Unbonded JPCP overlay over existing JPCP

### Project Selection

Calibration projects were selected from two primary databases, the MoDOT PMS and FHWA LTPP. Selection of candidate calibration projects covered all design types, material sources, mix designs, and climate patterns relevant to Missouri pavement design and construction.

The range of parameters included in the MoDOT PMS sections database were as follows:

- For new AC projects, construction was over crushed or large stone base layers on fine subgrades. The HMA wearing surfaces used 9.5 or 12.5 mm nominal aggregate size HMA mix. Intermediate HMA layer mix types considered were nominal aggregate size of 19.0 and 25.0 mm. Binder types included SuperPave Performance Grade (PG) 76-22, 70-22, and 64-22 grades, using virgin aggregates, and RAP contents ranging from about 12 to 24 percent. The projects were constructed over fine-grained soils. Projects were constructed from 2001 to 2010 and were located throughout the state.
- AC over AC projects had HMA overlay thicknesses in the range of 1.5 to 5 inches and were constructed over existing 9 to 12-inch thick HMA layers of AC pavements. AC

overlays used 9.5 or 12.55 mm nominal aggregate size HMA mix with varying RAP contents. For some of the projects, the existing HMA layer was milled up to 2 inches prior to HMA overlay placement. The existing pavement base type/subgrade were typical of base materials used by MoDOT for new AC pavements. Existing pavement condition was a mix of good/fair/poor. The existing pavement in several of the AC over AC projects used were considered as new AC pavement projects under the previous calibration effort. HMA overlays were constructed from 2006 to 2013.

- For AC overlay over existing JPCP, the overlay construction was completed in two lifts using 12.5 mm to 19 mm nominal aggregate size HMA layers with a total thickness ranging from 3.7 to 4.2 inches. HMA mixes used 9 to 40 percent RAP contents. PCC materials, base type, and their thicknesses varied, but were typical of MoDOT designs and specifications; subgrades were typical of Missouri soils. Existing pavement condition was a mix of good/fair/poor. The HMA overlays were constructed from 2006 to 2010.
- For new JPCP and unbonded JPCP overlay projects, the majority of projects comprised of PCC thickness greater than 10 inches, widened 14 ft lanes with tied shoulders, and joint spacing of 15 ft. The JPCP projects were doweled and constructed over an aggregate base and fine subgrade.

LTPP sections located in the state of Missouri were included in the calibration database. LTPP experiments included in the calibration were SPS-5, SPS-6, SPS-8, SPS-9, GPS-1, and GPS-6.

### **Development of Pavement ME Design Database**

Data from MoDOT and LTPP database were assembled in a format suitable for Pavement ME analyses. MoDOT conducted laboratory and field tests to obtain Level 1 data to the extent possible for use in the calibration as well as in future MoDOT designs. MERRA Climate data was obtained for all AC surfaced LTPP and MoDOT projects from the LTPP InfoPave Climate tool. For rigid pavements, the Pavement ME uses the NARR climate data that can be accessed directly from the software program interface.

Historical traffic records, in weight data format, from 18 installation sites for a 3-year period, 2015, 2016 and 2017 were obtained from MoDOT. The historical weight records were then analyzed to develop site-specific traffic inputs for the Pavement ME software: Vehicle Class Distribution, Number of Axles Per Truck, Monthly Adjustment Factors, and Axle Load Distribution Profiles. The traffic inputs were then further analyzed to evaluate conformance with generally accepted trends, presence of data clusters, outliers and errors. The outcome of raw WIM traffic data analysis and processing was Missouri specific default traffic inputs.

Layer materials and layer thickness data were assembled from various sources, which primarily included the use of laboratory testing and field testing results. The development of Missouri default Pavement ME data inputs involved the following activities:

- Loose samples of HMA materials and field cores from the AC surfaced PMS sections (New AC, AC over AC and AC over JPCP) were extracted for laboratory testing to develop HMA materials inputs required for design. Laboratory test results were provided for dynamic modulus, low temperature creep compliance, and indirect tensile strength

tests. HMA mixes used in these tests used MoDOT SP gradations and binder types with RAP contents ranging from 12 to 40 percent. These data were used in calibration and to develop the HMA materials library for MoDOT.

- Laboratory characterization of PCC materials was conducted under the 2009 calibration effort. No additional PCC tests were performed under this project. Data from previous testing covered all PCC gradations included in the MoDOT specifications. These data were also used to develop PCC materials library for MoDOT.
- Field core data were used to determine layer thicknesses.
- Field FWD test results were used for backcalculating subgrade resilient modulus for local calibration and models verification. FWD tests were performed only on New AC, AC over AC, and AC over JPCP projects.
- For performance data of PMS projects, time-series rutting, faulting, and IRI data were obtained from the MoDOT PMS database. For AC alligator cracking and transverse cracking, and JPCP transverse slab cracking, data were obtained by reviewing MoDOT PMS video imaging files and conducting a virtual distress survey as per LTPP distress data collection and reporting protocols.

### **Local Calibration of Distress Prediction Models**

Local calibration was performed for all AC distress models. For JPCP, the models were verified using a classification type analysis because the calibration sections did not have adequate distress development to develop a meaningful calibration model. Calibration was done to remove bias (consistent over- or under-prediction) and improve accuracy of prediction while verification was done to confirm accuracy and absence of bias. The outcomes of this effort were as follows:

- Significant improvements were made for AC alligator cracking, reflection fatigue cracking, thermal cracking, and transverse reflection cracking prediction models.
- A reasonable improvement in the total rutting model accuracy was achieved. Total rutting data contains considerable amount of variability. Thus, a significant improvement in  $R^2$  was not expected.
- For all the AC models, any significant bias was minimized or eliminated.
- The JPCP models were verified to determine their accuracy and lack of bias for Missouri conditions. The global models were deemed reasonable for MoDOT local conditions within a limited range of field distresses.

### **Sensitivity Analysis and Case Studies**

Sensitivity studies were done to help establish confidence in the new locally calibrated or verified models. Outcomes were very reasonable, and trends observed were as expected. Case studies were presented for New AC and AC over AC designs. The design inputs and site conditions were specific to Missouri.

# TABLE OF CONTENTS

<b>CHAPTER 1. INTRODUCTION.....</b>	<b>1</b>
Background.....	1
Overview of Pavement ME Design Adoption in Missouri.....	3
Need for Future Recalibration for MoDOT .....	5
Project Objectives .....	6
Project Scope .....	7
Organization of Report .....	7
<b>CHAPTER 2. IDENTIFICATION AND SELECTION OF PROJECTS .....</b>	<b>9</b>
Selection of Pavement Types and Distress Models for MoDOT Calibration.....	9
Identification and Selection of Pavement Projects for Local Calibration.....	10
Project Selection .....	10
<b>CHAPTER 3. DEVELOPMENT OF CALIBRATION DATABASE.....</b>	<b>22</b>
Selection of Hierarchical Input Levels .....	22
Data Assembly.....	23
Climate Data .....	25
Traffic Data.....	29
Field Data Collection and Analysis of Test Data.....	58
HMA Material Characterization .....	61
PCC Material Input Data .....	70
Performance Data.....	70
<b>CHAPTER 4. VERIFICATION OF <i>PAVEMENT ME DESIGN</i> GLOBAL DISTRESS MODELS .....</b>	<b>73</b>
Verification Methodology.....	73
Verification of Models for New AC and AC over AC pavements.....	75
Verification of Models for AC over JPCP Pavements.....	85
Model Verification for New JPCP and Unbonded JPCP Overlays .....	98
Summary of Model Verification Analysis Results .....	100
Recommendations.....	100

<b>CHAPTER 5. LOCAL CALIBRATION OF <i>PAVEMENT ME DESIGN FLEXIBLE</i></b>	
<b>PAVEMENT DISTRESS MODELS.....</b>	<b>101</b>
Total Alligator “Fatigue + Reflection” Cracking Model .....	101
Total Rutting and Rutting for AC, Base, and Subgrade .....	110
Total Transverse “Thermal + Reflection” Cracking.....	121
Pavement Smoothness (IRI) Models for New AC, AC over AC, and AC over JPCP .....	129
Summary of Recalibration for AC Surfaced Pavements .....	138
<b>CHAPTER 6. LOCAL CALIBRATION OF <i>PAVEMENT ME DESIGN RIGID</i></b>	
<b>PAVEMENT DESIGN DISTRESS MODELS.....</b>	<b>139</b>
Transverse Slab Cracking .....	139
Transverse Joint Faulting.....	147
Smoothness (IRI) .....	151
Summary .....	156
<b>CHAPTER 7. CASE STUDIES .....</b>	<b>157</b>
New AC Pavement Case Study.....	157
AC over AC Pavement.....	161
<b>CHAPTER 8. SUMMARY AND CONCLUSIONS.....</b>	<b>164</b>
Summary .....	164
Conclusions and Recommendations .....	168
<b>REFERENCES.....</b>	<b>169</b>
<b>APPENDIX A: NUMBER OF AXLES PER TRUCK FOR WIM SITES .....</b>	<b>A-1</b>
<b>APPENDIX B: LEVEL 1 HMA MATERIALS TEST RESULTS.....</b>	<b>B-1</b>

## LIST OF FIGURES

Figure 1. Location of MoDOT PMS New AC and AC over AC projects (Google, n.d.) .....	16
Figure 2. Location of MoDOT PMS new JPCP and unbonded overlays projects (Google, n.d.).....	17
Figure 3. Location of MoDOT PMS AC over JPCP projects (Google, n.d.) .....	17
Figure 4. Location of Missouri LTPP projects selected for verification and validation of Pavement ME distress models (Source: LTPP InfoPave Visualization tool).....	18
Figure 5. Average air temperature for Taney county (south) and Macon county (north) .....	26
Figure 6. Average precipitation for Taney County (south) and Macon County (north).....	26
Figure 7. Average frost depth for Taney county (south) and Macon county (north).....	26
Figure 8. Location of WIM sites (Google, n.d.) .....	29
Figure 9. Summary of truck class distribution by truck type.....	35
Figure 10. Comparison of site-specific vehicle class distribution with TTC-2 and TTC-4 .....	38
Figure 11. Comparison of site-specific vehicle class distribution with TTC-1 .....	38
Figure 12. Comparison of site specific vehicle class distribution with TTC-6 and TTC-9.....	39
Figure 13. Summary of number of single axles per truck.....	41
Figure 14. Summary of number of tandem axles per truck .....	41
Figure 15. Summary of number of tridem axles per truck.....	42
Figure 16. Summary of number of quad axles per truck .....	42
Figure 17. Summary of total number of axles per truck.....	43
Figure 18. Month to month variation in the number of Class 9 trucks at Site 1881 in 2015.....	43
Figure 19. Comparison of 50th percentile weight of single axles of Class 5 trucks.....	44
Figure 20. Load distribution of Class 5 single axles at Site 3021 (US 61 in Lewis County) .....	45
Figure 21. Load distribution of single axles of Class 5 trucks.....	45
Figure 22. Load distribution of single axles of Class 5 trucks at Sites 2001 and 2003 (US 63 in Macon County).....	46

Figure 23. Percent single axles of Class 5 trucks with loads heavier than 20,000 lb .....	47
Figure 24. Comparison of 50 <sup>th</sup> percentile weight of single axles of Class 9 trucks.....	48
Figure 25. Load distribution of single axles of Class 9 trucks.....	48
Figure 26. Load distribution of single axles of Class 9 trucks.....	49
Figure 27. Percent single axles of Class 9 trucks with loads heavier than 20,000 lb .....	49
Figure 28. Comparison of 50 <sup>th</sup> percentile weight of tandem axles of Class 9 trucks .....	50
Figure 29. Load distribution of tandem axles of Class 9 trucks .....	51
Figure 30. Load distribution of tandem axles of Class 9 trucks .....	51
Figure 31. Percent single axles of Class 9 trucks with loads heavier than 46,000 lb .....	52
Figure 32. Test layout for flexible pavements used in the MEPDG calibration.....	58
Figure 33. Average rut depth versus year for Project AOA1 .....	71
Figure 34. Average rut depth versus year for Project AOA2 .....	71
Figure 35. Average smoothness (IRI) versus year for Project F1.....	72
Figure 36. Average smoothness (IRI) versus year for Project F5.....	72
Figure 37. Pavement ME Design global calibration predicted versus measured AC alligator cracking.....	76
Figure 38. Verification of the AC alligator cracking and fatigue damage models with Pavement ME Design global coefficients, using Missouri flexible pavement projects .....	76
Figure 39. Pavement ME Design global calibration predicted versus measured total rutting for New AC and AC over AC pavements.....	78
Figure 40. Photo showing transverse cracking from shrinkage of the AC surface due to asphalt binder hardening.....	79
Figure 41. USDA Plant Hardiness zone map for Missouri (USDA 2017).....	80
Figure 42. Pavement ME Design global calibration predicted versus measured transverse cracking .....	82
Figure 43. Pavement ME Design global calibration predicted transverse cracking versus age for LTPP project 0501 (New AC pavement) .....	82

Figure 44. Pavement ME Design global calibration predicted transverse cracking versus age for LTPP project 0504 (AC over AC pavement) .....	83
Figure 45. Pavement ME Design global calibration predicted transverse cracking versus age for LTPP project 0801 (New AC pavement) .....	83
Figure 46. Pavement ME Design global calibration predicted transverse cracking versus age for LTPP project 1002 (AC over AC pavement) .....	84
Figure 47. Pavement ME Design global calibration predicted transverse cracking versus age for LTPP project 1008 (AC over AC pavement) .....	84
Figure 48. Pavement ME Design global calibration predicted versus measured alligator cracking for AC over JPCP .....	86
Figure 49. Pavement ME Design global calibration predicted alligator cracking versus age for LTPP project 0604 (AC over JPCP) .....	87
Figure 50. Pavement ME Design global calibration predicted alligator cracking versus age for LTPP project 0606 (AC over JPCP) .....	87
Figure 51. Pavement ME Design global calibration predicted alligator cracking versus age for LTPP project 0602 (AC over JPCP) .....	88
Figure 52. Pavement ME Design global calibration predicted alligator cracking versus age for LTPP project 0662 (AC over JPCP) .....	88
Figure 53. Pavement ME Design global calibration predicted alligator cracking versus age for LTPP project 0665 (AC over JPCP) .....	89
Figure 54. Pavement ME Design global calibration predicted versus measured AC rutting for AC over JPCP .....	90
Figure 55. Pavement ME Design global calibration predicted rutting versus age for LTPP project 0604 (AC over JPCP) .....	91
Figure 56. Pavement ME Design global calibration predicted rutting versus age for LTPP project 0606 (AC over JPCP) .....	91
Figure 57. Pavement ME Design global calibration predicted rutting versus age for LTPP project 0608 (AC over JPCP) .....	92
Figure 58. Pavement ME Design global calibration predicted rutting versus age for LTPP project 0664 (AC over JPCP) .....	92
Figure 59. Pavement ME Design global calibration predicted rutting versus age for LTPP project 0665 (AC over JPCP) .....	93

Figure 60. Pavement ME Design global calibration predicted versus measured total transverse cracking for composite AC over JPCP.....	95
Figure 61. Pavement ME Design global calibration predicted versus measured total transverse cracking for composite AC over JPCP (showing SPS-6 and SPS-9 projects) .....	95
Figure 62. Pavement ME Design global calibration predicted transverse cracking versus age for LTPP project 0603 (composite AC over JPCP).....	96
Figure 63. Pavement ME Design global calibration predicted transverse cracking versus age for LTPP project 0604 (composite AC over JPCP).....	96
Figure 64. Pavement ME Design global calibration predicted transverse cracking versus age for LTPP project 0663 (AC over JPCP) .....	97
Figure 65. Pavement ME Design global calibration predicted transverse cracking versus age for LTPP project 0901 (AC over JPCP) .....	97
Figure 66. Pavement ME Design global calibration predicted transverse cracking versus age for LTPP project 0665 (AC over JPCP) .....	98
Figure 67. Distribution of transverse cracking data in LTPP data used for model verification.....	99
Figure 68. Distribution of joint faulting data in LTPP data used for model verification .....	99
Figure 69. AC alligator cracking and fatigue damage model with Pavement ME Design local calibration coefficients, using all Missouri LTPP and PMS flexible pavement projects.....	105
Figure 70. Pavement ME Design local calibration model predicted versus measured AC alligator cracking for Missouri LTPP and PMS flexible pavement projects.....	106
Figure 71. Impact of AC thickness on local calibration model predicted AC alligator cracking (New AC design) .....	107
Figure 72. Impact of AC overlay thickness on local calibration predicted AC alligator cracking (AC over AC design).....	107
Figure 73. Impact of fatigue in existing pavement and overlay thickness on local calibration model predicted AC alligator cracking (AC over AC design) .....	108
Figure 74. Impact of climate on local calibration model predicted AC alligator cracking (New AC design).....	108

Figure 75. Impact of HMA air voids on local calibration model predicted AC alligator cracking for Missouri .....	109
Figure 76. Pavement ME Design local calibration model predicted versus measured total rutting for New AC and AC over AC pavements.....	112
Figure 77. Pavement ME Design local calibration model predicted rutting versus age for LTPP project 0502 (AC over AC pavement) .....	113
Figure 78. Pavement ME Design local calibration model predicted rutting versus age for LTPP project 0504 (AC over AC pavement) .....	114
Figure 79. Pavement ME Design local calibration model predicted rutting versus age for LTPP project 0508 (AC over AC pavement) .....	114
Figure 80. Pavement ME Design local calibration model predicted rutting versus age for LTPP project 0608 (AC over JPCP).....	115
Figure 81. Pavement ME Design local calibration model predicted rutting versus age for LTPP project 0662 (AC over JPCP).....	115
Figure 82. Pavement ME Design local calibration model predicted rutting versus age for LTPP project 0901 (AC over JPCP).....	116
Figure 83. Pavement ME Design local calibration model predicted rutting versus age for LTPP project 0903 (AC over JPCP).....	116
Figure 84. Pavement ME Design local calibration model predicted rutting versus age for MoDOT PMS project FDA1-S1 (New AC pavement) .....	117
Figure 85. Pavement ME Design local calibration model predicted rutting versus age for MoDOT PMS project FDA3 (New AC pavement).....	117
Figure 86. Pavement ME Design local calibration model predicted rutting versus age for MoDOT PMS project AOA3 (AC over AC pavement).....	118
Figure 87. Pavement ME Design local calibration model predicted rutting versus age for MoDOT PMS project AOA1 (AC over AC pavement) .....	118
Figure 88. Impact of AC thickness on local calibration predicted total rutting for Missouri.....	119
Figure 89. Impact of climate on local calibration predicted total rutting for Missouri .....	119
Figure 90. Impact of HMA air voids on local calibration predicted total rutting for Missouri.....	120

Figure 91. Impact of HMA air voids and overlay thickness on local calibration predicted total rutting for Missouri .....	120
Figure 92. Pavement ME Design local calibration model predicted versus measured transverse cracking .....	123
Figure 93. Pavement ME Design local calibration predicted versus measured transverse cracking for LTPP project 0505 (AC over AC) .....	125
Figure 94. Pavement ME Design local calibration versus measured transverse cracking for LTPP project 0802 (New AC) .....	125
Figure 95. Pavement ME Design local calibration versus measured transverse cracking for MoDOT PMS project AOA2 (AC over AC) .....	126
Figure 96. Pavement ME Design local calibration versus measured transverse cracking for LTPP project 0665 (AC over JPCP) .....	126
Figure 97. Impact of AC thickness on local calibration predicted thermal transverse cracking for Missouri .....	127
Figure 98. Impact of climate on local calibration predicted thermal transverse cracking for Missouri .....	127
Figure 99. Impact of climate and air voids on local calibration predicted thermal transverse cracking for Missouri .....	128
Figure 100. Pavement ME Design local calibration predicted versus field measured IRI for New AC and AC over AC pavements .....	131
Figure 101. Pavement ME Design predicted versus measured IRI for project FDA2 (New AC) .....	132
Figure 102. Pavement ME Design local calibration predicted versus measured IRI for LTPP project 0502 (AC over AC) .....	132
Figure 103. Pavement ME Design local calibration predicted versus measured IRI for project AOA4 (AC over AC) .....	133
Figure 104. Impact of AC thickness on local calibration model predicted IRI .....	133
Figure 105. Impact of climate on local calibration predicted IRI .....	134
Figure 106. Impact of HMA air voids on local calibration predicted IRI .....	134
Figure 107. Pavement ME Design local calibration model predicted versus measured IRI for AC over JPCP .....	136

Figure 108. Pavement ME Design local calibration model predicted versus measured IRI for LTPP project 0660 .....	137
Figure 109. Pavement ME Design local calibration model predicted versus measured IRI for MoDOT PMS project AOC1 .....	137
Figure 110. Pavement ME Design local calibration model predicted versus measured IRI for MoDOT PMS project AOC4 .....	138
Figure 111. Histogram showing distribution of JPCP transverse cracking for the projects utilized in calibration and validation .....	141
Figure 112. Histogram showing distribution of residual (measured minus predicted transverse cracking) for the projects utilized in calibration and validation.....	141
Figure 113. Pavement ME Design global model predicted and measured transverse cracking versus fatigue damage for the projects utilized in calibration and validation .....	142
Figure 114. Impact of PCC thickness (8 through 12 inches) on predicted transverse slab cracking for Missouri .....	144
Figure 115. Impact of PCC CTE on predicted transverse slab cracking for Missouri .....	145
Figure 116. Impact of widened slab and PCC thickness on predicted transverse slab cracking for Missouri .....	145
Figure 117. Impact of shoulder type and PCC thickness on predicted slab cracking for Missouri.....	146
Figure 118. Impact of PCC flexural strength on predicted transverse slab cracking for Missouri.....	146
Figure 119. Histogram showing distribution of mean joint faulting for the projects utilized for model verification/calibration.....	148
Figure 120. Histogram showing distribution of residual (measured minus predicted transverse joint faulting) for the projects utilized for model verification/calibration .....	149
Figure 121. Impact of PCC thickness and widened slab on predicted transverse joint faulting for Missouri.....	150
Figure 122. Impact of PCC CTE on predicted transverse joint faulting for Missouri.....	151
Figure 123. Impact of PCC dowel size on predicted transverse joint faulting for Missouri .....	151

Figure 124. Impact of PCC thickness on predicted IRI for Missouri .....	153
Figure 125. Plot showing impact of PCC CTE on predicted IRI for Missouri.....	154
Figure 126. Impact of widened slab and PCC thickness on predicted IRI for Missouri .....	154
Figure 127. Impact of shoulder type and PCC thickness on predicted IRI for Missouri.....	155
Figure 128. Impact of PCC flexural strength on predicted IRI for Missouri.....	155
Figure 129. Plot showing distribution of ambient temperature at project site.....	157
Figure 130. Plot showing distribution of precipitation and windspeed at project site.....	157
Figure 131. Plot showing vehicle class distribution at project site.....	158
Figure 132. Plot showing truck hourly distribution at project site .....	158

## LIST OF TABLES

Table 1. Pavement ME Design distress and overall condition metrics used for pavement evaluation (AASHTO 2010).....	2
Table 2. Pavement ME Design distress models selected for verification and local calibration .....	9
Table 3. Pavement ME Design parameters used for developing sampling template.....	10
Table 4. Sampling template for MoDOT PMS New AC projects in local calibration .....	12
Table 5. Sampling template for AC over AC MoDOT PMS projects in local calibration .....	12
Table 6. Sampling template for MoDOT PMS AC over JPCP projects in local calibration .....	13
Table 7. Sampling template for new JPCP and unbonded JPCP overlay over existing JPCP projects selected for local calibration .....	13
Table 8. Location and construction dates of the calibration projects .....	14
Table 9. List of LTPP sections included in the local calibration .....	19
Table 10. Layer thicknesses, and site parameters of LTPP sections used in local calibration .....	20
Table 11. Input data predominant hierarchical level .....	23
Table 12. Summary of climate data for New AC, AC over AC, and AC over JPCP sections .....	27
Table 13. Description of MoDOT WIM sites selected for traffic analysis.....	30
Table 14. Lane and travel direction of WIM sites .....	31
Table 15. Data availability of WIM sites for years 2015-2017 .....	32
Table 16. Monthly breakdown of available data .....	33
Table 17. Site-specific distribution of truck classes .....	34
Table 18. Truck traffic classification (TTC) group description.....	36
Table 19. Recommended TTC groups for WIM sites.....	37
Table 20. Nationwide averages for number of axles per truck.....	39
Table 21. Axles per truck statistics for MoDOT WIM sites.....	40

Table 22. Traffic volume inputs used for FDA, AOA, and AOC section (from MoDOT) .....	53
Table 23. Summary of traffic volume inputs used in calibration of JPCP projects (Data provided by MoDOT).....	54
Table 24. Summary of Level 3 vehicle/truck class distribution data used in local calibration .....	55
Table 25. Summary of Level 1 vehicle/truck class distribution in flexible pavement projects .....	56
Table 26. Summary of Level 1 vehicle/truck class distribution in rigid pavement projects .....	57
Table 27. Backcalculated subgrade modulus used for MoDOT calibration sections .....	59
Table 28. MoDOT HMA material type selection .....	61
Table 29. HMA materials sampling plan .....	62
Table 30. Laboratory characterization testing procedures and sampling requirements for MEPDG HMA dynamic modulus, AC binder $G^*$ and phase angle $\delta$ , HMA creep compliance and HMA as-placed volumetric properties .....	62
Table 31. Pseudo Binder Stiffness and Phase Angles for MoDOT Binders.....	64
Table 32. Laboratory characterization test results for HMA dynamic modulus, psi.....	66
Table 33. Laboratory characterization of Level 1 HMA creep compliance and tensile strength test data for HMA mix SP190 15-57 with 4.0 and 6.5 percent air voids .....	67
Table 34. Laboratory characterization of Level 1 HMA creep compliance and tensile strength test data for HMA mix SP250 16-68 with 4.0 and 6.5 percent air voids .....	67
Table 35. Representative HMA mixtures selected from laboratory test data for Level 1 inputs to Pavement ME .....	68
Table 36. Data sources and availability for condition data.....	70
Table 37. Statistical comparison of field measured and Pavement ME Design predicted alligator cracking goodness of fit for New AC and AC over AC pavements .....	75
Table 38. Hypothesis testing for field measured and Pavement ME Design predicted alligator cracking curve slope and intercept for New AC and AC over AC pavements .....	75

Table 39. Paired t-test results for field measured and Pavement ME Design predicted alligator cracking observations for New AC and AC over AC pavements .....	75
Table 40. Statistical comparison of field measured and Pavement ME Design predicted rutting goodness of fit for New AC and AC over AC pavements .....	78
Table 41. Hypothesis testing for field measured and Pavement ME Design predicted rutting curve slope and intercept for New AC and AC over AC pavements .....	78
Table 42. Paired t-test results for field measured and Pavement ME Design predicted rutting observations for New AC and AC over AC pavements .....	78
Table 43. Statistical goodness of fit assessment for field measured, and Pavement ME Design predicted transverse cracking for New AC and AC over AC pavements .....	80
Table 44. Hypothesis testing for field measured and Pavement ME Design predicted transverse cracking curve slope and intercept for New AC and AC over AC pavements .....	81
Table 45. Paired t-test results for field measured and Pavement ME Design predicted transverse cracking observations for New AC and AC over AC pavements .....	81
Table 46. Statistical comparison of field measured and Pavement ME Design predicted AC alligator cracking for AC over JPCP .....	85
Table 47. Hypothesis testing for field measured and Pavement ME Design predicted alligator cracking curve slope and intercept AC over JPCP.....	85
Table 48. Paired t-test results for field measured and Pavement ME Design predicted alligator cracking observations for AC over JPCP.....	85
Table 49. Statistical comparison of field measured and Pavement ME Design predicted AC rutting goodness of fit for AC over JPCP .....	89
Table 50. Hypothesis testing for field measured and Pavement ME Design predicted AC rutting curve slope and intercept for AC over JPCP .....	89
Table 51. Paired t-test results for field measured and Pavement ME Design predicted AC rutting observations for AC over JPCP .....	90
Table 52. Statistical comparison of field measured and Pavement ME Design predicted transverse cracking goodness of fit for AC over JPCP .....	94
Table 53. Hypothesis testing for field measured and Pavement ME Design predicted transverse cracking curve slope and intercept for composite AC over JPCP.....	94

Table 54. Paired t-test results for field measured and Pavement ME Design predicted transverse cracking observations for composite AC over JPCP .....	94
Table 55. Summary of model’s verification results and recommendations for improvement.....	100
Table 56. Summary of local coefficients for the alligator cracking model .....	104
Table 57. Locally calibrated alligator cracking model goodness of fit for New AC and AC over AC pavements.....	105
Table 58. Bias test results for locally calibrated alligator cracking model for New AC and AC over AC pavements.....	105
Table 59. Paired t-test results for field measured and Pavement ME Design predicted alligator cracking observations for New AC and AC over AC pavements .....	105
Table 60. Summary of local coefficients for the total rutting model.....	111
Table 61. Statistical comparison of field measured and Pavement ME Design predicted rutting goodness of fit for New AC and AC over AC pavements.....	112
Table 62. Hypothesis testing for field measured and Pavement ME Design predicted rutting curve slope and intercept for New AC and AC over AC pavements .....	112
Table 63. Paired t-test results for field measured and Pavement ME Design predicted rutting observations for New AC and AC over AC pavements .....	112
Table 64. Summary of local coefficients for thermal cracking and reflection cracking.....	123
Table 65. Statistical comparison of field measured and Pavement ME Design predicted transverse cracking goodness of fit for New AC, AC over AC, and AC over JPCP .....	124
Table 66. Hypothesis testing for field measured and Pavement ME Design predicted transverse cracking curve slope and intercept for New AC, AC over AC, and AC over JPCP.....	124
Table 67. Paired t-test results for field measured and Pavement ME Design predicted transverse cracking observations for New AC, AC over AC, and AC over JPCP .....	124
Table 68. Summary of local coefficients for the New AC and AC over AC smoothness model .....	130
Table 69. Statistical comparison of field measured and Pavement ME Design predicted IRI goodness of fit for New AC and AC over AC pavements .....	130

Table 70. Hypothesis testing for field measured and Pavement ME Design predicted IRI slope and intercept for New AC and AC over AC pavements .....	131
Table 71. Paired t-test results for field measured and Pavement ME Design predicted IRI observations for New AC and AC over AC pavements .....	131
Table 72. Summary of local calibration coefficients for the AC over JPCP smoothness model .....	135
Table 73. Statistical comparison of field measured and Pavement ME Design predicted rutting goodness of fit for AC over JPCP.....	135
Table 74. Hypothesis testing for field measured and Pavement ME Design predicted rutting curve slope and intercept for AC over JPCP .....	135
Table 75. Paired t-test results for field measured and Pavement ME Design predicted rutting observations for AC over JPCP .....	135
Table 76. Statistical comparison of field measured and Pavement ME Design predicted transverse cracking goodness of fit for new JPCP and unbonded JPCP overlays.....	142
Table 77. New JPCP and JPCP overlays faulting model coefficients .....	148
Table 78. Confusion matrix table showing measured versus predicted transverse joint faulting.....	149
Table 79. Trial design for New AC design .....	159
Table 80. Summary of New AC design thicknesses and predicted distress/IRI.....	160
Table 81. Trial AC overlay structure .....	161
Table 82. Summary of optimized AC overlay thickness and predicted distress/IRI .....	162
<u>Tables in Appendix A</u>	
Table A - 1. Number of axles per truck for MoDOT WIM sites .....	A-1
<u>Tables in Appendix B</u>	
Table B - 1. Dynamic modulus inputs for MoDOT HMA mixes, psi .....	B-1
Table B - 2. Indirect tensile strength inputs for MoDOT HMA mix designs.....	B-6
Table B - 3. Creep compliance inputs for MoDOT HMA mix designs, D(t) 1/psi .....	B-7

# CHAPTER 1. INTRODUCTION

## BACKGROUND

The Mechanistic-Empirical (ME) Pavement Design procedure was formally accepted in the American Association of State Highway and Transportation Officials (AASHTO) Guide for design and evaluation of new, reconstructed, and rehabilitated flexible, rigid, and semi-rigid pavement structures in 2008 (AASHTO 2015). The design procedure and practices for its implementation built upon findings and products from a series of national research efforts including National Cooperative Highway Research Program (NCHRP) projects, 1-37A (ARA, 2004), 1-40B (AASHTO 2010), 1-40D (ARA, 2007), 20-07/Task 327 (AASHTO 2015), 1-41 (Lytton et al., 2010), 9-30A (Von Quintus, et al., 2012). The design procedure is supported in practice by the AASHTOWare Pavement ME Design software program. Design Build 2.5.5 was the latest version available at the time of preparation of this report. As an AASHTOWare product, Pavement ME is supported, maintained, and progressively enhanced by AASHTO (AASHTO, 2019a, 2019b).

The following pavement types are supported by the current AASHTOWare Pavement ME tool:

- New designs – Flexible pavement that includes pavements with an asphalt concrete (AC) surface layer, Jointed Plain Concrete Pavements (JPCP) that includes pavements with portland cement concrete (PCC) slabs with transverse joints on the surface layer, Continuously Reinforced Concrete Pavement (CRCP), and Semi-Rigid Pavement.
- Rehabilitation designs – AC overlay on existing AC or PCC layers, bonded PCC over existing JPCP/CRCP, Unbonded JPCP/CRCP over existing JPCP/CRCP, JPCP/CRCP over existing AC, and JPCP restoration.

The Pavement ME design procedure utilizes project-specific inputs for traffic, climate, and materials, and combines them with mechanistic and ME algorithms to simulate pavement responses under truck- and climate-induced loads. The critical responses form the basis for estimating damage caused by both truck traffic and climate cycles. Damage is computed using critical responses and established transfer functions. The design period is divided into hourly time increments, and damage is accumulated incrementally during these time increments based on mechanistic response of the pavement to truck and climate load applications. Empirical models are used to relate damage to distress metrics that typically characterize pavement structural health condition. Empirical models are also used to relate predicted distress to International Roughness Index (IRI), the metric used to characterize overall ride quality and functional condition of the pavement (ARA, 2004). A listing of the distress types that can be used to establish performance criteria in the Pavement ME Design is presented in Table 1.

The Pavement ME Design procedure is, fundamentally, an iterative process for the selection of a feasible or optimized design. The AASHTO Pavement ME Design tool is used to select a preliminary pavement design for the given project site. The preliminary design is generally a typical design used by the agency and may include the pavement type, material types and layer thicknesses, design features, and material properties consistent with material test results or agency specifications. Site conditions considered in the design include traffic inputs, climate,

and subgrade properties. The software program simulates the interactions of key material properties, design features, and site conditions in hourly time increments to compute critical pavement responses and incremental and accumulated damage. The governing distress calibration models used for the analysis are used by AASHTO Pavement ME Design to predict distress development and smoothness loss over the design or analysis period. By comparing predicted distress and IRI at a given reliability level at the end of the design period to the agency threshold values, the design is either accepted or further optimized iteratively. Agencies typically perform economic and value analyses external to the AASHTOWare tool for construction. (AASHTO 2015)

Table 1. Pavement ME Design distress and overall condition metrics used for pavement evaluation (AASHTO 2010)

Pavement Type	Alligator (Bottom-Up Fatigue) Cracking	Alligator Reflection Cracking	AC Thermal Cracking	Transverse Reflection Cracking	Chemically Stabilized Layer Fatigue Fracture	AC Rutting	Total Rutting	Transverse (Slab) Cracking	Transverse Joint Faulting	Punchouts	Smoothness (IRI)
New AC	X		X			X	X				X
AC over AC and AC over Rubblized PCC	X	X	X	X		X	X				X
AC over Semi-Rigid	X	X	X	X	X	X	X				
AC over JPCP	X		X	X		X		X			X
AC over CRCP	X		X	X		X				X	X
New JPCP and Bonded PCC over JPCP								X	X		X
Unbonded JPCP Overlays								X	X		X
New CRCP and Bonded PCC over CRCP										X	X
Unbonded CRCP overlays										X	X

Many state highway agencies in the United States continue to take steps to implement the Pavement ME Design as their pavement design standard through local calibration and implementation efforts. In fact, local implementation of the Pavement ME procedure is much

more than just a statistical adjustment (calibration) of the performance models; it includes various other activities specific to an agency such as developing appropriate local inputs, revising local design standards, customizing the software for design automation and developing functional user guide documents for routine use.

## **OVERVIEW OF PAVEMENT ME DESIGN ADOPTION IN MISSOURI**

Missouri Department of Transportation (MoDOT) was one of the early adopters of the ME design procedure, which was formerly referred to as the ME Pavement Design Guide (MEPDG). It was one of the first agencies to initiate research and mobilize resources to implement the MEPDG. From 2004 to 2009, MoDOT conducted traffic studies, performed laboratory testing of hot mix asphalt (HMA), portland cement concrete (PCC), base and soils materials, undertook field testing, and calibrated distress models.

MoDOT's initial implementation tasks concluded in 2009 with the MoDOT study RI04-002, titled, "*Implementing the AASHTO Mechanistic Empirical Pavement Design Guide in Missouri*" (Mallela et al. 2009). Under this study, the 2009 version of the AASHTO MEPDG tools distress and smoothness prediction models were validated and calibrated for new pavement designs. A MoDOT specific AASHTO MEPDG User Manual was also developed. While the study was initiated with a broader scope in mind, its narrower focus on new pavement designs was primarily due to the extent of data that was available at the time. This limited its coverage of rehabilitated pavement types. In addition, since the time the study was completed, several enhancements have been incorporated into the ME design software to reflect ongoing research addressing gaps in the methodologies and advancements to the different ME models.

The 2009 MoDOT study, as described previously, provided a basis for the use of ME Design by the agency. Key findings, and recommendations from this study are as follows:

- Identification of Pavement Types of Interest to MoDOT – For ME Design usage mostly on heavy/medium routes, New AC, New JPCP, AC on rubblized PCC, AC over AC, AC on JPCP, and PCC overlays were identified. Note that although several rehabilitation types of interest were contemplated, they could not be evaluated in-depth due to the lack of mature in-service sections at that point in time.
- Development of Local Calibration Projects Factorial – This study identified key pavement design features and material layer properties. The factorial of calibration sections included projects from Long-Term Pavement Performance (LTPP) experiments and MoDOT Pavement Management System (PMS). A total of seven flexible pavement projects and 27 rigid pavement projects (20 with tied shoulders) were selected from the PMS and supplemented with LTPP sections. Majority of PMS AC and PCC sections were less than 12 and 20 years in service. This also included the selection of hierarchical input level based on importance and DOT capabilities and resources. Calibration for rehabilitation design was recommended for a future date.
- Decisions on Traffic Data – Data from 11 Weigh-in-motion (WIM) sites were analyzed and they represented two to seven years of data, ranging from 5-12 months of the year. MEPDG specific input parameters were found to align with default truck traffic classification (TTC) one, two, and six axle load spectra, number of axles per truck, and

hourly truck distributions. Special analyses were recommended if overloaded axles exceed defaults by 10 percent, or if spring and summer traffic are 30 percent higher than average. MoDOT has collected additional WIM data since 2008, and new WIM sites need to be analyzed and verified against previous findings.

- Decisions on Climate Data – The research grade software program for MEPDG included 18 default weather stations in the state of Missouri. This MEPDG version used enabled the generations of virtual weather stations for project specific locations using interpolated data from weather stations within a 20 mile radius of a project location. Therefore, weather stations from neighboring States within 20 miles of the state border were included. The current AASHTOWare Pavement ME (version 2.5.5) utilizes weather data from two sources, Modern-Era Retrospective analysis for Research and Applications, Version 2 (MERRA-2) managed by the National Aeronautics and Space Administration (NASA) Goddard Earth Sciences (GES) Data and Information Services Center (DISC) and the North American Regional Reanalysis (NARR) produced by the National Centers for Environmental Prediction (NCEP). MERRA-2 data is used for flexible pavement analysis and NARR data files are used for rigid pavement analysis.
- Decisions on Materials data – Material testing and field testing were performed by MoDOT and its contractors for the 2009 study.
  - HMA materials test data – Eight (8) HMA mixtures covering Stone Mix Asphalt (SMA), Polymer Modified Asphalt (PMA), neat and Marshall mixes used in surface, intermediate, and base courses were tested. The study concluded that:
    - MEPDG provides reasonable prediction of  $|E^*|$  for both unmodified and modified binders.
    - MEPDG permanent deformation model coefficients appear to be dependent on mix type (important consideration for layer-by-layer rutting calibration).
    - MEPDG Level 3 creep compliance estimates are higher than corresponding Level 1 values.
    - MEPDG Level 3 estimates of indirect tensile strengths were lower than the corresponding Level 1 values.
  - PCC Test Data –Six PCC mixtures with five gradation types were tested and data analyzed. Findings showed:
    - Default values could be established for all inputs.
    - Correlations for flexural strength and elastic modulus were not consistent with default models and MoDOT correlations were recommended.
    - PCC mixes showed lower Coefficient of Thermal Expansion (CTE) than default values. Corrected CTE values based on AASHTO T 336 did not show errors as large as national LTPP samples did, yet lower than measured values.
  - Unbound Materials – Resilient modulus values were determined and  $k_1$ ,  $k_2$ ,  $k_3$  values derived for predominant base type and three subgrade types, AASHTO classes A-2-6, A-4, and A-7-6.

Since 2009, MoDOT has increasingly used recycled materials in HMA for highway pavement construction. Recognizing the need for proper design and control during

production and construction, MoDOT has used reclaimed asphalt pavement (RAP) and reclaimed asphalt shingles (RAS) in varying percentages to determine acceptable levels of replacement. These mixes were not included in the 2009 calibration efforts.

- Validation and calibration of Distress and IRI Prediction Models – The 2009 calibration effort evaluated the accuracy of the global prediction models. For distress types where significant bias was noted and where adequate performance data were available, the models were recalibrated using statistical methods.
- Recommendations – The study made recommendations for future recalibration and implementation based on future needs of the agency. These recommendations touched upon future data collection and laboratory testing necessary to support a calibration effort maximizing the Level 1 data to the extent possible.

### **NEED FOR FUTURE RECALIBRATION FOR MODOT**

MoDOT has been using the AASHTOWare Pavement ME Design since 2004 for traditional pavement design and alternative contracting. Since 2009, several enhancements have been made to the Pavement ME Design procedure and the AASHTOWare Pavement ME tool. During this time, MoDOT has also gained valuable experience in the implementation and adoption of this procedure. Experience gained by other agencies nationwide has also been exchanged through various discussion forums, workshops, user groups meetings, and other technical interactions within the industry. Concurrently, new mix designs, test methods, material specifications, and construction specifications have been established at MoDOT. These general factors warrant a review and recalibration of the current global distress prediction models for future MoDOT designs. Other factors specific to MoDOT that support the need for recalibration now include:

- Need for Rehabilitation Design – MoDOT anticipates that a significant number of future design projects will involve rehabilitation of existing pavements. With the ability to assemble data for overlay designs, and reasonable performance data available on rehabilitation projects for use in calibration, local calibration of rehabilitation design are essential and achievable at this stage.
- Updates to Material Types in Use – MoDOT has increasingly adopted RAP and RAS in HMA construction and focused on performing laboratory tests to generate level 1 data for calibration and future designs. The ongoing laboratory testing efforts to determine material properties necessary for Pavement Design ME make it necessary to include sections with RAP and RAS mixes in local calibration efforts.
- Updates to Traffic Data – WIM data collected post 2008 needs analysis and verification. These efforts can lead to procedures for urban interstates and other haul routes.
- Availability of Additional Data – Additional data available relative to the previous study for revising previous calibration. Performance data after six additional years of service are available on most sections.
- Field Test Data – Field testing and data collection can be performed using a field sampling plan like LTPP sections. FWD deflection testing data can also be used to establish reasonable backcalculated modulus values.

- Availability of Level 1 Inputs – MoDOT conducted HMA materials testing programs at in-house laboratories and through collaboration with Missouri University of Science and Technology.
- Enhancements to Pavement ME Design Procedure and AASHTOWare Pavement ME – The MEPDG version used in 2009 underwent comprehensive reviews, and revisions and enhancements. A summary of the enhancements is summarized below (ARA 2019):
  - New climate data from MERRA-2 and NARR data sources.
  - Recalibration of the rigid pavement models (2016) to correct bias due to erroneous CTE inputs.
  - Technical audit of the design procedure and models leading to recalibration of the flexible pavement models in 2018. This includes revisions to the model forms for some of the distress prediction equations. These changes are particularly relevant to flexible pavement fatigue cracking prediction models.
  - Incorporation of a new ME based reflection cracking model adapted after research conducted under National Cooperative Highway Research Program (NCHRP) Project 1-41 for use in design of AC overlays.
  - New design modules for the ME design of semi-rigid pavements (i.e., AC over cementitious treated base) and thin bonded PCC over existing AC pavement.

MoDOT therefore initiated a recalibration of the AASHTOWare Pavement ME. Design Build 2.5.5 was used. This report summarizes the research findings from this study.

## **PROJECT OBJECTIVES**

MoDOT initiated this project to realize the benefit from the enhancements listed above and expand use of the tool beyond New AC pavement and JPCP designs. The project goals were to refine and update the 2009 calibration effort to reflect new enhancements and expand the scope of use of the tool by MoDOT. The objectives of this implementation study were to:

- Update the materials database library with Level 1 laboratory test data for contemporary pavement material properties, including reclaimed materials.
- Perform local calibration of distress prediction models for pavement types of interest to MoDOT.
- Fully document the local calibration work, including clear guidance for changing calibration coefficients.
- Provide recommendations and precise details of any suggested/incorporated changes.

The key activities performed to achieve study objectives are presented below:

1. Develop a detailed work plan and implementation roadmap.
2. Develop a field test plan and laboratory test plan to obtain material inputs of the highest hierarchical level practical within the project duration.
3. Conduct laboratory and field testing to characterize materials properties and pavement condition.
4. Update default traffic input libraries and develop project specific traffic inputs for calibration.

5. Update climate data libraries and develop project specific climate inputs for calibration.
6. Conduct analysis to verify and validate existing Pavement ME Design procedures and models.
7. Confirm or adjust input default values for Missouri conditions.
8. Confirm or adjust the calibration coefficients to avoid biased designs.
9. Recommend any changes in policy and procedure that will be needed.
10. Conduct analysis to calibrate Pavement ME Design models for local Missouri conditions.
11. Perform sensitivity analysis for newly calibrated Pavement ME Design models.
12. Develop default traffic and materials data libraries.
13. Develop draft and final reports documenting all key project activities.

## **PROJECT SCOPE**

This project covers the expected use of the AASHTOWare Pavement ME Design procedure for new and rehabilitated projects in Missouri. Therefore, the local calibration was performed with the inclusion of pavement types applicable to MoDOT practices and the corresponding distress models. The pavement types and distress models calibrated are as follows:

- New AC and AC overlaid on AC pavements
  - Total alligator (bottom-up fatigue + reflected) cracking (Note: This distress type could not be verified in the previous effort since none of the Missouri pavement sections chosen for verification exhibited fatigue cracking.)
  - Total transverse (low temperature + reflected) cracking
  - Total rutting
  - Smoothness
- Composite pavements, which comprise of AC overlaid on PCC pavements
  - Total alligator cracking
  - Total transverse (low temperature + reflected) cracking
  - Total rutting
  - Smoothness
- Rigid pavements (new JPCP and JPCP overlays)
  - Transverse fatigue mid panel cracking
  - Transverse joint faulting
  - Smoothness

## **ORGANIZATION OF REPORT**

This report provides a detailed description of the work performed and includes relevant results to support the project findings and research conclusions. The report is organized in eight chapters. After this introductory chapter, Chapter 2 describes the methodology employed for identification and selection of pavement projects for local calibration. Discussions include criteria for selection of pavement projects for calibration, selection of hierarchical input levels, and data assembly strategies. Chapter 3 summarizes work done leading to the development of the calibration project database. Next, Chapter 4 describes the verification of the global models. Chapters 5 and 6 describe local calibration of pavement ME models for flexible and rigid pavements, respectively. Specific issues described and discussed include goodness of fit and

evaluations for the presence of bias, and methodologies for improving the predictive ability of the distress models and minimizing bias. Chapter 7 presents two case studies showing examples of use of the locally calibrated tool for pavement design in Missouri. Summary of study findings, conclusions, and recommendations for future research are presented in Chapter 8.

## CHAPTER 2. IDENTIFICATION AND SELECTION OF PROJECTS

### SELECTION OF PAVEMENT TYPES AND DISTRESS MODELS FOR MoDOT CALIBRATION

The project team selected pavement types that are used in current and future MoDOT pavement designs. Therefore, based on discussions with MoDOT, the following new and rehabilitated pavement types were selected:

- New AC and referred to as full depth asphalt or *FDA* sections in this report
- AC overlays of existing AC pavements, referred to as *AOA* in this report
- Composite pavements or AC overlays of existing PCC/JPCP pavements, referred to as *AOC*
- New JPCP
- Unbonded JPCP overlays of existing rigid pavements, referred to as UB

A combination of distress types and IRI are utilized for pavement design evaluation using the Pavement ME Design tool. The distress types used for the evaluation of the preliminary designs and design iterations, as per the scope of this study, are shown in Table 2.

Table 2. Pavement ME Design distress models selected for verification and local calibration

Pavement Types Selected for Local Calibration	Alligator (Bottom-Up Fatigue) Cracking	Alligator Reflection Cracking	AC Thermal Cracking	Transverse Reflection Cracking	AC Rutting	Total Rutting	Transverse (Slab) Cracking	Transverse Joint Faulting	Smoothness (IRI)
New AC	X		X		X	X			X
AC over AC	X	X	X	X	X	X			X
AC over JPCP	X		X	X	X		X		X
New JPCP							X	X	X
Unbonded JPCP Overlays							X	X	X

## IDENTIFICATION AND SELECTION OF PAVEMENT PROJECTS FOR LOCAL CALIBRATION

### Development of Sampling Template and Plan

Identification and selection of pavement projects for local calibration begins with developing a sampling plan to identify and select projects representative of the agency's pavement network. A general rule followed in selecting pavement projects for use in calibration is that the projects must represent current and future agency practices. Thus, for the projects selected the pavement design, material selection, construction practices and site (traffic, climate, and subgrade) conditions represented those in Missouri. It was also necessary that these projects have available detailed design, materials, construction records, and performance data. The design, materials, and construction data are key inputs for the Pavement ME Design tool. Performance data is necessary for the validation and calibration of the distress models. Sampling templates were developed to identify and select in-service projects for analysis. The parameters considered for the calibration matrix are presented in Table 3.

Table 3. Pavement ME Design parameters used for developing sampling template

Design Input Parameter	Pavement Type				
	New AC	AC over AC	AC over JPCP	New JPCP	Unbonded JPCP Overlays
Wearing/intermediate HMA layers thickness	X				
AC overlay thickness		X	X		
HMA mix type (9.5-, 12.5-, 19.0-, 25.0-mm)	X	X			
Asphalt binder type (PG-grades)	X	X	X		
HMA mix type (RAP or RAS content levels)	X	X	X		
Base type (crushed stone and large stone)	X			X	X
Climate zones [approximate latitude]: south [ $<38^{\circ}$ ], central [ $38.5^{\circ}$ to $39.5^{\circ}$ ], and north [ $>39.5^{\circ}$ ]	X	X	X	X	X
PCC slab thickness				X	
PCC overlay thickness					X
Load transfer				X	X
Slab width/shoulder type				X	X

### PROJECT SELECTION

A combination of simple random and stratified sampling techniques was utilized for the development of the calibration matrix. While simple random sampling technique was utilized to randomly select projects for populating the sampling template, stratified sampling was used to

divide the parameters presented in Table 3 into smaller homogeneous subgroups (strata) as needed. For example, AC thickness of  $\leq 6$  inches versus  $> 6$  inches, RAP contents of  $<20\%$  and  $20-40\%$ . Climatic regions considered were the southern, central, and northern regions of the state. The goal was to ensure that projects selected represented the full range of values used by MoDOT for any given parameter.

Using the parameters of interest, templates for project identification and selection were developed. The sampling templates were populated with projects obtained from LTPP and the MoDOT PMS.

### **Projects Selected from the MoDOT Pavement Management System**

Projects selected from the MoDOT PMS provided data critical for the calibration of the distress models in this study because the design inputs are representative of MoDOT's current specifications and material test procedures. The following summarizes the parameters included in the calibration template for MoDOT PMS sections:

- For New AC projects, construction was over crushed or large stone base layers on fine subgrades. The HMA wearing surfaces used 9.5 or 12.5 mm nominal aggregate size HMA mix. Intermediate HMA layer mix types considered were nominal aggregate size of 19.0 and 25.0 mm. Binder types included SuperPave Performance Grade (PG) 76-22, 70-22, and 64-22 grades, using virgin aggregates, and RAP contents ranging from about 12 to 24 percent. The projects were constructed over fine-grained soils. Projects were constructed from 2001 to 2010 and were located throughout the state.
- AC over AC projects had HMA overlay thicknesses in the range of 1.5 to 5 inches and were constructed over existing 9 to 12-inch thick HMA layers of AC pavements. AC overlay used 9.5 or 12.5 mm nominal aggregate size HMA mix with varying RAP contents. For some of the projects, the existing HMA layer was milled up to 2 inches prior to HMA overlay placement. The existing pavement base type/subgrade were typical of base materials used by MoDOT for New AC pavements. Existing pavement condition was a mix of good/fair/poor. The existing pavement in several of the AC over AC projects used were considered as New AC pavement projects under the previous calibration effort. HMA overlays were constructed from 2006 to 2013.
- For AC overlay over existing JPCP, the overlay construction was completed in two lifts using 12.5 mm to 19 mm nominal aggregate size HMA layers with a total thickness ranging from 3.7 to 4.2 inches. HMA mixes used 9 to 40 percent RAP contents. PCC materials, base type, and their thicknesses varied, but were typical of MoDOT designs and specifications; subgrades were typical of Missouri soils. Existing pavement condition was a mix of good/fair/poor. The HMA overlays were constructed from 2006 to 2010.
- For new JPCP and unbonded JPCP overlay projects, the majority of projects comprised of PCC thickness greater than 10 inches, widened 14 ft. lanes with tied shoulders, and joint spacing of 15 ft. The JPCP projects were doweled and constructed over an aggregate base and fine subgrade.

The selected projects are included in the calibration matrix for New AC, AC over AC, AC on JPCP, and rigid pavements shown in Table 4 through Table 7, respectively. Note that, in Table 4 through Table 7, the projects are identified by their Cell ID. As stated previously, the Cell IDs use the prefix FDA, AOA, AOC, and UB for New AC, AC over AC, AC on JPCP and unbonded JPCP overlay projects respectively. Note that the PMS sections do not cover all cells of the template. For each Cell ID, the corresponding MoDOT Project ID is presented in Table 8. Table 8 also presents the location and construction history for the project. Cell IDs are used as the reference for each project through the remainder of this report.

Table 4. Sampling template for MoDOT PMS New AC projects in local calibration

Climate	Base Type	Total AC Thickness			
		≤ 10 inch		> 10 inch	
		Surface Layer AC Binder		Surface Layer AC Binder	
		0 to 20% RAP/RAS	20 to 40% RAP/RAS	0 to 20% RAP/RAS	20 to 40% RAP/RAS
Central	Crushed Stone				
	Large Stone	FDA1-S2 <sup>4</sup>	FDA1-S1 <sup>4</sup>		
South	Crushed Stone		FDA3 <sup>1</sup>	FDA4 <sup>3,4</sup>	
	Large Stone			FDA6 <sup>1,2</sup> , FDA2 <sup>4</sup>	

<sup>1</sup>Virgin binder in surface layer, i.e. 0 percent RAP/RAS.

<sup>2</sup>Virgin binder in intermediate layer.

<sup>3</sup>Variable/unknown RAP/RAS content in surface layer.

<sup>4</sup>Variable/unknown RAP/RAS content in intermediate layer.

Table 5. Sampling template for AC over AC MoDOT PMS projects in local calibration

Climate	Base Type	AC Overlay Thickness			
		1 to 2 inch		2 to 6 inch	
		AC Overlay Binder Type		AC Overlay Binder Type	
		0 to 20% RAP	20 to 40% RAP	0 to 20% RAP	20 to 40% RAP
North	Crushed stone	AOA5 <sup>2</sup>			AOA4 <sup>1</sup>
	Rock base				
Central	Crushed stone	AOA1 <sup>1</sup>			AOA3
	Rock base				
South	Crushed stone				
	Rock base	AOA2-S1		AOA2-S2 <sup>1,3</sup>	

<sup>1</sup>AC overlay thickness: Includes mill and fill.

<sup>2</sup>Virgin binder in overlay HMA.

<sup>3</sup>AC overlay has variable RAP content.

Table 6. Sampling template for MoDOT PMS AC over JPCP projects in local calibration

<b>AC overlay thickness ranging from 3.6 to 4.2 inch</b>			
<b>Climate</b>	<b>Overlay Lower Lift Binder Type</b>	<b>HMA Overlay Top Lift Binder Type</b>	
		<b>0 to 20% RAP</b>	<b>20 to 40% RAP</b>
North	0 to 20% RAP	AOC3	
	20 to 40% RAP	AOC1 <sup>1</sup>	
Central	0 to 20% RAP	AOC5 (20% RAP)	
	20 to 40% RAP		AOC2 <sup>2</sup>
South	0 to 20% RAP		
	20 to 40% RAP	AOC4	

<sup>1</sup>Virgin binder in top lift of the HMA overlay.

<sup>2</sup>Project has variable RAP content.

Table 7. Sampling template for new JPCP and unbonded JPCP overlay over existing JPCP projects selected for local calibration

<b>Climate</b>	<b>Base Type</b>	<b>PCC Thickness</b>			
		<b>&lt; 10 inch</b>		<b>≥ 10 inch</b>	
		<b>Edge Support</b>		<b>Edge Support</b>	
		<b>None</b>	<b>Widened and Tied</b>	<b>None</b>	<b>Widened and Tied</b>
North/South	Crushed Stone	B1, C1	D1, D3		F1, F2, F3, F4, F5, F6, F7, F8, F9, F10
	Large Stone				G1, G2, G3
	PCC <sup>1</sup>	UB1, UB2, UB3, UB4		UB5	

\*All pavements have joint spacing of 15 ft. and doweled joints.

The MoDOT calibration project sections had different truck traffic loading conditions, subgrade soil conditions, and pavement layer material properties. These topics are discussed in the next chapter of the report.

Table 8. Location and construction dates of the calibration projects

Cell ID	Sample Unit	Rte.	Dir.	MoDOT Project ID	Begin Log	End Log	Latitude, deg	Longitude, deg	Original Construction Year	Overlay Construction Year
<b>New AC Design Projects</b>										
FDA1	S1	5	N	J5P0590	127.5	127.7	38.125	-93.093	2008	
FDA1	S2	5	N	J5P0590	128.5	128.7	38.114	-93.081	2008	
FDA2	S1	65	N	J8P0609B	10	10.2	36.624	-93.222	2006	
FDA3	S1	66	W	J7S0594	4.6	4.8	37.084	-94.443	2010	
FDA4	S1	266	W	J8S0851	0.6	0.8	37.214	-93.393	2008	
FDA6	S1	65	N	J8P0609	3	3.2	36.535	-93.246	2001	
<b>AC overlay on Existing AC Projects</b>										
AOA1	S1	13	S	J7P0824D	166.2	166.4	38.101	-93.707	2000	2010
AOA2	S1	65	N	J8P2268	27.8	28	36.877	-93.232	2000	2012
AOA2	S2	65	S	J8P2268	285.1	285.3	36.880	-93.233	2000	2012
AOA3	S1	21	S	J3S2009P	77.8	78	37.676	-90.716	1999	2009
AOA4	S1	63	N	J5P0964	235.33	235.519	39.199	-92.329	2001	2013
AOA5	S1	210	W	J4S1737	10.437	10.627	39.232	-94.188	1996	2006
<b>AC overlay on JPCP Projects</b>										
AOC1	S1	35	S	J1D0600J	74.74	74.94	39.543	-94.273	1996	2006
AOC2	S1	100	W	J6D0600J	26.15	26.34	38.586	-90.656	1996	2005
AOC3	S1	63	S	J2P0773	44.4	44.6	39.998	-92.476	1994	2008
AOC4	S1	60	E	J9P0596	192.2	192.4	36.987	-91.546	1997	2010
AOC5	S1	61	N	J3D0600A	274.4	274.6	39.025	-90.980	1996	2006
<b>New JPCP Projects</b>										
B1	S1	6	W	J1U0402	206.509	206.609	39.784	-94.763	1995	
C1	S1	AB	W	AC-STP-113	2.169	2.269	37.239	-89.529	1997	
D1	S1	92	W	J4P0889	29.948	30.048	39.372	-94.789	1995	
D3	S1	TT	E	J5P0381	2	2.1	38.956	-92.392	1995	
F1	S1	36	W	J1P0489B	147.64	147.74	39.751	-94.143	1996	
F1	S2	36	W	J1P0489B	150.9	151	39.750	-94.108	1996	
F1	S3	36	W	J1P0489B	153.02	153.12	39.750	-94.087	1996	
F1	S4	36	W	J1P0489B	154.89	154.99	39.737	-94.030	1996	
F2	S1	24	E	J3P0284	211.489	211.589	39.931	-91.482	1997	
F3	S1	54	W	J5P0409	77.89	77.99	38.883	-91.954	1995	
F3	S2	54	W	J5P0409	79.23	79.33	38.868	-91.971	1997	

Table 8. Location and construction dates of the calibration projects, continued

Cell ID	Sample Unit	Rte.	Dir	MoDOT Project ID	Begin Log	End Log	Latitude, deg	Longitude, deg	Original Construction Year	Overlay Construction Year
F3	S3	54	W	J5P0409	81.22	81.32	38.839	-91.971	1995	
F4	S1	54	W	J5P0410	83.34	83.44	38.812	-91.986	1995	
F5	S1	54	E	J5P0411C	183.732	183.832	38.760	-92.046	1993	
F5	S2	54	E	J5P0411C	185.615	185.715	38.781	-92.023	1993	
F5	S3	54	E	J5P0411C	187.135	187.235	38.796	-92.006	1993	
F6	S1	54	E	J5P0412C	177.312	177.412	38.678	-92.096	1994	
F6	S2	54	E	J5P0412C	179.272	179.372	38.706	-92.087	1994	
F6	S3	54	E	J5P0412C	181.492	181.592	38.732	-92.064	1994	
F7	S1	7	S	J4P0861D	71.521	71.621	38.409	-93.850	1997	
F7	S2	7	S	J4P0861D	73.081	73.181	38.394	-93.828	1997	
F8	S1	60	E	J0P0571	271.349	271.449	36.795	-90.373	1997	
F8	S2	60	E	J0P0571	272.049	272.149	36.795	-90.360	1997	
F9	S1	60	W	J0P0572	65.13	65.23	36.791	-90.248	1997	
F9	S2	60	W	J0P0572	68.63	68.73	36.793	-90.312	1997	
F10	S1	74	E	J0U0412C	7.94	8.04	37.291	-89.562	1995	
G1	S1	63	S	J5P0621	144.866	144.966	38.629	-92.196	1994	
G1	S2	63	S	J5P0621	145.966	146.066	38.615	-92.188	1994	
G2	S1	M	E	J6S064E	0.548	0.648	38.375	-90.495	1998	
G2	S2	M	E	J6S064E	1.988	2.088	38.364	-90.474	1998	
G3	S1	M	E	J6S0641	3.268	3.278	38.358	-90.455	1998	
G3	S2	M	E	J6S0641	5.318	5.418	38.352	-90.419	1998	
G3	S3	M	E	J6S0641	6.228	6.328	38.349	-90.401	1998	
Unbonded Overlay on JPCP Projects (Projects not used in recalibration)										
UB2	S2	44	W	J8I0633	200.417	200.517	37.271	-93.089		
UB3	S1	55	S	J0I0833	196.015	196.115	36.161	-89.753		
UB3	S2	55	S	J0I0833	199.515	199.615	36.114	-89.767		
UB3	S3	55	S	J0I0833	202.895	202.905	36.079	-89.810		
UB3	S4	55	S	J0I0833	206.465	206.565	36.043	-89.853		
UB4	S1	255	S	J6I1486	0.526	0.626	38.502	-90.321		
UB4	S2	255	S	J6I1486	1.626	1.726	38.492	-90.294		
UB5	S1	412	E	J0P0600D	30.94	31.04	36.234	-89.905		
UB5	S2	412	E	J0P0600D	32.45	32.55	36.234	-89.878		

The locations of the selected calibration projects from the MoDOT PMS are shown in Figure 1, Figure 2, and Figure 3 below for flexible pavement, rigid pavement and composite pavement sections, respectively. Note the flexible sections include New AC and AC over AC projects. Likewise, the rigid pavement sections include all PCC surfaced pavements. The projects cover all site conditions including climate variations in the state relevant to distress development.



Figure 1. Location of MoDOT PMS New AC and AC over AC projects (Google, n.d.)



Figure 2. Location of MoDOT PMS new JCP and unbonded overlays projects (Google, n.d.)



Figure 3. Location of MoDOT PMS AC over JCP projects (Google, n.d.)

## Projects Selected from FHWA Long Term Pavement Performance Database

The LTPP experiments include field sections in the state of Missouri. The majority of these sections are flexible pavement projects. Figure 4 shows a map with the location of the LTPP project sites in Missouri and indicates that the projects are well distributed across the northern, central, and southern parts of the state. Table 9 provides the list of LTPP sections located in Missouri and that were used in this study. This table summarizes the defined experiment type, county location, the roadway, functional class, climate zone, and date of original construction. The LTPP experiments included in the calibration and the pavement types therein are:

- SPS-5 – AC overlay on existing AC pavement
- SPS-6 – AC overlay on existing JPCP
- SPS-8 – New AC and JPCP with minimal traffic (SPS-8 was designed to study the effects of environmental factors in the absence of heavy loads)
- SPS-9 – AC overlay on JCP with different AC binder types
- GPS -1 – AC surfaced pavements with unbound granular base
- GPS-6A - Existing AC overlay on AC Pavement
- GPS-6B - AC Overlay with conventional AC on AC Pavement, no milling
- GPS-6S - AC Overlay on AC pavement with milling and/or fabric pretreatment

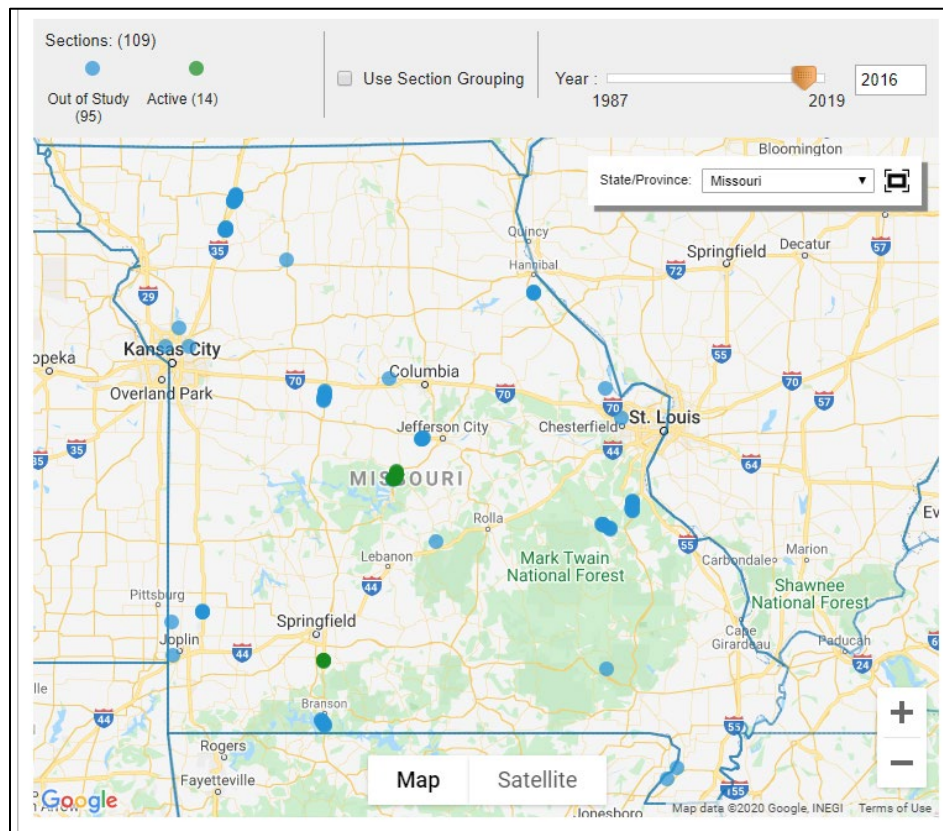


Figure 4. Location of Missouri LTPP projects selected for verification and validation of Pavement ME distress models (Source: LTPP InfoPave Visualization tool)

Table 9. List of LTPP sections included in the local calibration

<b>LTPP State and Section ID</b>	<b>LTPP Study</b>	<b>County</b>	<b>Route, Direction</b>	<b>Design Type</b>	<b>Functional Class*</b>	<b>Climatic Zone</b>	<b>Construction Date</b>
29-0501	SPS-5	Taney	US-65, NB	New AC	RPA-O	WNF	Oct-1981
29-0502	SPS-5	Taney	US-65, NB	AC/AC	RPA-O	WNF	Oct-1981
29-0503	SPS-5	Taney	US-65, NB	AC/AC	RPA-O	WNF	Oct-1981
29-0504	SPS-5	Taney	US-65, NB	AC/AC	RPA-O	WNF	Oct-1981
29-0505	SPS-5	Taney	US-65, NB	AC/AC	RPA-O	WNF	Oct-1981
29-0506	SPS-5	Taney	US-65, NB	AC/AC	RPA-O	WNF	Oct-1981
29-0507	SPS-5	Taney	US-65, NB	AC/AC	RPA-O	WNF	Oct-1981
29-0508	SPS-5	Taney	US-65, NB	AC/AC	RPA-O	WNF	Oct-1981
29-0509	SPS-5	Taney	US-65, NB	AC/AC	RPA-O	WNF	Oct-1981
29-0603	SPS-6	Harrison	I-35, SB	AC/JPCP	RPA-I	WF	Jul-1975
29-0604	SPS-6	Harrison	I-35, SB	AC/JPCP	RPA-I	WF	Jul-1975
29-0606	SPS-6	Harrison	I-35, SB	AC/JPCP	RPA-I	WF	Jul-1975
29-0607	SPS-6	Harrison	I-35, SB	AC/JPCP	RPA-I	WF	Jul-1975
29-0608	SPS-6	Harrison	I-35, SB	AC/JPCP	RPA-I	WF	Jul-1975
29-0659	SPS-6	Harrison	I-35, SB	AC/JPCP	RPA-I	WF	Jul-1975
29-0660	SPS-6	Harrison	I-35, SB	AC/JPCP	RPA-I	WF	Jul-1975
29-0661	SPS-6	Harrison	I-35, SB	AC/JPCP	RPA-I	WF	Jul-1975
29-0662	SPS-6	Harrison	I-35, SB	AC/JPCP	RPA-I	WF	Jul-1975
29-0663	SPS-6	Harrison	I-35, SB	AC/JPCP	RPA-I	WF	Jul-1975
29-0664	SPS-6	Harrison	I-35, SB	AC/JPCP	RPA-I	WF	Jul-1975
29-0665	SPS-6	Harrison	I-35, SB	AC/JPCP	RPA-I	WF	Jul-1975
29-0801	SPS-8	Christian	SW Outer Rd, SB	New AC	RLC	WF	Jul-1998
29-0802	SPS-8	Christian	SW Outer Rd, SB	New AC	RLC	WF	Jul-1998
29-0807	SPS-8	Christian	SW Outer Rd, SB	JPCP	RLC	WF	Jul-1998
29-0808	SPS-8	Christian	SW Outer Rd, SB	JPCP	RLC	WF	Jul-1998
29-A801	SPS-8	Harrison	US-61, NB	New AC	RLC	WF	Dec-1998
29-A802	SPS-8	Harrison	US-61, NB	New AC	RLC	WF	Dec-1998
29-0901	SPS-9J	Pettis	US-65, SB	AC/JPCP	RPA-O	WF	Apr-1966
29-0902	SPS-9J	Pettis	US-65, SB	AC/JPCP	RPA-O	WF	Apr-1966
29-0903	SPS-9J	Pettis	US-65, SB	AC/JPCP	RPA-O	WF	Apr-1966
29-0959	SPS-9J	Pettis	US-65, SB	AC/JPCP	RPA-O	WF	Apr-1966

Table 9. List of LTPP sections included in the calibration, continued

LTPP State and Section ID	LTPP Study	County	Route, Direction	Design Type	Functional Class*	Climatic Zone	Construction Date
29-0960	SPS-9J	Pettis	US-65, SB	AC/JPCP	RPA-O	WF	Apr-1966
29-0961	SPS-9J	Pettis	US-65, SB	AC/JPCP	RPA-O	WF	Apr-1966
29-0962	SPS-9J	Pettis	US-65, SB	AC/JPCP	RPA-O	WF	Apr-1966
29-0963	SPS-9J	Pettis	US-65, SB	AC/JPCP	RPA-O	WF	Apr-1966
29-0964	SPS-9J	Pettis	US-65, SB	AC/JPCP	RPA-O	WF	Apr-1966
29-1002	GPS-1	Cole	Other-3, WB	New AC	RMC	WF	Apr-1986
29-1005	GPS-1	Miller	US-54, WB	New AC	RPA-O	WF	May-1974
29-1008	GPS-1	Jasper	State-171, SB	New AC	RPA-O	WF	Apr-1986
29-1010_1	GPS-6S	Pulaski	I-44, EB	New AC	RPA-I	WF	Aug-1980
29-1010_2	GPS-6S	Pulaski	I-44, EB	AC/AC	RPA-I	WF	Aug-1980
29-5403	GPS-6B	Dunklin	US-412, EB	AC/AC	RMA	WNF	Oct-1965
29-5413	GPS-6B	Dunklin	US-412, EB	AC/AC	RPA-O	WNF	Oct-1965
29-6067	GPS-6A	Carter	US-60, EB	AC/AC	RPA-O	WNF	Jun-1965

\*RPA-O is Rural Principal Arterial – Other; RPA-I is Rural Principal Arterial – Interstate.  
 RLC is Rural Local Collector; RMC is Rural Major Collector; RMA is Rural Minor Arterial

Table 10 summarizes other site parameters and design parameters for all LTPP sections used in the calibration database. This table provides the layer thicknesses for each layer type in the structural design of the project. Also listed in Table 10 are site specific factors, such as the initial daily truck traffic in the design lane, and the location reference.

Table 10. Layer thicknesses, and site parameters of LTPP sections used in local calibration

SHRP_ID	AC Overlay Thickness, in	AC Layer Thickness, in	PCC Thickness, in	Unbound Base Thickness, in	Subgrade Type	Initial Daily Truck Traffic (Design Lane)	Latitude	Longitude
29-0501	N/A	8.4		4	A-4	218	36.5	-93.125
29-0502	2.1	8.4		4.5	A-4	487	36.5	-93.125
29-0503	4.9	8.5		4	A-4	487	36.5	-93.125
29-0504	4.7	8.1		4	A-4	487	36.5	-93.125
29-0505	2.2	8.8		4	A-4	487	36.5	-93.125
29-0506	3.9	5.7		6	A-4	487	36.5	-93.125
29-0507	6.3	7.2		4	A-4	487	36.5	-93.125

Table 10. Layer thicknesses, and site parameters of LTPP sections used in local calibration, continued

SHRP_ID	AC Overlay Thickness, in	AC Layer Thickness, in	PCC Thickness, in	Unbound Base Thickness, in	Subgrade Type	Initial Daily Truck Traffic (Design Lane)	Latitude	Longitude
29-0508	7.1	6.2		4	A-4	487	36.5	-93.125
29-0509	4.2	6.1		4	A-4	487	36.5	-93.125
29-0603	4	N/A	9.1	4.8	A-4	1408	40	-93.75
29-0603	4	8	N/A	4.8	A-4	1408	40	-93.75
29-0604	4	N/A	9.1	4.5	A-4	1408	40	-93.75
29-0606	4	N/A	8.9	3.5	A-4	1408	40	-93.75
29-0608	8	N/A	9.4	5	A-4	1408	40	-93.75
29-0660	7.9	N/A	9.7	4.2	A-4	1408	40	-93.75
29-0661	12.6	N/A	9.4	4.2	A-4	1408	40	-93.75
29-0662	8	N/A	9.4	4.5	A-4	1408	40	-93.75
29-0663	12.4	N/A	9.5	4.5	A-4	1408	40	-93.75
29-0664	7.9	N/A	9.7	5.1	A-4	1408	40	-93.75
29-0665	4.7	N/A	9.1	4	A-4	1408	40	-93.75
29-0801	N/A	4.7	N/A	7.9	A-4	10	37	-93.125
29-0802	N/A	7.5	N/A	11.5	A-4	10	37	-93.125
29-A801	N/A	6.9	N/A	11.5	A-4	10	37	-93.125
29-A802	N/A	6.9	N/A	11.5	A-4	10	37	-93.125
29-0901	3.7	N/A	8	4	A-4	547	39	-93.125
29-0902	4.4	N/A	8	5.8	A-4	547	39	-93.125
29-0903	4.2	N/A	8	4.9	A-4	547	39	-93.125
29-0959	4.3	N/A	8.1	4.5	A-7-6	547	39	-93.125
29-0960	4	N/A	8.1	4.3	A-4	547	39	-93.125
29-0961	3.5	N/A	7.8	4.3	A-4	547	39	-93.125
29-0962	4.2	N/A	8.1	4.5	A-4	547	39	-93.125
29-0963	4	N/A	8.1	4.4	A-4	547	39	-93.125
29-0964	4.2	N/A	8.0	4.3	A-4	547	39	-93.125
29-1002	N/A	6.8	N/A	7.5	A-4	41	38.5	-92.5
29-1005	N/A	8.9	N/A	3.9	A-6	192	38	-92.5
29-1008	N/A	11.4	N/A	4.4	A-6	128	37	-94.375
29-5403	2.2	2.2	N/A	6.2	A-4	313	36	-90
29-5413	3.5	3.8	N/A	5	A-4	313	36	-90
29-6067	2.2	5.9	N/A	4	A-2-6	139	37	-90.625
29-1010-1	N/A	13.8	N/A	4.2	A-2-7	1757	38	-92.5
29-1010-2	7.7	13.4	N/A	4.2	A-2-7	3010	38	-92.5

## **CHAPTER 3. DEVELOPMENT OF CALIBRATION DATABASE**

Data required for AASHTOWare Pavement ME analyses and performance data required for distress model calibration were assembled to develop a project database. Data assembly comprises of five main activities, (1) selecting hierarchical input level for key inputs, (2) processing climate, traffic, construction, design, materials, and subgrade data, (3) assembling supplemental data derived from field testing, laboratory characterization, and on-site forensic investigations, (4) extracting pavement performance data from agency pavement management data or interpreting distress images, and (5) integrating all data into a project calibration database. The development of the project calibration database is described in the following sections.

### **SELECTION OF HIERARCHICAL INPUT LEVELS**

The Pavement ME Design requires a significant number of inputs for the simulation of pavement distress development through the various algorithms and ME models. Sensitivity analysis in past studies has shown that not all inputs significantly impact predicted distress and smoothness. Further, agency practices and resources place a practical limitation on the data items that can be acquired and assembled in various levels of detail. The AASHTO MEPDG Local Calibration Guide therefore provides users or agencies some flexibility for establishing inputs to the design procedure. Inputs may be provided in three hierarchical levels, Levels 1 to 3, each associated with a different level of accuracy in input values and therefore a different level of reliability in the predicted distresses. The guidance provided is summarized as follows:

- Level 1 inputs provide the highest level of accuracy and, hence, are expected to have the lowest level of uncertainty or error in the predictions. Level 1 inputs are typically laboratory test results for the specific materials or site-specific test results.
- Level 2 inputs provide an intermediate level of accuracy and would be closest to the typical procedures used in earlier editions of the AASHTO Pavement Design Guide. Level 2 inputs may be derived through correlations with other easily determined index properties.
- Level 3 inputs are considered to have lowest level of accuracy. Inputs typically would be user-selected values based on national averages, engineering experience, or typical averages of an input for the region or state.

A general rule of thumb is to select the highest hierarchical level for critical inputs that significantly impact predicted distress and smoothness. Examples of such critical inputs are truck traffic volumes, layer thicknesses and material properties that show high impact on performance, or those that tend to vary from one mix design to the other. Levels 2 and 3 inputs can be selected for less critical inputs. For this implementation study a mix of all levels of inputs was utilized as described in Table 11. For material properties considered critical for pavement performance predictions, MoDOT provided laboratory- or field-test results. Specifically, the material test results were representative of the values typical of current and future mix designs adopted by MoDOT.

Table 11. Input data predominant hierarchical level

<b>Input Type</b>	<b>Input Data Elements</b>	<b>Hierarchical Level</b>
Traffic	Truck volume distribution and vehicle class distribution	Level 1 project specific data from MoDOT
	Axle load distributions	Level 1 or 2 site-specific computed using MoDOT WIM data or national defaults when data not available
	Monthly Adjustment Factors	Level 1 when available, or default
	All others	Level 3 Pavement ME defaults
Climate	Temperature, wind speed, percent sunshine, precipitation, and, relative humidity	AASHTOWare procedure; MERRA data for flexible pavements and NARR data for rigid pavements. Not associated with hierarchical level.
AC Materials	HMA dynamic modulus	Level 1 Laboratory testing (for PMS sections) Level 2 computed (for LTPP sections)
	Air voids	Level 1 field air void data from MoDOT and LTPP database
	Binder	Level 1 for PMS sections; Level 3 defaults for LTPP sections
	HMA creep compliance & indirect tensile strength	Level 1 laboratory test data for PMS sections; Level 2 computed data for LTPP sections
	Other inputs	Level 3 Pavement ME defaults
PCC Materials	Strength over time and mix design inputs	Level 1 strength data from previous laboratory test results for different MoDOT specification gradations. Level 2 and 3 for CTE and other inputs.
Unbound Base and Subgrade	Resilient modulus Atterberg limits, & gradation	Level 1 backcalculated data and field test data for PMS sections, and Level 3 data from LTPP database for LTPP sections.
Performance	Distress & smoothness	Level 1: Field measured

## DATA ASSEMBLY

This step involved extraction, review, and conversion to appropriate units for all data required as inputs for the Pavement ME Design. The principal sources of data for this local calibration effort were:

1. Standard Data Release 30 (2016) available from the LTPP InfoPave™ online portal (<https://infopave.fhwa.dot.gov>) for all LTPP sections
2. MoDOT databases or records for traffic data, pavement performance data, design features, and construction records for the PMS sections

3. Field data to backcalculate layer modulus from falling weight deflectometer tests, and layer information from cores for the PMS sections
4. Laboratory test data for material characterization of MoDOT mix designs for PMS sections
5. Final report for MoDOT Study RI04-002 (Mallela et al., 2009) for data assembled for the PMS sections during the previous study.

Although the calibration sections used were in-service with varying levels of distresses observed, the information extracted covered historical data relevant to the time of construction. The data collected included material properties, historical traffic, design features, and historical performance. Inventory type data such as project location, highway functional class, number of lanes, etc. were also retrieved. The findings from the data assembly effort are discussed below for LTPP projects and for the PMS projects used in the calibration.

### **LTPP Projects**

All the LTPP projects had information in sufficient detail required for developing Pavement ME Design input files. The hierarchical levels for the inputs available were appropriate and in agreement with recommendations.

LTPP data tables were used to obtain construction dates, layer types (identified by layer number in the database), layer thicknesses, AC material gradation, AC binder grade, AC content, subgrade and base gradation (and therefore AASHTO classifications), subgrade and base layer Atterberg limits, granular layer modulus, PCC unit weight, CTE, strength and modulus, curing type used during construction, performance data at the time of rehabilitation for rehabilitation projects, and performance data after construction for new and rehabilitation designs.

### **PMS Projects**

An initial review of materials and performance data readily available in MoDOT databases concluded that the existing data were inadequate for the calibration exercise. As a result, additional laboratory and field testing were required to obtain suitable project specific data. The calibration projects included for New AC (Cell IDs FDA), AC over AC (Cell IDs AOA), and AC on JPCP (Cell IDs AOC) were identified as those requiring additional data. The rigid pavement projects used in this calibration effort were also used during the 2009 calibration (Mallela et al., 2009), and data assembled from the 2009 study were used as needed.

A laboratory test plan was developed by the project team recommending the standard test protocols to be utilized, the test parameters to be included, number of test repetitions, and the sampling rates. The laboratory test plan also focused on maximizing Level 1 input data for HMA materials. The HMA mix designs were selected for the laboratory test plan to serve two purposes, first to provide inputs of representative mixtures for the current calibration, and second, to develop a materials library for MoDOT's future use. Analysis of the HMA materials test data is described later in this chapter.

A field test plan was also developed for New AC, AC over AC, and AC over PCC sections. Field tests were conducted to collect pavement layer information and to estimate material properties for materials not included in the laboratory test plans. Field cores were used to establish the layer types and thicknesses, gradations of the materials, and to evaluate interlayer conditions. FWD testing was performed to determine backcalculated layer properties, most essential for subgrade layers (note that laboratory test data were utilized for the HMA layers). Details of the field test plan and analyses of FWD data are discussed later in this chapter.

For traffic inputs, available MoDOT WIM data were assembled and analyzed to develop traffic vehicle class, axle load, and hourly/monthly truck volume distributions. Details of the traffic analyses are presented in later sections of this chapter.

Performance data were available in different formats for the PMS section. Historical IRI and rutting data were obtained for all sections from MoDOT's transportation management system. However, for cracking data, MoDOT collected Automatic Road Analyzer (ARAN) vehicle pavement condition data, including images, for the calibration sections in the study. Distress images were processed in accordance with the LTPP Distress Identification Manual (Miller, J.S., and Bellinger, W.Y., 2014) to obtain field data for all distresses identified in Table 2.

Finally, all assembled data were reviewed for accuracy, reasonableness, and consistency. Evaluation comprised of a review of the assembled data to identify erroneous entries and outliers. The review included visual inspection of time series plots showing the progression of distress and IRI to determine if the observed trends were reasonable, computing mean values and variance of key inputs to identify potential anomalies (e.g., significant increase in variance indicates potential outliers and errors). Identified anomalies were rectified where possible by substituting with data from other reliable sources such as LTPP.

## **CLIMATE DATA**

MERRA Climate data was obtained for all AC surfaced LTPP and MoDOT projects from the LTPP InfoPave Climate tool. The tool provides a visual interface to access MERRA data, and extracts data in the format required for the Pavement ME software program. MERRA utilizes a reanalysis model to combine computed climate data with ground, ocean, atmospheric, and satellite-reported observations resulting in a uniformly gridded dataset of meteorological data. MERRA meteorological data is reported hourly for 0.5 degrees latitude by 0.67 degrees longitude spatial resolution (approximately 31 x 37 miles). Likewise, the Pavement ME provides access to the NARR data in a format suitable for Pavement ME analysis of rigid pavements. Project location defined by latitude and longitude was used to obtain the MERRA or NARR grid data file. Specific data obtained for Pavement ME was temperature, wind speed, percent sunshine precipitation and relative humidity.

Figure 5 and Figure 6 show plots of ambient temperature and precipitation for two counties in Missouri, Taney in the south and Macon in the north. Figure 7 shows depth of frost penetration for the two sites estimated using the Pavement ME Design's Integrated Climatic Model (ICM). The plots show the northern county being slightly colder than the southern county, and particularly, the winter months show about 10 degrees lower temperatures in the North.

However, the frost penetration was significantly more in the north. Precipitation was about the same, although the precipitation is higher in the north during summer, and lower in the fall. Note that these data represent the climate patterns for the two specific sites and may not necessarily demonstrate a typical comparison between all northern and southern climates. There is every possibility that systematic variations occur from micro-climate patterns at a given site, or the presence of mountains, valleys, water bodies, or topographical variations.

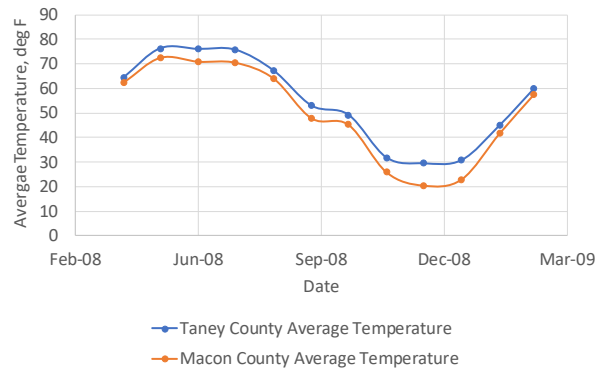


Figure 5. Average air temperature for Taney county (south) and Macon county (north)

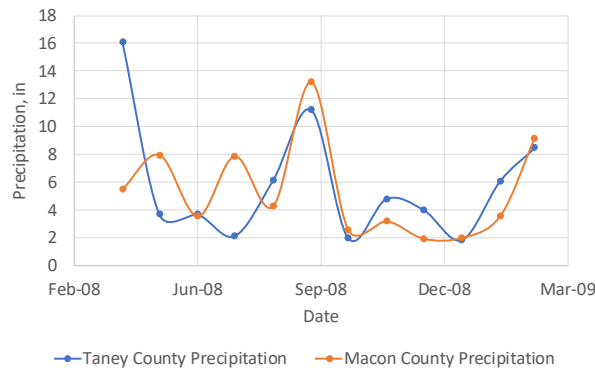


Figure 6. Average precipitation for Taney County (south) and Macon County (north)

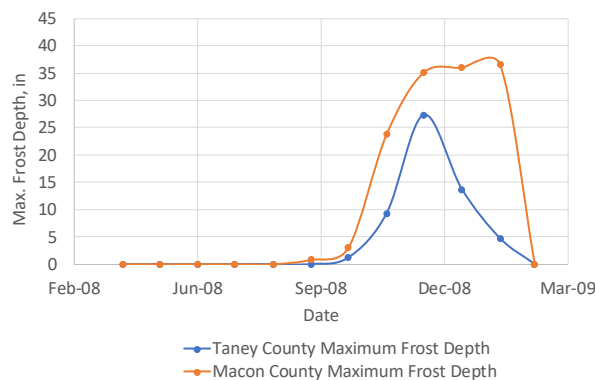


Figure 7. Average frost depth for Taney county (south) and Macon county (north)

Table 12 provides a summary of the climate data for all calibration sections selected. Data for each section is, essentially, a representative parameter or an index meant to capture the overall climate pattern from the large dataset of hourly measurements. These parameters are significant because they are inputs to Pavement ME model predictions that are influenced by the climate. A review of these data shows that, in general, the latitude is a good indicator of the mean annual air temperature (MAAT), with increasing MAAT values at lower latitudes. The freezing index and average number of freeze-thaw cycles increase at higher latitudes. These trends indicate the climate patterns in the calibration files are less likely to have microclimate influences.

Table 12. Summary of climate data for New AC, AC over AC, and AC over JPCP sections

Calibration Section	Latitude, degrees	Longitude, degrees	Mean Annual Air Temperature, °F	Mean Annual Precipitation (inch)	Freezing Index (Deg F -Days)	Average Annual Number of Freeze-Thaw Cycles
AOA1	38	-93.75	56.71	49.42	384.28	78.12
AOA2	37	-93.125	56.18	53.27	323.96	80.31
AOA3	37.5	-90.625	56.19	55.87	324.23	82.21
AOA4	39	-92.5	54.69	46.88	561.52	86.79
AOC1	39.5	-94.375	53.52	44.05	557.18	90.54
AOC2	38.5	-90.625	55.36	48.82	402.70	82.67
AOC3	40	-92.5	52.03	47.49	678.09	91.27
AOC4	37	-91.25	57.07	53.61	254.69	79.52
AOC5	39	-91.25	54.26	50.10	518.55	85.03
FDA1	38	-93.125	55.59	49.28	369.08	84.37
FDA2	36.5	-93.125	57.31	49.70	221.99	75.31
FDA3	37	-94.375	56.75	47.09	287.53	73.94
FDA4	37	-93.125	55.97	53.67	292.91	80.31
FDA6	36.5	-93.125	57.02	50.43	220.10	75.31
B1*	39.774	-94.907	53.63	36.38	644.42	67.36
D1*	39.299	-94.718	54.56	38.17	525.47	68.54
D3*	39.774	-94.907	53.63	36.38	644.42	67.36
F10*	37.225	-89.571	58.41	44.72	214.81	54.42
F1*	39.774	-94.907	54.06	36.47	587.22	67.36
F2*	39.943	-91.194	53.88	38.84	576.94	66.16
F3*	38.817	-92.218	56.35	39.61	343.06	67.02
F5*	39.774	-94.907	53.56	37.09	643.02	67.36
F6*	38.591	-92.156	56.45	40.49	359.65	64.77
F7*	38.704	-93.183	55.44	39.56	428.17	64.99

Table 12. Summary of climate data for New AC, AC over AC, and AC over JPCP sections, continued

Calibration Section	Latitude	Longitude	Mean Annual Air Temperature, °F	Mean Annual Precipitation (inch)	Freezing Index (Deg F -Days)	Average Annual Number of Freeze-Thaw Cycles
F8*	36.773	-90.325	59.61	46.80	169.78	48.48
F9*	36.773	-90.325	59.61	46.80	169.78	48.48
G1*	38.591	-92.156	56.45	40.49	359.65	64.77
G2*	38.571	-90.157	56.59	40.86	353.59	59.54
G3*	38.571	-90.157	56.59	40.86	353.59	59.54
LTPP Site 0500 <sup>#</sup>	36.5	-93.125	57.15	46.99	205.32	75.31
LTPP Site 0600 <sup>#</sup>	40	-93.75	52.74	40.76	602.31	92.90
LTPP Site 0800 <sup>#</sup>	37	-93.125	56.64	48.87	271.84	80.31
LTPP Site 0800 <sup>#*</sup>	37.24	-93.39	57.18	43.42	256.56	61.11
LTPP Site 0900 <sup>#</sup>	39	-93.125	54.82	45.67	421.50	86.53
LTPP Section 1002	38.5	-92.5	54.65	43.41	367.41	87.66
LTPP Section 1005	38	-92.5	55.62	47.68	344.74	83.38
LTPP Section 1008	37	-94.375	56.71	44.44	237.48	74.03
LTPP Section 1010 <sup>#</sup>	38	-92.5	55.71	45.51	322.78	83.38
LTPP Section 5403	36	-90	59.59	50.18	118.97	60.88
LTPP Section 5413	36	-90	59.59	50.18	118.97	60.88
LTPP Section 6067	37	-90.625	57.04	49.57	197.62	77.84
LTPP Section A800 <sup>#</sup>	39.5	-91.25	54.11	44.77	520.14	85.09

<sup>#</sup>Multiple calibration projects at site

\*Rigid pavement sections, climate data from NAAR

## TRAFFIC DATA

### Traffic Data Sources

The MoDOT Traffic/Collection unit is responsible for installation of weigh-in motion sites, traffic data collection, processing, and reporting. Historical traffic records, in weight data format, from 18 installation sites for a 3-year period, 2015, 2016 and 2017 was obtained from MoDOT for this study. The objective of the traffic data analysis was to assemble traffic inputs for the calibration projects, and to also create traffic libraries. Figure 8 and Table 13 present the geographic location, including route, milepost, geo-coordinates, and county, of MoDOT WIM installation sites. Table 14 identifies the lane and direction of travel associated with each WIM site.

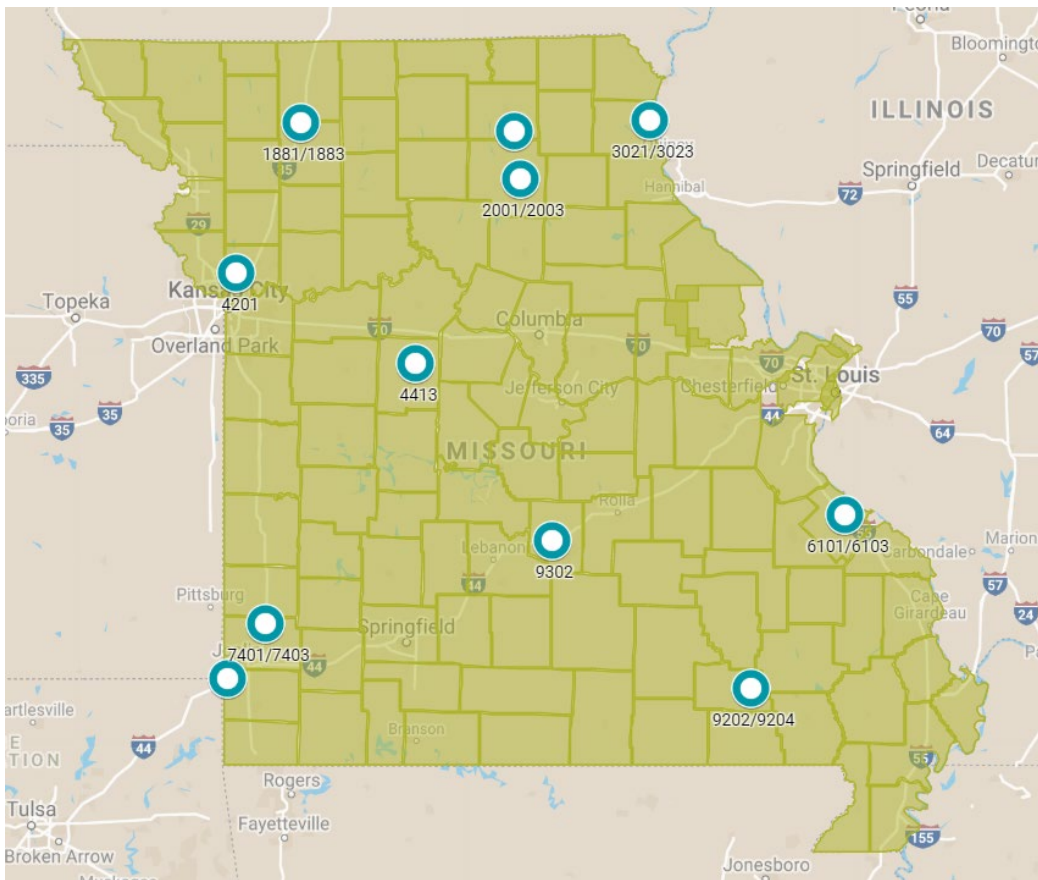


Figure 8. Location of WIM sites (Google, n.d.)

Table 13. Description of MoDOT WIM sites selected for traffic analysis

Station ID	Site Number	Route	Location	Direction	District	County	Log	Latitude	Longitude
1881	031-000188-1	IS 35	2.0 miles N/O RT B	North	Northwest	Daviess	82.734	40.131	-94.0506
1883	031-000188-3	IS 35	2.0 miles N/O RT B	South	Northwest	Daviess	31.694	40.13102	-94.051
2001	061-000200-1	US 63	0.9 miles N/O RT DD	North	Northeast	Macon	280.539	39.81555	-92.473
2003	061-000200-3	US 63	0.9 miles N/O RT DD	South	Northeast	Macon	57.205	39.81559	-92.4733
2021	0000202-1	US 63	1.4 miles S/O RT KK	North	Northeast	Adair	299.452	40.08044	-92.5119
2023	0000202-3	US 63	1.4 miles S/O RT KK	South	Northeast	Adair	38.3	40.08035	-92.5121
3021	056-000302-1	US 61	0.4 miles N/O MO 16	North	Northeast	Lewis	368.003	40.14084	-91.5393
3023	056-000302-3	US 61	0.4 miles N/O MO 16	South	Northeast	Lewis	25.002	40.14087	-91.5396
4201	024-000420-1	IS 435	0.1 miles N/O 108TH ST	North	Kansas City	Clay	29.428	39.28989	-94.51
4413	080-000441-3	US 65	3.0 miles N/O RTS H-HH	South	Kansas City	Pettis	143.441	38.78598	-93.2255
6101	095-000610-1	IS 55	0.3 miles N/O MO 32	North	Southeast	Ste. Genevieve	150.751	37.93947	-90.1274
6103	095-000610-3	IS 55	55 0.3 miles N/O MO 32	South	Southeast	Ste. Genevieve	59.113	37.93924	-90.1276
7401	049-000740-1	IS 49	US 71 1.6 miles S/O RTS H-K	North	Southwest	Jasper	59.719	37.32028	-94.3021
7403	049-000740-3	IS 49	US 71 1.6 miles S/O RTS H-K	South	Southwest	Jasper	119.002	37.3203	-94.3024
7602	073-000760-2	IS 44	0.3 miles W/O weight scales	East	Southwest	Newton	2.406	37.00472	-94.5759
9202	018-000920-2	US 60	0.5 miles W/O MO 21 S JCT	East	Southeast	Carter	240.38	36.93937	-90.8179
9204	018-000920-4	US 60	0.5 miles W/O MO 21 S JCT	West	Southeast	Carter	100.419	36.93954	-90.8177
9302	085-000930-2	IS 44	1.5 miles W/O RT H	East	Central	Pulaski	154.93	37.79219	-92.2435

Table 14. Lane and travel direction of WIM sites

Station	Route	Direction	Lane 1	Lane 2	ID
1881	IS-35 N	North	X		1881_1_1
1883	IS-35 S	South	X		1883_5_1
2001	US-63 N	North	X	X	2001_1_1, 2001_1_2
2003	US-63 S	South	X	X	2003_5_1, 2003_5_2
2021	US-63 N	North	X	X	2021_1_1, 2021_1_2
2023	US-63 S	South	X	X	2023_5_1, 2023_5_2
3021	US-61 N	North	X		3021_1_1
3023	US-61 S	South	X		3023_5_1
4201	IS-435 N	North	X		4201_1_1
6101	IS-55 N	North	X		6101_1_1
6103	IS-55 S	South	X		6103_5_1
7401	IS-49 N	North	X		7401_1_1
7403	IS-49 S	South	X		7403_5_1
9202	US-60 E	East	X		9202_3_1
9204	US-60 W	West	X		9204_7_1
9302	IS-44 E	West	X		9302_3_1
4413	US-65 S	South	X		4413_5_1
7602	IS-44 E	East	X		7602_3_1

### Traffic Data Analysis Approach

WIM data files, in weight data format, were processed and analyzed to develop traffic inputs for the AASHTOWare Pavement ME software. The truck weight records were first processed to convert text strings to useable fields in accordance with the FHWA Traffic Monitoring Guide. The historical weight records were then analyzed to develop the following site-specific traffic inputs for the Pavement ME software:

- Vehicle Class Distribution
- Number of Axles Per Truck
- Monthly Adjustment Factors
- Axle Load Distribution Profiles

The traffic inputs were then further analyzed to evaluate the following:

- Conformance with generally accepted trends
- Presence of data clusters
- Outliers and errors in the overall trends
- Comparison of Missouri specific traffic inputs with Level 3 national defaults

## Traffic Data Availability and Quality

The WIM data was available for 3 years: 2015 through 2017. In order to develop statistically robust site-specific values, the adequacy of available data was evaluated. Table 15 summarizes the data availability, in terms of the number of days and percent days, for each site over the 3-year period. Only Site 2021 (US 63 NB in Adair County) had nearly complete raw data. Site 1883 (I-35 SB in Daviess County) had less than 6 months of data over the 3-year period. The remaining sites had raw data for about 40 to 70 percent of the days. Some sites, including Site 1881 (I-35 NB in Daviess County), Sites 3021 and 3023 (US 61 NB and SB in Lewis County) had almost no data collected in 2017, while Site 4413 (US 65 in Pettis County) had raw data collected for only a single month in 2015. Table 16 summarizes the number of months in the 3-year period for which raw data is available for more than 21 days with a breakdown by year. The table also presents supplemental information on the number of months with no data as well as those with 20 days of data or less.

Table 15. Data availability of WIM sites for years 2015-2017

Site	Direction	Lane	Data Availability (Number of Days in a Year)			Percent Availability over a 3-year Period (1096 days)
			2015	2016	2017	
1881	1	1	273	143	8	39
1883	5	1	168	14	9	17
2001	1	1	226	178	165	52
2001	1	2	232	186	165	53
2003	5	1	180	146	165	45
2003	5	2	180	146	165	45
2021	1	1	331	331	364	94
2021	1	2	331	331	364	94
2023	5	1	185	102	130	38
2023	5	2	185	103	130	38
3021	1	1	264	181	0	41
3023	5	1	264	168	0	39
4202	1	1	131	153	312	54
4413	5	1	34	304	322	60
6101	1	1	208	301	191	64
6103	5	1	218	301	191	65
7401	1	1	293	122	64	44
7403	5	1	293	122	64	44
7602	3	1	125	196	163	44
9202	3	1	256	251	279	72
9204	7	1	257	251	279	72
9302	3	1	268	278	309	78

Table 16. Monthly breakdown of available data

Site	Direction	Lane	Number of Months (Over a 3-year Period) with data:			Number of Months with More than 21 Days of Data		
			≥ 21 days	< 21 days	No data	2015	2016	2017
1881	1	1	13	6	17	9	4	0
1883	5	1	5	5	26	5	0	0
2001	1	1	17	9	10	6	5	6
2001	1	2	18	9	9	7	5	6
2003	5	1	16	4	16	6	4	6
2003	5	2	16	3	17	6	4	6
2021	1	1	34	0	2	11	11	12
2021	1	2	34	0	2	11	11	12
2023	5	1	12	8	16	5	4	3
2023	5	2	12	8	16	5	4	3
3021	1	1	15	3	18	8	7	0
3023	5	1	13	5	18	8	5	0
4202	1	1	19	6	11	3	5	11
4413	5	1	23	2	11	1	11	11
6101	1	1	22	11	3	7	11	4
6103	5	1	22	11	3	7	11	4
7401	1	1	15	5	16	9	4	2
7403	5	1	15	5	16	9	4	2
7602	3	1	14	10	12	3	7	4
9202	3	1	24	9	3	7	8	9
9204	7	1	24	9	3	7	8	9
9302	3	1	29	5	2	8	10	11

This information was critical to ascertain whether reliable monthly adjustment factors can be developed. It was observed, as shown in Table 16, that none of the sites had adequate data (more than 21 days in a month) to represent each of the twelve months in a calendar year. While most sites had partial year data, Site 2021, which had data for 94 percent of the days, had missing data in December for years 2015 and 2016. Therefore, the available data were not considered as adequate for reliable monthly adjust factors. Default values were used for this input category.

### Traffic Data Processing

The weigh-in motion data files were processed to develop default traffic inputs for the AASHTOWare Pavement ME. Truck weight records were first processed to convert text strings into useable fields in accordance with the FHWA Traffic Monitoring Guide (TMG). The historical weight records were then analyzed to develop the following site-specific traffic inputs for the Pavement ME software: Vehicle Class Distribution, Number of Axles Per Truck, Monthly Adjustment Factors, and Axle Load Distribution profiles. The traffic inputs were then further analyzed to evaluate conformance with generally accepted trends, presence of data

clusters, outliers and errors in the overall trends, and comparison of Missouri specific traffic inputs with Level 3 national defaults.

### Vehicle Class Distribution

WIM data was processed individually for each site. The weight data were analyzed to compute the distribution of trucks at each WIM site. Table 17 summarizes the distribution truck classes, as standardized by FHWA Vehicle Classes 4 through 13, for each WIM site by direction and lane of travel.

Table 17. Site-specific distribution of truck classes

WIM Station			Vehicle/Truck Class Distribution (percent)									
Station ID	Direction	Lane	VC 4	VC 5	VC 6	VC 7	VC 8	VC 9	VC 10	VC 11	VC 12	VC 13
1881	1	1	1.7	5.0	5.3	0.0	5.6	75.6	0.5	4.7	1.5	0.1
1883	5	1	2.1	7.5	3.1	0.0	5.7	75.4	0.6	4.1	1.4	0.1
2001	1	1	3.3	36.7	7.6	0.2	11.8	38.8	0.9	0.6	0.0	0.1
2001	1	2	3.1	21.5	6.9	0.2	9.3	56.5	0.7	1.5	0.1	0.2
2003	5	1	3.4	36.4	6.2	0.3	9.0	43.0	0.5	1.1	0.0	0.1
2003	5	2	4.1	27.0	6.6	0.3	10.6	49.6	0.6	1.1	0.0	0.1
2021	1	1	5.0	34.6	5.0	0.2	10.8	43.3	0.5	0.4	0.0	0.2
2021	1	2	2.9	18.8	6.4	0.2	8.7	60.5	0.6	1.7	0.0	0.2
2023	5	1	2.3	34.4	4.5	0.3	6.1	51.6	0.3	0.4	0.0	0.1
2023	5	2	2.8	39.8	4.4	0.3	7.7	43.5	0.4	1.0	0.0	0.1
3021	1	1	0.8	4.5	2.6	0.1	3.6	85.5	0.7	1.8	0.3	0.1
3023	5	1	1.1	5.0	2.1	0.1	3.6	85.2	0.6	1.8	0.4	0.1
4201	1	1	2.4	10.8	5.6	0.4	6.3	71.0	0.8	0.7	1.8	0.2
4413	5	1	4.3	20.8	12.8	0.1	7.7	52.8	0.7	0.5	0.1	0.2
6101	1	1	2.4	7.2	2.4	0.1	5.0	78.0	0.6	2.9	1.2	0.2
6103	5	1	2.4	7.0	4.7	0.1	5.6	75.5	0.6	2.7	1.2	0.2
7401	1	1	1.9	7.4	2.9	0.1	6.1	77.4	0.9	2.4	0.7	0.2
7403	5	1	1.6	6.6	4.3	0.2	7.0	75.4	1.9	2.3	0.6	0.1
7602	3	1	3.5	5.6	1.3	0.0	4.0	79.9	0.3	3.3	2.0	0.1
9202	3	1	2.5	11.8	5.1	0.8	8.3	69.2	0.6	1.4	0.2	0.1
9204	7	1	2.5	12.6	5.4	0.4	8.0	68.3	0.7	1.4	0.4	0.3
9302	3	1	2.0	6.4	1.5	0.1	3.5	80.3	0.4	3.8	1.9	0.1

Figure 9 presents the distribution by vehicle type, namely, buses, single unit trucks, single trailer trucks, and multi-trailer sites. More than half the sites appear to be on single trailer routes with predominantly Class 9 trucks, while the roadways at the remaining sites appears to carry a mix of single-trailer and single-unit trucks, predominantly of Class 9 and Class 5 types. The proportions of buses and multi-trailer trucks average around 2.6 percent statewide, and generally, less than 6.5 percent at individual sites.

### Site Specific Vehicle Class Distribution

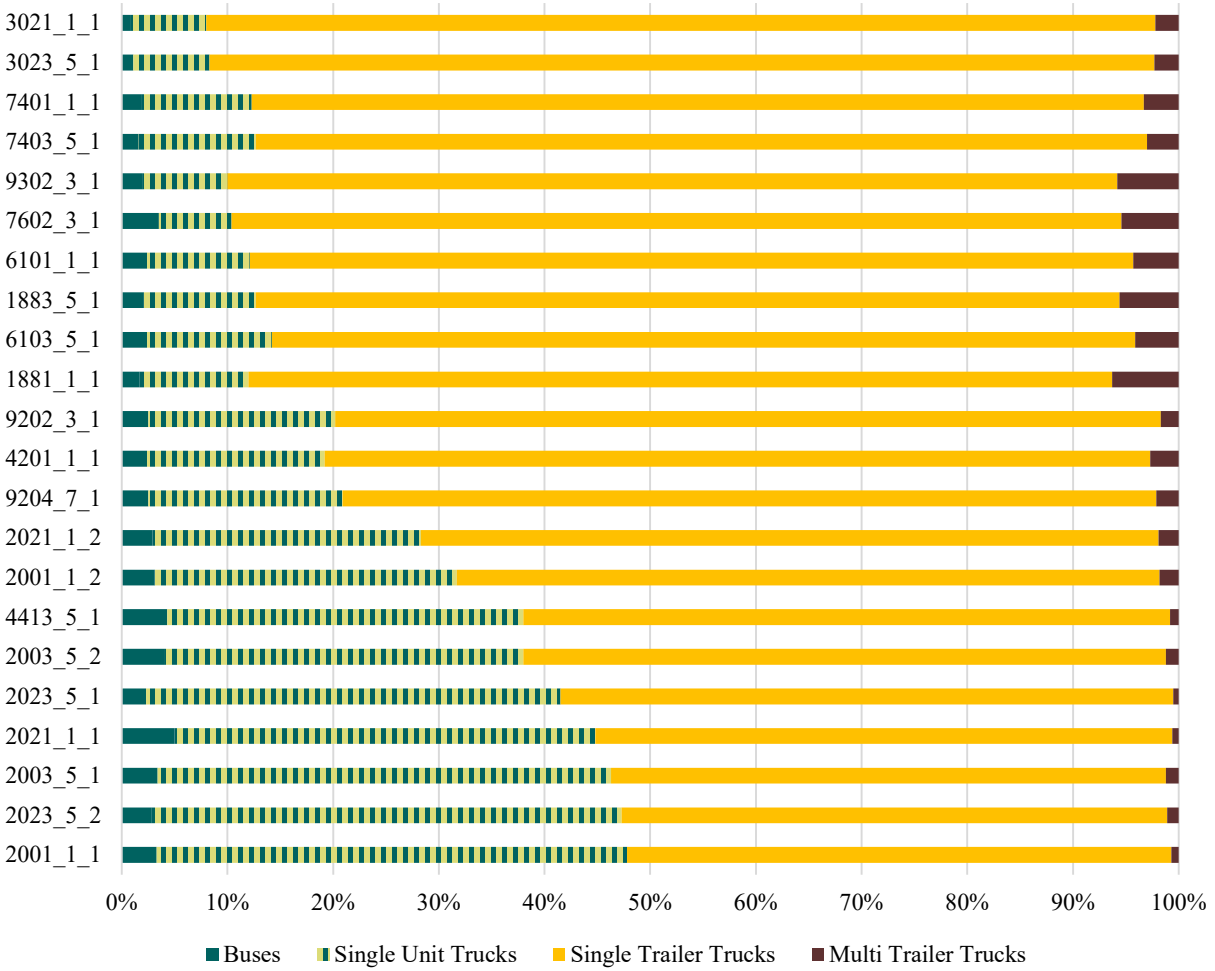


Figure 9. Summary of truck class distribution by truck type

Since the AASHTOWare Pavement ME software allows both user-input truck distributions as well as the option to select national defaults from 17 groups of truck traffic classifications (TTC), site-specific truck distributions were compared with TTC groups. Table 18 presents the percentage of each truck type expected in each TTC group.

Table 18. Truck traffic classification (TTC) group description

TTC Group	TTC Description	Vehicle/Truck Class Distribution (percent)									
		VC 4	VC 5	VC 6	VC 7	VC 8	VC 9	VC 10	VC 11	VC 12	VC 13
1	Major single-trailer truck route (type I)	1.3	8.5	2.8	0.3	7.6	74	1.2	3.4	0.6	0.3
2	Major single-trailer truck route (Type II)	2.4	14.1	4.5	0.7	7.9	66.3	1.4	2.2	0.3	0.2
3	Major single- and multi- trailer truck route (Type I)	0.9	11.6	3.6	0.2	6.7	62	4.8	2.6	1.4	6.2
4	Major single-trailer truck route (Type III)	2.4	22.7	5.7	1.4	8.1	55.5	1.7	2.2	0.2	0.4
5	Major single- and multi- trailer truck route (Type II).	0.9	14.2	3.5	0.6	6.9	54	5	2.7	1.2	11
6	Intermediate light and single-trailer truck route (I)	2.8	31	7.3	0.8	9.3	44.8	2.3	1	0.4	0.3
7	Major mixed truck route (Type I)	1	23.8	4.2	0.5	10.2	42.2	5.8	2.6	1.3	8.4
8	Major multi-trailer truck route (Type I)	1.7	19.3	4.6	0.9	6.7	44.8	6	2.6	1.6	11.8
9	Intermediate light and single-trailer truck route (II)	3.3	34	11.7	1.6	9.9	36.2	1	1.8	0.2	0.3
10	Major mixed truck route (Type II)	0.8	30.8	6.9	0.1	7.8	37.5	3.7	1.2	4.5	6.7
11	Major multi-trailer truck route (Type II)	1.8	24.6	7.6	0.5	5	31.3	9.8	0.8	3.3	15.3
12	Intermediate light and single-trailer truck route (III)	3.9	40.8	11.7	1.5	12.2	25	2.7	0.6	0.3	1.3
13	Major mixed truck route (Type III)	0.8	33.6	6.2	0.1	7.9	26	10.5	1.4	3.2	10.3
14	Major light truck route (Type I)	2.9	56.9	10.4	3.7	9.2	15.3	0.6	0.3	0.4	0.3
15	Major light truck route (Type II)	1.8	56.5	8.5	1.8	6.2	14.1	5.4	0	0	5.7
16	Major light and multi-trailer truck route	1.3	48.4	10.8	1.9	6.7	13.4	4.3	0.5	0.1	12.6
17	Major bus route	36.2	14.6	13.4	0.5	14.6	17.8	0.5	0.8	0.1	1.5

The comparison of site-specific truck distributions with TTC groups adopted a cluster analysis approach. The Euclidean distance, which calculates the square root of the sum of squares of differences between the vehicle class percentages between site-specific and TTC groups, was used to identify the clusters. The resulting TTC group assignment on a site-by-site basis is summarized in Table 19, and graphically compared in Figure 10, Figure 11, and Figure 12. The recommended TTC groups are listed as follows:

- TTC 1 – Predominantly single-trailer trucks, and low to moderate amount of buses and multi-trailer trucks

- TTC 2 – Predominantly single-trailer trucks, but with a low percentage of single-unit trucks, and low to moderate amount of buses and multi-trailer trucks
- TTC 4 – Predominantly single-trailer trucks with a low to moderate amount of single-unit trucks, and low to moderate amount of buses and multi-trailer trucks
- TTC 6 – Mixed truck traffic with a higher percentage of single-trailer trucks, and low to moderate amount of buses and multi-trailer trucks
- TTC 9 – Mixed truck traffic with about equal percentages of single-unit and single trailer trucks, and low to moderate amount of buses and multi-trailer trucks

Table 19. Recommended TTC groups for WIM sites

WIM Station			Truck Traffic Classes
WIM Station ID	Direction	Lane	
1881	1	1	TTC 1
1883	5	1	TTC 1
2001	1	1	TTC 6 / TTC 9
2001	1	2	TTC 4
2003	5	1	TTC 6
2003	5	2	TTC 6
2021	1	1	TTC 6
2021	1	2	TTC 4
2023	5	1	TTC 6
2023	5	2	TTC 6
3021	1	1	TTC 1
3023	5	1	TTC 1
4201	1	1	TTC 1 / TTC 2
4413	5	1	TTC 4
6101	1	1	TTC 1
6103	5	1	TTC 1
7401	1	1	TTC 1
7403	5	1	TTC 1
7602	3	1	TTC 1
9202	3	1	TTC 2
9204	7	1	TTC 2
9302	3	1	TTC 1

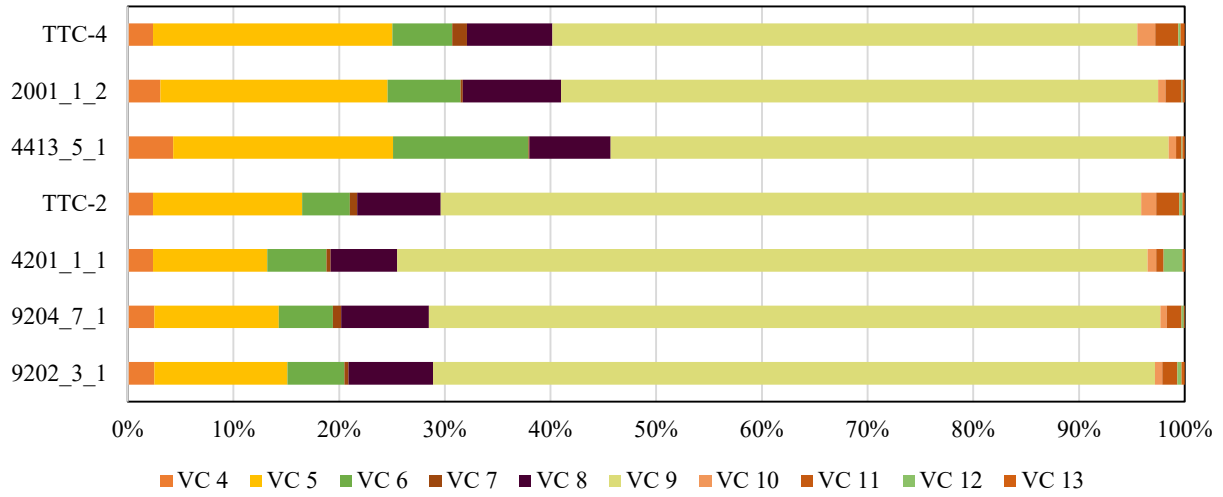


Figure 10. Comparison of site-specific vehicle class distribution with TTC-2 and TTC-4

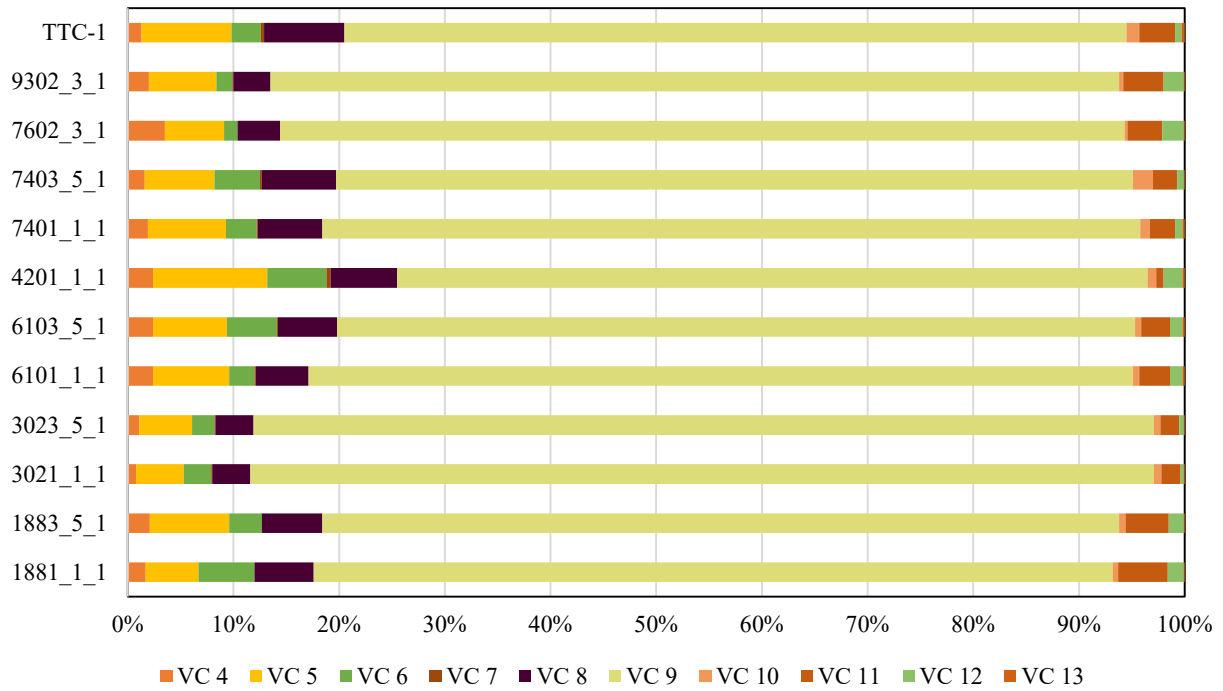


Figure 11. Comparison of site-specific vehicle class distribution with TTC-1

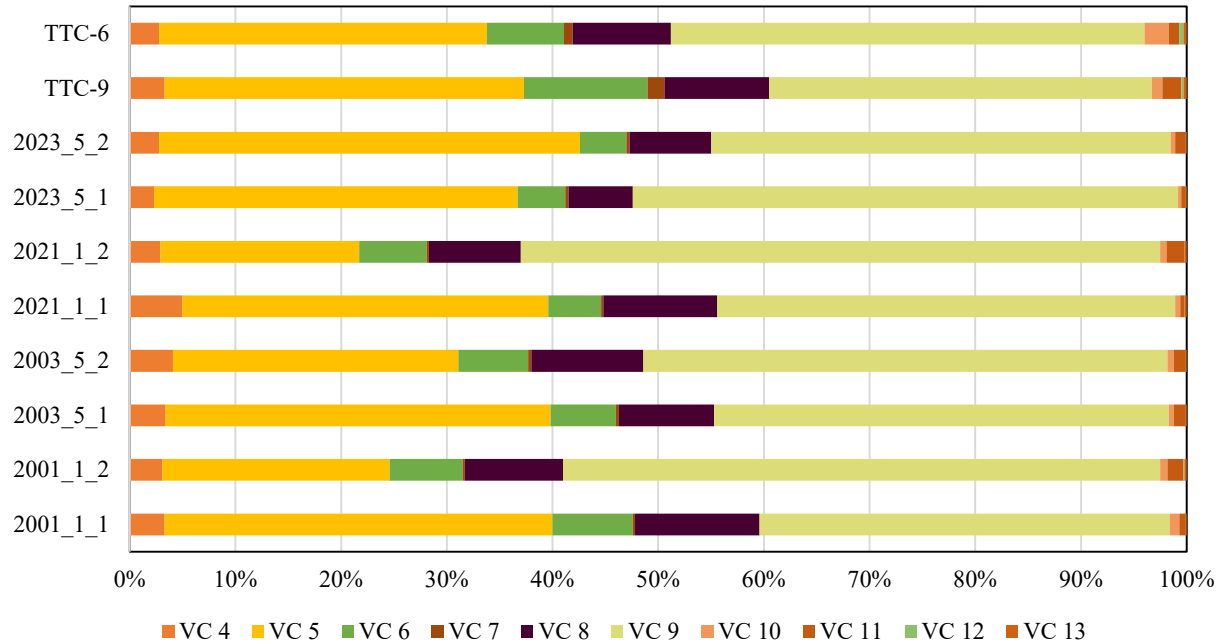


Figure 12. Comparison of site specific vehicle class distribution with TTC-6 and TTC-9

### Number of Axles Per Truck

The axles per truck factor indicate the average number of axles for each axle type (single, tandem, tridem, and quad axles) in each vehicle class. Table 20 presents the nation-wide or Level 3 averages of the number of axles for each vehicle class. The axles per truck values of each WIM site were calculated by grouping axles in traffic records by each axle type (4 axle types) and vehicle class (10 classes) and dividing the total number of axles in each group by the corresponding total number of trucks. The statistical summary of site-specific axles per truck values is presented in Table 21.

Table 20. Nationwide averages for number of axles per truck

Vehicle Class	Single	Tandem	Tridem	Quad	Total Number of Axles
4	1.62	0.39	0.00	0.00	2.4
5	2.00	0.00	0.00	0.00	2.0
6	1.02	0.99	0.00	0.00	3.0
7	1.00	0.26	0.83	0.00	4.01
8	2.38	0.67	0.00	0.00	3.72
9	1.13	1.93	0.00	0.00	4.99
10	1.19	1.09	0.89	0.00	6.04
11	4.29	0.26	0.06	0.00	4.99
12	3.52	1.14	0.06	0.00	5.98
13	2.15	2.13	0.35	0.00	7.46

Table 21. Axles per truck statistics for MoDOT WIM sites

Vehicle Class	Single			Tandem			Tridem			Quad		
	Min	Ave	Max	Min	Ave	Max	Min	Ave	Max	Min	Ave	Max
VC 4	1.63	1.86	1.93	0.09	0.22	0.46	0.00	0.00	0.00	0.00	0.00	0.00
VC 5	2.00	2.00	2.00	0.00	0.00	0.00	0.00	0.00	0.00	0.00	0.00	0.00
VC 6	1.00	1.00	1.00	1.00	1.00	1.00	0.00	0.00	0.00	0.00	0.00	0.00
VC 7	0.99	1.00	1.14	0.00	0.00	0.05	0.92	1.00	1.00	0.00	0.00	0.00
VC 8	2.06	2.25	2.47	0.54	0.75	0.92	0.00	0.00	0.01	0.00	0.00	0.00
VC 9	1.03	1.27	1.41	1.53	1.82	1.90	0.00	0.01	0.02	0.00	0.00	0.02
VC 10	1.04	1.17	1.61	0.92	1.03	1.11	0.71	0.89	0.97	0.00	0.02	0.13
VC 11	5.00	5.00	5.00	0.00	0.00	0.00	0.00	0.00	0.00	0.00	0.00	0.00
VC 12	3.20	3.99	4.00	0.20	0.99	1.00	0.00	0.01	0.80	0.00	0.00	0.00
VC 13	1.00	1.28	2.11	0.24	0.64	2.25	0.00	0.99	1.56	0.09	0.31	0.67

Figure 13 through Figure 17 present the site-specific single, tandem, tridem, quad, and total axles per truck, respectively, for various vehicle classes, their statistical spread among various sites, along with the corresponding national defaults. The following observations can be derived from the data presented:

- The computed axles per truck values were generally consistent among sites, particularly for key truck classes, Class 5 (two-axle, six-tire, single-unit trucks) and Class 9 (five-axle single-trailer trucks). The axles per truck values exhibited high variability among Class 13 (seven or more axle multi-trailer trucks).
- When the computed axles per truck values are compared among various sites, the number of single and tandem axles generally exhibited a high level of consistency. The number of single axles of Class 10 (six or more axle single-trailer trucks) and Class 13 (seven or more axle multi-trailer trucks) exhibited variability among various sites. Similar variations were observed Class 4 (buses) and Class 8 (four or fewer axle single-trailer trucks). Vehicle Class 7 (four or more axle single-unit trucks) and Class 10 (six or more axle single-trailer trucks) had almost the same number of tridem axles with very little variability. Quad axles appeared to be prevalent only among Class 10 (six or more axle single-trailer trucks) and Class 13 (seven or more axle multi-trailer trucks).
- Missouri-specific values were in good agreement with national defaults for all truck classes except for multi-trailer trucks.

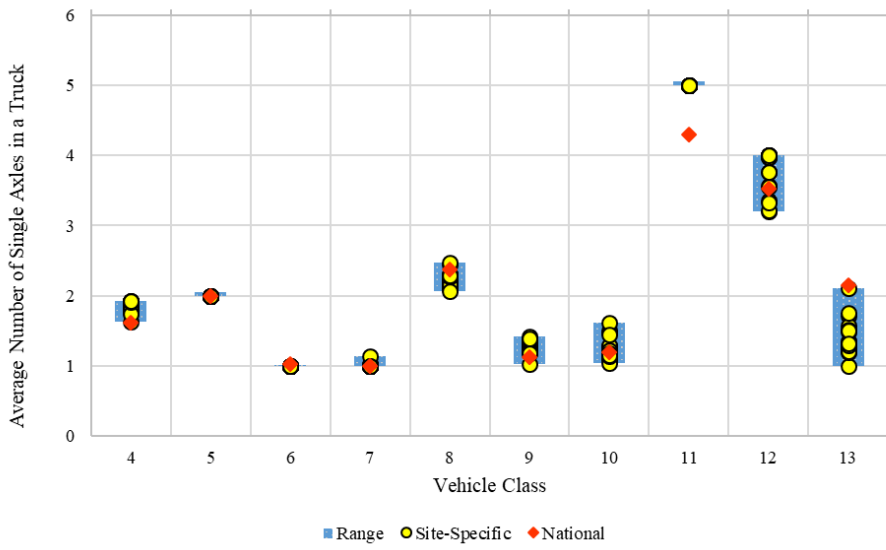


Figure 13. Summary of number of single axles per truck

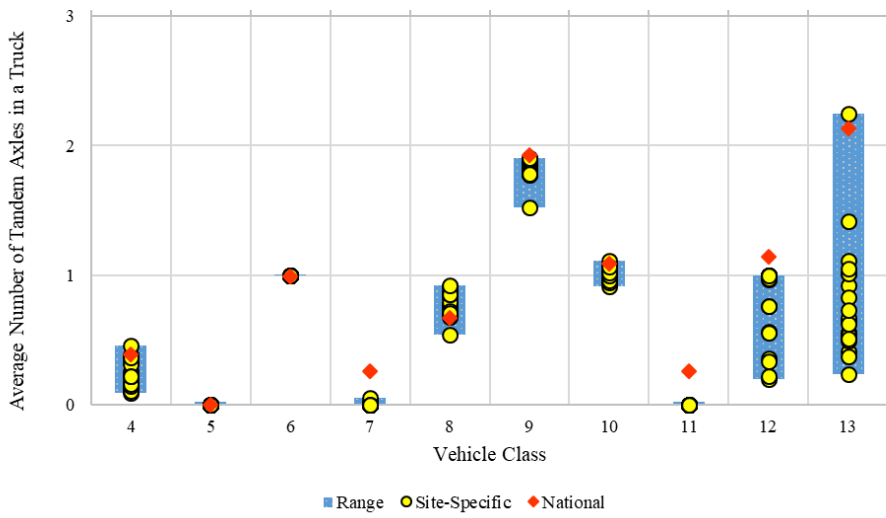


Figure 14. Summary of number of tandem axles per truck

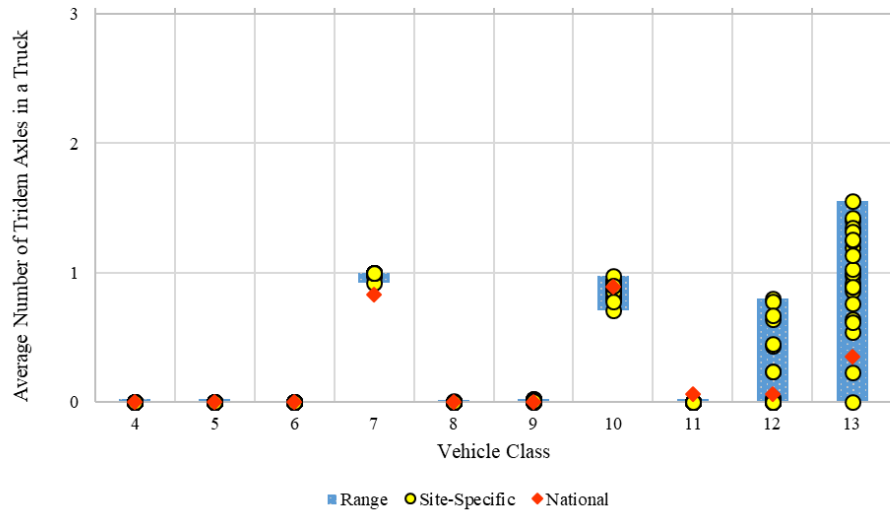


Figure 15. Summary of number of tridem axles per truck

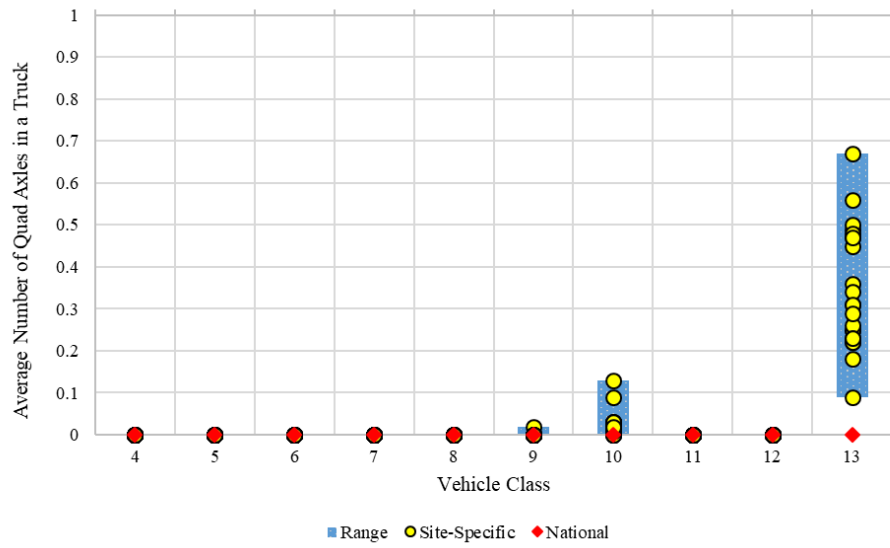


Figure 16. Summary of number of quad axles per truck

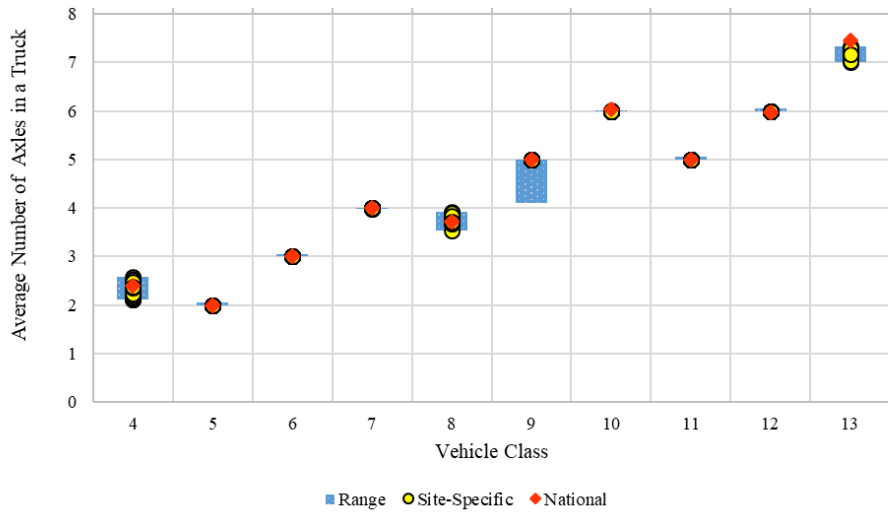


Figure 17. Summary of total number of axles per truck

### Monthly Adjustment Factors

As discussed earlier (see Table 13 and Table 14), none of the sites had adequate data to represent all twelve months of a year. In addition, some sites had data with unusual volume across different months of a year. Figure 18 presents an example with Site 1881, where the volume of Class 9 trucks in May 2015 was approximately one-half of those of preceding and succeeding months. Given these observations, computing reliable monthly adjustment factors was considered infeasible.

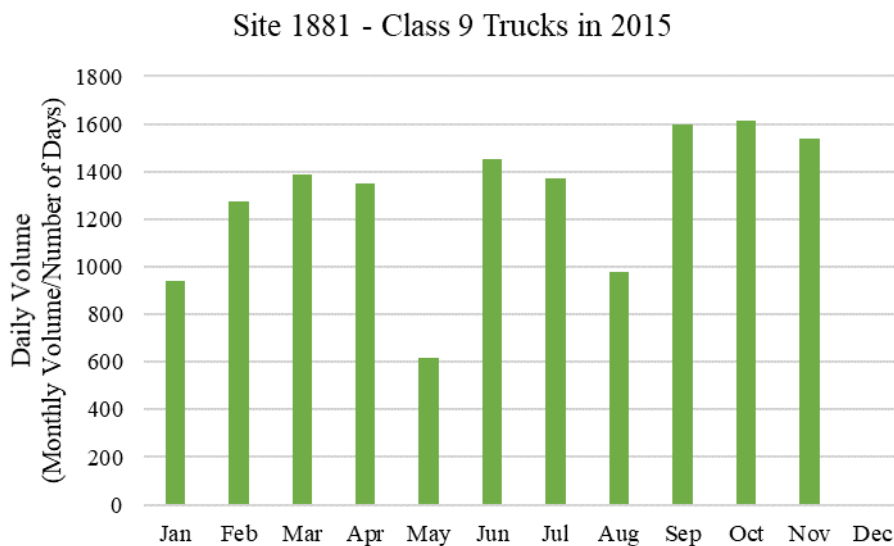


Figure 18. Month to month variation in the number of Class 9 trucks at Site 1881 in 2015

## Axle Load Distribution

The site-specific axle load distribution factors were computed for each site using weight files. Further analysis was performed to compare how well the site-specific axle load distributions compared with the Level 3 national defaults. The comparison focused on the following aspects of axle load distributions:

- General shape of the distribution, i.e., unimodal or bimodal
- 50<sup>th</sup> Percentile weight of the distribution, which is computed by multiplying the percentage of the total axle applications within each load bin by the corresponding load upon consideration of site-specific vehicle class distribution and axles per truck factors.
- Percent axles that are heavier than legal load
  - Single axles > 20,000 lb.
  - Tandem axles > 46,000 lb.

Single and tandem axles of Class 5 and Class 9 trucks were selected for comparison purposes. Note that Class 5 and Class 9 trucks constitute about 80 percent of the truck distribution.

### *Single Axle of Class 5 Trucks*

Figure 19 compares the relative difference of site-specific 50<sup>th</sup> percentile weight of single axles of Class 5 trucks with that of the Level 3 national defaults. In general, the weights of single axles of Class 5 trucks were lighter than the Level 3 defaults. Site 3021 was an exception. Class 5 trucks at this location, whose axle load distribution is shown in Figure 20, were about 5 percent heavier than the national defaults.

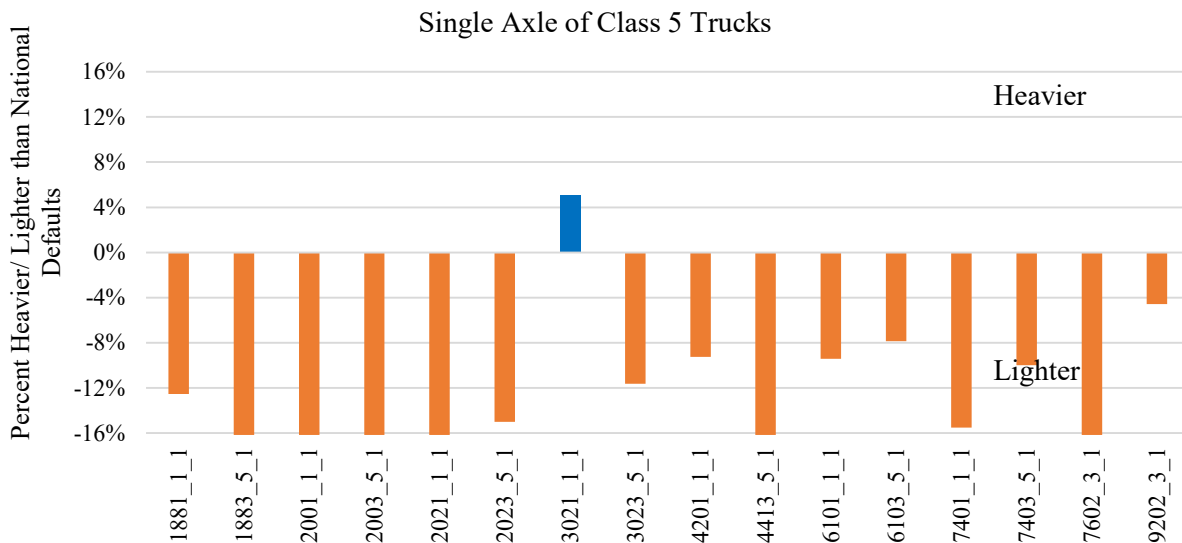


Figure 19. Comparison of 50th percentile weight of single axles of Class 5 trucks

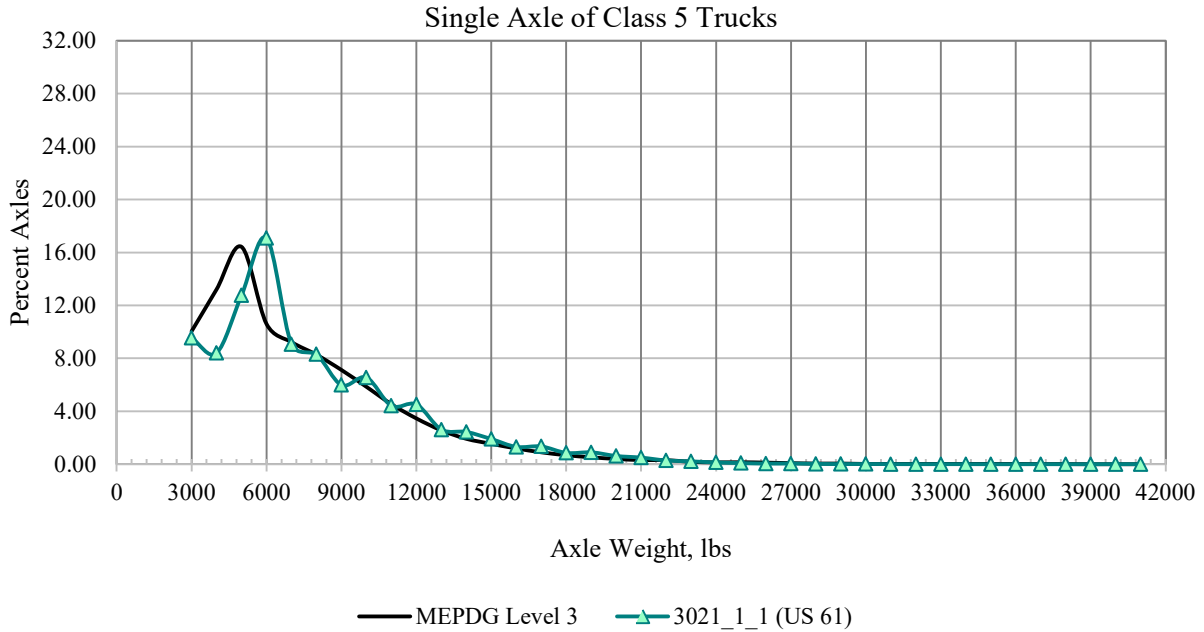


Figure 20. Load distribution of Class 5 single axles at Site 3021 (US 61 in Lewis County)

Figure 21 presents the single axle load profiles of Class 5 trucks measured at various MoDOT sites. The overall shape of these load profiles generally agreed with that of the Level 3 defaults.

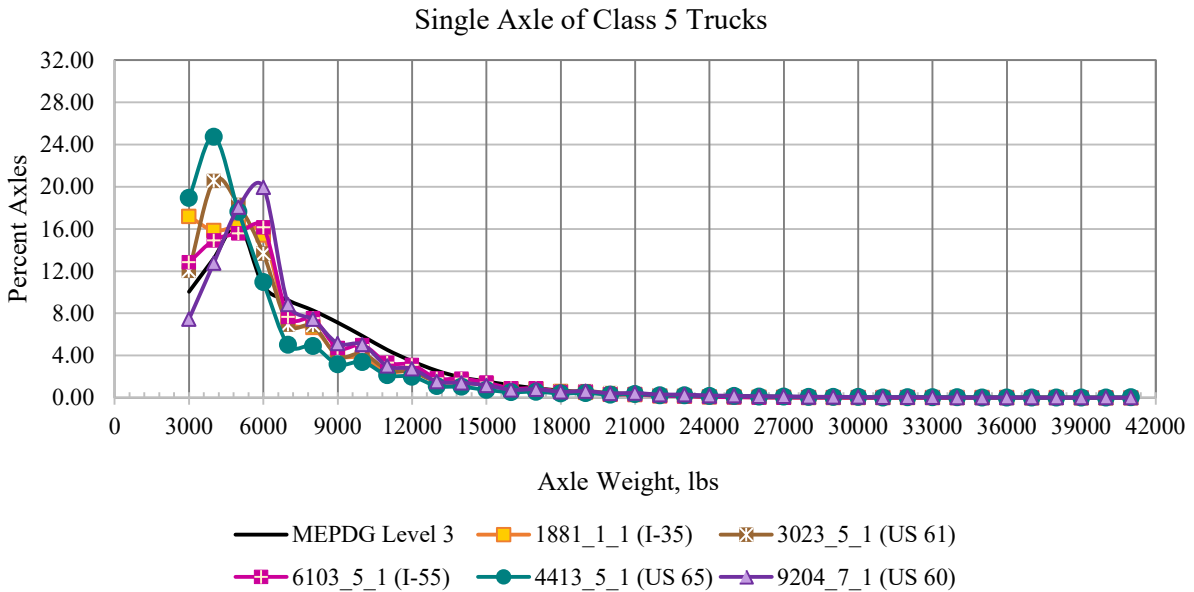


Figure 21. Load distribution of single axles of Class 5 trucks

Figure 22 presents the axle load profiles of Class 5 trucks at Sites 2001 and 2003. Site 2001 (US 63 NB in Macon County) seemed to carry 40 percent of the single axles that were lighter than 3,500 lb., while the load distribution of Class 5 trucks on the other direction (Site 2003, US 63 SB), somewhat appeared to agree with the general shape of the load profile.

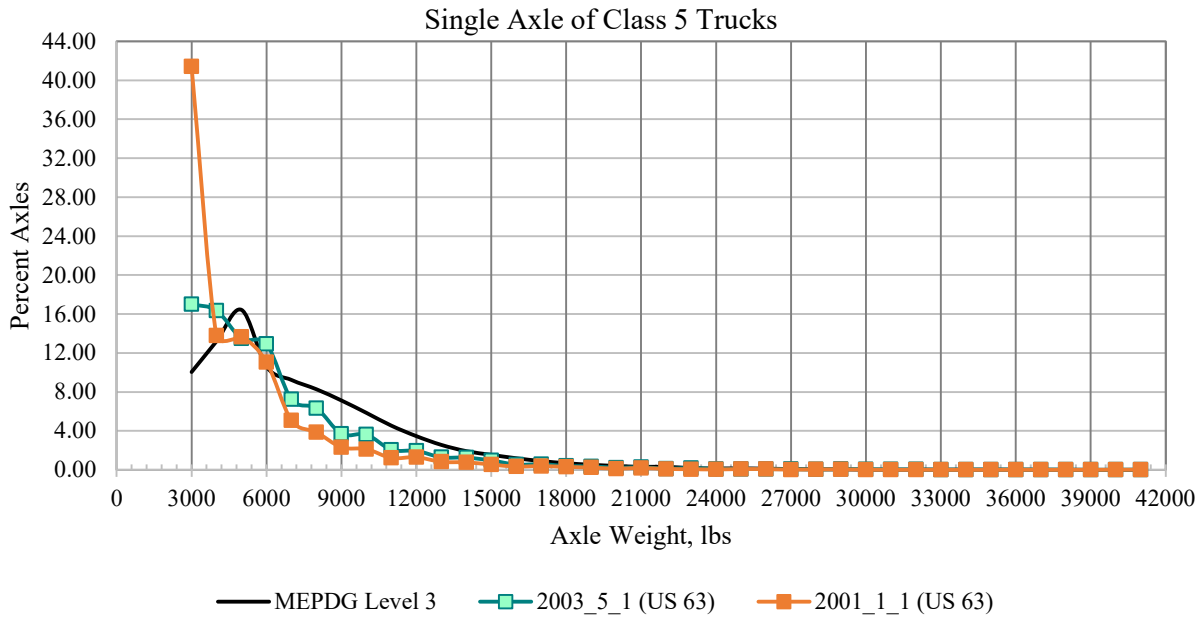


Figure 22. Load distribution of single axles of Class 5 trucks at Sites 2001 and 2003 (US 63 in Macon County)

The proportion of single axles of Class 5 trucks heavier than 20,000 lb. was computed for each WIM site. Threshold values of 20,000 and 46,000 lb. were selected for single and tandem axles, respectively, based on the maximum allowable load that Missouri allows for trucks under regular operations. Figure 23 presents the percent of single axles of Class 5 trucks that were heavier than the 20,000-lb threshold. Heavier single axles were generally fewer, generally less than 1.5 percent, at most MoDOT sites. Site 4413 (US 65 in Pettis County) and Site 9204 (US 60 WB in Carter County) had slightly heavier axles. In summary, Class 5 trucks in MoDOT WIM sites were generally lighter than the Level 3 defaults.

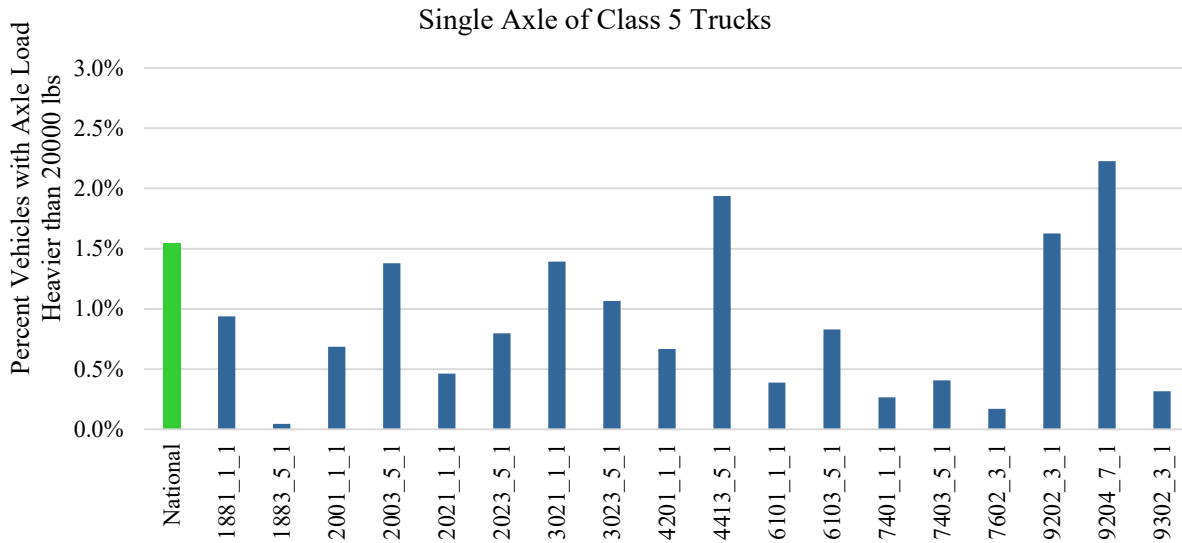


Figure 23. Percent single axles of Class 5 trucks with loads heavier than 20,000 lb.

### *Single Axle of Class 9 Trucks*

Figure 24 compares the relative difference of site-specific 50<sup>th</sup> percentile weight of single axles of Class 9 trucks with that of the Level 3 defaults. On an average, single axles of Class 9 trucks were about 6 to 9 percent heavier than the Level 3 defaults. Sites 2001 and 2003 (US 63 in Macon County) were an exception. Figure 25 and Figure 26 present the load distribution profile of single axles of Class 9 trucks at various sites. The overall shape of the axle load profiles at various sites generally agreed with the unimodal distribution of a typical single axle of Class 9 trucks.

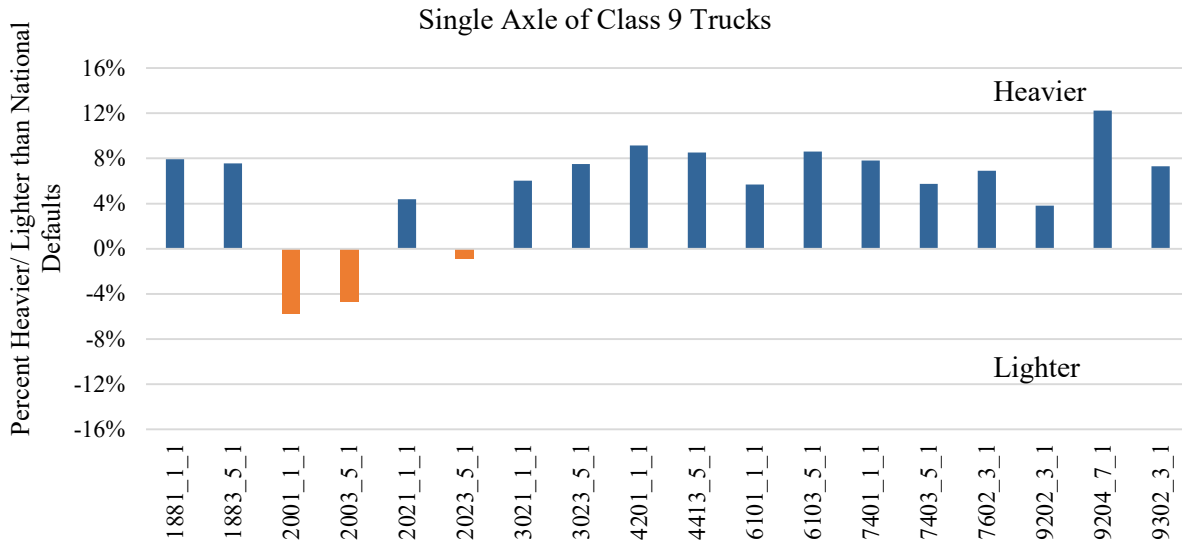


Figure 24. Comparison of 50<sup>th</sup> percentile weight of single axles of Class 9 trucks

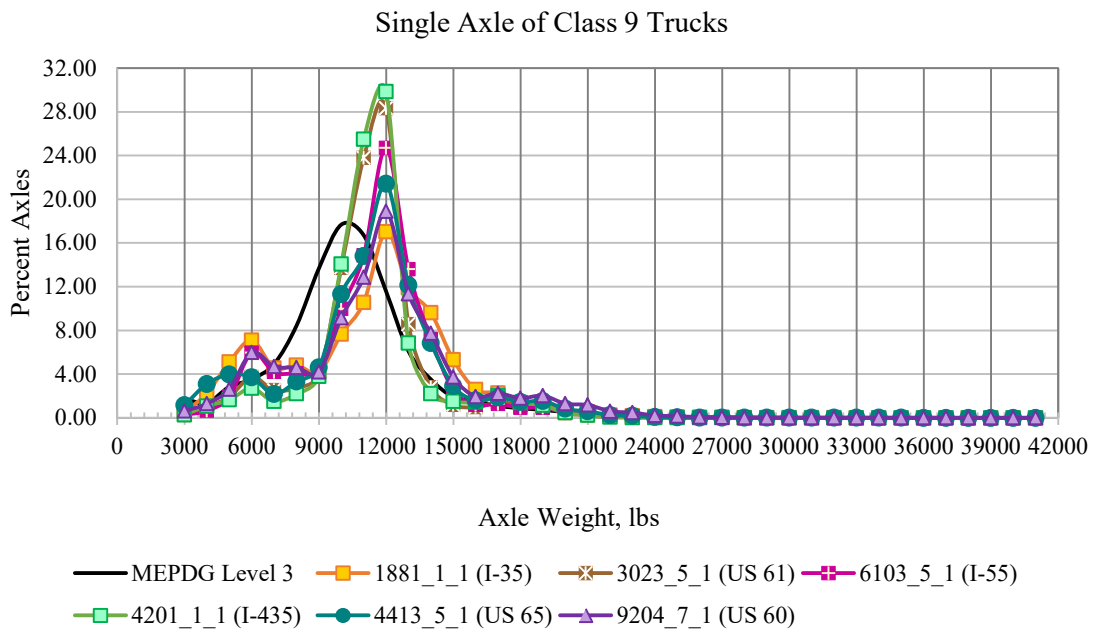


Figure 25. Load distribution of single axles of Class 9 trucks

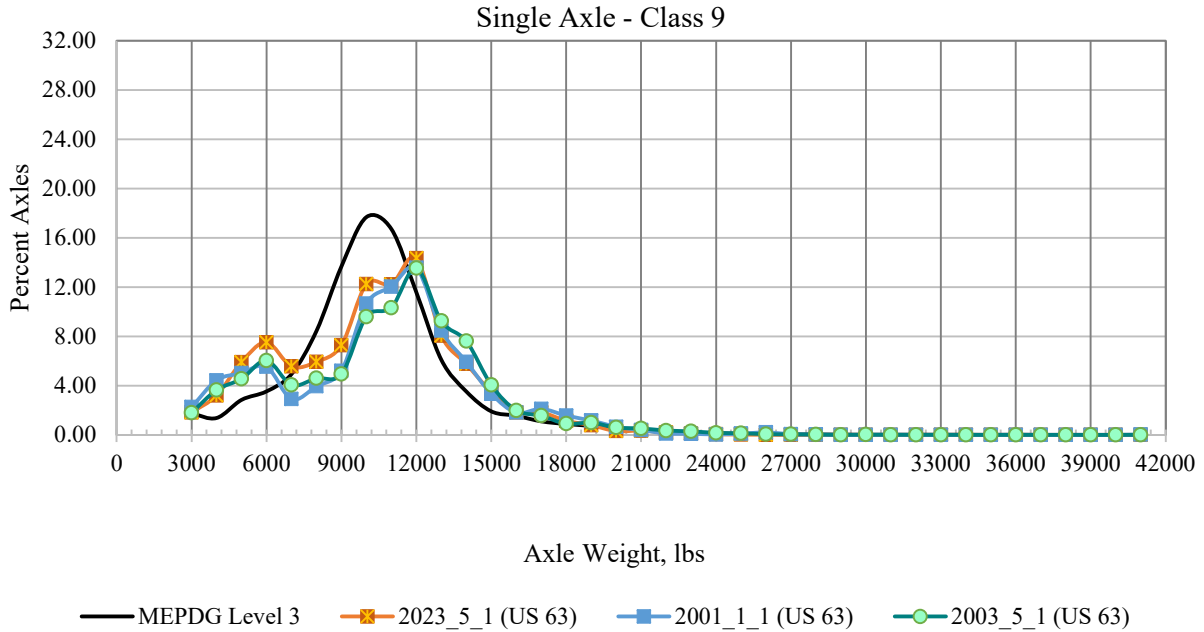


Figure 26. Load distribution of single axles of Class 9 trucks

Figure 27 presents the percent of single axles of Class 9 trucks that were heavier than the 20,000-lb threshold. Heavier single axles of Class 9 trucks at MoDOT sites varied within 1 percent at most sites, and hence, are not considered a significant deviation from the Level 3 defaults.

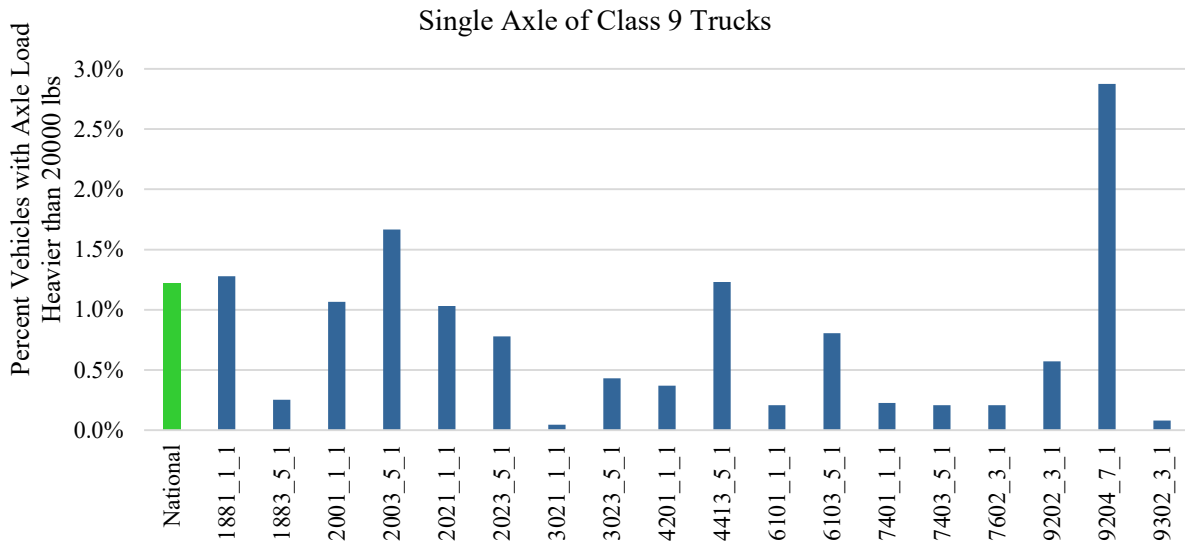


Figure 27. Percent single axles of Class 9 trucks with loads heavier than 20,000 lb.

### Tandem Axle of Class 9 Trucks

Figure 28 compares the relative difference of site-specific 50<sup>th</sup> percentile weight of tandem axles of Class 9 trucks with that of the Level 3 national defaults. The figure indicates a mixed trend with site specific weights on both heavier and lighter side of the Level 3 defaults, and in some cases, their differences exceeded 10 percent.

Figure 29 and Figure 30 present the load distribution profiles of tandem axles of Class 9 trucks. The bimodal load profile shape of tandem axles at various MoDOT site agrees with the front-rear pattern of a Class 9 truck tandem axle. Figure 31 presents the percent axles of Class 9 trucks that were heavier than the 46,000-lb threshold for tandem axles. Heavier tandem axles were generally less than one-half percent of total axles, albeit with some exceptions. Site 2001 and Site 2003 (US 63 in Macon County), whose single axles of Class 5 and Class 9 trucks were on the lighter side of Level 3 defaults, exhibited a different pattern. In comparison with other MoDOT sites, Sites 2001 and Site 2003 appeared to carry proportionately higher percent of heavier tandem axles of Class 9 trucks.

Appendix A contains the axles per truck by site calculated from all WIM data for MoDOT. The data are summarized in Table A - 1.

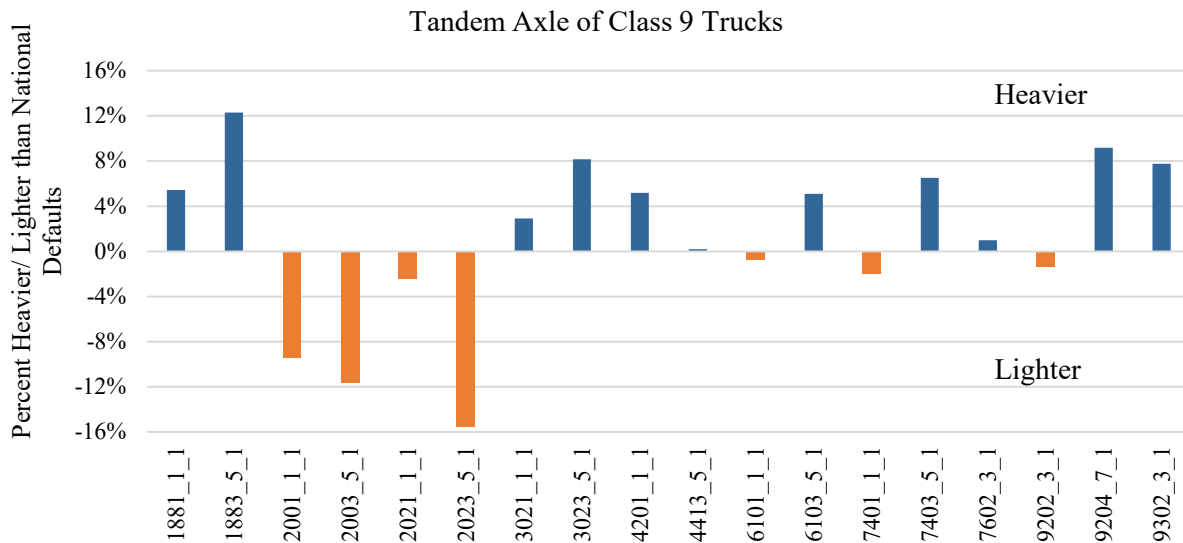


Figure 28. Comparison of 50<sup>th</sup> percentile weight of tandem axles of Class 9 trucks

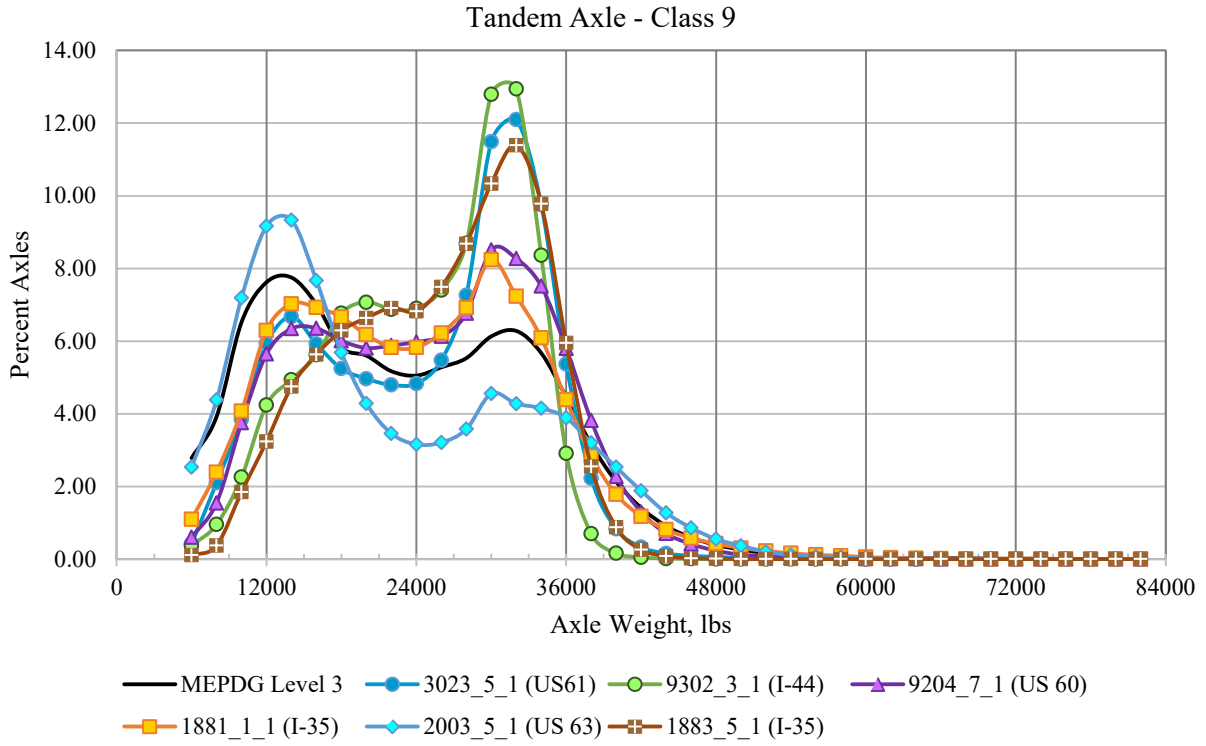


Figure 29. Load distribution of tandem axles of Class 9 trucks

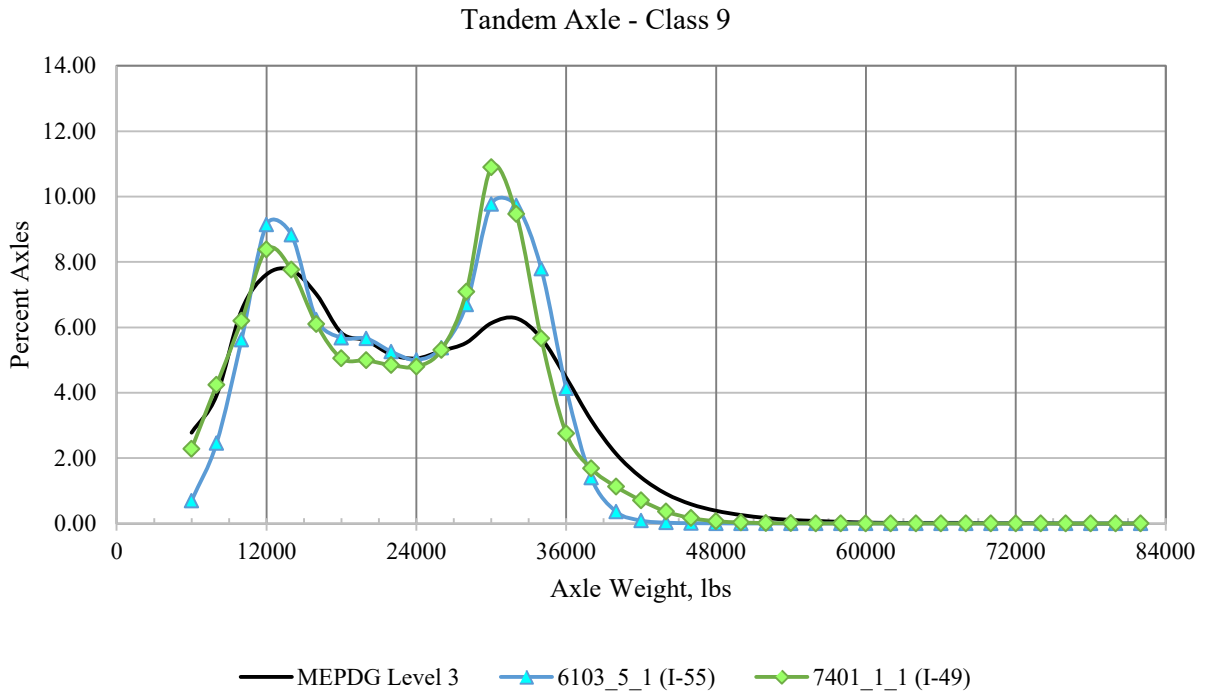


Figure 30. Load distribution of tandem axles of Class 9 trucks

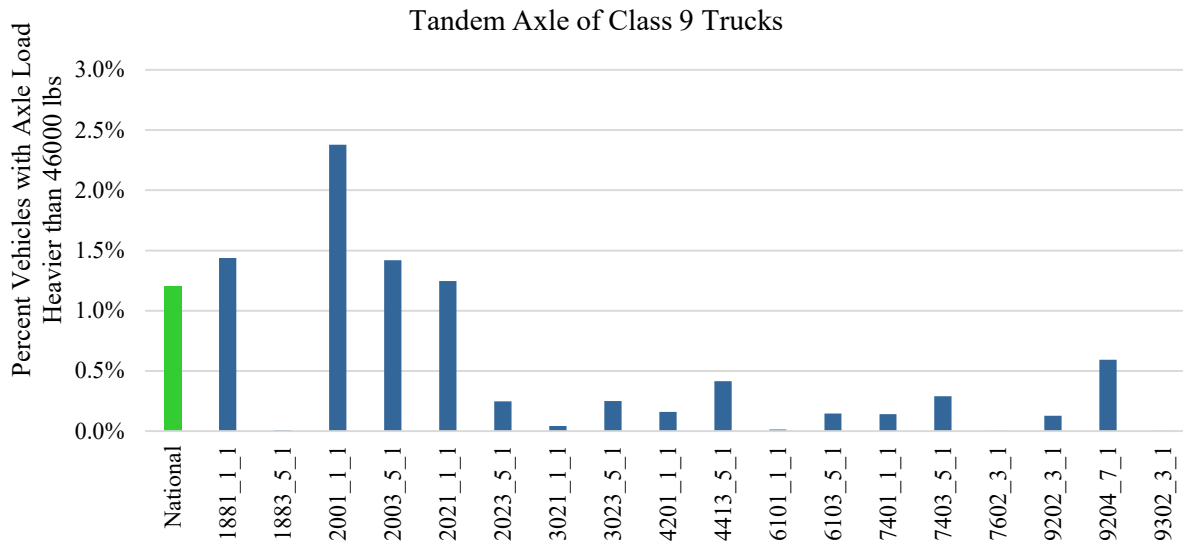


Figure 31. Percent single axles of Class 9 trucks with loads heavier than 46,000 lb.

### Traffic Inputs Assembled for Calibration

Missouri specific default traffic inputs for the AASHTO Pavement ME Design tool were developed based on the analysis of raw WIM traffic data described in the previous sections. WIM sites were assigned to the PMS projects selected for calibration based on location on the specific highway, proximity of the project to the WIM site, and the likelihood of traffic patterns changing between project location and the WIM site. In cases where WIM data were not available, default TTCs were used based on the functional class and traffic volume.

For all the calibration sections, MoDOT provided traffic volume, truck traffic distribution, future growth type, and growth rate based on project specific traffic count data. Summaries of project specific traffic volume data used for calibration are presented in Table 22 and Table 23 for flexible and rigid pavements, respectively. Project specific vehicle class distribution data were available from MoDOT for several calibration projects. In the absence of level 1 data, level 3 AASHTOWare Pavement ME defaults were used. A summary of level 3 truck traffic classifications used for the calibration sections is presented in Table 24. As noted, level 3 data were used for selecting New AC, AC over AC, AC over PCC, and JPCP sections. Project specific vehicle class distribution data used for calibration are presented in Table 25 and Table 26 for flexible and rigid pavements respectively.

Table 22. Traffic volume inputs used for FDA, AOA, and AOC section (from MoDOT)

<b>Project and Section</b>	<b>Construction Year</b>	<b>Base Year AADTT*</b>	<b>AADT in 2017*</b>	<b>Directional Distribution, percent</b>	<b>Peak Hour</b>	<b>Percent Trucks*</b>	<b>Growth Rate*, percent</b>
FDA1- S1	2008	75	814	51.0	8.48	8.48	-0.87
FDA1- S2	2008	75	814	51.0	8.48	8.48	-0.87
FDA2	2006	1185	10,752	N/A	8.46	10.60	-0.35
FDA3	2010	1199	11,916	50.5	8.93	9.57	-0.70
FDA4	2008	439	4,362	50.0	7.36	10.61	0.61
FDA6	2008	617	9,955	N/A	7.70	7.60	2.51
AOA1	2010	1792	6,171	N/A	7.68	30.85	0.89
AOA2 - NB	2012	1659	14,958	51.5	8.02	6.21	1.76
AOA2 - SB	2012	1659	13,583	49.5	8.16	6.41	1.62
AOA3	2009	282	1,580	50.3	8.80	17.03	-0.57
AOA4	2013	940	7909	N/A	12.50	12.28	0.84
AOA5	2006	620	6,362	50.0	9.60	8.42	-1.24
AOC1	2006	3977	12,272	N/A	6.34	35.58	0.89
AOC2	2005	778	7,532	N/A	9.60	8.72	-1.30
AOC3	2008	500	2,776	N/A	8.07	18.79	0.49
AOC4	2005	721	2,923	N/A	6.57	23.78	-0.30
AOC5	2010	2482	9,878	N/A	9.40	25.62	0.28

\*Base year AADTT calculated based on AADT in 2017, percent trucks, and growth rate

Table 23. Summary of traffic volume inputs used in calibration of JPCP projects (data provided by MoDOT)

Project	Sample Unit	Construction Year*	Base Year AADTT*	AADT in 2017	Directional Distribution, percent	Peak Hour, percent	Percent Trucks	Growth Rate, percent
B1	S1	1995	252	4,086	50.8/ 49.2	10.52	6.32	0.11
C1	S1	1997	3154	2,441	48.3/ 51.70	4.38	12.91	-1.13
D1	S1	1995	11255	8,630	47.9/ 52.10	12.56	8.52	-1.06
D3	S1	1995	14144	17,567	50.2/ 49.80	9.79	5.03	1.10
F1	S1	1996	5869	4,612	N/A	7.07	29.54	-1.02
F1	S2	1996	4338	4,848	N/A	7.32	32.26	0.56
F1	S3	1996	4338	4,848	N/A	7.32	32.26	0.56
F1	S4	1996	3840	4,292	N/A	7.36	37.42	0.56
F2	S1	1997	8715	9,308	N/A	8.18	8.92	0.34
F3	S1	1994	4292	5,338	N/A	8.82	20.29	1.06
F3	S2	1994	5716	7,346	N/A	8.48	15.82	1.24
F3	S3	1994	6120	6,458	N/A	9.51	20.18	0.24
F4	S1	1994	5654	6,629	N/A	9.43	15.55	0.75
F5	S1	1993	5452	6,878	N/A	8.69	18.08	1.09
F5	S2	1993	6248	6,983	N/A	8.69	17.87	0.49
F5	S3	1993	6248	6,983	N/A	8.69	17.87	0.49
F6	S1	1994	6210	7,410	N/A	9.85	18.06	0.84
F6	S2	1994	6078	7,015	N/A	9.85	11.72	0.67
F6	S3	1994	5878	6,878	N/A	8.69	18.06	0.74
F7	S1	1997	6782	8,668	N/A	7.76	16.64	1.39
F7	S2	1997	6782	8,668	N/A	7.76	16.64	1.39
F8	S1	1997	4673	5,112	N/A	9.39	22.06	0.47
F8	S2	1997	4673	5,112	N/A	9.39	22.06	0.47
F9	S1	1997	4999	6,299	N/A	8.43	18.27	1.30
F9	S2	1997	4665	5,878	N/A	8.44	28.75	1.30
F10	S1	1995	4027	4,975	N/A	9.61	11.18	1.07
G1	S1	1994	8388	11,726	N/A	9.76	9.87	1.73
G1	S2	1994	8388	11,726	N/A	9.76	9.87	1.73
G2	S1	1998	4934	5,093	N/A	9.84	9.12	0.17
G2	S2	1998	4934	5,093	N/A	9.84	9.12	0.17
G3	S1	1998	4934	5,093	N/A	9.84	9.12	0.17
G3	S2	1998	7806	9,289	N/A	10.37	5.03	1.00

Table 23. Summary of traffic volume inputs used in calibration of JPCP projects (data provided by MoDOT), continued

Project	Sample Unit	Construction Year*	Base Year AADTT*	AADT in 2017	Directional Distribution, percent	Peak Hour, percent	Percent Trucks	Growth Rate, percent
G3	S3	1998	17230	19,227	48.3/ 51.70	9.78	5.65	0.61
H1	S1	1998	5378	5,848	N/A	7.40	41.39	0.46
H1	S2	1998	5378	5,848	N/A	7.40	41.39	0.46
H2	S1	1998	15907	17,811	N/A	6.87	40.37	0.63
UB2	S2	2000	16088	17,811	N/A	6.87	40.37	0.63
UB3	S1	2002	9545	9,373	N/A	6.41	41.06	-0.12
UB3	S2	2002	9545	9,373	N/A	6.41	41.06	-0.12
UB3	S3	2002	7979	7,584	N/A	6.42	41.07	-0.33
UB3	S4	2002	7830	8,041	N/A	6.42	41.06	0.18
UB4	S1	2004	40503	44,557	N/A	7.73	18.44	0.77
UB4	S2	2004	29750	32,535	N/A	9.17	18.44	0.72
UB5	S1	2003	3937	3,546	N/A	8.71	24.55	-0.71
UB5	S2	2003	3902	3,618	N/A	7.96	21.48	-0.52
UB5	S3	2003	3902	3,618	N/A	7.96	21.48	-0.52
UB5	S4	2003	3807	3,780	N/A	7.96	25.78	-0.05
Base year AADTT calculated based on AADT in 2017, percent trucks, and growth rate								

Table 24. Summary of Level 3 vehicle/truck class distribution data used in local calibration

Project and Section (Includes New AC, AC over AC, AC over PCC and JPCP)	Default AASHTOWare TTC Class
FDA1	ME TTC2
FDA4	ME TTC3
AOA1	ME TTC 5
AOA2	ME TTC 1
AOA3	ME TTC 2
AOC2	ME TTC 9
D1/S1	ME TTC 13
D3/S1	ME TTC 11
F2/S1	ME TTC 8
F7/S1 and S2	ME TTC 8
F10/S1	ME TTC 5

Table 25. Summary of Level 1 vehicle/truck class distribution in flexible pavement projects

<b>Project</b>	<b>Class 4 BUS (%)</b>	<b>Class 5 2D (%)</b>	<b>Class 6 SU3 (%)</b>	<b>Class 7 SU4- (%)</b>	<b>Class 8 ST4- (%)</b>	<b>Class 9 ST5 (%)</b>	<b>Class 10 ST6+ (%)</b>	<b>Class 11 MT5- (%)</b>	<b>Class 12 MT6 (%)</b>	<b>Class 13 MT7+ (%)</b>	<b>WIM Site</b>
FDA2	7.72	48.86	6.14	0.09	8.42	26.49	0.09	2.02	0.09	0.09	*
FDA3	3.77	47.37	1.84	0.09	38.60	2.89	1.49	3.77	0.00	0.18	*
FDA6	3.83	29.85	14.27	2.64	5.15	40.29	1.32	2.64	0.00	0.00	*
AOA4	2.98	19.34	6.17	1.34	21.30	40.95	1.95	1.34	0.10	4.53	*
AOA5	4.47	31.10	10.43	2.05	12.48	37.43	1.12	0.00	0.37	0.56	*
AOC1	2.25	14.39	3.99	0.05	3.55	69.81	0.76	3.92	1.26	0.05	1883
AOC3	9.21	31.67	6.14	0.77	14.40	35.12	0.58	1.34	0.00	0.77	2023
AOC4	3.88	12.09	5.04	1.15	8.63	62.45	1.87	1.29	0.00	3.60	9202
AOC5	7.11	23.21	4.07	0.83	7.66	49.35	1.42	1.22	0.28	4.86	3021
*Default axle load distributions and monthly adjustment factors were used											

Table 26. Summary of Level 1 vehicle/truck class distribution in rigid pavement projects

Section	Sample Unit	Class 4 BUS (%)	Class 5 2D (%)	Class 6 SU3(%)	Class 7 SU4 (%)	Class 8 ST4 (%)	Class 9 ST5 (%)	Class 10 ST6+ (%)	Class 11 MT5- (%)	Class 12 MT6 (%)	Class 13 MT7+ (%)
B1	S1	16.67	51.16	4.26	0.39	7.75	18.60	0.00	0.00	0.00	1.16
C1	S1	2.22	20.63	12.38	1.59	10.16	46.98	0.95	2.22	0.00	3.17
F1	S1	3.30	11.09	2.79	0.37	4.99	71.00	1.25	1.62	0.59	2.94
F1	S2	5.75	13.30	3.39	0.26	5.31	65.98	0.90	1.53	0.58	2.94
F1	S3	5.75	13.30	3.39	0.26	5.31	65.98	0.90	1.53	0.58	2.94
F1	S4	5.75	13.30	3.39	0.26	5.31	65.98	0.90	1.53	0.58	2.94
F3	S1	4.71	9.97	12.47	0.65	10.90	55.22	1.48	0.74	0.28	3.51
F3	S2	4.71	9.97	12.47	0.65	10.90	55.22	1.48	0.74	0.28	3.51
F3	S3	6.45	30.01	8.21	0.38	12.28	38.22	1.00	0.38	0.38	2.84
F4	S1	2.13	14.35	5.24	0.68	18.33	51.60	1.26	0.68	0.39	5.33
F5	S1	7.45	27.16	10.26	0.40	11.70	37.98	0.80	0.56	0.24	3.45
F5	S2	7.45	27.16	10.26	0.40	11.70	37.98	0.80	0.56	0.24	3.45
F5	S3	7.45	27.16	10.26	0.40	11.70	37.98	0.80	0.56	0.24	3.45
F6	S1	1.34	11.19	5.84	1.34	6.45	64.96	1.82	0.97	0.36	5.84
F6	S2	1.34	11.19	5.84	1.34	6.45	64.96	1.82	0.97	0.36	5.84
F6	S3	1.34	11.19	5.84	1.34	6.45	64.96	1.82	0.97	0.36	5.84
F8	S1	5.23	21.01	4.61	0.62	9.75	51.95	0.98	1.95	0.27	3.55
F8	S2	5.23	21.01	4.61	0.62	9.75	51.95	0.98	1.95	0.27	3.55
F9	S1	4.17	18.33	5.21	0.78	12.77	52.74	0.96	1.82	0.35	2.78
F9	S2	4.17	18.33	5.21	0.78	12.77	52.74	0.96	1.82	0.35	2.78
G1	S1	7.35	34.23	10.29	0.69	15.82	27.23	0.78	0.95	0.09	2.77
G1	S2	7.35	34.23	10.29	0.69	15.82	27.23	0.78	0.95	0.09	2.77
G2	S1	8.41	50.65	19.83	1.08	9.27	9.70	0.22	0.22	0.00	0.86
G2	S2	8.41	50.65	19.83	1.08	9.27	9.70	0.22	0.22	0.00	0.86
G3	S1	8.41	50.65	19.83	1.08	9.27	9.70	0.22	0.22	0.00	0.86
G3	S2	8.41	50.65	19.83	1.08	9.27	9.70	0.22	0.22	0.00	0.86
G3	S3	8.19	39.28	14.26	2.85	16.38	10.86	1.29	0.37	0.00	6.81

## FIELD DATA COLLECTION AND ANALYSIS OF TEST DATA

Primary objective of field testing was to perform FWD testing for the backcalculation of layer moduli, and to collect cores to verify pavement layer materials and thickness information. Time and budget allocation for field testing permitted testing of New AC, AC over AC, and AC on PCC sections, bearing Cell IDs FDA, AOA and AOC respectively. The project team recommended using 1000-ft sampling units for each project. Figure 32 shows the general test layout for FWD testing on AC surfaced pavements. Field core samples were also collected from the same segment of the project.

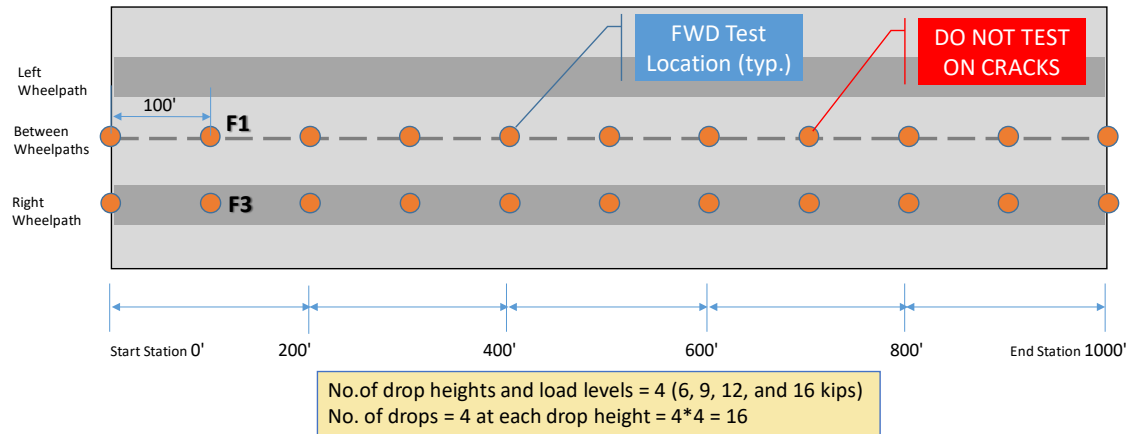


Figure 32. Test layout for flexible pavements used in the MEPDG calibration

FWD tests were performed in two test passes, one along mid-lane (i.e. between wheel paths) and the other along the wheel path identified as test lanes F1 and F3 respectively in Figure 32. Testing was performed at a spacing of 100 feet. The latitude, longitude, and elevation of the start and end of the test segment was recorded. The presence of cracks and/or other pavement distresses manifesting on the pavement surface can cause erroneous results. Therefore, locations with distress manifestation on the surface of the pavement were avoided for FWD testing. An alternate test point in its closest vicinity was used instead.

The seven-sensor configuration typically used by MoDOT and in the early LTPP testing was used for the FWD testing performed for the calibration sections. Sensor offsets, as measured from the center of the load plate, are 0, 8, 12, 18, 24, 36, and 60 inches for deflection sensors, D1 through D7. Four load levels, target load levels and acceptable load range for each drop height were consistent with LTPP FWD testing. The acceptable load range for each drop height is between 90 percent and 110 percent of the target value. Target loads were 6,000 lb. (26.7 kN), 9,000 lb. (40 kN), 12,000 lb. (53.4 kN), and 16,000 lb. (71.2 kN). A total of 16 drops, 4 drops per drop height, was used at each test location. At each test location, deflection measurements were made at all four drop heights. At each drop height, 4 repetitions were made. Therefore, deflection measurements were recorded for a total of 16 drops, i.e. 4 drops at each drop height \* 4 drop heights = 16 drops.

## Core Data

Cores extracted from the pavement sections were examined to verify material types used in the different layer, and to determine layer thicknesses. Average layer thicknesses determined from the cores were used in the Pavement ME analyses. The results are not summarized in this section but are presented in the description of HMA mixes utilized for each layer.

## Backcalculation of Layer Moduli

Backcalculation was performed using EVERCALC™ to determine elastic layer moduli of the in-situ materials. Table 27 presents the results of the backcalculation for subgrade materials for all the MoDOT PMS sections. The backcalculated subgrade resilient value was multiplied by a factor of 0.35 to convert it to a laboratory tested in-situ resilient modulus value, which is a normally accepted practice for making the field to laboratory test estimation. The root mean squared error was limited to between 2 to 3 percent and therefore deflection basins that provided results beyond this tolerance level were ignored. In general, deflection basins from 9,000 and 12,000-lb drop loads provided acceptable results from the field test data.

Table 27. Backcalculated subgrade modulus used for MoDOT calibration sections

Section	FWD Test Location	FWD Test Location Description	Backcalculated Subgrade Modulus, ksi	RMSE	Pavement ME Input for Subgrade Modulus, psi
FDA1 - S1	F1	Center	54.91	1.10	
FDA1 - S1	F3	Wheel path	50.81	1.37	
FDA1	S1	All	53.19	1.22	18,615
FDA1 - S2	F1	Center	35.78	1.44	
FDA1 - S2	F3	Wheel path	36.46	1.39	
FDA1 - S2	S2	All	36.13	1.42	12,645
FDA2	F1	Center	71.09	2.02	
FDA2	F3	Wheel path	66.59	1.88	
FDA2	ALL	All	68.39	1.94	23,936
FDA3	F1	Center	64.83	1.24	
FDA3	F3	Wheel path	69.33	1.18	
FDA3	ALL	All	66.76	1.22	23,366
FDA4	F1	Center			
FDA4	F3	Wheel path	55.05	2.11	19,269
FDA4	ALL	All			
FDA6	F1	Center	60.43	2.14	
FDA6	F3	Wheel path	60.03	2.13	
FDA6	ALL	All	60.18	2.13	21,063
AOA1	F1	Center	52.70	1.45	
AOA1	F3	Wheel path	50.21	1.14	
AOA1	ALL	All	51.76	1.33	18,117

Table 27. Backcalculated subgrade modulus used for MoDOT calibration sections, continued

<b>Section</b>	<b>FWD Test Location</b>	<b>FWD Test Location Description</b>	<b>Backcalculated Subgrade Modulus, ksi</b>	<b>RMSE</b>	<b>Pavement ME Input for Subgrade Modulus, psi</b>
AOA2 - S1	F1	Center	48.21	1.25	
AOA2 - S1	F3	Wheel path	49.09	0.92	
AOA2 - S1	S1	All	48.67	1.07	17,036
AOA2 - S2	F1	Center	40.67	1.94	
AOA2 - S2	F3	Wheel path	40.54	1.72	
AOA2 - S2	S2	All	40.61	1.85	14,214
AOA3	F1	Center	30.00	0.91	
AOA3	F3	Wheel path	38.66	2.14	
AOA3	ALL	All	35.36	1.67	12,377
AOA4	F1	Center	24.53	0.95	
AOA4	F3	Wheel path	23.38	1.69	
AOA4	ALL	All	24.04	1.27	8,415
AOA5	F1	Center	25.81	2.29	
AOA5	F3	Wheel path	25.63	2.43	
AOA5	ALL	All	25.71	2.37	8,997
AOC1	F1	Center	23.36	0.88	
AOC1	F3	Wheel path	20.70	0.99	
AOC1	ALL	All	23.23	0.88	8,132
AOC2	F3	Wheel path	33.48	1.04	
AOC2	F3	All	33.48	1.04	11,717
AOC3	F1	Center	31.59	0.88	
AOC3	F3	Wheel path	23.91	1.40	
AOC3	ALL	All	27.84	1.13	9,744
AOC4	F1	Center	35.12	1.46	
AOC4	F3	Wheel path	40.83	0.92	
AOC4	ALL	All	36.95	1.29	12,932
AOC5	F1	Center	31.26	0.81	
AOC5	F3	Wheel path	31.03	1.09	
AOC5	ALL	All	31.23	0.84	10,930

## HMA MATERIAL CHARACTERIZATION

Several HMA mix types are used by MoDOT for flexible pavement designs and AC overlays. HMA mix designation is based on binder type and nominal aggregate size that defines the combined aggregate gradation per MoDOT specifications (MoDOT, 2018). Mix type selections are based upon location, layer type being considered (surface or base layers), and anticipated traffic levels. Table 28 presents a list common and specialty MoDOT HMA mix types.

Table 28. MoDOT HMA material type selection

Traffic Levels	Mix Types	
	Surface Mixtures	Intermediate/Base Course Mixtures
<b>Interstate/ Heavy</b>	SP125BSM w/ PG 76-22 SP095BSM w/ PG 76-22 SP125B w/ PG 76-22 SP095B w/ PG 76-22	SP190B w/ PG 76-22 SP250B w/ PG 76-22
<b>High</b>	SP125C w/ PG 70-22 SP125CLP w/ PG 70-22 SP095C w/ PG 70-22 SP095CLP w/ PG 70-22	SP190C w/ PG 70-22 SP250C w/ PG 70-22
<b>Medium</b>	SP095C w/ PG 64-22 SP125C w/ PG 64-22	SP190C w/ PG 64-22 SP250C w/ PG 64-22
<b>Low</b>	BP-1 w/ PG 64-22 BP-2 w/ PG 64-22 BP-3 w/ PG 64-22 SL w/ PG 64-22	BB w/ PG 64-22

A material sampling and testing plan was developed and used to obtain HMA materials for laboratory testing to obtain Level 1 defaults of HMA dynamic modulus, HMA creep compliance and indirect tensile strength, and associated HMA volumetric properties. The sampling and testing plan were comprehensive to ensure that all common HMA mix types were characterized. The plan also covered all the primary sources of aggregates from the seven MoDOT Districts, Northwest (NW) District, Kansas City District, Northeast (NE) District, St. Louis (STL) District, Central District, Southwest (SW) District, and Southeast (SE) District. This was to ensure that aggregate material properties were reflected in default inputs for the Pavement ME Design tool. The HMA materials sampling plan is presented in Table 29. Description of testing protocols and standards, test temperatures, loading frequencies are presented in Table 30.

Table 29. HMA materials sampling plan

MoDOT Region	Percent RAP	Binder/Mix Type						
		PG 76-22		PG 70-22		PG 64-22		
		SP-125	SP-190	SP-125	SP-190	SP-125	SP-190	BB-1
NW and Kansas City Districts	0 to 20	✓		✓		✓		✓
	20 to 40		✓		✓		✓	✓
NE and STL Districts	0 to 20	✓		✓		✓		✓
	20 to 40		✓		✓		✓	✓
SW District	0 to 20	✓		✓		✓		✓
	20 to 40		✓		✓		✓	✓
SE District	0 to 20	✓		✓		✓		✓
	20 to 40		✓		✓		✓	✓

Table 30. Laboratory characterization testing procedures and sampling requirements for MEPDG HMA dynamic modulus, AC binder G\* and phase angle  $\delta$ , HMA creep compliance and HMA as-placed volumetric properties

Material Property	Test Standard		Test Temperature, deg. F	Test Frequency, Hz
Dynamic Modulus	AASHTO T342: Determining Dynamic Modulus of Hot-Mix Asphalt Concrete Mixtures		14, 40, 70, 100, 130	0.1, 1, 10, 25
Asphalt binder G* and phase angle $\delta$	AASHTO T 315	Determining the Rheological Properties of Asphalt Binder Using a Dynamic Shear Rheometer (DSR)	40, 55, 70, 85, 100, 115, 130	N/A
	AASHTO T 316	Viscosity Determination of Asphalt Binder Using Rotational Viscometer	40, 55, 70, 85, 100, 115, 130	N/A
	AASHTO T 319	Quantitative Extraction and Recovery of Asphalt Binder from Asphalt Mixtures	40, 55, 70, 85, 100, 115, 130	N/A
	AASHTO T 164	Quantitative Extraction of Bitumen from Bituminous Paving Mixtures	40, 55, 70, 85, 100, 115, 130	N/A
Creep Compliance and Indirect Tensile Strength	AASHTO T 322: Determining the Creep Compliance and Strength of Hot Mix Asphalt (HMA) Using the Indirect Tensile Test Device		-4, 14, 32	1, 2, 5, 10, 20, 50, 100* (Loading Time, secs)

Table 30. Laboratory characterization testing procedures and sampling requirements for MEPDG HMA dynamic modulus, AC binder  $G^*$  and phase angle  $\delta$ , HMA creep compliance and HMA as-placed volumetric properties, continued

In place air voids	AASHTO T 166	Bulk Specific Gravity of Compacted Bituminous Mixtures Using Saturated Surface-Dry Specimens	N/A	N/A
	AASHTO T 209	Theoretical Maximum Specific Gravity and Density of Hot-Mix Asphalt Paving Mixtures	N/A	N/A
	AASHTO T 269	Percent Air Voids in Compacted Dense and Open Asphalt Mixtures	N/A	N/A
In place volumetric binder content	AASHTO T 308	Determining the Asphalt Binder Content of Hot-Mix Asphalt (HMA) by the Ignition Method	N/A	N/A

Field work to retrieve HMA cores and production of loose material for laboratory testing was done by MoDOT engineers and technicians. Raw data from AMPT dynamic modulus testing were provided by MoDOT and processed data from creep compliance and indirect tensile strength tests were provided by Lusher (2017). The test results were reviewed by the project team. Post quality review and data processing, the laboratory test data were summarized and used to develop the Level 1 HMA properties required by the Pavement ME Design tool. These Level 1 inputs were also used as inputs for PMS projects used in calibration. Level 1 HMA material inputs for dynamic modulus, creep compliance, and indirect tensile strength are tabulated in Appendix B. The research team also provided a materials library for MoDOT to use in future designs. The following section describes the processing of laboratory test data to develop HMA material inputs for the AASHTO Pavement ME.

**Preparation of Dynamic Modulus Inputs**

The dynamic modulus ( $E^*$ ) of select MoDOT HMA mixtures, which were measured using the Asphalt Mixture Performance Tester (AMPT) in the laboratory, were converted into mix-specific, Level 1 inputs compatible for the AASHTOWare Pavement ME software. This process involved two steps:

1. Development of Pseudo Level 1 Asphalt Binder Inputs
2. Development of dynamic modulus master curves using *MasterSolver*.

Development of Pseudo Level 1 Asphalt Binder Inputs

MEPDG Level 1 inputs require the use of laboratory measured rheology properties of asphalt binders (i.e. viscosity,  $\eta$  or complex shear modulus,  $G^*$  and phase angle,  $\delta$  at different

temperatures) in conjunction with the laboratory measured  $E^*$  of asphalt concrete mixtures. The purpose of using binder properties in the MEPDG is to predict ASTM A<sub>i</sub>-VTS<sub>i</sub> viscosity parameters, a linear relationship that explains the change in binder viscosity with temperature, and to further determine viscosity-based shift factors to establish the HMA  $E^*$  master curve.

Under this effort, binder characterization tests were not available at the time of this research to characterize the rheological properties of the binders used in MoDOT mixtures. To allow the use of laboratory measured  $E^*$  values in the Pavement ME Design software, binder stiffness ( $G^*$ ) and phase angle ( $\delta$ ) values were back cast using the estimated  $E^*$  shift factors and  $G^* - \eta$  conversion relationships in the MEPDG (2004). The following relationships binder viscosity, binder stiffness, and temperature were used:

$$\eta = \frac{G^*}{10} \left( \frac{1}{\sin \delta} \right)^{4.8628} \quad (1)$$

$$\log \log \eta = A + VTS \log T_R \quad (2)$$

where:

$G^*$  = binder complex shear modulus, Pa.

$\delta$  = binder phase angle, °

$\eta$  = binder viscosity, cP.

$T_R$  = temperature in Rankine.

A, VTS = regression parameters indicating intercept and slope, respectively, of the relationship between binder viscosity and temperature. Note that Level 3 binder A-VTS parameters were used for back casting

Table 31 presents the assumed  $G^*$  and  $\delta$  values at different temperatures for each performance-grade binder. Note that the values presented in Table 31 are approximate; however, these binder  $G^*$  estimates are compatible with mixture  $E^*$  values.

Table 31. Pseudo Binder Stiffness and Phase Angles for MoDOT Binders

PG-High	PG-Low	VTS	A	Temp (°F)	G* (Pa)	Delta
64	-22	-3.68	10.98	168.8	645	87.2
				158	1329	85.9
				147.2	2899	84.3
70	-22	-3.426	10.299	168.8	1357	82.0
				158	2744	80.3
				147.2	5830	78.4
76	-22	-3.024	9.2	168.8	2451	74.3
				158	4614	72.5
				147.2	9022	70.5

## Development of Dynamic Modulus Master Curves

The AMPT measured  $E^*$  values were modeled to fit with a single sigmoidal function for each function. While the development of master curves is not a requirement for developing HMA inputs, this exercise allowed to prevent the possibility of optimization problems when the analytical engine of the AASHTOWare Pavement ME software performs curve fitting internally.

The master curves were developed using *MasterSolver*, a Microsoft Excel application that was developed under NCHRP Project 9-29 (Bonaquist, 2011), to facilitate curve fitting of AMPT measurements and develop MEPDG compatible inputs.

The dynamic modulus master curves were modeled to fit the following sigmoidal function, as required by the MEPDG:

$$\log|E^*| = \log(\text{Min}) + \frac{(\log(\text{Max}) - \log(\text{Min}))}{1 + e^{\beta + \gamma \log \omega_r}} \quad (3)$$

where:

- $|E^*|$  = dynamic modulus
- Max = limiting maximum modulus, ksi
- Min = limiting minimum modulus, ksi
- $\omega_r$  = reduced the frequency, Hz
- $\beta, \gamma$  = fitting parameters

Note that the *MasterSolver* application adopts the Arrhenius equation to compute shift factors and reduced frequencies using time-temperature superposition principles. The use of Arrhenius equation, as described below, allows calculating shift factors without the need for additional binder testing (Bonaquist, 2010).

$$\log(\omega_r) = \log(\omega) + \frac{\Delta E_a}{19.14714} \left( \frac{1}{T} - \frac{1}{T_r} \right) \quad (4)$$

where:

- $\Delta E_a$  = activation energy
- T = test temperature, °K
- $T_r$  = reference temperature, °K
- $\omega$  = loading frequency at the test temperature, Hz

The dynamic modulus inputs of all MoDOT mixtures, developed using *MasterSolver*, are presented in Table B - 1 of Appendix B.

Examples of laboratory HMA dynamic modulus test outputs are provided in Table 32. Table 32 presents HMA dynamic modulus data for a selected 19-mm and 25-mm, i.e. SP190 and SP250 gradations with 4 and 6.5 percent air voids. The selected mix designs are SP190 15-57 and SP250 16-68 with about 20% and 24% RAP contents respectively. The binder type used for both mixes is PG 70-22. Based on the results, the procedure described above resulted in dynamic modulus values that show the expected trends. The laboratory HMA dynamic modulus shows that increase in percent air voids from 4 to 6.5 resulted in a decrease in HMA dynamic

modulus. Also, for a given air void level, increasing temperature decreased HMA dynamic modulus while increasing test loading frequency increased dynamic modulus.

Table 32. Laboratory characterization test results for HMA dynamic modulus, psi

Mix Designation	Air Voids	Test Temperature (°F)	Test Frequency (Hz)			
			0.1	1	10	25
SP190 15-57	4.00%	14	2616082	2926111	3129390	3187432
		40	1689799	2228124	2652634	2785565
		70	637925	1135526	1712420	1935956
		100	167077	372970	748379	944819
		130	49106	104626	237195	325898
SP190 15-57	6.50%	14	2328973	2667627	2907584	2979811
		40	1405610	1910186	2345957	2491482
		70	504238	900543	1395959	1600998
		100	136406	289567	571639	724339
		130	42870	85632	182356	246059
SP250 16-68	4.00%	14	2509491	2860320	3098437	3167823
		40	1543094	2095846	2555740	2704459
		70	562050	1015499	1573931	1799837
		100	155864	333967	665841	844814
		130	51870	102234	218422	295714
SP250 16-68	6.50%	14	2221141	2605137	2880545	2963585
		40	1255924	1784669	2261278	2423411
		70	418699	782714	1272572	1484046
		100	115380	243225	492920	634501
		130	40615	76320	157812	212629

### Creep Compliance and Tensile Strength Testing

Cold temperature creep compliance and tensile strength testing was performed by Missouri University of Science and Technology as part of level 1 laboratory testing of HMA materials. Testing was performed in accordance with AASHTO T 322. Test samples included top lifts extracted from the full depth, AC over AC, and AC on PCC pavements. In addition, all laboratory loose mix samples were compacted to two levels of air voids for the Level 1 tests. Tensile strength tests were performed at 14°F and are summarized in Table B - 2 of Appendix B. Creep test results were reported at 32, 14, and -4°F and summarized in Table B - 3 of Appendix B for top lift cores and loose mix samples. These values were used to develop the HMA materials library and were also used as inputs in analyses required for local calibration of models.

Examples of laboratory derived Level 1 HMA creep compliance and tensile strength test data are presented in Table 33 and Table 34 for mixes SP190 15-57, and SP250 16-68 respectively. They correspond to the same mixes for which dynamic modulus values are presented in Table 32. The data shows significant decrease in tensile strength with increase in air voids (3.4 to 6.5 percent).

Creep compliance increases with increased air voids, as is expected. A summary of materials defaults used for PMS projects is presented in Table 35.

Table 33. Laboratory characterization of Level 1 HMA creep compliance and tensile strength test data for HMA mix SP190 15-57 with 4.0 and 6.5 percent air voids

Mix #	SP190 15-57				SP190 15-57			
Lab ID	16PJ5B012				16PJ5B012			
Test ID	SS012-4.0				SS012-6.5			
Specimen Type	Sawn				Sawn			
Target Voids (%)	4.0				6.5			
Test Date	8/24/17				8/25/17			
Gmm	2.438				2.438			
Lab ID	16PJ5B012				16PJ5B012			
Average Air Voids	3.79				6.45			
Std Dev., Percent	0.10				0.00			
Time, Sec	Level 1 Creep Compliance D(t), 1/psi				Level 1 Creep Compliance D(t), 1/psi			
	At -20C	At -10C	At 0C	Indirect Tensile Strength, psi	At -20C	At -10C	At 0C	Indirect Tensile Strength, psi
1	2.0061E-07	2.3911E-07	3.0981E-07	626	2.2671E-07	2.5324E-07	2.9311E-07	514
2	2.0698E-07	2.4332E-07	3.3074E-07		2.3477E-07	2.7116E-07	3.2577E-07	
5	2.1723E-07	2.6602E-07	3.7926E-07		2.4619E-07	2.8314E-07	3.6115E-07	
10	2.2374E-07	2.7348E-07	4.1625E-07		2.5395E-07	3.0233E-07	3.9814E-07	
20	2.3067E-07	2.9564E-07	4.5502E-07		2.6593E-07	3.2229E-07	4.5348E-07	
50	2.4130E-07	3.1665E-07	5.3575E-07		2.8098E-07	3.5431E-07	5.3348E-07	
100	2.4994E-07	3.3638E-07	6.2479E-07		2.9972E-07	3.7662E-07	6.1935E-07	

Table 34. Laboratory characterization of Level 1 HMA creep compliance and tensile strength test data for HMA mix SP250 16-68 with 4.0 and 6.5 percent air voids

Mix #	SP250 16-68				SP250 16-68			
Lab ID	16PJ5B013				16PJ5B013			
Test ID	SS013-4.0				SS013-6.5			
Specimen Type	Sawn				Sawn			
Target Voids (%)	4.0				6.5			
Test Date	8/17/17				8/18/17			
Gmm	2.495				2.495			
Lab ID	16PJ5B013				16PJ5B013			
Average Air Voids	4.08				6.36			
Std Dev., Percent	0.30				0.06			
Time, Sec	Level 1 Creep Compliance D(t), 1/psi				Level 1 Creep Compliance D(t), 1/psi			
	At -20C	At -10C	At 0C	Indirect Tensile Strength, psi	At -20C	At -10C	At 0C	Indirect Tensile Strength, psi
1	2.5837E-07	3.3654E-07	4.4914E-07	579	3.1604E-07	3.7181E-07	5.6851E-07	450
2	2.6992E-07	3.4964E-07	4.8454E-07		3.2695E-07	3.9236E-07	6.3273E-07	
5	2.7428E-07	3.7620E-07	5.5233E-07		3.4258E-07	4.2230E-07	7.2495E-07	
10	2.8573E-07	3.9440E-07	6.1430E-07		3.5278E-07	4.4718E-07	8.1932E-07	
20	2.9839E-07	4.1555E-07	6.8242E-07		3.6812E-07	4.7590E-07	9.6313E-07	
50	3.1649E-07	4.6078E-07	8.2525E-07		3.9204E-07	5.3032E-07	1.1799E-06	
100	3.2749E-07	4.9555E-07	9.7065E-07		4.1232E-07	5.8023E-07	1.4250E-06	

Table 35. Representative HMA mixtures selected from laboratory test data for Level 1 inputs to Pavement ME

Section	Layer No.	HMA Course	Layer Thickness, in	Mix ID	NMAS	Binder Type	Loose Mix ID	Rep. Mix ID/Type
Project Type: FDA1 Project ID: J5P0590 Route: Rte 5 Section: 1	1	Wearing	1.74	SP125 07-35	SP125	PG70-22	16PJ5B016	SP125 16-44
	2	Binder 1	2.56	SP250 07-46	SP250	PG70-22	16PJ5B013	SP250 16-68
	3	Binder 2	2.99	SP250 08-19A	SP250	PG64-22	Level 3*	N/A
Project Type: FDA1 Project ID: J5P0590 Route: Rte5 Section: 2	1	Wearing	1.87	SP125 08-18	SP125	PG70-22	16PJ5B016	SP125 16-44
	2	Binder 1	2.58	SP250 07-46	SP250	PG70-22	16PJ5B013	SP250 16-68
	3	Binder 2	3.44	SP250 08-19A	SP250	PG64-22	Level 3*	N/A
Project Type: FDA2 Project ID: J8P0609B Route: US65, Taney	1	Wearing	1.66	SP125 06-139	SP125	PG70-22	16PJ5B011	SP125 15-60
	2	Binder 1	3.33	SP250 06-122	SP250	PG70-22	16PJ5B013	SP250 16-68
	3	Binder 2	2.72	SP250 06-122	SP250	PG70-22	16PJ5B013	SP250 16-68
	4	Binder 3	4.07	SP250 06-122	SP250	PG70-22	16PJ5B013	SP250 16-68
Project Type: FDA3 Project ID: J7S0594 Route: MO66, Jasper	1	Wearing	1.95	SP095 10-116A	SP095	PG76-22	16PJ5B007	SP095 16-63
	2	Binder 1	3.15	SP250 10-85A	SP250	PG76-22	Level 3*	N/A
	3	Binder 2	3.75	SP250 10-88	SP250	PG70-22	16PJ5B013	SP250 16-68
Project Type: FDA4 Project ID: J8S0851 Route: Rte266, Greene	1	Wearing	2.04	SP125 08-20	SP125	PG64-22	16PJ5B009	SP125 16-39
	2	Binder 1	3.32	SP250 08-103	SP250	PG64-22	Level 3*	N/A
	3	Binder 2	5.58	SP250 08-103	SP250	PG64-22	Level 3*	N/A
Project Type: FDA6 Project ID: J8P0609 Route: US65, Taney	1	Wearing	1.85	SP125 07-92	SP125	PG70-22	16PJ5B011	SP125 15-60
	2	Binder 1	1.93	SP250 08-133	SP250	PG64-22	Level 3*	N/A
	3	Binder 2	2.40	SP250 07-9	SP250	PG64-22	Level 3*	N/A
	4	Binder 3	4.31	SP250 07-9	SP250	PG64-22	Level 3*	N/A
	5	Binder 4	2.57	SP250 07-9	SP250	PG64-22	Level 3*	N/A
	6	Binder 5	1.55	SP250 07-9	SP250	PG64-22	Level 3*	N/A
Project Type: AOAI Project ID: J7P0824D Route: Rte13, St. Clair	1	Wearing	1.69	SP125 10-31	SP125	PG70-22	16PJ5B011	SP125 15-60

Table 35. Representative HMA mixtures selected from laboratory test data for Level 1 inputs, continued

Section	Layer No.	HMA Course	Layer Thickness, in	Mix ID	NMAS	Binder Type	Loose Mix ID	Rep. Mix ID/Type
Project Type: AOA2 Project ID: J8P2268 Route: US65N, Christian	1	Wearing	1.33	SP095 12-51	SP095	PG64-22H	16PJ5B003 (SMA)	SP095 16-13
Project Type: AOA2 Project ID: J8P2268 Route: US65S, Christian	1	Wearing	2.05	SP125 12-48	SP125	PG64-22H	16PJ5B014	SP125 16-66
Project Type: AOA3 Project ID: J3S2009P Route: MO 21, Iron	1	Wearing	5.89	BP09-80	BP09	PG64-22	16PJ5B001	BP2 15-87
Project Type: AOA4 Project ID: J5P0964 Route: US63, Boone	1	Wearing	2.45	SP125 13-86	SP125	PG64-22H	16PJ5B014	SP125 16-66
Project Type: AOA5 Project ID: J4S1737 Route: MO210, Ray	1	Wearing	1.62	SP125 06-125	SP125	PG64-22	16PJ5B009	SP125 16-39
Project Type: AOC1 Project ID: J1D0600J Route: I35, Clinton	1	Wearing	1.82	SP125 06-45	SP125	PG76-22	16PJ5B006	SP125 16-9
	2	Binder	2.26	SP190 06-36	SP190	PG76-22	16PJ5B002	SP190 15-27
Project Type: AOC2 Project ID: J6D0600 Route: MO100, St. Louis	1	Wearing	1.81	SP125 05-143	SP125	PG70-22	16PJ5B011	SP125 15-60
	2	Binder	1.84	SP190 05-118	SP190	PG70-22	16PJ5B008	SP190 14-18
Project Type: AOC3 Project ID: J2P0773 Route: Rte63, Macon	1	Wearing	1.75	SP125 08-24	SP125	PG64-22	16PJ5B009	SP125 16-39
	2	Binder	1.96	SP190 08-23	SP190	PG64-22	16PJ5B010	SP190 15-48
Project Type: AOC4 Project ID: J9P0596 Route: US60, Shannon	1	Wearing	2.01	SP125 10-110	SP125	PG70-22	16PJ5B011	SP125 15-60
	2	Binder	2.13	SP190 10-11	SP190	PG70-22	16PJ5B012	SP190 15-57
Project Type: AOC5 Project ID: J3D0600A Route: Rte61, Lincoln	1	Wearing Surf	1.76	SP125 06-150	SP125	PG70-22	16PJ5B011	SP125 15-60
	2	Binder	2.43	SP190 06-149	SP190	PG70-22	16PJ5B012	SP190 15-57
*Pavement ME default models compute dynamic modulus and estimate creep compliance for given gradation and binder type.								

## PCC MATERIAL INPUT DATA

Input data for PCC materials were obtained from the previous calibration study (Mallela, et al., 2009). Level 1 strength data were available for each gradation type.

## PERFORMANCE DATA

Pavement distress and smoothness data were obtained from several sources. For LTPP projects, condition data was assembled directly from the LTPP database (<https://infopave.fhwa.dot.gov>, accessed 2017). LTPP data tables contained time series alligator cracking, transverse cracking, rutting, and IRI data for HMA surfaced pavements. For AC overlays, transverse cracking reported represented sum total of low temperature cracking and transverse cracking reflected from the underlying existing HMA layer or PCC slab. The alligator cracking reported for AC overlay of existing AC pavements represented sum total of post AC overlay fatigue cracking and cracking reflected from the underlying existing AC layer.

For PMS projects, time-series rutting, faulting, and IRI data were obtained from MoDOT PMS database. Note that faulting was available only for the year 2017. For AC alligator cracking and transverse cracking, and JPCP transverse cracking, data were obtained by reviewing MoDOT's ARAN files and conducting a virtual distress survey as per LTPP distress data collection and reporting protocols. Note that distress data collection video logs were available for only 2017.

Summaries of condition data sources and availability is presented in Table 36. Plots showing distress data assembled for selected PMS projects are presented in Figure 33 through Figure 36. These figures show examples of the different performance periods from a data standpoint, and the extent of data available for the local calibration.

Table 36. Data sources and availability for condition data

Pavement Type	Performance Indicator	Source of Data
New AC	Alligator cracking	LTPP, Review of MoDOT Survey Images
	Transverse thermal cracking	LTPP, Review of MoDOT Survey Images
	Rutting	LTPP, MoDOT PMS
	IRI	LTPP, MoDOT PMS
AC over AC	Alligator cracking	LTPP, Review of MoDOT Survey Images
	Transverse thermal cracking	LTPP, Review of MoDOT Survey Images
	Rutting	LTPP, MoDOT PMS
	IRI	LTPP, MoDOT PMS
	Reflection fatigue cracking	LTPP, Review of MoDOT Survey Images
	Reflection transverse cracking	LTPP, Review of MoDOT Survey Images
JPCP	Faulting	LTPP, MoDOT PMS
	Transverse cracking	LTPP, Review of MoDOT Survey Images
	IRI	LTPP, MoDOT PMS
AC over PCC	Reflection transverse cracking	LTPP, Review of MoDOT Survey Images



Figure 33. Average rut depth versus year for Project AOA1



Figure 34. Average rut depth versus year for Project AOA2



Figure 35. Average smoothness (IRI) versus year for Project F1

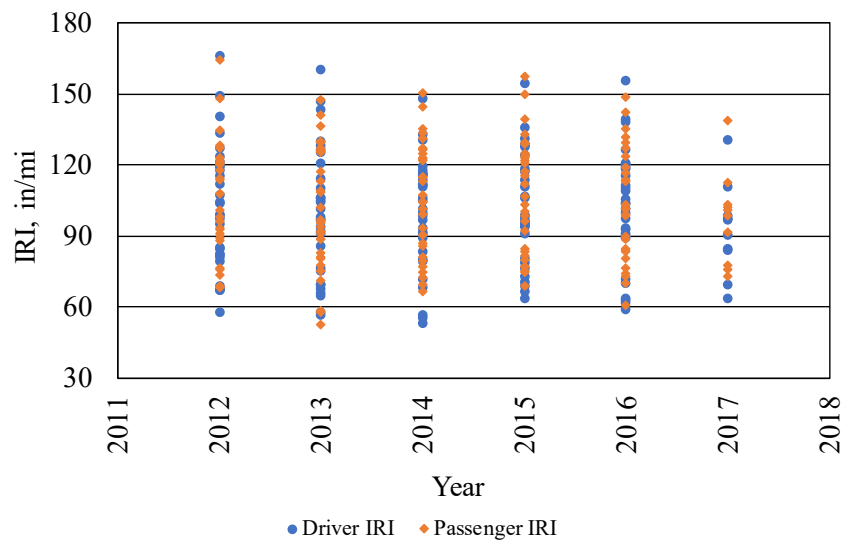


Figure 36. Average smoothness (IRI) versus year for Project F5

# CHAPTER 4. VERIFICATION OF *PAVEMENT ME DESIGN* GLOBAL DISTRESS MODELS

## VERIFICATION METHODOLOGY

A key step in Pavement ME Design tool implementation is performance of statistical analysis to determine suitability of the tool's global models for local state conditions. Global in this context implies models calibrated to reflect the entire continental U.S. pavement design and construction practices and site conditions. Local implies same conditions and practices specific to Missouri. The AASHTO MEDPG Local Calibration Guide outlines strategies for assessing global models' suitability. Details of the procedure followed to verify the models is:

1. For the selected projects, using the data assembled, develop Pavement ME Design input files.
2. Develop dataset of relevant field measured distress and IRI data available for each project. The dataset must include age distress measurements, which are necessary to access mechanistic response data.
3. Run Pavement ME Design for each selected project and extract predicted pavement distresses and IRI (at 50 percent reliability) corresponding to ages for which measured distress and IRI data is available.
4. Perform statistical analysis to assess goodness of fit and presence of bias as described below:
  - a. Goodness of Fit: Develop a linear regression model to define the relationship between the dependent variable, MEPDG-predicted distress/IRI (Y variable), and the explanatory variable, measured distress/IRI (X variable).

$$Y_i = b_0 + m(X_i) \quad (5)$$

Review outputs of the regression analysis (i.e., coefficient of determination ( $R^2$ )).  $R^2$  is the proportion of variance in the Pavement ME Design predicted distress/IRI that is predictable from the measured distress/IRI and it ranges from 0 to 1. An  $R^2$  of 0 implies no relationship between measured and predicted distress/IRI. An  $R^2$  of 1 implies the measured distress/IRI can be predicted without error.

- b. Bias
  - i. Hypothesis 1: Determine whether the linear regression model developed using measured and MEPDG predicted distress/IRI has an intercept ( $b_0$ ) of zero. Using the results of the linear regression analysis, test the following null and alternative hypotheses to determine if the fitted linear regression model has an intercept ( $b_0$ ) of zero:
    - $H_0: b_0 = 0$
    - $H_A: b_0 \neq 0$

A rejection of the null hypothesis ( $p\text{-value} < 0.05$ ) would imply the linear model had an intercept significantly different from zero at the 5 percent significant level. This indicates that using the distress/IRI model within

the range of very low measured distress/IRI values will produce biased predictions.

- i. Hypothesis 2: Determine whether the linear regression model developed using measured and MEPDG predicted distress/IRI has a slope ( $m$ ) of 1.0:
  - Using the results of the linear regression analysis, test the following null and alternative hypothesis to determine if the fitted linear regression model has a slope ( $m$ ) of 1.0:
    - $H_0: m = 1.0$ .
    - $H_A: m \neq 1.0$ .

A rejection of the null hypothesis ( $p\text{-value} < 0.05$ ) would imply that the linear model has a slope significantly different from 1.0 at the 5 percent significant level. This indicates that using the distress/IRI model outside the range of measured distress/IRI used for analysis will produce biased predictions.

- ii. Hypothesis 3: Paired t-test was done to determine whether the measured and MEPDG predicted distress/IRI represented the same population of distress/IRI. The paired t-test was performed as follows:
  - Perform a paired t-test to test the following null and alternative hypothesis:
    - $H_0$ : Mean measured distress/IRI - mean predicted distress/IRI = 0.
    - $H_A$ : Mean measured distress/IRI - mean predicted distress/IRI  $\neq$  0.

A rejection of the null hypothesis ( $p\text{-value} < 0.05$ ) would imply the measured and MEPDG distress/IRI are from different populations. This indicates that, for the range of distress/IRI used in analysis, the MEPDG model will produce biased predictions.

Assessment of goodness of fit is done by comparing the statistical analysis output  $R^2$  with those reported from the global models. A rule of thumb test is also applied. For bias, a rejection of any of the three null hypotheses indicates some form of bias in predicted distress/IRI although the outcome of the paired t-test (hypothesis 3) is most critical. Models that successfully passed all three tests were deemed to be unbiased. The presence of bias does not necessarily imply that the prediction model is inadequate and cannot be deployed for use in analysis. It only means that there is some bias present along the range of possible distress/IRI predictions. For example, the IRI models may produce unbiased predictions for the typical IRI range of 30 to 250 in/mi. The same model may, however, produce biased predictions for measured IRI values close to zero. Such a model can be used without modifications through local calibration.

For the verification of global models for MoDOT sections, only the LTPP sections were used. During the verification activity, a complete dataset of inputs was available for the LTPP projects.

## VERIFICATION OF MODELS FOR NEW AC AND AC OVER AC PAVEMENTS

### Total Alligator “Fatigue + Reflection” Cracking Model for New AC and AC over AC

Field measured and Pavement ME Design predicted alligator cracking data were evaluated to determine model goodness of fit and evaluate inherent bias in Pavement ME Design predicted alligator “fatigue + reflection” cracking. The results of the evaluation of the system of models that result in predicted alligator cracking for New AC and AC over AC pavements are presented in Table 37, Table 38, and Table 39.

Table 37. Statistical comparison of field measured and Pavement ME Design predicted alligator cracking goodness of fit for New AC and AC over AC pavements

<b>R-Square = 7.3%, SEE = 0.97141 percent</b>					
<b>Source</b>	<b>DF</b>	<b>Sum of Squares</b>	<b>Mean Square</b>	<b>F Value</b>	<b>Pr &gt; F</b>
<b>Model</b>	1	7.406	7.406	7.85	0.0061
<b>Error</b>	100	94.363	0.943		
<b>Corrected Total</b>	101	101.770			

Table 38. Hypothesis testing for field measured and Pavement ME Design predicted alligator cracking curve slope and intercept for New AC and AC over AC pavements

<b>Variable</b>	<b>DF</b>	<b>Parameter Estimate</b>	<b>Standard Error</b>	<b>t Value</b>	<b>Pr &gt;  t </b>	<b>95% Confidence Limits</b>	
<b>Intercept</b>	1	0.27733	0.10312	2.69	0.0084	0.07273	0.48192
<b>Slope</b>	1	0.03057	0.00779	3.92	< 0.0001	0.01512	0.04602

Table 39. Paired t-test results for field measured and Pavement ME Design predicted alligator cracking observations for New AC and AC over AC pavements

<b>N</b>	<b>Mean</b>	<b>Std Dev</b>	<b>Std Err</b>	<b>Minimum</b>	<b>Maximum</b>	<b>t Value</b>	<b>Pr &gt;  t </b>
102	-4.2074	11.6950	1.1580	-62.8384	6.4608	-3.63	0.0004

The information in Table 37, Table 38, and Table 39 show the following:

- Goodness of fit was generally poor, with an  $R^2 < 7.3$  percent, which implies extremely poor relationship between the Pavement ME Design predicted and field-measured alligator cracking.
- The null hypothesis, intercept = 0, was rejected as p-value was less than 0.05.
- Test for predicted versus measured cracking slope = 1 reported a p-value < 0.0001 which indicated slope was not 1.0. This is an indication of bias in predicted alligator cracking.
- Paired t-test reports a p-value of 0.0004. The null hypothesis is thus rejected and measured and predicted cracking are from different populations.

Figure 37 shows a comparison of the predicted and the measured alligator cracking, and Figure 38 shows the same comparison as a function of calculated damage. These figures show that the

global calibration model consistently under-predicted alligator cracking with increasing levels of AC fatigue damage, which is another indication of bias.

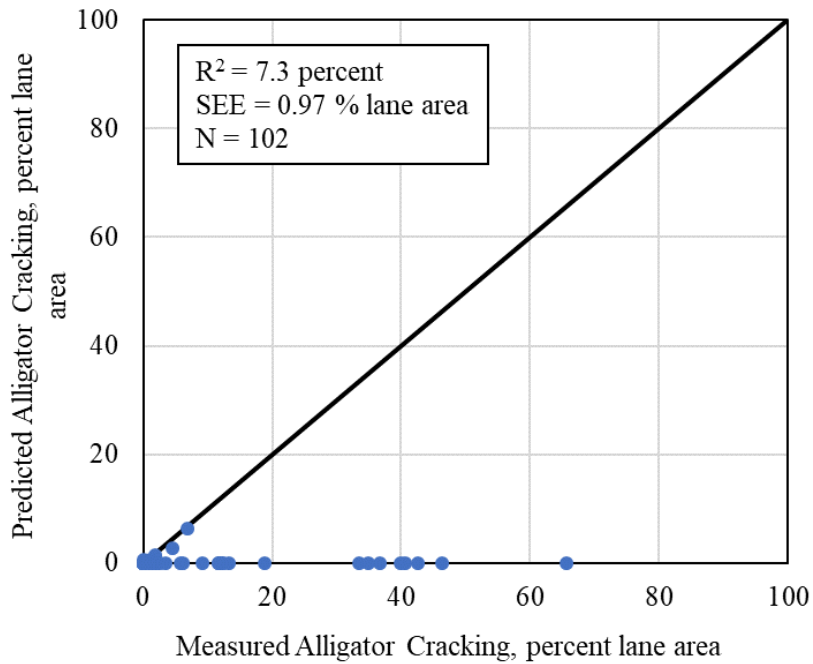


Figure 37. Pavement ME Design global calibration predicted versus measured AC alligator cracking

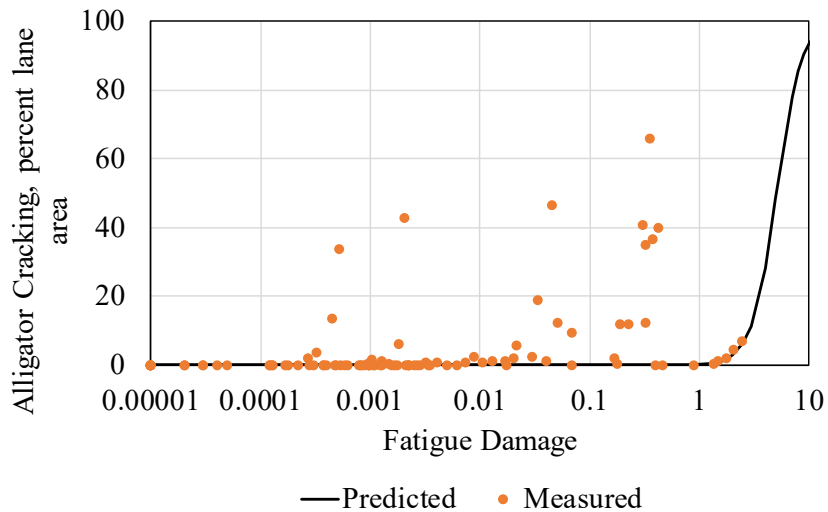


Figure 38. Verification of the AC alligator cracking and fatigue damage models with Pavement ME Design global coefficients, using Missouri flexible pavement projects

Version 2.5.2 and later versions of the Pavement ME Design procedure incorporates a revised HMA fatigue and alligator cracking prediction model. The revised model form categorizes

HMA thickness into three subgroups (<5, 5 to 12, and > 12 inches) and the calibration coefficients are a function of HMA thickness. The deviation in alligator cracking prediction from the global model, as seen in Figure 37 and Figure 38, is fairly large. Although, such low goodness of fit of the global model was observed under other local calibration efforts (Darter et al., 2014 and Mallela et al., 2013), the low goodness of fit for MoDOT data may also be influenced by the revised global models.

It is worth noting that one possible reason for longitudinal cracking at low fatigue damage levels is misinterpreting segregation as fatigue. During the development of the new PMED top-down cracking model, a careful analysis of the LTPP longitudinal cracking data was conducted to separate probable construction-related cracking, i.e. segregation, from true longer-term fatigue cracking. It was determined that the best way to resolve this, this was by relating low damage to segregation and higher damage to fatigue. This is of no consequence to the current local calibration effort.

The results of the statistical evaluation lead to the conclusion that the Pavement ME Design alligator cracking model did not adequately predict alligator cracking for Missouri local conditions. Local calibration of the Pavement ME Design alligator cracking model was thus recommended. Figure 38 shows that shifting the s-shaped curve to the left may be adequate to significantly improve accuracy of predictions. In other words, the LTPP calibration sections physically manifest distresses at a lower magnitude of damage relative to the global calibration. Figure 38 shows significant amounts of alligator cracking occurring within the range of 0.1 to 1.0 fatigue damage. The Pavement ME Design global model shows cracking steeply increasing with fatigue damage ranging from 10 to 100. Therefore, a shift of the fatigue damage versus alligator cracking model will significantly improve accuracy of predictions.

### **Rutting for New AC and AC over AC**

Measured and Pavement ME Design predicted total rutting data were analyzed to characterize goodness of fit and identify bias in Pavement ME Design predictions. The results are presented in Table 40, Table 41, and Table 42, and they suggest the following:

- Goodness of fit was poor, with an  $R^2 = 25.8$  percent, which implies a weak relationship between the Pavement ME Design and field-measured rutting.
- The null hypothesis intercept = 0 was accepted as p-value was 0.2445, greater than 0.05. This implies that predictions of smaller rutting values had insignificant levels of bias.
- The null hypothesis, slope = 1.0, was rejected as p-value was less than 0.05. This is an indication of the presence of significant bias in higher values of predicted total rutting.
- The paired t test used to determine whether the mean difference between measured and predicted total rutting is zero was rejected as p-value was less than 0.05. This is another indication of the presence of significant bias in higher values of predicted total rutting.
- Figure 39 shows predicted versus field measured rutting for all the projects evaluated. The plot shows a consistent over prediction of rutting, which is another indicator of bias.

Table 40. Statistical comparison of field measured and Pavement ME Design predicted rutting goodness of fit for New AC and AC over AC pavements

R-Square = 25.8 %, SEE = 0.1408 in					
Source	DF	Sum of Squares	Mean Square	F Value	Pr > F
Model	1	1.00674	1.00674	50.77	< 0.0001
Error	146	2.89499	0.01983		
Corrected Total	147	3.90173			

Table 41. Hypothesis testing for field measured and Pavement ME Design predicted rutting curve slope and intercept for New AC and AC over AC pavements

Variable	DF	Parameter Estimate	Standard Error	t Value	Pr >  t	95% Confidence Limits	
Intercept	1	0.03272	0.02800	1.17	0.2445	-0.02262	0.08806
Slope	1	1.41050	0.07128	19.79	<0.0001	1.26963	1.55138

Table 42. Paired t-test results for field measured and Pavement ME Design predicted rutting observations for New AC and AC over AC pavements

N	Mean	Std Dev	Std Err	Minimum	Maximum	t Value	Pr >  t
148	0.0664	0.1412	0.0116	-0.1708	0.4546	5.72	< 0.0001

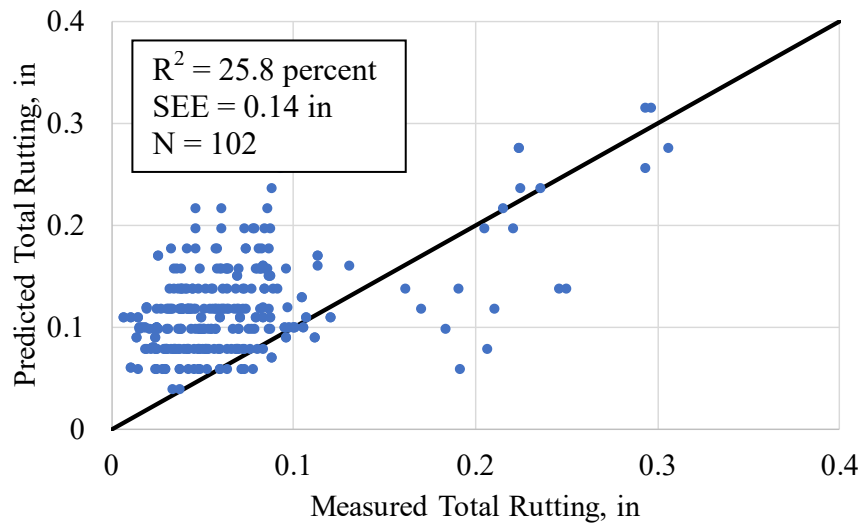


Figure 39. Pavement ME Design global calibration predicted versus measured total rutting for New AC and AC over AC pavements

## Total Transverse “Thermal + Reflection” Cracking for New AC and AC over AC

The Pavement ME Design simulates low temperature contraction of asphalt mixes that lead to tensile stresses and the formation of transverse thermal cracks. The reflection of existing transverse cracking in underlying AC layers to the AC surface is also simulated. However, other mechanisms that could cause transverse cracking such as shrinkage of the HMA (due to, for example, asphalt binder/mix hardening) are not considered (see Figure 40). This may have a considerable impact on accuracy of predictions in hotter climates such as the southern parts of the state of Missouri where transverse cracking due to shrinkage is more likely than low temperature cycles.



Figure 40. Photo showing transverse cracking from shrinkage of the AC surface due to asphalt binder hardening

LTPP classifies the entire state of Missouri as a single climate/temperature zone (e.g., freeze). The transverse cracking model in Pavement ME characterizes climate into two regions, one with MAAT greater than 57°F and the other with MAAT less than 57°F. The transverse cracking model adjusts for the climatic region in the calibration process. This definition of climate essentially classifies the entire state of Missouri as a single climate zone — cold region.

A review of average temperatures, precipitation, and freezing index from the MERRA climate data presented in Figure 5 through Figure 7 showed that average temperature conditions in the northern counties of the state are a little lower than in the southern counties. However, the freezing conditions were more significant. The United States Department of Agriculture (USDA) classifies the United States into 3 climate zones to define plant hardiness. The classification is based on average annual extreme minimum temperature conditions, which fundamentally, also trigger the initiation of AC thermal cracking. The Plant Hardiness Zone Map for Missouri is presented as Figure 41 (USDA 2017). For model’s verification only, projects from the Moderate and High Freeze zones were utilized to ensure that potential deficiencies in goodness of fit and bias will not be due to the model’s inherent deficiencies described because they cannot be corrected through recalibration.

Measured and Pavement ME Design predicted transverse cracking data for projects within the moderate and high freeze zones were evaluated to determine model goodness of fit and bias. The results are presented in Table 43, Table 44, and Table 45.

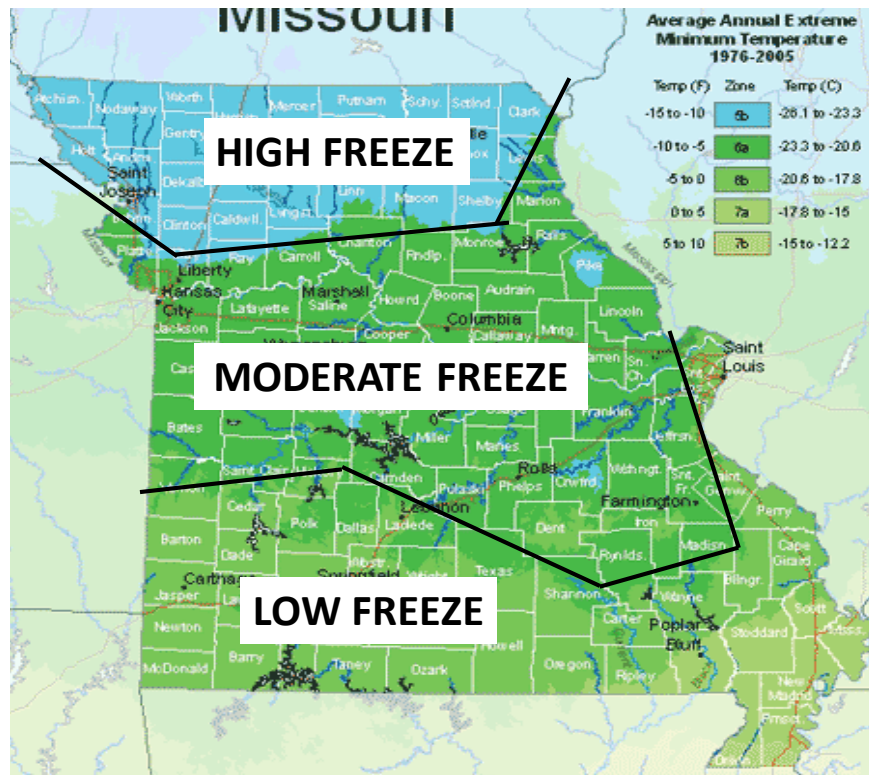


Figure 41. USDA Plant Hardiness zone map for Missouri (USDA 2017)

Table 43. Statistical goodness of fit assessment for field measured, and Pavement ME Design predicted transverse cracking for New AC and AC over AC pavements

R-Square = 1.42 %, SEE = 206.7 ft/mi					
Source	DF	Sum of Squares	Mean Square	F Value	Pr > F
Model	1	61465	61465	1.44	0.2332
Error	100	4272160	42722		
Corrected Total	101	4333625			

Table 44. Hypothesis testing for field measured and Pavement ME Design predicted transverse cracking curve slope and intercept for New AC and AC over AC pavements

Variable	DF	Parameter Estimate	Standard Error	t Value	Pr >  t	95% Confidence Limits	
Intercept	1	71.63415	22.05769	3.25	0.0016	27.87232	115.39598
Slope	1	0.0002014	0.01634	0.01	< 0.0001	-0.03221	0.03261

Table 45. Paired t-test results for field measured and Pavement ME Design predicted transverse cracking observations for New AC and AC over AC pavements

N	Mean	Std Dev	Std Err	Minimum	Maximum	t Value	Pr >  t
102	-427.1	1263.4	125.1	-6996.0	979.8	-3.41	0.0009

The information in Table 43, Table 44, and Table 45 show the following:

- Goodness of fit was poor, with an  $R^2 = 34.8$  percent, which implies a weak relationship between the Pavement ME Design transverse cracking predictions and field-measured/observed transverse cracking.
- The null hypothesis intercept = 0 was rejected as p-value was 0.0016 and thus less than 0.05 (5 percent significance level).
- The null hypothesis slope = 1.0 was rejected as p-value of 0.0016 was less than 0.05.
- Paired t-test reported a p-value of < 0.0001. The predicted and measured cracking values were thus deemed to belong to different populations as the null hypothesis was rejected.
- Rejection of all three hypotheses was an indication of the presence of bias in predicted rutting.

The plots presented in Figure 42 shows that the model consistently under-predicted transverse cracking, another indication of bias. It was concluded that the Pavement ME Design transverse cracking model did not adequately predict transverse cracking for Missouri local conditions. Local calibration of the Pavement ME Design transverse cracking model for Missouri was thus recommended.

Figure 43 through Figure 47 illustrate examples of the Pavement ME Design transverse cracking model prediction for New AC pavement and AC over AC pavements. The information presented shows the following:

- The LTPP SPS-5, SPS-8, and GPS-1 (ID 1008) projects reported low values of transverse cracking after 10 to 20 years in service. All projects were mostly in Zone 6b in Figure 41.
- Project 1002 reported significant levels of cracking after 4 years in service. This project is located in zone 6a in Figure 41.
- The reported transverse cracking seemed to show higher sensitivity to temperature, i.e. the distress development is temperature driven, as projects 0501, 0800, and 1002 used AC-20 binders but reported very different levels of cracking. Projects 0500 AC overlay mix binder was PG 64-22/PG 64-28 and project 1008 reported binder type penetration grade 60-70.

- More detailed review of mix properties (binder content, air voids, etc.) to characterize possibility for shrinkage was done as part of local calibration of the transverse cracking models.

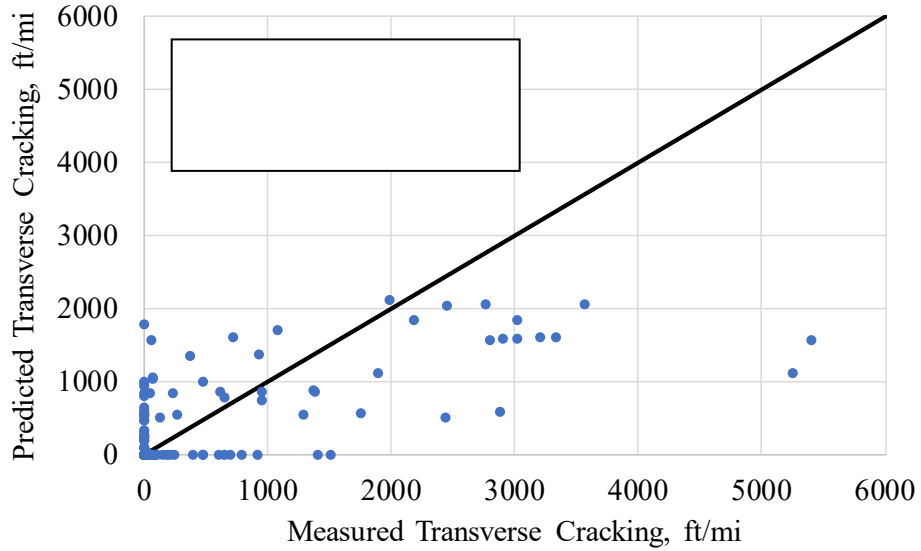


Figure 42. Pavement ME Design global calibration predicted versus measured transverse cracking

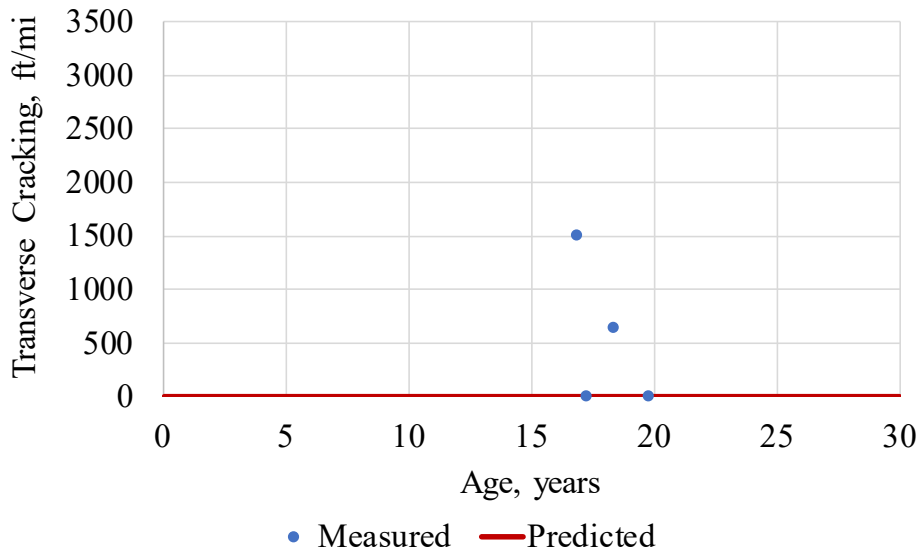


Figure 43. Pavement ME Design global calibration predicted transverse cracking versus age for LTPP project 0501 (New AC pavement)

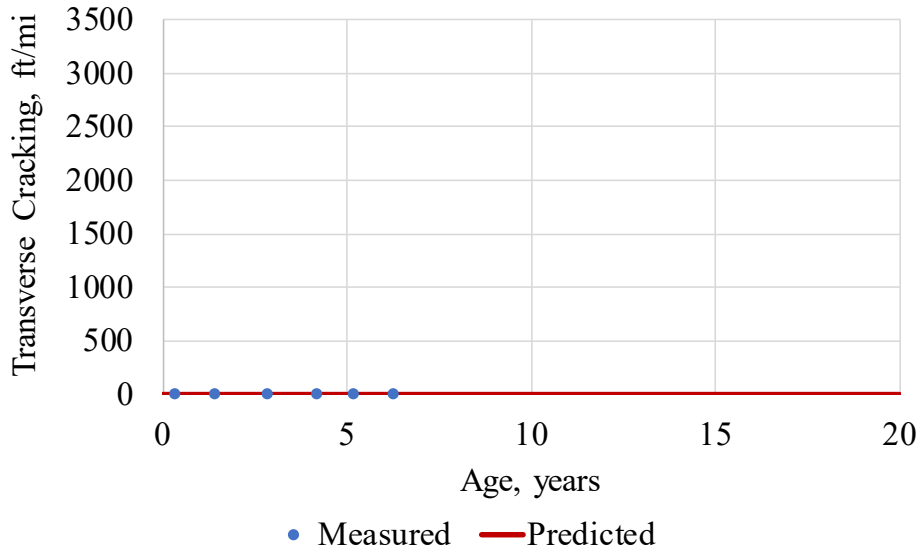


Figure 44. Pavement ME Design global calibration predicted transverse cracking versus age for LTPP project 0504 (AC over AC pavement)

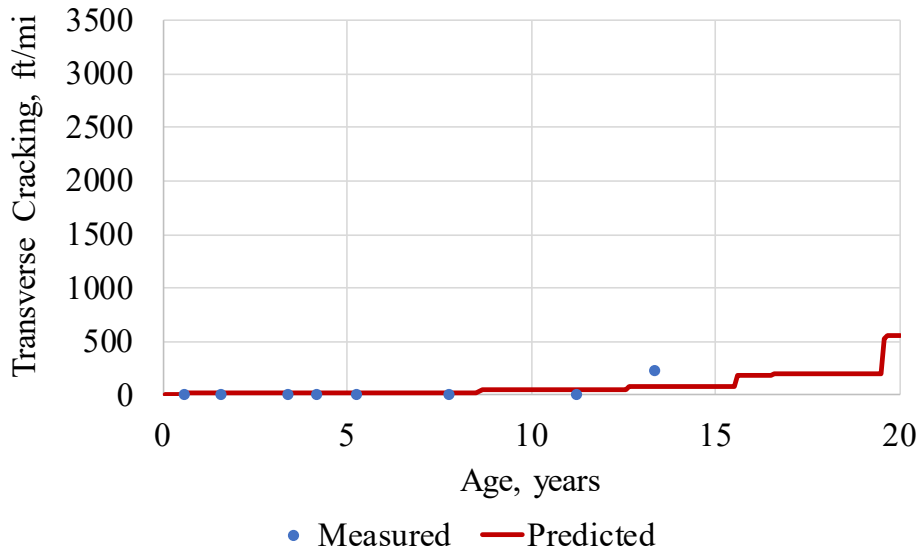


Figure 45. Pavement ME Design global calibration predicted transverse cracking versus age for LTPP project 0801 (New AC pavement)

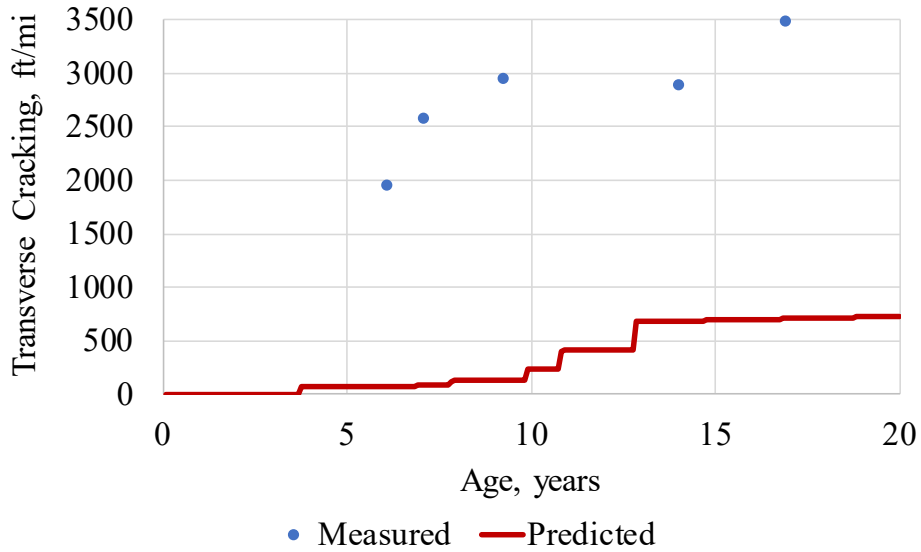


Figure 46. Pavement ME Design global calibration predicted transverse cracking versus age for LTPP project 1002 (AC over AC pavement)

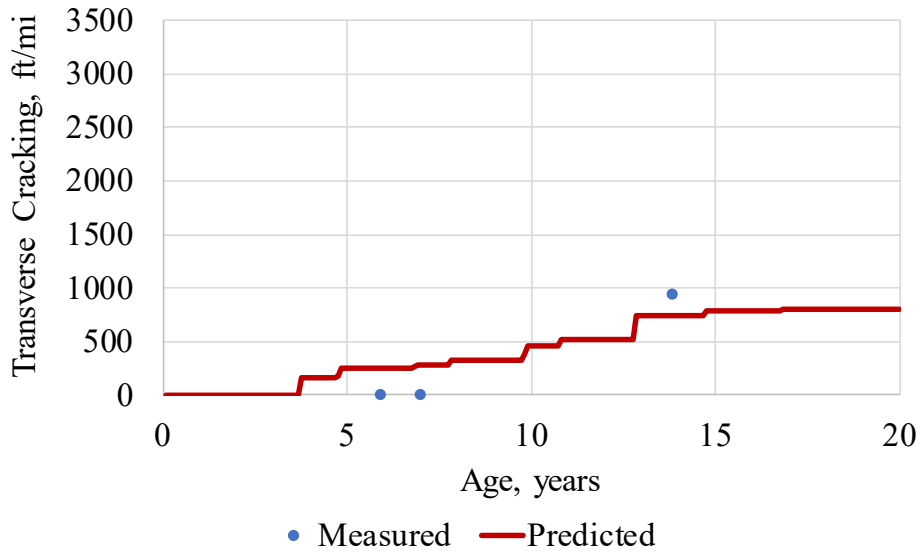


Figure 47. Pavement ME Design global calibration predicted transverse cracking versus age for LTPP project 1008 (AC over AC pavement)

## IRI for New AC and AC over AC

The IRI prediction model for New AC and AC over AC pavements uses outputs from other distress prediction models of Pavement ME including fatigue cracking, rutting, and transverse cracking. Since these models were not regarded to be adequate and will need some adjustments, verification of the IRI prediction model will not be conclusive. It was therefore not verified.

## VERIFICATION OF MODELS FOR AC OVER JPCP PAVEMENTS

### AC Alligator Cracking for AC over JPCP

For composite pavements (AC overlay over intact PCC), only the AC alligator fatigue cracking model was verified as there was no existing alligator cracking in the underlying PCC layer. The results of verification are presented in Table 46, Table 47, and Table 48.

Table 46. Statistical comparison of field measured and Pavement ME Design predicted AC alligator cracking for AC over JPCP

R-Square = 0 %, SEE = 0 %					
Source	DF	Sum of Squares	Mean Square	F Value	Pr > F
Model	1	0	0	-	-
Error	65	0	0		
Corrected Total	66	0			

Table 47. Hypothesis testing for field measured and Pavement ME Design predicted alligator cracking curve slope and intercept AC over JPCP

Variable	DF	Parameter Estimate	Standard Error	t Value	Pr >  t	95% Confidence Limits	
Intercept	1	0.00000100	0	Infnty	< 0.0001	0.0000010	0.00000100
Slope	1	5.70867E-8	1.6909E-8	3.38	< 0.0001	2.3325E-8	9.084763E-8

Table 48. Paired t-test results for field measured and Pavement ME Design predicted alligator cracking observations for AC over JPCP

N	Mean	Std Dev	Std Err	Minimum	Maximum	t Value	Pr >  t
67	-2.5796	6.2543	0.7641	-33.4430	1E-6	-3.92	0.0012

The information in Table 46, Table 47, and Table 48 show that goodness of fit as well as bias in the alligator cracking prediction could not be properly characterized as the Pavement ME Design model basically predicted no cracking for AC placed over existing PCC layer. This is not unexpected as the likelihood of the AC layer developing fatigue damage in significant quantities is extremely low. Although zero predictions of alligator cracking on AC over JPCP was as expected, some LTPP SPS-9 projects reported significant amounts of alligator cracking (for example, up to 25 percent for 0902, approximately 10 percent for 0961, and over 30 percent for

0962). The amounts of alligator cracking reported seems excessive for AC overlays over a thin 8-in existing JPCP. Several possibilities such as the examples below must be investigated to fully understand this anomaly such as:

- Reported alligator cracking is erroneous and other forms of HMA material defect in the wheel path may be wrongly characterized as alligator cracking.
- Underlying thin 8-in PCC develops longitudinal cracking in the wheel path post AC overlay, and
- The model is under predicting fatigue damage and thus fatigue cracking.

Figure 48 through Figure 53 illustrate the Pavement ME Design global calibration model prediction of alligator cracking for composite AC over JPCP LTPP projects in Missouri. The causes of excessive fatigue cracking in the AC overlay was investigated as part of local calibration of the model.

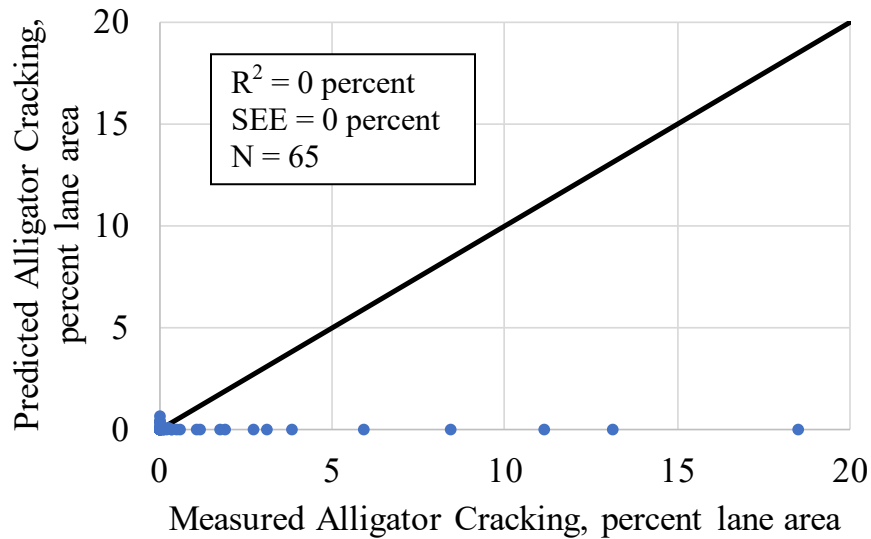


Figure 48. Pavement ME Design global calibration predicted versus measured alligator cracking for AC over JPCP

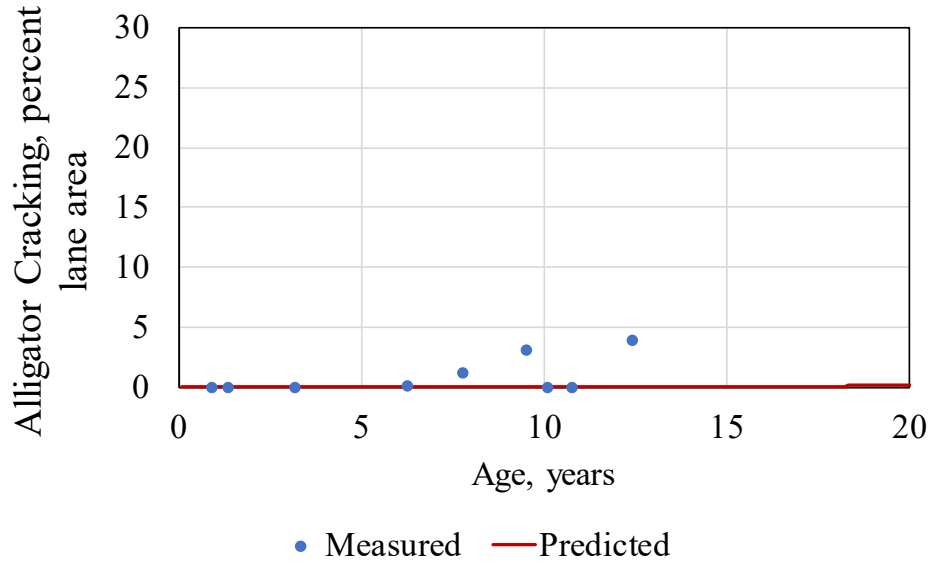


Figure 49. Pavement ME Design global calibration predicted alligator cracking versus age for LTPP project 0604 (AC over JPCP)

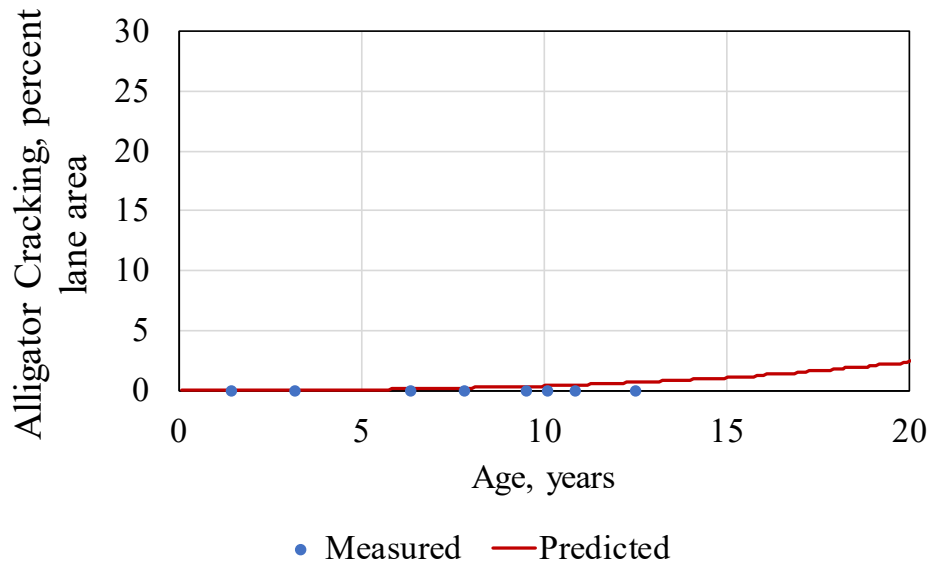


Figure 50. Pavement ME Design global calibration predicted alligator cracking versus age for LTPP project 0606 (AC over JPCP)

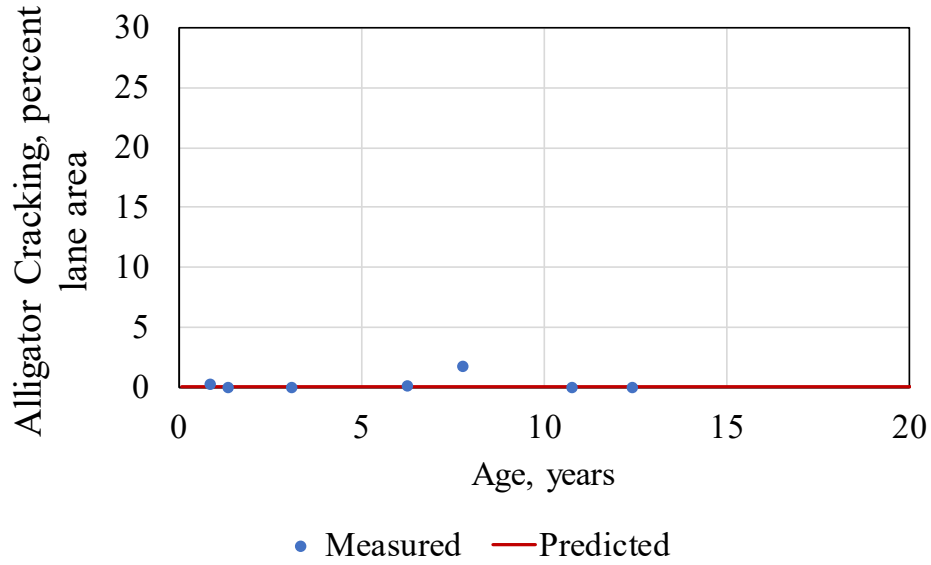


Figure 51. Pavement ME Design global calibration predicted alligator cracking versus age for LTPP project 0602 (AC over JPCP)

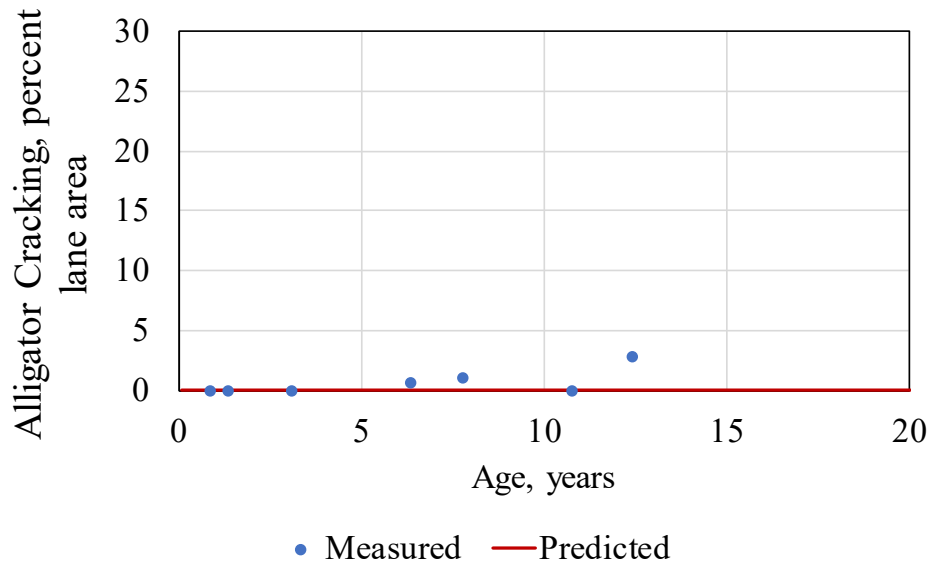


Figure 52. Pavement ME Design global calibration predicted alligator cracking versus age for LTPP project 0662 (AC over JPCP)

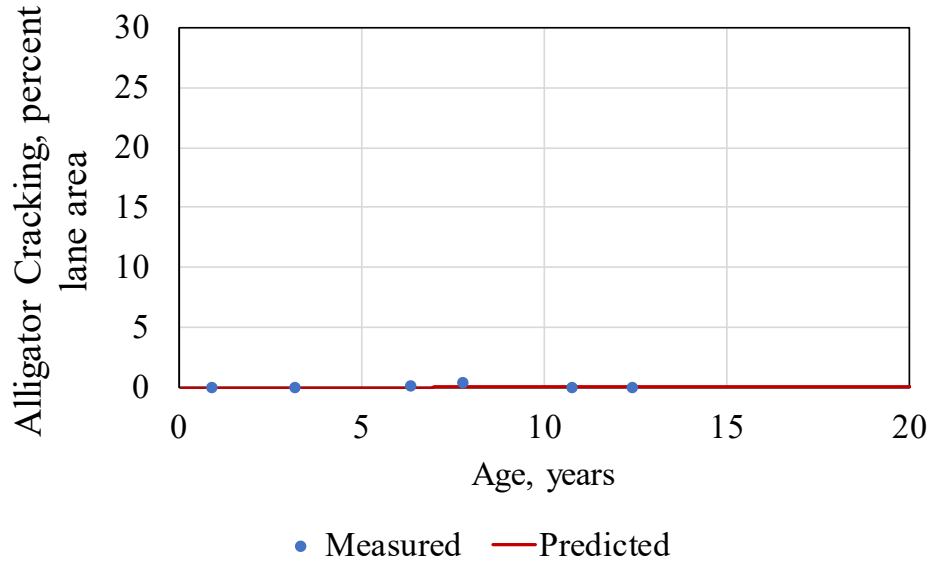


Figure 53. Pavement ME Design global calibration predicted alligator cracking versus age for LTPP project 0665 (AC over JPCP)

### AC Rutting for AC over JPCP

Measured and Pavement ME Design predicted rutting data were statistically compared to determine model goodness of fit and bias. Note rutting occurs only in the AC overlay for composite pavements and thus only the AC rutting model was evaluated. The results are presented in Table 49, Table 50, and Table 51.

Table 49. Statistical comparison of field measured and Pavement ME Design predicted AC rutting goodness of fit for AC over JPCP

R-Square = 0.58 %, SEE = 0.09691 in					
Source	DF	Sum of Squares	Mean Square	F Value	Pr > F
Model	1	0.00612	0.00612	0.65	0.4212
Error	111	1.04245	0.00939		
Corrected Total	112	1.04857			

Table 50. Hypothesis testing for field measured and Pavement ME Design predicted AC rutting curve slope and intercept for AC over JPCP

Variable	DF	Parameter Estimate	Standard Error	t Value	Pr >  t	95% Confidence Limits	
Intercept	1	0.21743	0.02301	9.45	< 0.0001	0.17184	0.26302
Slope	1	1.78034	0.11988	14.85	< 0.0001	1.54280	2.01787

Table 51. Paired t-test results for field measured and Pavement ME Design predicted AC rutting observations for AC over JPCP

N	Mean	Std Dev	Std Err	Minimum	Maximum	t Value	Pr >  t
113	0.1070	0.1077	0.0101	-0.0469	0.3484	10.56	< 0.0001

The information in Table 49, Table 50, and Table 51 show the following:

- Goodness of fit was poor, with an  $R^2 = 0.58$  percent. This implies a reasonable relationship between the Pavement ME Design rutting predictions and field-measured/observed rutting.
- All three null hypotheses intercept = 0, slope = 1.0, and predicted/measured rutting belonging to the same population were rejected as reported p-values were less than 0.05. Thus, predicted rutting was biased.

Figure 54 shows a plot of global calibration predicted versus measured AC rutting for AC over JPCP. The plot in Figure 54 shows that the model consistently over predicted rutting. Very similar trends were observed for New AC and AC over AC pavements. It was, therefore, concluded that the Pavement ME Design AC rutting model did not adequately predict AC rutting for Missouri local conditions. Local calibration of the Pavement ME Design rutting model for Missouri was thus recommended. Figure 55 through Figure 59 illustrate the Pavement ME Design AC rutting model prediction of AC rutting for select AC over JPCP LTPP projects.

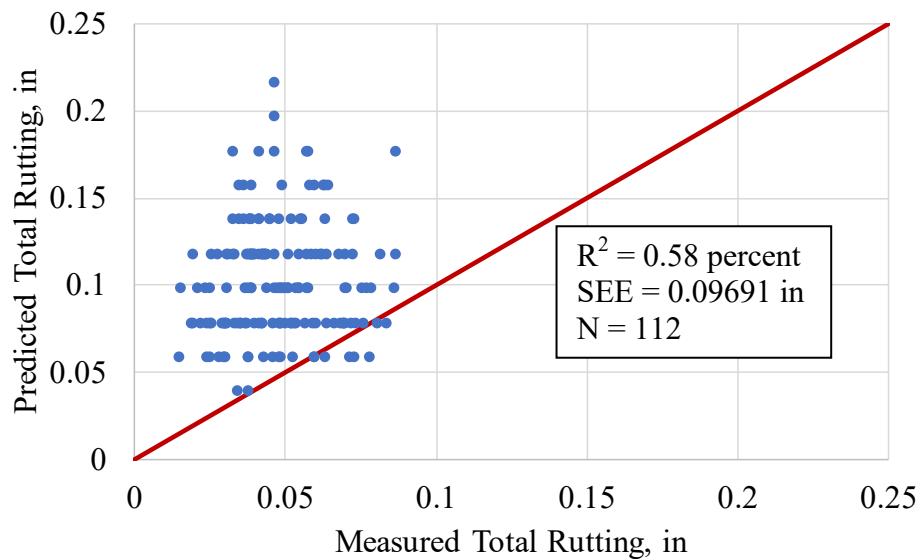


Figure 54. Pavement ME Design global calibration predicted versus measured AC rutting for AC over JPCP

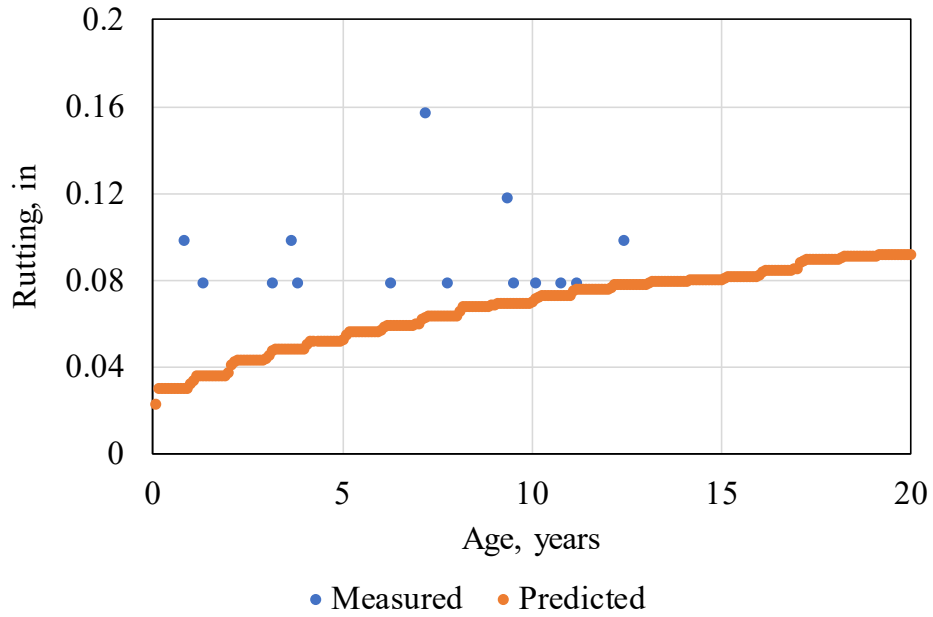


Figure 55. Pavement ME Design global calibration predicted rutting versus age for LTPP project 0604 (AC over JPCP)

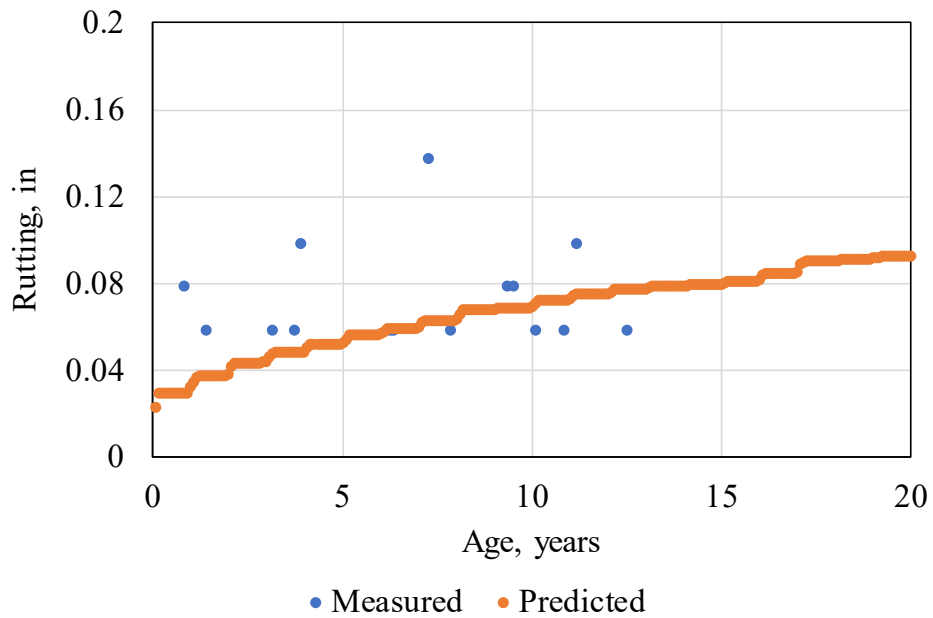


Figure 56. Pavement ME Design global calibration predicted rutting versus age for LTPP project 0606 (AC over JPCP)

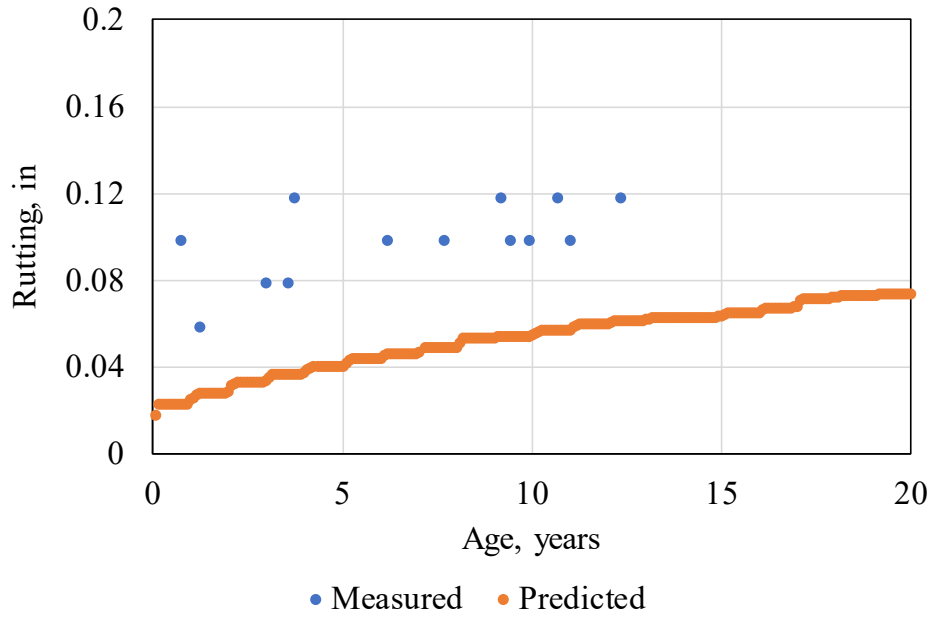


Figure 57. Pavement ME Design global calibration predicted rutting versus age for LTPP project 0608 (AC over JPCP)

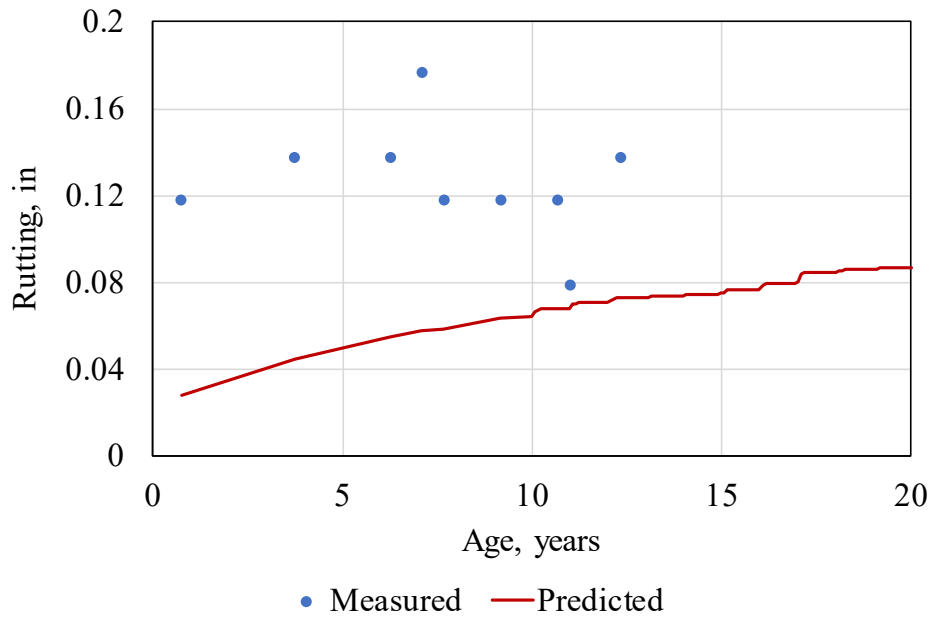


Figure 58. Pavement ME Design global calibration predicted rutting versus age for LTPP project 0664 (AC over JPCP)

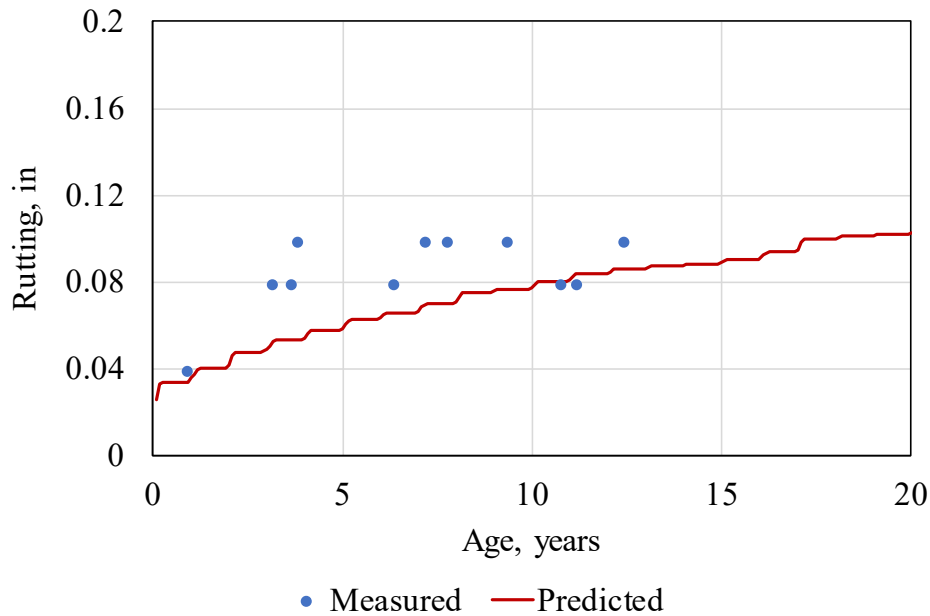


Figure 59. Pavement ME Design global calibration predicted rutting versus age for LTPP project 0665 (AC over JPCP)

### Total Transverse “Thermal + Reflection” Cracking for AC over JPCP

Total transverse cracking in composite AC over JPCP can occur due to a combination of the following mechanisms (1) low temperature thermal cracking in the AC layer, (2) shrinkage of the AC surface due to HMA mix asphalt binder hardening, and (3) reflection of existing transverse cracking and transverse joints in the underlying PCC. For the projects included in this evaluation, underlying PCC transverse cracking were repaired (full depth repairs and patching) prior to AC overlay placement. This may introduce some extra joints in the underlying PCC. However, there was no evidence of active existing transverse cracks. Since the Pavement ME Design does not predict AC transverse cracking initiated by shrinkage due to asphalt binder hardening, predicted transverse cracking may be less than measured. This would be more apparent in the southern counties of the state rather than the northern counties as previously explained.

Measured and Pavement ME Design predicted transverse cracking data were evaluated to determine model goodness of fit and bias in Pavement ME Design predicted transverse cracking. The results are presented in Table 52, Table 53, and Table 54. Note that most of the projects were located in zones with high potential for low temperature transverse cracking (see Figure 41).

Table 52. Statistical comparison of field measured and Pavement ME Design predicted transverse cracking goodness of fit for AC over JPCP

<b>R-Square = 37.6 %, SEE = 547.62 ft/mi</b>					
Source	DF	Sum of Squares	Mean Square	F Value	Pr>F
Model	1	8662662	8662662	28.89	<.0001
Error	48	14394789	299891		
Corrected Total	49	23057451			

Table 53. Hypothesis testing for field measured and Pavement ME Design predicted transverse cracking curve slope and intercept for composite AC over JPCP

Variable	DF	Parameter Estimate	Standard Error	t Value	Pr >  t	95% Confidence Limits	
Intercept	1	-142.8035	137.9008	-1.04	0.3056	-420.0717	134.46477
Slope	1	0.31922	0.03971	8.04	< 0.0001	0.23941	0.39902

Table 54. Paired t-test results for field measured and Pavement ME Design predicted transverse cracking observations for composite AC over JPCP

N	Mean	Std Dev	Std Err	Minimum	Maximum	t Value	Pr >  t
50	-1144.4	874.8	123.7	-2973.8	115.4	-9.25	< 0.0001

The information in Table 52, Table 53, and Table 54 show the following:

- Goodness of fit was poor, with an  $R^2 = 37.6$  percent, which implies some relationship between the Pavement ME Design transverse cracking predictions and field-measured/observed transverse cracking exists. However, it is not at an acceptable level.
- The null hypothesis intercept = 0 was accepted as p-value was 0.3056 and thus greater than 0.05.
- The null hypotheses, slope = 1, and measured and predicted cracking belong to the same population were, however, rejected as computed p-value < 0.05. This is an indication of the presence of bias in predicted transverse cracking.
- The plot of measured versus predicted cracking presented in Figure 60 shows that the Pavement ME Design model consistently under-predicted transverse cracking, another indication of bias.
- Figure 61 shows that Pavement ME Design predicted transverse cracking much more accurately ( $R^2 = 43$  percent) for the SPS-6 projects located in colder climates and constructed with Superpave mixes. Transverse cracking predictions for the SPS-9 projects in slightly milder climates constructed with conventional asphalt binders was poor ( $R^2 = 8$  percent).

It was concluded, therefore, that the Pavement ME Design transverse cracking model did not adequately predict transverse cracking for Missouri local conditions. Local calibration of the Pavement ME Design transverse cracking model for Missouri was thus recommended. The

impact of mix type and properties and location (climate) on accuracy of the Pavement ME Design transverse cracking model was investigated in much more detail as part of local calibration. Figure 60 through Figure 66 illustrate the Pavement ME Design transverse cracking model prediction of transverse cracking for AC over JPCP projects.

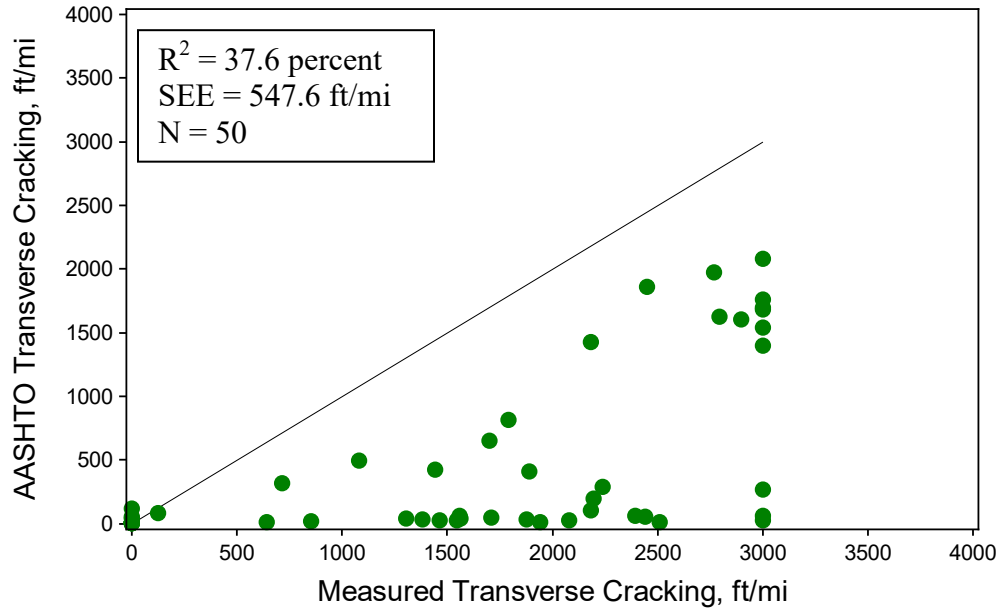


Figure 60. Pavement ME Design global calibration predicted versus measured total transverse cracking for composite AC over JPCP

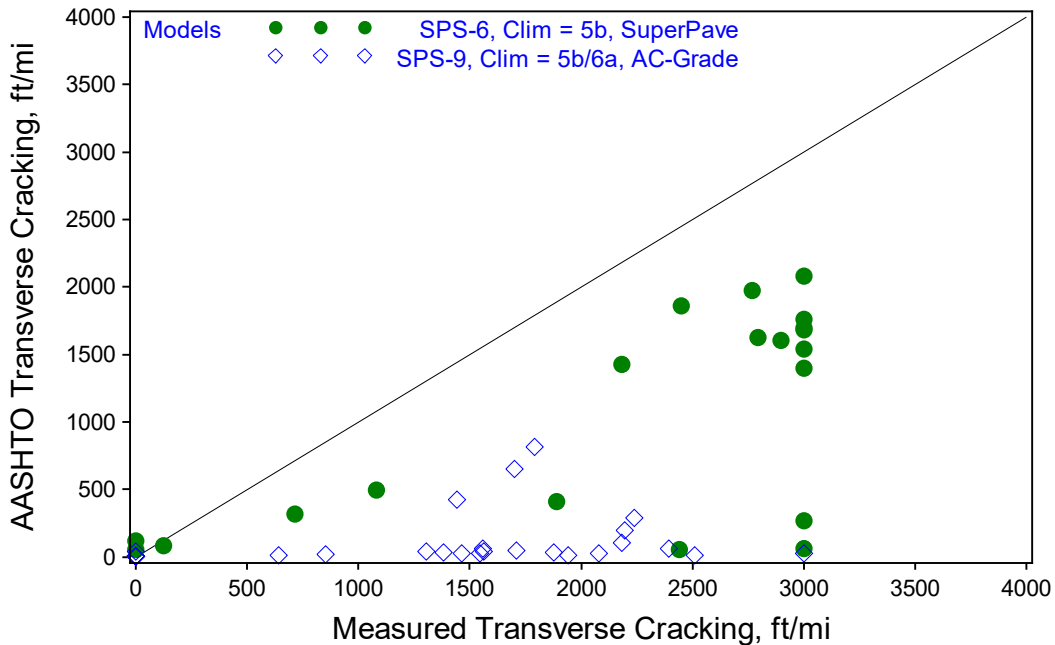


Figure 61. Pavement ME Design global calibration predicted versus measured total transverse cracking for composite AC over JPCP (showing SPS-6 and SPS-9 projects)

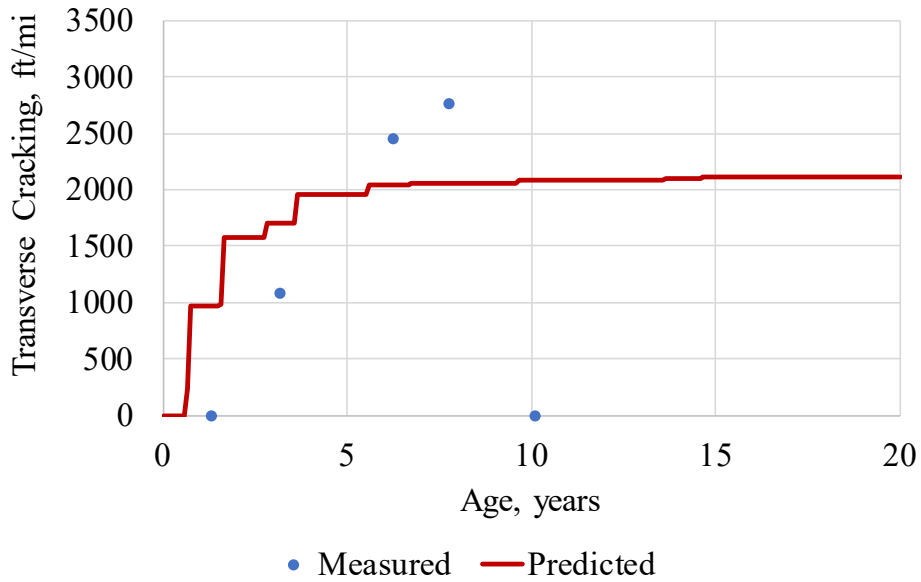


Figure 62. Pavement ME Design global calibration predicted transverse cracking versus age for LTPP project 0603 (composite AC over JPCP)

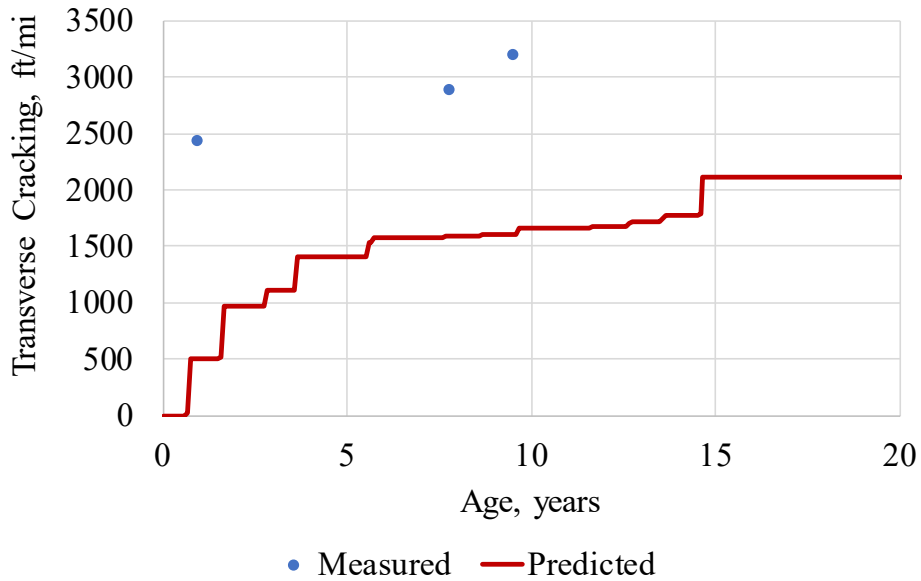


Figure 63. Pavement ME Design global calibration predicted transverse cracking versus age for LTPP project 0604 (composite AC over JPCP)

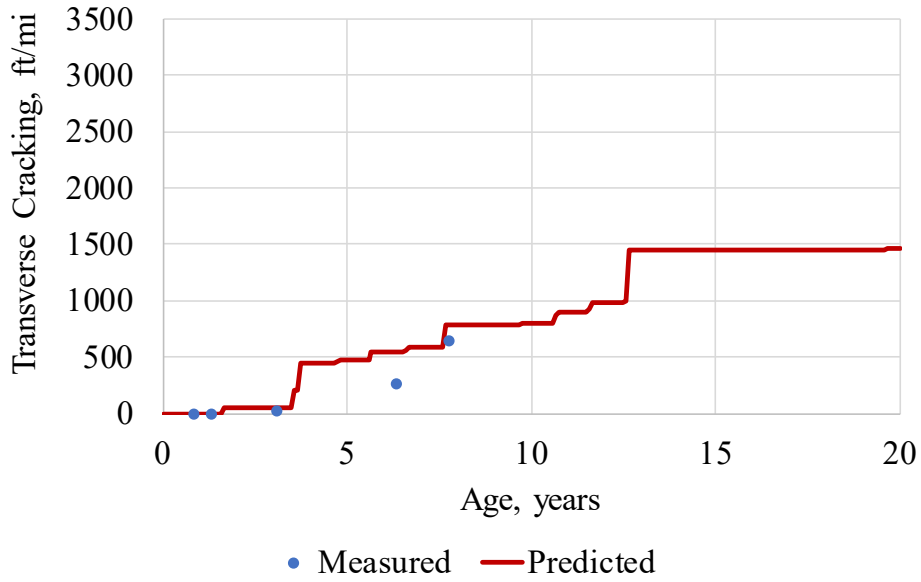


Figure 64. Pavement ME Design global calibration predicted transverse cracking versus age for LTPP project 0663 (AC over JPCP)

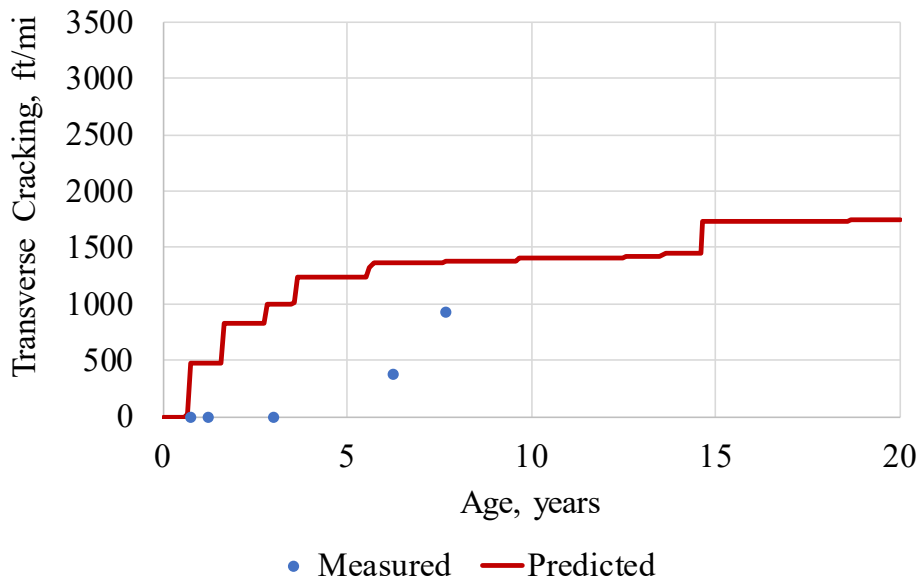


Figure 65. Pavement ME Design global calibration predicted transverse cracking versus age for LTPP project 0901 (AC over JPCP)

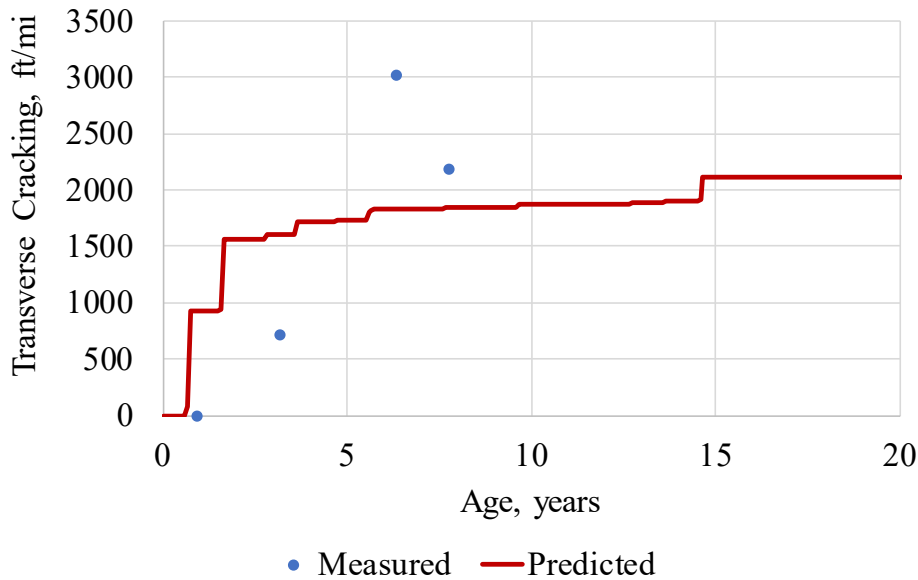


Figure 66. Pavement ME Design global calibration predicted transverse cracking versus age for LTPP project 0665 (AC over JPCP)

### IRI for AC over JPCP

The IRI prediction model for AC over JPCP is a function of the outputs obtained from the Pavement ME Design distress prediction models for the design. Since these models were not regarded to be adequate and will need some adjustments, verification of the IRI prediction models would not be logical.

### MODEL VERIFICATION FOR NEW JPCP AND UNBONDED JPCP OVERLAYS

#### Transverse Cracking for JPCP

Figure 67 presents a distribution of the transverse cracking data available from the LTPP JPCP projects assembled. The information in Figure 67 shows that approximately 80 percent of all projects report zero (0) percent cracking. The remaining projects, with the exception of one, reported 3 percent or less cracking. A full regression-based model verification as outlined in the AASHTO Local MEPDG Calibration Guide was hence not feasible as key regression outputs used for model assessment would not be meaningful. Accordingly, a non-regression classification analysis approach was used to assess model’s reasonableness as part of local calibration. This approach, described in detail in Chapter 6, allows for checking the model’s reasonableness and, if possible, minor adjustments to improve accuracy and precision as needed.

#### Transverse Joint Faulting for JPCP

Figure 68 presents a distribution of the transverse joint faulting data available from the JPCP projects assembled. The information in Figure 68 shows that approximately 50 percent of all

projects report zero (0) inch joint faulting. The remaining projects report 0.02 in or less transverse joint faulting. With approximately all projects reporting no more than 0.02 in faulting a full regression-based model verification as outlined in the AASHTO Local MEPDG Calibration Guide was thus not feasible as key regression outputs used for model assessment would not be meaningful. A non-regression classification analysis approach was thus used to assess model's reasonableness as part of local calibration. This approach described in detail in Chapter 5 allows for checking models reasonableness and making minor adjustments to improve accuracy and precision as needed.

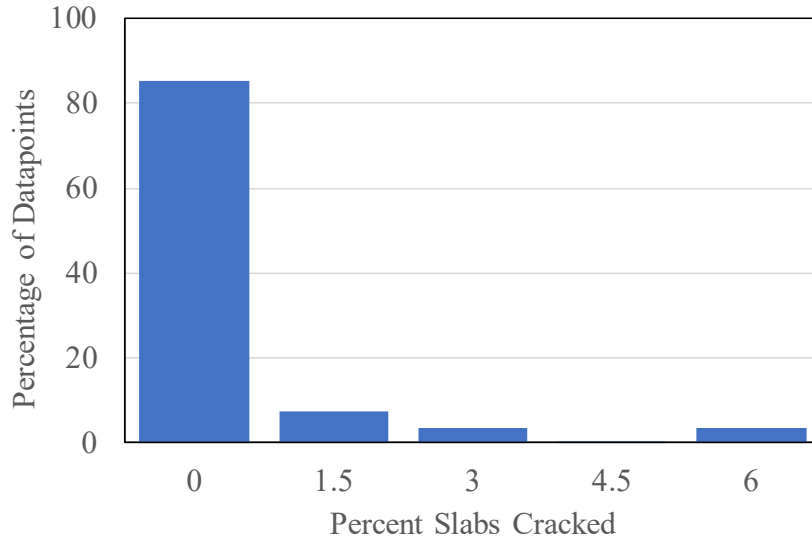


Figure 67. Distribution of transverse cracking data in LTPP data used for model verification

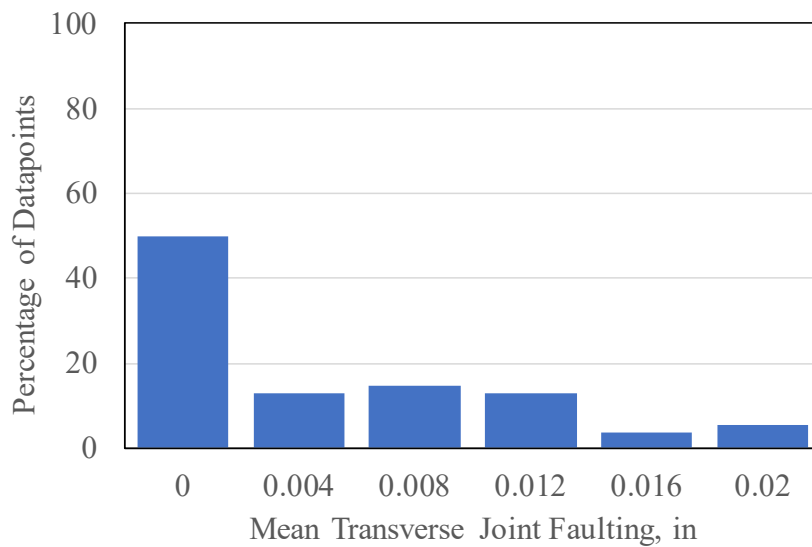


Figure 68. Distribution of joint faulting data in LTPP data used for model verification

## JPCP IRI

The JPCP IRI prediction model uses outputs from other distress models in Pavement ME Design. The dataset lacked mature distress data for full verification in this case. Since these models were not certified to be adequate, or inadequate either, verification of the IRI prediction model was not performed under this activity. A larger dataset with the MoDOT PMS section data will be used for verification and validation.

## SUMMARY OF MODEL VERIFICATION ANALYSIS RESULTS

The verification analyses presented in this chapter shows significant levels of bias and lack of goodness of fit in the global models when applied to local Missouri conditions. A summary of the results is presented in Table 55. The results show need for local calibration for the New AC, AC over AC, and AC over JPCP models. A more detailed/advanced verification, and if possible, adjustment is needed for the JPCP models.

Table 55. Summary of model’s verification results and recommendations for improvement

<b>Pavement Type</b>	<b>Performance Indicators</b>	<b>Goodness of Fit</b>	<b>Bias</b>	<b>RECOMMENDATIONS</b>
New AC and AC over AC	Alligator cracking	Poor	Yes	Recalibration
	Transverse cracking	Poor	Yes	Recalibration
	Rutting	Moderate	Yes	Recalibration
AC over AC	Reflection fatigue cracking	Poor	Yes	Recalibration
	Reflection transverse cracking	Poor	Yes	Recalibration
AC over JPCP	Reflection fatigue cracking	Inconclusive		Recalibration
	Reflection transverse cracking	Poor	Yes	Recalibration
All AC surfaced pavements	IRI	N/A	N/A	Recalibration
New JPCP and unbonded JPCP overlay	Transverse slab cracking	N/A	N/A	Verify using classification methods. Adjust models if needed
	Faulting	N/A	N/A	
	IRI	N/A	N/A	

## CHAPTER 5. LOCAL CALIBRATION OF *PAVEMENT ME DESIGN* FLEXIBLE PAVEMENT DISTRESS MODELS

### TOTAL ALLIGATOR “FATIGUE + REFLECTION” CRACKING MODEL

Total alligator cracking comprises alligator fatigue cracking that initiates at the bottom of the AC layer and propagates to the surface with repeated application of heavy truck axles, and alligator cracking reflected from the underlying existing AC layers.

#### Alligator Fatigue Cracking

Alligator fatigue cracking prediction begins with the computation of the incremental AC bottom-up fatigue damage using Equation 6 (AASHTO 2015).

$$DI = \sum(\Delta DI)_{j,m,l,p,T} = \sum \left( \frac{n}{N_{f-HMA}} \right)_{j,m,l,p,T} \quad (6)$$

where:

- $n$  = actual number of axle load applications within a specific time period
- $j$  = axle load interval
- $m$  = axle load type (single, tandem, tridem, quad, or special axle configuration)
- $l$  = truck type using the truck classification groups included in the MEPDG
- $p$  = month
- $T$  = median temperature for the five temperature intervals or quintiles used to subdivide each month, °F
- $N_{f-HMA}$  = allowable number of axle load applications for a flexible pavement and AC overlays to fatigue cracking

The allowable number of axle load applications needed for the incremental fatigue damage computation, and calculated on a constant stress criterion, is expressed as (AASHTO 2015):

$$N_{f-HMA} = C * k_1 * \beta_{f1} (\varepsilon_t)^{-k_2 \beta_{f2}} (E_{HMA})^{-k_3 \beta_{f3}} \quad (7)$$

where:

- $N_{f-HMA}$  = allowable number of axle load applications for a flexible pavement and AC overlays to initiate fatigue cracking
- $\varepsilon_t$  = tensile strain at critical locations, in/in
- $E_{HMA}$  = dynamic modulus of the HMA, psi
- $k_1, k_2, k_3$  = laboratory regression coefficients
- $\beta_{f1}, \beta_{f2}, \beta_{f3}$  = local or field calibration constants
- $C$  = Laboratory to field adjustment factor expressed as:

$$C = 10^M \quad (8)$$

where:

$$M = 4.84 \left( \frac{V_{be}}{V_a + V_{be}} - 0.69 \right) \quad (9)$$

$V_{be}$  = effective asphalt content by volume, percent  
 $V_a$  = percent air voids in the HMA mixture (in situ only, not mixture design)

In the development of the fatigue model under NCHRP 1-37A (ARA, 2004), the global calibration factors were assigned the following values:

$\beta_{f1} = C_H * \beta'_{f1}$ , where  $C_H$  is the thickness correction term shown in equation 10.  
 $\beta'_{f1} = 1.0$   
 $\beta_{f2} = 1.2$   
 $\beta_{f3} = 1.5$   
 $C_H$  = thickness correction term for bottom-up cracking is as follows:

$$C_H = \frac{1}{0.000398 + \frac{0.003602}{1 + e^{(11.02 - 3.49H_{HMA})}}} \quad (10)$$

where:

$H_{HMA}$  = total AC thickness, in

Note that the thickness correction factor has a different relationship to AC thickness for the top-down cracking model, which is not being calibrated for MoDOT under the current research study. Since 2004, the bottom-up fatigue model was revised over time and the version 2.5.5 of the AASHTOWare Pavement ME uses the following global calibration factors:

$\beta_{f1} = 0.02054$  for  $H_{HMA} < 5$  inch,  
 $0.001032$  for  $H_{HMA} > 12$  inch, and  
 $5.014 * H_{HMA}^{3.416}$  for  $5 \text{ inch} \leq H_{HMA} \leq 12 \text{ inch}$   
 $\beta_{f2} = 1.38$   
 $\beta_{f3} = 0.88$

Alligator cracking is calculated from the cumulative damage over time (Equation 6) using the relationship presented as Equation 11. (AASHTO 2015)

$$FC_{Bottom} = \left(\frac{1}{60}\right) \left(\frac{C_4}{1 + e^{(C_1 C_1^* + C_2 C_2^* \text{Log}(DI_{Bottom}))}}\right) \quad (11)$$

where:

$FC_{Bottom}$  = area of alligator cracking that initiates at the bottom of the AC layers, percent of total lane area  
 $DI_{Bottom}$  = cumulative damage index at the bottom of the AC layer  
 $C_{1,2,4}$  = Regression constants;  $C_4 = 6,000$ ;  $C_1 = 1.00$ ; and  $C_2 = 1.00$

$$C_1^* = -2C_2^* \quad (12)$$

$$C_2^* = -2.40874 - 39.748(1 + H_{HMA})^{-2.856} \quad (13)$$

where:

$H_{HMA}$  = total AC thickness, in

### Alligator Reflection Cracking

Alligator reflection cracking prediction begins with estimation of crack tip location beginning at the bottom of the AC overlay and progressing incrementally through the AC overlay thickness (note location is characterized in terms of length of distance between bottom of the AC overlay to crack tip). This is done using an adaptation of the Paris/Erdogan crack progression model presented as Equation 14 (Titus-Glover et al. 2016).

$$\Delta C_{CrackTip} = \sum_{i=1}^N \{ (k_1 A [K_I]^n) + (k_2 A [K_{II}]^n) + (k_3 A [K_{III}]^n) \} \quad (14)$$

where:

$\Delta C_{CrackTip}$  = crack total length  
 $k_1, k_2, k_3$  = regression coefficients  
 $K_I$  = bending crack propagation mode stress intensity factor (SIF)  
 $K_{II}$  = shearing crack propagation mode SIF  
 $K_{III}$  = thermal crack propagation mode SIF  
 $A, n$  = AC fracture properties  
 $N$  = total thermal/traffic load increments (cumulative number of daily axle loading/temperature cycles)

The crack tip location (or crack length) is determined sequentially for each small increment of time to enable accurate computation of location-specific stresses and strains that drive crack progression through the AC overlay thickness. Damage is defined as the ratio of crack length and AC overlay thickness and is computed as follows (Titus-Glover et al. 2016).

$$D_T = \frac{\sum_{i=1}^N \{ (C_1 k_1 A [K_I]^n) + (C_2 k_2 A [K_{II}]^n) + (C_3 k_3 A [K_{III}]^n) \}}{h_{OL}} \quad (15)$$

where:

$D_T$  = total damage  
 $C_{1,2,3}$  = regression coefficients  
 $h_{OL}$  = AC overlay thickness

All other variables are as previously defined. Computed total damage is related to field estimates of alligator reflection cracking using the equation below (Titus-Glover et al. 2016).

$$PRC = \frac{100}{C_4 + e^{(C_5 \log D_T)}} \quad (16)$$

where:

$PRC$  = percentage of existing alligator cracking in the underlying AC reflected  
 $D_T$  = total damage  
 $C_4, C_5$  = calibration coefficients

## Calibration of the Alligator Fatigue and Reflection Cracking Model

The alligator “fatigue + reflection” cracking model was recalibrated to improve goodness of fit and reduce bias. As described above, the fatigue cracking and the reflective cracking are two different distress mechanisms and governed by independent equations for the two types of cracking. Each model is derived using different calibration coefficients. Since the exact cause of alligator cracking observed at the surface of AC overlays is not reported, it is difficult to apportion the cause of cracking to fatigue or reflection from sublayers. As such, calibration of the two models was done simultaneously.

Results of the model’s recalibration are presented in Table 56 through Table 59, and Figure 69 and Figure 70. Table 56 presents coefficients of the global model and the locally calibrated model. Comparison of the two sets of coefficients shows considerable difference. It is to be noted here, that the changes to  $\beta_{fl}$  will impact the top-down fatigue and top-down cracking model predictions within the AASHTOWare program. However, because the top-down cracking model is not being calibrated under this effort, the corresponding calibration factors have not been readjusted. It is recommended that the global models be used to evaluate top-down cracking predictions, should MoDOT consider this distress in future designs.

Table 56. Summary of local coefficients for the alligator cracking model

Model	Model Coefficient	Local Missouri	Global AASHTOWare Pavement ME Version 2.5.5
AC Fatigue	$\beta_{fl}$ for $H_{HMA} < 5$ in	<b>8.316E-05</b>	0.02054
	$\beta_{fl}$ for $H_{HMA} > 12$ in	<b>8.316E-05</b>	0.001032
	$\beta_{fl}$ for $5 \text{ in} \leq H_{HMA} \leq 12 \text{ in}$	<b>8.316E-05</b>	$5.014 * H_{HMA}^{3.416}$
AC Cracking- Bottom Up	C1	<b>-0.31</b>	1.31
	C2 < 5 in	<b>1.367</b>	2.158
	C2 > 12 in	<b>2.067</b>	3.9666
	C2 (5 in < hac < 12 in)	<b>0.867+0.1*hac</b>	0.867+0.2583*hac
	C3	6000	6000
	Standard Deviation	<b>1.13 + 0.7236*Dam<sup>0.4654</sup></b>	$1.13 + 13/(1+e^{(7.57-15.5*\text{LOG10}(\text{Dam}+0.0001)))}$
Fatigue Reflective Cracking	C1	<b>0.0456</b>	0.38
	C2	<b>0.0083</b>	1.66
	C3	2.72	2.72
	C4	105.4	105.4
	C5	-7.02	-7.02

Based on results in Table 57 through Table 59, the coefficient of determination improved significantly for the new recalibrated model (i.e. from 0.07 to 0.80). Tables 58 and 59 shows all three p-values from the bias hypothesis testing to be greater than 0.05 and thus there was no bias at the 5 percent significance level.

Table 57. Locally calibrated alligator cracking model goodness of fit for New AC and AC over AC pavements

<b>R-Square = 80.5%, RMSE = 4.94 percent, COV = 132.0, N = 85</b>					
Source	DF	Sum of Squares	Mean Square	F Value	Pr > F
Model	1	8469.14837	8469.14837	346.48	<.0001
Error	84	2053.25630	24.44353		
Corrected Total	85	10522			

Table 58. Bias test results for locally calibrated alligator cracking model for New AC and AC over AC pavements

Variable	DF	Parameter Estimate	Standard Error	t Value	Pr >  t	95% Confidence Limits	
Intercept	1	0.53247	0.56036	0.95	0.3447	-0.58187	1.64682
Slope	1	0.94482	0.04752	19.88	0.2488	0.85034	1.03930

Table 59. Paired t-test results for field measured and Pavement ME Design predicted alligator cracking observations for New AC and AC over AC pavements

N	Mean	Std Dev	Std Err	Minimum	Maximum	t Value	Pr >  t
86	0.2914	4.9716	0.5361	-15.3696	34.4895	0.54	0.5881

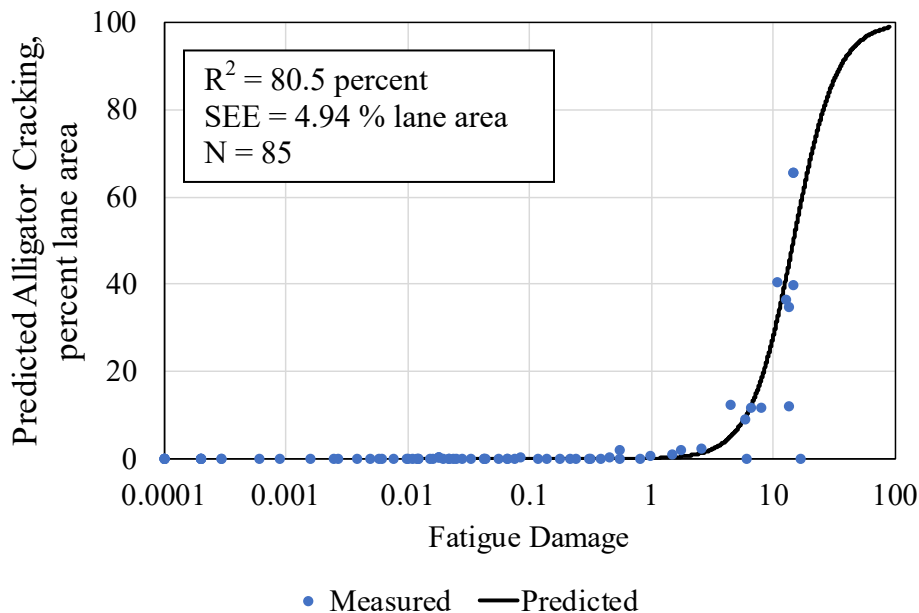


Figure 69. AC alligator cracking and fatigue damage model with Pavement ME Design local calibration coefficients, using all Missouri LTPP and PMS flexible pavement projects

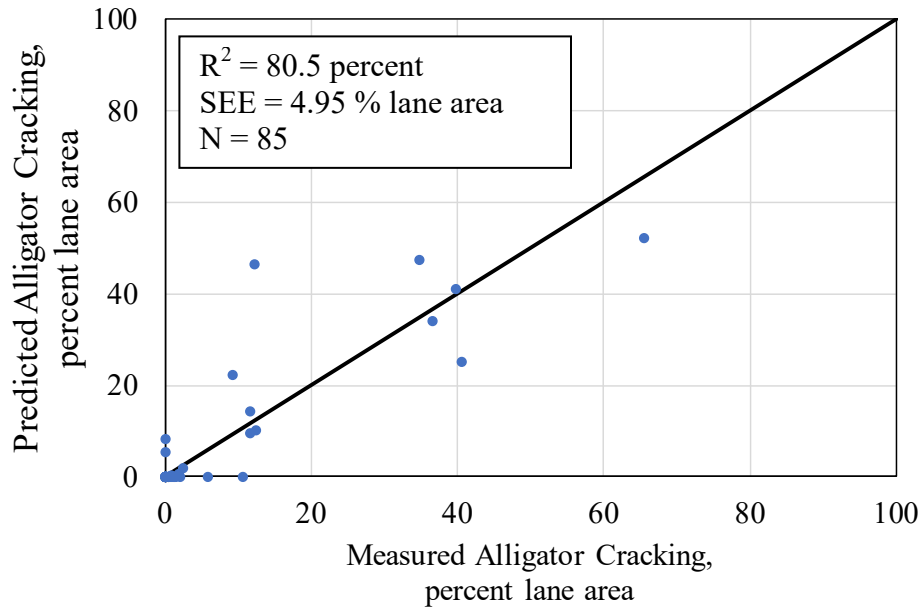


Figure 70. Pavement ME Design local calibration model predicted versus measured AC alligator cracking for Missouri LTPP and PMS flexible pavement projects

Additional verification of recalibrated models was done through sensitivity analysis and evaluation of the reasonableness of the trends observed in relation to varying parameters. For all sensitivity analyses presented in this report, the baseline design for New AC pavements used a 9-inch AC layer structure over crushed aggregate base on an AASHTO A-7-6 subgrade soil. The AC structure consisted of 3-inch thick AC layer of SP125 15-60 surface mix with 20 percent RAP content, over 3 inch thick SP 190 15-48, over 3 inch thick SP 250 16-68 HMA mixes. Level 1 inputs were used from the MoDOT materials library. A 20-year design life with a cumulative traffic of 2 million trucks was used. The rehabilitation design used AC overlay on an existing 9-inch AC pavement. The analyses assumed two cases, the first with no pre-existing fatigue cracking, and the second with pre-existing fatigue cracking of 10 percent at the time of rehabilitation, which is a typical for a rehabilitation project. The cumulative traffic at the end of the 20-year rehabilitation design life was 7 million trucks. The use of level 1 HMA materials inputs provides an opportunity to evaluate the value of engineering the mix design to control any specific distress type.

As part of the sensitivity analyses, impacts of AC thickness, site location (ambient temperature), and HMA mix air voids on predicted alligator cracking were investigated. The results are presented in Figure 71, through Figure 75. Please note that, while the trends in sensitivity analyses will generally apply to most designs, the quantitative discussion included on the sensitivity analyses are specific to the designs used in the analyses.

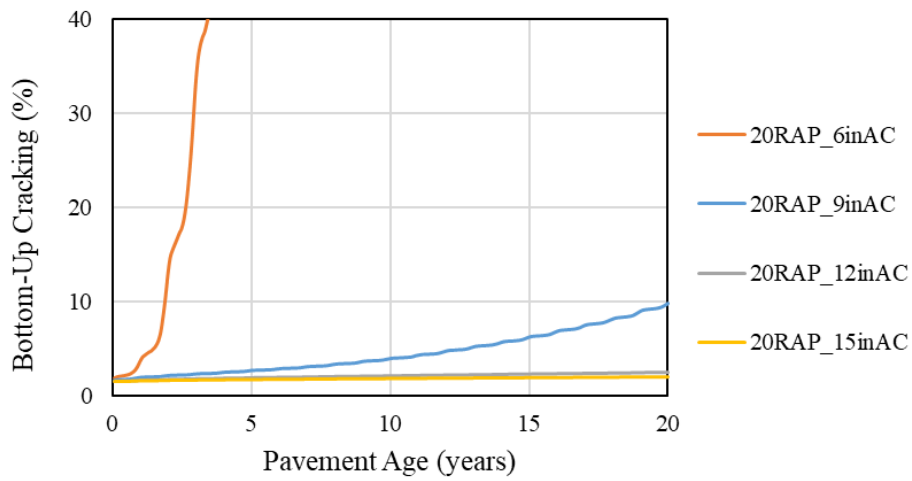


Figure 71. Impact of AC thickness on local calibration model predicted AC alligator cracking (New AC design)

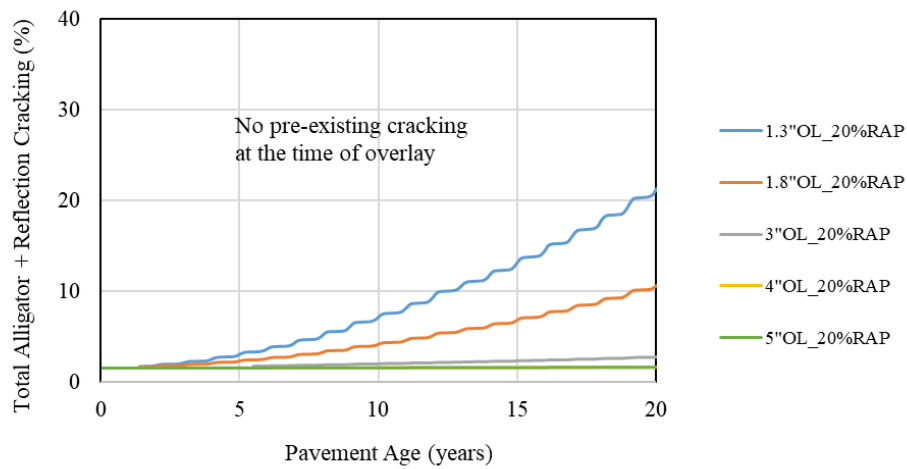


Figure 72. Impact of AC overlay thickness on local calibration predicted AC alligator cracking (AC over AC design)

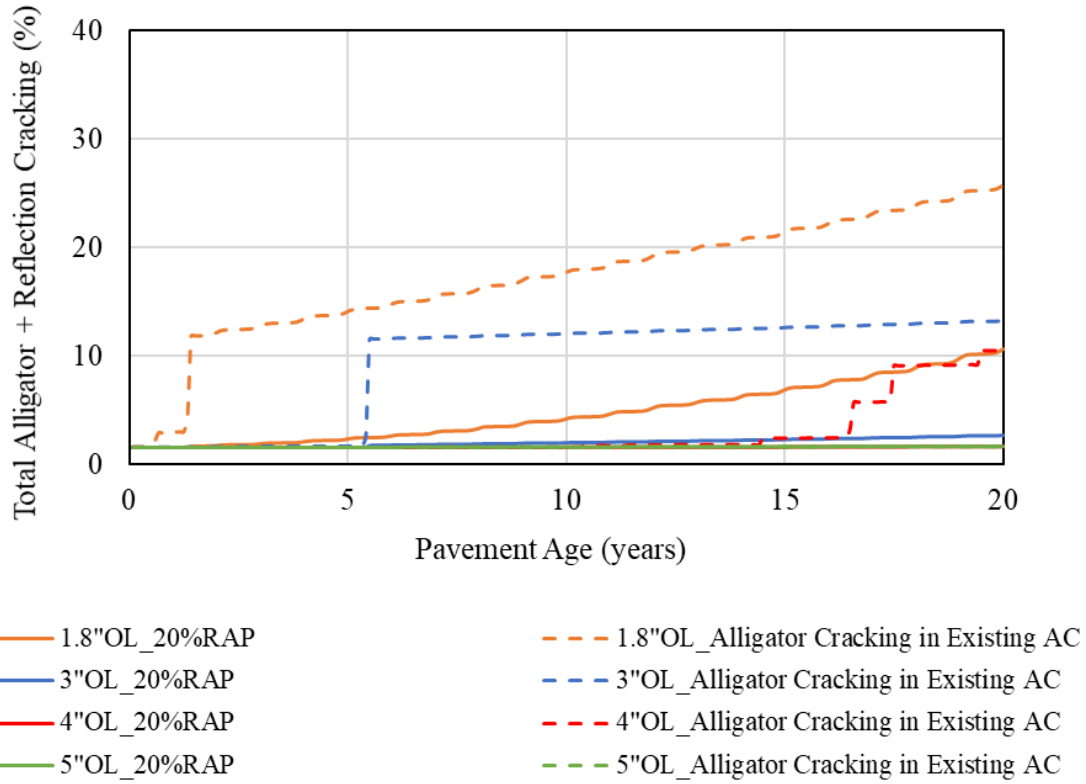


Figure 73. Impact of fatigue in existing pavement and overlay thickness on local calibration model predicted AC alligator cracking (AC over AC design)

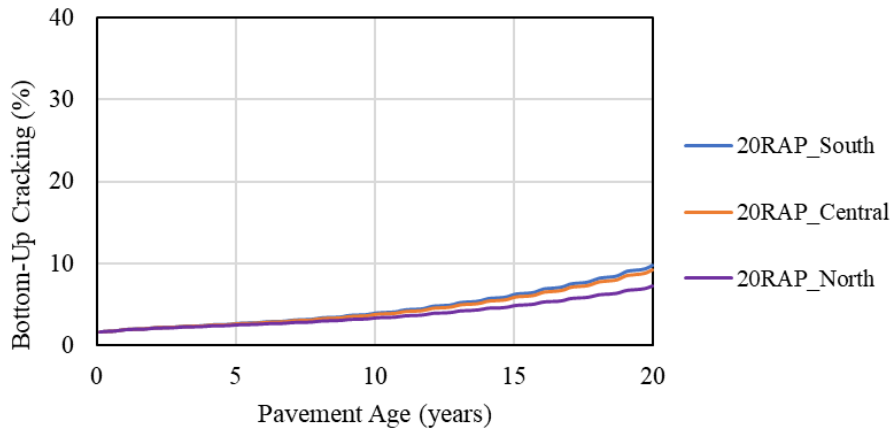


Figure 74. Impact of climate on local calibration model predicted AC alligator cracking (New AC design)

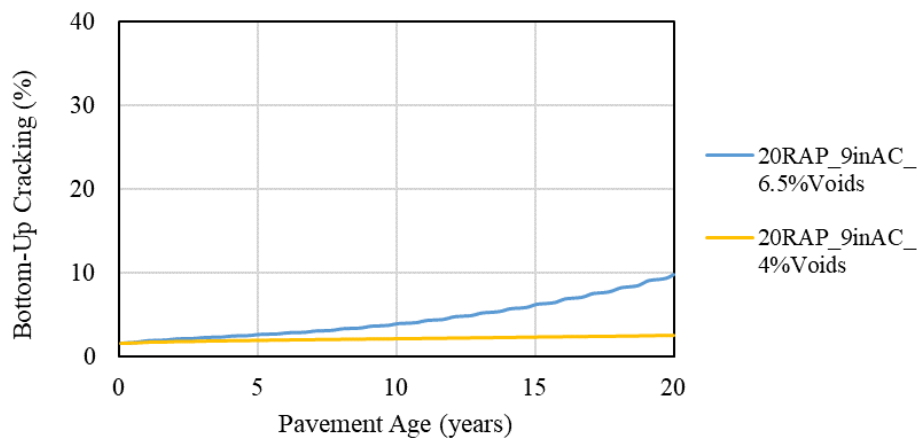


Figure 75. Impact of HMA air voids on local calibration model predicted AC alligator cracking for Missouri

The sensitivity analysis results suggest the following:

- Predictions of alligator cracking using the locally calibrated model is significantly influenced by AC thickness as shown in Figure 71, Figure 72 and Figure 73. For a New AC design (Figure 71) a 9-in increase in thickness (from 6 to 15 inches) results in almost completely eliminating fatigue cracking in the design (i.e., reduction from 100 percent to 2 percent cracking). Increasing the thickness from 6 to 9 inches results in an acceptable fatigue cracking level for the design. Further, increasing the thickness to 12 almost results in negligible cracking, while any further increase, say to 15 inches, will diminish the benefit of increasing thickness. Likewise, Figure 72 shows that the design life can be substantially extended with increased AC overlay thicknesses. Increasing the overlay thickness from 1.3 to 3 inches offers an additional 40 percent design life for a design criterion of 10 percent cracking. As seen in Figure 73, the fatigue cracking reported for rehabilitation designs combines cracking from tensile strain-induced fatigue damage and reflection from cracking in underlying layers. Existing cracking in the existing pavement increases total fatigue cracking and increased overlay thickness reduces the cracking manifested on the surface. The impact of thickness was deemed reasonable.
- Figure 74 shows that climate has a reasonable impact on predicted alligator cracking. The warmer (southern and central) regions of the state exhibited higher levels of alligator cracking when compared to the colder northern climate. HMA temperature does have a significant impact on dynamic modulus, stress, and strain. The stiffer mixes in the north is expected to exhibit lower levels of strain when subjected to similar truck loading and thus less fatigue damage and associated alligator cracking.
- Figure 75 shows impact of HMA mix air voids on cracking with higher air voids (high of optimum) HMA mix exhibiting higher levels of cracking. This is as expected, as higher than optimum air voids reduce AC stiffness, and increase fatigue damage and cracking.

In summary the sensitivity analyses results validate the calibration of the total alligator cracking model for Missouri.

### TOTAL RUTTING AND RUTTING FOR AC, BASE, AND SUBGRADE

Rutting is a manifestation of accumulated plastic or permanent strain in the AC, unbound base/subbase layers, and subgrade/foundation soil. Rutting is predicted by calculating the plastic vertical strain accumulated in each pavement layer due to applied truck axle loading. This is equivalent to the summation of all plastic vertical strain at the mid-depth of each pavement layer within the pavement structure, accumulated in each time increment over a given analysis period. Pavement ME Design approach to estimating total pavement rutting is based on the universal laboratory derived strain hardening relationship presented in Equation 17 and 21 for AC and unbound base/subgrade layers, respectively:

$$\Delta_{p(HMA)} = \varepsilon_{p(HMA)} h_{HMA} = \beta_{1r} k_z \varepsilon_{r(HMA)} 10^{k_{1r}} n^{k_{2r}} \beta_{2r} T^{k_{3r}} \beta_{3r} \quad (17)$$

where:

- $\Delta_{p(HMA)}$  = accumulated permanent or plastic vertical deformation in the AC layer/sublayer, in
- $\varepsilon_{p(HMA)}$  = accumulated permanent or plastic axial strain in the AC layer/sublayer, in/in
- $\varepsilon_{r(HMA)}$  = resilient or elastic strain calculated by the structural response model at the mid-depth of each AC sublayer, in/in
- $h_{(HMA)}$  = thickness of the AC layer/sublayer, in
- $n$  = number of axle load repetitions
- $T$  = mix or pavement temperature, °F
- $k_z$  = depth confinement factor
- $k_{1r}, k_{2r}, k_{3r}$  = global field calibration parameters
- $\beta_{1r}, \beta_{2r}, \beta_{3r}$  = local or mixture field calibration constants

$$k_z = (C_1 + C_2 D) 0.328196^D \quad (18)$$

$$C_1 = -0.1039(H_{HMA})^2 + 2.4868H_{HMA} - 17.342 \quad (19)$$

$$C_2 = 0.0172(H_{HMA})^2 - 1.7331H_{HMA} + 27.428 \quad (20)$$

where:

- $D$  = depth below the surface, in
- $H_{HMA}$  = total AC thickness, in

The relationship for the unbound layer is expressed as:

$$\Delta_{p(soil)} = \beta_{s1} k_{s1} \varepsilon_v h_{soil} \left( \frac{\varepsilon_p}{\varepsilon_r} \right) e^{-\left( \frac{\rho}{n} \right)^\beta} \quad (21)$$

where:

- $\Delta_{p(Soil)}$  = permanent or plastic deformation for the unbound layer/sublayer, in.

- $n$  = number of axle load applications
- $\varepsilon_o$  = intercept determined from laboratory repeated load permanent deformation tests, in/in
- $\varepsilon_r$  = resilient strain imposed in laboratory test to obtain material properties  $\varepsilon_o$ ,  $\beta$ , and  $\rho$ , in/in
- $\varepsilon_v$  = average vertical resilient or elastic strain in the layer/sublayer and calculated by the structural response model, in/in
- $h_{Soil}$  = thickness of the unbound layer/sublayer, in
- $k_{sI}$  = global calibration coefficients;  $k_{sI}=1.673$  for granular materials and 1.35 for fine-grained materials
- $\beta_{sI}$  = local calibration constant for the rutting in the unbound layers (base or subgrade). Note that  $\beta_{sI}$  represents the subgrade layer while  $\beta_{BI}$  represents the base layer

$$\text{Log}\beta = -0.61119 - 0.017638(W_c) \quad (22)$$

$$\rho = 10^9 \left( \frac{C_o}{(1-(10^9)^\beta)} \right)^{\frac{1}{\beta}} \quad (23)$$

$$C_o = \text{Ln} \left( \frac{a_1 M_r^{b_1}}{a_9 M_r^{b_9}} \right) = 0.0075 \quad (24)$$

where:

- $W_c$  = water content, percent
- $M_r$  = resilient modulus of the unbound layer or sublayer, psi
- $a_{1,9}$  = regression constants;  $a_1=0.15$  and  $a_9=20.0$
- $b_{1,9}$  = regression constants;  $b_1=0.0$  and  $b_9=0.0$

For AC over AC pavement, accumulation of additional rutting in the underlying layers is assumed to be minimal. Also, as a portion of the existing AC surface is milled or filled, initial rutting is assumed to be minimal.

### Calibration of the Rutting Models

Results of rutting model's recalibration are presented in Table 60, Table 61, Table 62, and Table 63. Figure 76 presents a plot of measured versus predicted total rutting. Missouri calibration coefficients presented in Table 60 indicates a significant deviation from the global calibration coefficients. This is as expected as the global models predicted significantly higher levels of rutting relative to field measurements in Missouri.

Table 60. Summary of local coefficients for the total rutting model

Model	Model Coefficient	Local Missouri	Global AASHTOWare Pavement ME Version 2.5.5
AC Rutting	Br1	<b>0.899</b>	0.4
Base Rutting	BS1	<b>1.0798</b>	1.0
Subgrade Rutting	BS1	<b>0.9779</b>	1.0

Table 61. Statistical comparison of field measured and Pavement ME Design predicted rutting goodness of fit for New AC and AC over AC pavements

R-Square = 34.36%, RMSE = 0.05031 inch COV = 41.11140, N = 307					
Source	DF	Sum of Squares	Mean Square	F Value	Pr > F
Model	1	0.40536	0.40536	160.15	<.0001
Error	306	0.77452	0.00253		
Corrected Total	307	1.17988			

Table 62. Hypothesis testing for field measured and Pavement ME Design predicted rutting curve slope and intercept for New AC and AC over AC pavements

Variable	DF	Parameter Estimate	Standard Error	t Value	Pr >  t	95% Confidence Limits	
Intercept	1	0.02704	0.00806	3.35	0.0009	0.01118	0.04290
Slope	1	1.00338	0.02297	43.68	0.8830	0.95818	1.04859

Table 63. Paired t-test results for field measured and Pavement ME Design predicted rutting observations for New AC and AC over AC pavements

N	Mean	Std Dev	Std Err	Minimum	Maximum	t Value	Pr >  t
308	0.00382	0.0510	0.00291	-0.1127	0.1413	1.31	0.1895

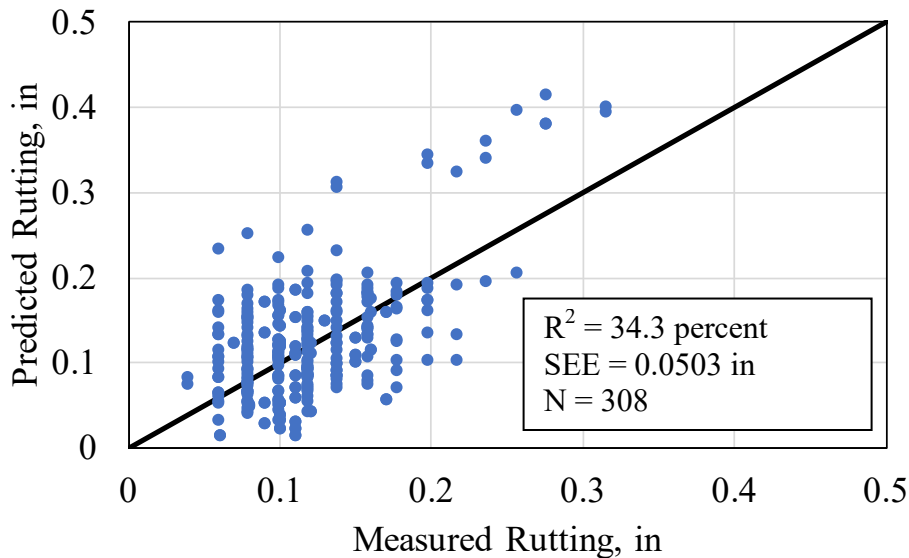


Figure 76. Pavement ME Design local calibration model predicted versus measured total rutting for New AC and AC over AC pavements

Table 61 shows a slight increase in rutting model’s goodness of fit statistic  $R^2$  (from 0.26 to 0.34). Noise in field measured rutting data negatively impacts goodness of fit statistics. Therefore, the  $R^2$  of 34 percent is considered reasonable. Table 62 and Table 63 show the results of bias testing for Missouri’s recalibrated rutting models. The information presented shows that two of the three hypotheses tests (slope of the  $y = x$  curve is not equal to 1 and measured and predicted rutting belong to different populations) were rejected. It was thus concluded that bias was mostly absent at the 95 percent significant level with the exception of near-zero rutting predictions. As threshold rutting values used to evaluate pavement performance and maintenance needs are typically greater than 0.25 in, this source of bias was not considered as significant for the use of this model.

Predicted and field measured rutting versus age is shown for select calibration projects in Figure 77 through Figure 87. The projects selected cover LTPP and MoDOT PMS sections and include different flexible pavement types that use the rutting prediction model, i.e. New AC, AC over AC, and AC over JPCP. The plots in these figures show reasonable predictions of rutting. The plots also illustrate the noise in field measured rutting data, which can negatively impact  $R^2$  obtained for the model.

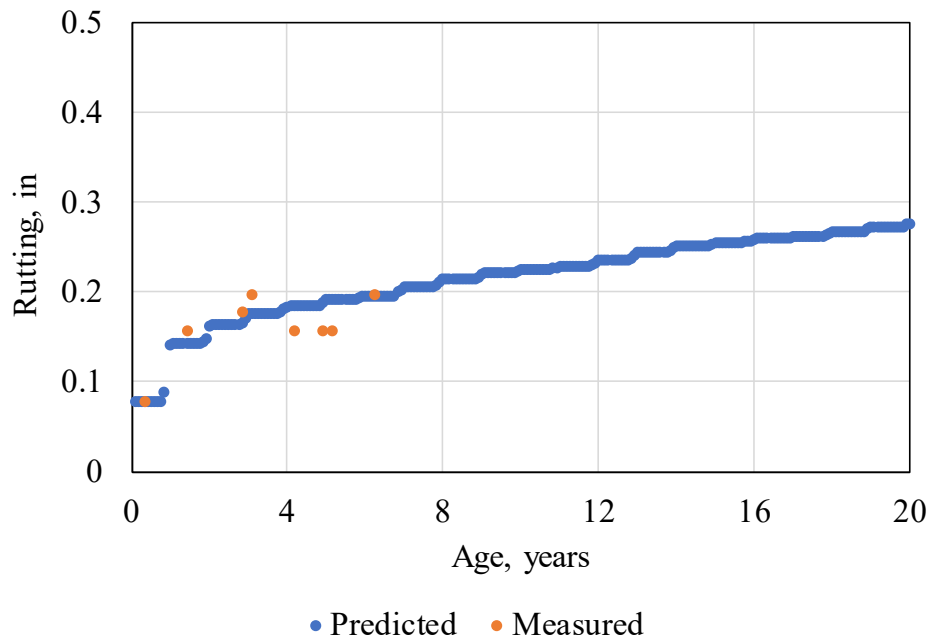


Figure 77. Pavement ME Design local calibration model predicted rutting versus age for LTPP project 0502 (AC over AC pavement)

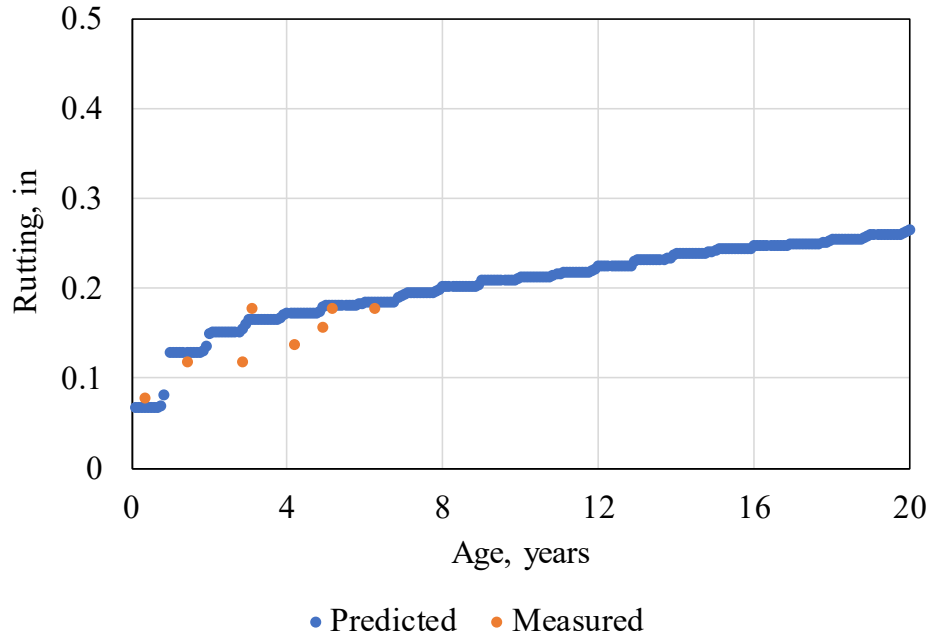


Figure 78. Pavement ME Design local calibration model predicted rutting versus age for LTPP project 0504 (AC over AC pavement)

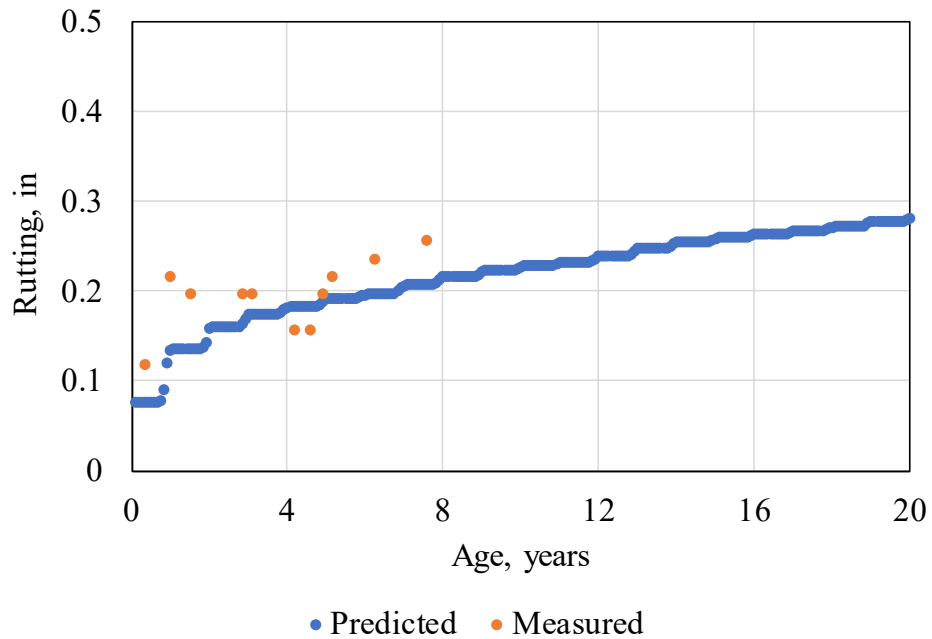


Figure 79. Pavement ME Design local calibration model predicted rutting versus age for LTPP project 0508 (AC over AC pavement)

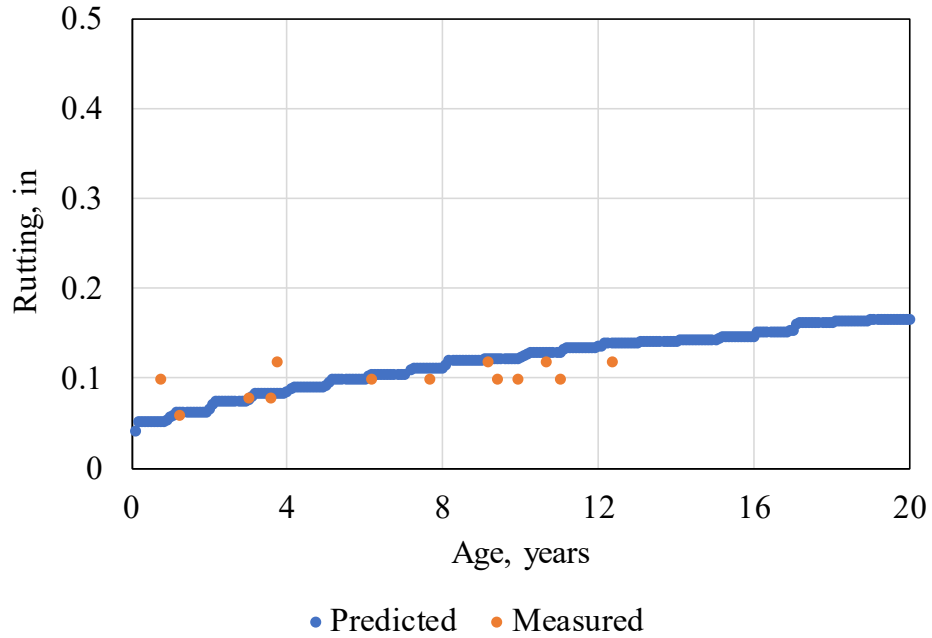


Figure 80. Pavement ME Design local calibration model predicted rutting versus age for LTPP project 0608 (AC over JPCP)

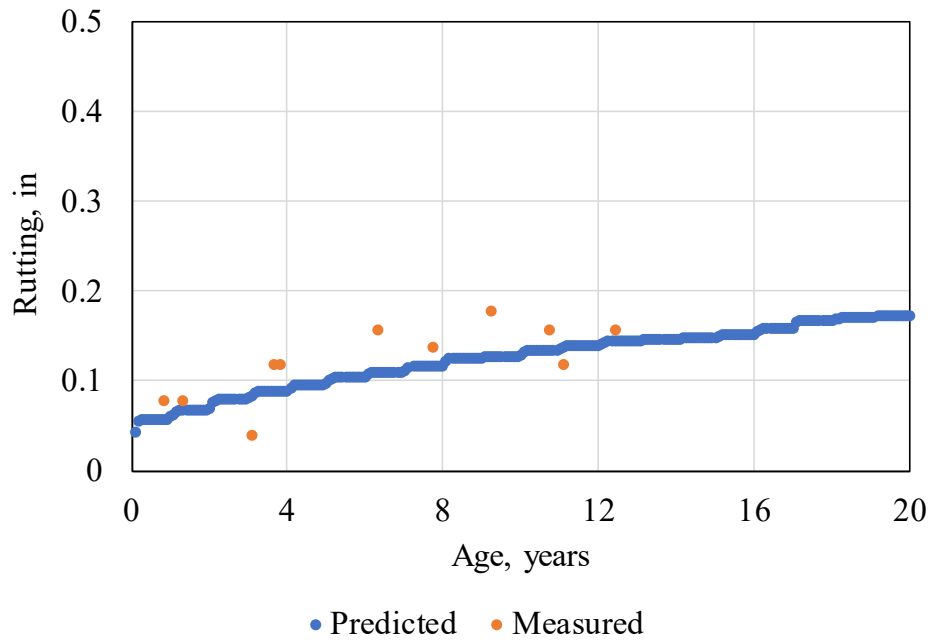


Figure 81. Pavement ME Design local calibration model predicted rutting versus age for LTPP project 0662 (AC over JPCP)

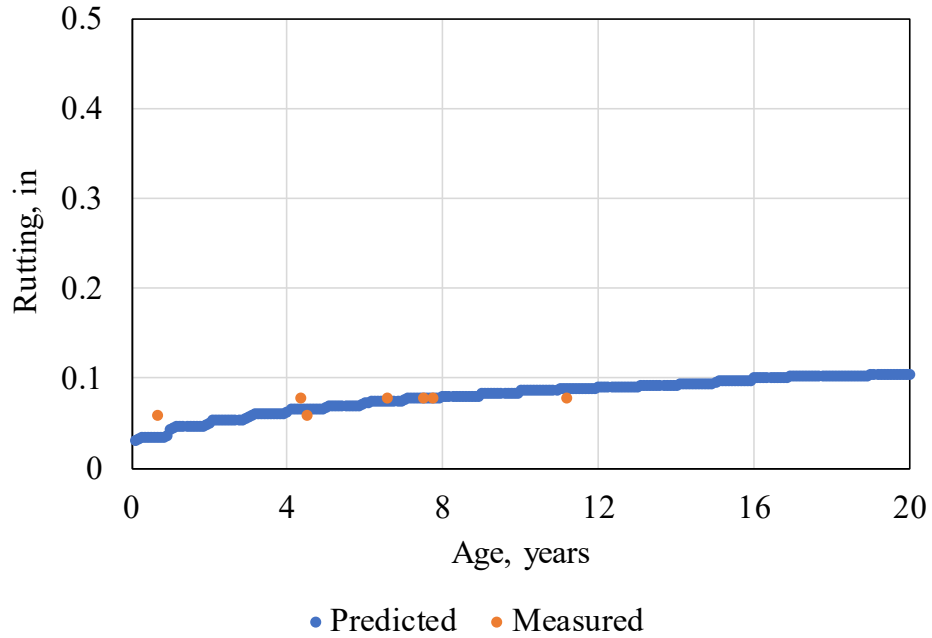


Figure 82. Pavement ME Design local calibration model predicted rutting versus age for LTPP project 0901 (AC over JPCP)

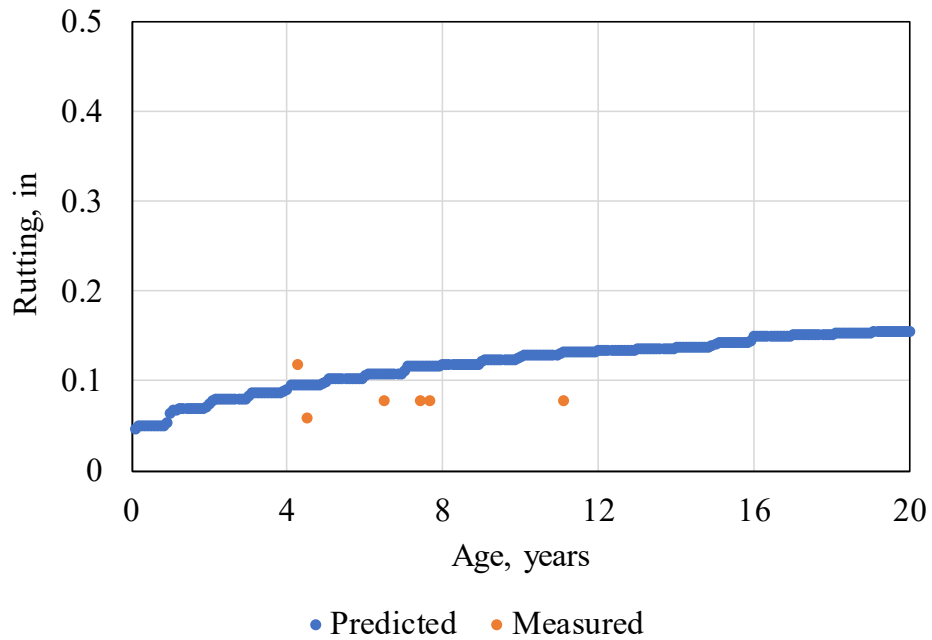


Figure 83. Pavement ME Design local calibration model predicted rutting versus age for LTPP project 0903 (AC over JPCP)

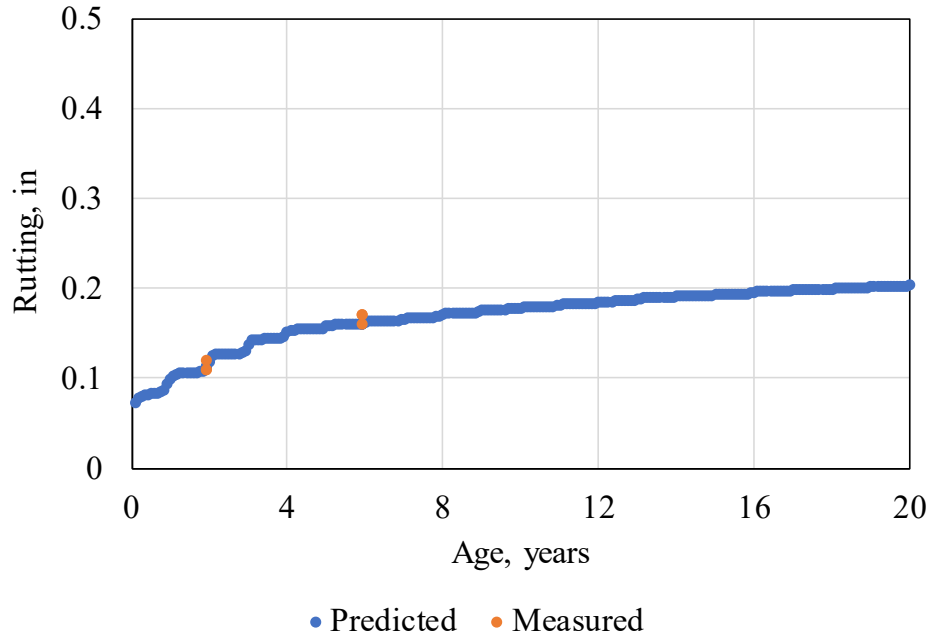


Figure 84. Pavement ME Design local calibration model predicted rutting versus age for MoDOT PMS project FDA1-S1 (New AC pavement)

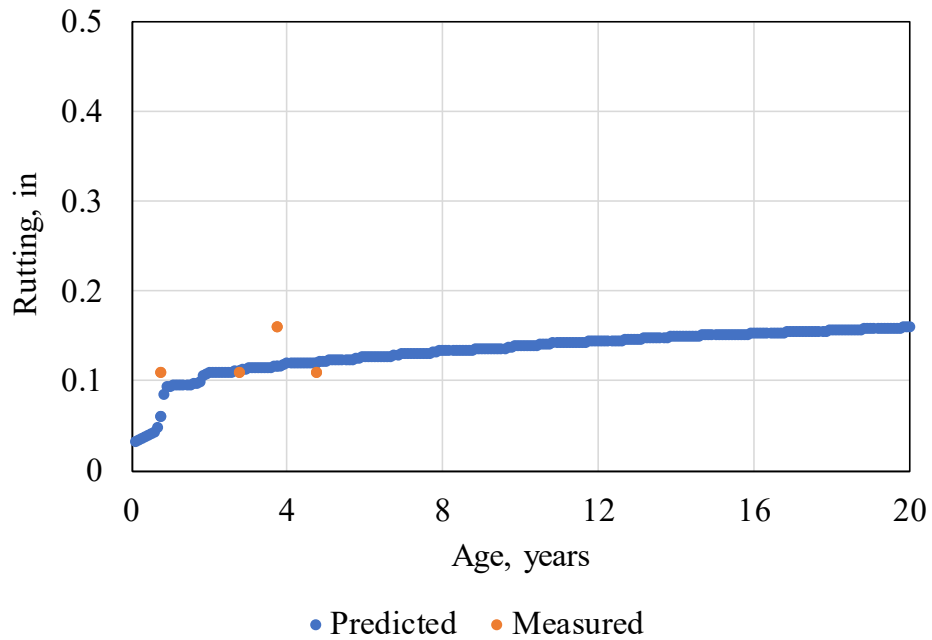


Figure 85. Pavement ME Design local calibration model predicted rutting versus age for MoDOT PMS project FDA3 (New AC pavement)

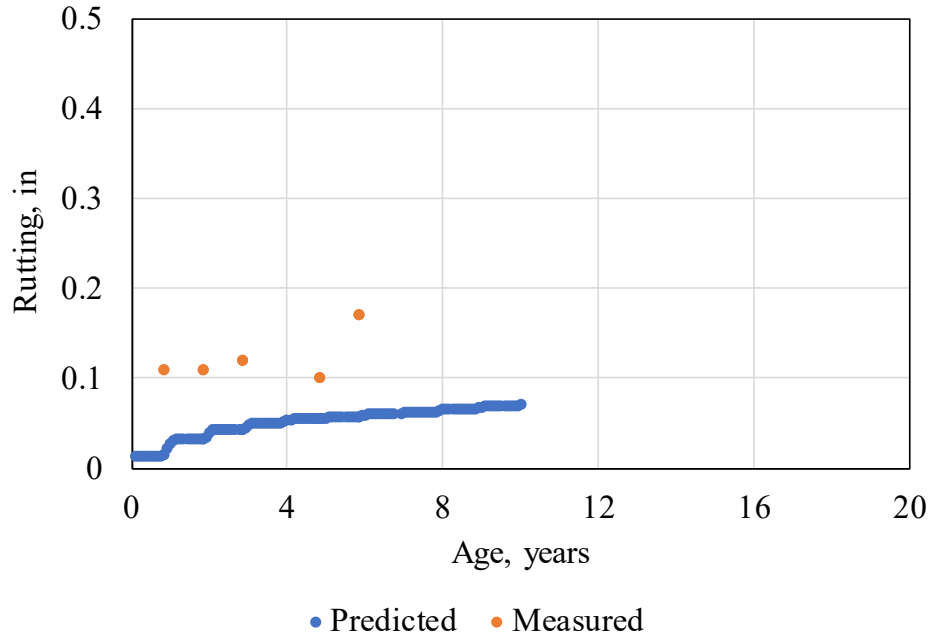


Figure 86. Pavement ME Design local calibration model predicted rutting versus age for MoDOT PMS project AOA3 (AC over AC pavement)

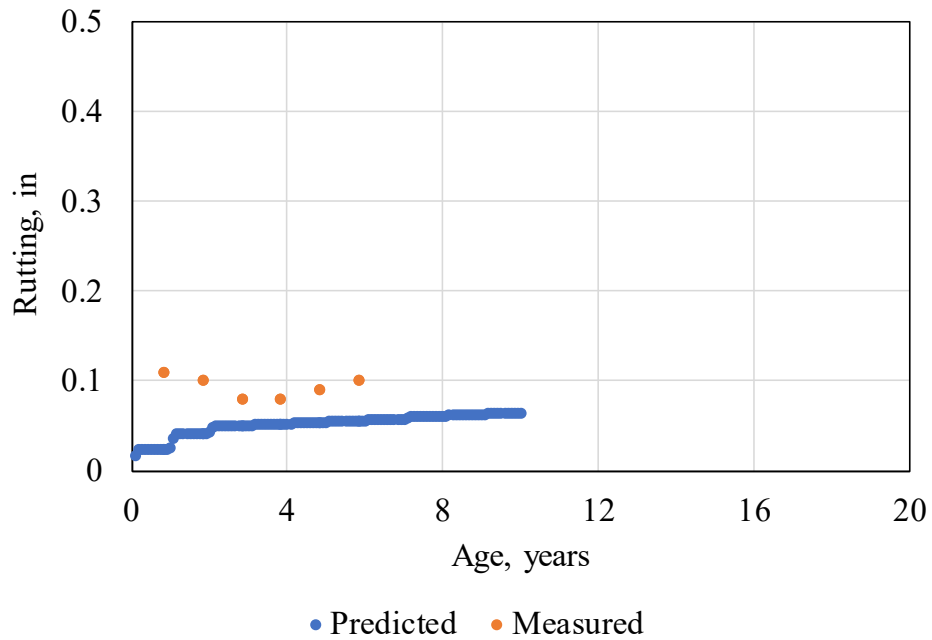


Figure 87. Pavement ME Design local calibration model predicted rutting versus age for MoDOT PMS project AOA1 (AC over AC pavement)

As stated in the previous section describing the validation of the alligator cracking model, sensitivity analyses were used to validate the rutting model as well. The same designs for New AC and AC over AC designs were used for the evaluation of critical parameters that are sensitive to rutting prediction. Specifically impacts of AC thickness, location (ambient temperature), and HMA mix air voids on predicted total rutting were investigated. The results are presented in Figure 88, through Figure 91.

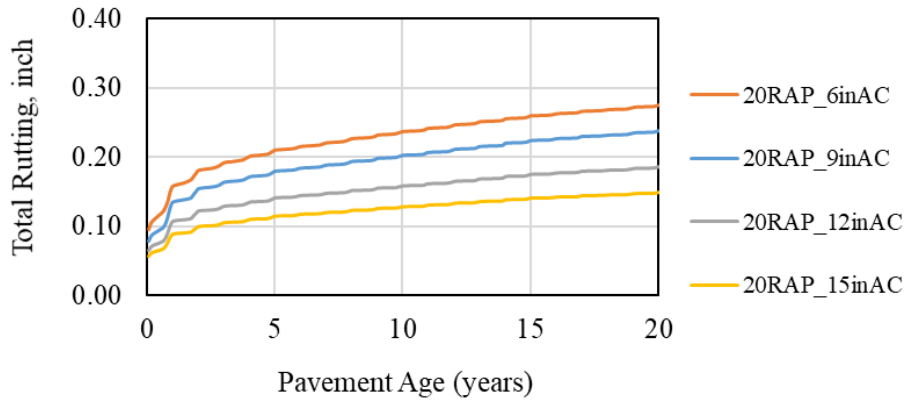


Figure 88. Impact of AC thickness on local calibration predicted total rutting for Missouri

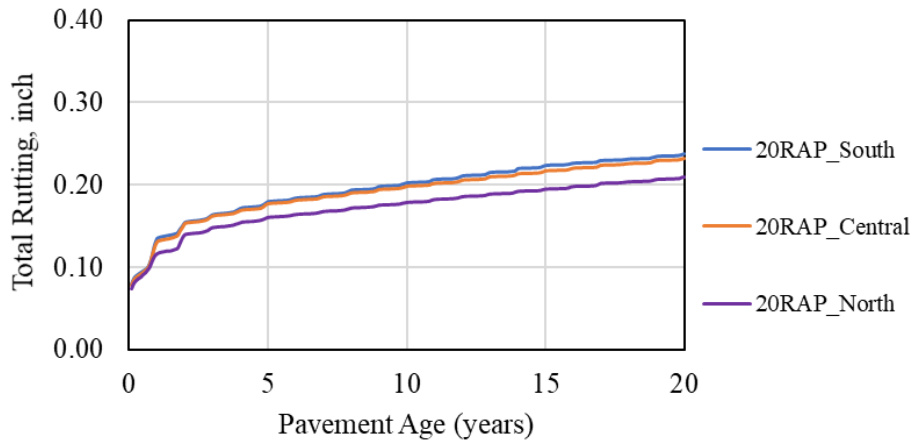


Figure 89. Impact of climate on local calibration predicted total rutting for Missouri

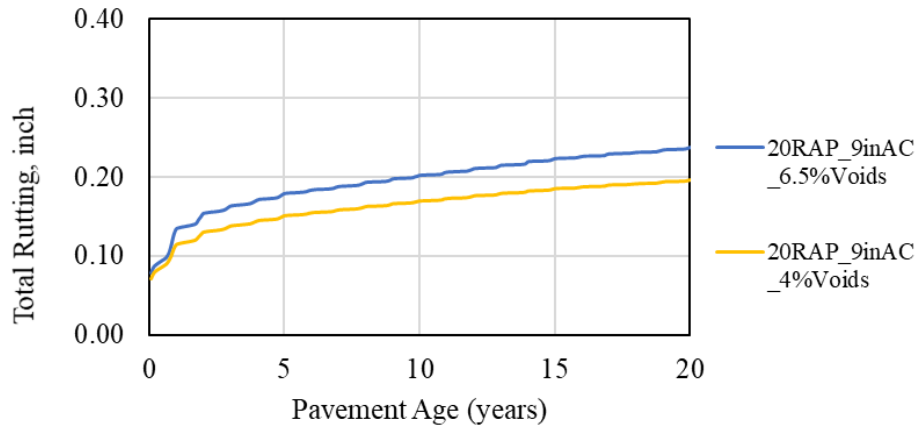


Figure 90. Impact of HMA air voids on local calibration predicted total rutting for Missouri

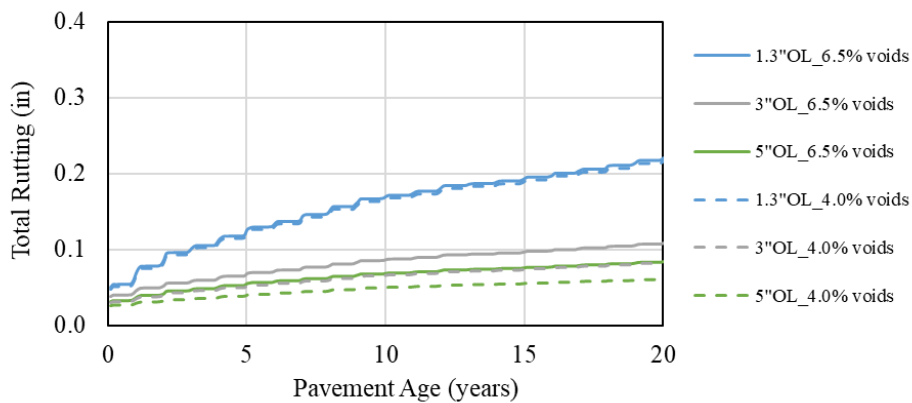


Figure 91. Impact of HMA air voids and overlay thickness on local calibration predicted total rutting for Missouri

Results of the sensitivity analyses presented in Figure 88 through Figure 91 show the following:

- Predictions of total rutting using the locally calibrated model are significantly influenced by AC thickness as shown in Figure 88. A 9-inch increase in thickness (from 6 to 15 inches) results in a reduction in rutting of 0.125 in. A 100 percent increase in thickness (6 to 12 inches) causes a reduction of 0.09 inches in rutting. Similar trends were noticed on the impact of AC overlay thickness on rutting. The effect of thickness would vary depending on the stiffness of the subgrade. The impact of thickness on predicted total rutting was therefore deemed reasonable.
- Figure 89 shows that the warmer (south) region of the state exhibited higher levels of total rutting when compared to the colder (north) region. HMA temperature does have a significant impact on dynamic modulus, stress, and strain. The stiffer mixes in the north

is expected to exhibit lower levels of vertical strain when subjected to similar truck loading and thus less accumulation of plastic strain and rutting.

- Figure 90 and Figure 91 shows impact of HMA mix air voids on rutting. Mixes with higher air voids (high of optimum) exhibit higher levels of total rutting. This is as expected as higher than optimum air voids do result in less AC layer stiffness, higher strain levels and rutting. Higher air voids also imply greater ability for consolidation of the HMA mix under traffic loading. Poor consolidation manifests itself as rutting. Figure 91, a sensitivity plot for the effect of AC thickness and voids in AC over AC design, also shows the interaction effect of mix design and structural design for rutting prediction. At very low AC thickness levels, the benefit of lower air voids diminishes. However, at higher AC overlay thickness levels (between 3 and 5 inches), Figure 91 demonstrates that a low air voids level can provide the same benefit of increasing thickness.

In summary the sensitivity analyses results validate the calibration of the rutting prediction model in New AC, AC over AC, and AC over JPCP designs for Missouri.

## TOTAL TRANSVERSE “THERMAL + REFLECTION” CRACKING

### Low Temperature Thermal Cracking

Thermal crack development and propagation is induced by thermal stresses generated by thermal cooling cycle, and is predicted using the expression (AASHTO 2015):

$$\Delta C = A(\Delta K)^n \quad (25)$$

where:

$\Delta C$  = change in the crack depth due to a cooling cycle

$\Delta K$  = change in the stress intensity factor due to a cooling cycle

$A, n$  = fracture parameters for the HMA mixture

Experimental results indicate that reasonable estimates of  $A$  and  $n$  can be obtained from the indirect tensile creep compliance and strength of the HMA in accordance with equations 26 and 27 (AASHTO 2015):

$$A = 10^{k_t \beta_t (4.389 - 2.52 \text{Log}(E_{HMA} \sigma_m^n))} \quad (26)$$

$$n = 0.8 \left[ 1 + \frac{1}{m} \right] \quad (27)$$

where:

$k_t$  = coefficient determined through global calibration for each input level

$E_{HMA}$  = HMA indirect tensile modulus, psi

$\sigma_m$  = mixture tensile strength, psi

$m$  = m-value derived from the indirect tensile creep compliance curve

$\beta_t$  = local or mixture calibration factor

Stress intensity factor,  $K$ , was incorporated in the Pavement ME Design procedure through the use of a simplified equation developed from theoretical finite element studies (equation 28):

$$K = \sigma_{tip} \left( 0.45 + 1.99(C_o)^{0.56} \right) \quad (28)$$

where:

- $\sigma_{tip}$  = far-field stress from pavement response model at depth of crack tip, psi
- $C_o$  = current crack length, ft

The amount of transverse cracking is predicted using an assumed relationship between the probability distribution of the log of the crack depth to AC layer thickness ratio and the percent of cracking. Equation 29 shows the expression used to determine the amount of thermal cracking (AASHTO 2015):

$$TC = \beta_{t1} N \left[ \frac{1}{\sigma_d} \text{Log} \left( \frac{C_d}{H_{HMA}} \right) \right] \quad (29)$$

where:

- $TC$  = thermal cracking, ft/mi
- $\beta_{t1}$  = regression coefficient determined through global calibration
- $N[z]$  = standard normal distribution evaluated at  $[z]$
- $\sigma_d$  = standard deviation of the log of the depth of cracks in the pavement (0.769), in
- $C_d$  = crack depth, in
- $H_{HMA}$  = thickness of AC layers, in

### Transverse Reflection Cracking

Transverse reflection cracking prediction was done using the model forms presented as Equations 14, 15, and 16 for alligator reflection cracking. Note that for the Pavement ME Design procedure, the model forms for reflection cracking are the same regardless of the underlying crack type because the mode of crack propagation (i.e., bending, shear, and thermal) are applicable to all existing crack types. The rate of crack propagation and the weights assigned to the different propagation modes differ by crack type. As previously described, transverse cracking due to shrinkage of the HMA binder/mix hardening is not considered by Pavement ME Design. This may have a considerable impact on accuracy of predictions in the warmer parts of Missouri where transverse cracking is more likely to be due to shrinkage rather than low temperature cycles.

### Calibration of Transverse Thermal and Reflection Cracking Model

LTPP classifies a major part of Missouri under the wet freeze climate zone. The Pavement ME Design tool low temperature thermal cracking model divides all climate into two zones according to reported MAAT value in the climate data. The divide is at a MAAT value of 57 °F. A review of MAAT computed for all the projects utilized for local calibration indicates MAAT values for sections in the Moderate and High Freeze zones of Figure 41 are less than 57 °F (see Table 12). Therefore, the thermal cracking model for MAAT < 57 °F and the transverse reflection cracking models were calibrated. The models were calibrated simultaneously for both New AC and AC over AC pavements and AC over JPCP. Model coefficients for the locally

calibrated prediction model are presented in Table 64. Figure 92 shows a plot of predicted versus measured transverse cracking.

Table 64. Summary of local coefficients for thermal cracking and reflection cracking

Model	Model Coefficient	Local Missouri	Global AASHTOWare Pavement ME Version 2.5.5
Low temperature HMA cracking	K1	<b>0.61</b>	1.0
Reflection transverse cracking	C1	<b>0.6</b>	3.22
	C2	<b>0.5</b>	25.7
	C3	<b>4280.1</b>	0.1
	C4	<b>254.4</b>	133.4
	C5	<b>-261.6</b>	-72.4
	K1	0.012	0.012
	K2	0.005	0.005
	K3	1	1

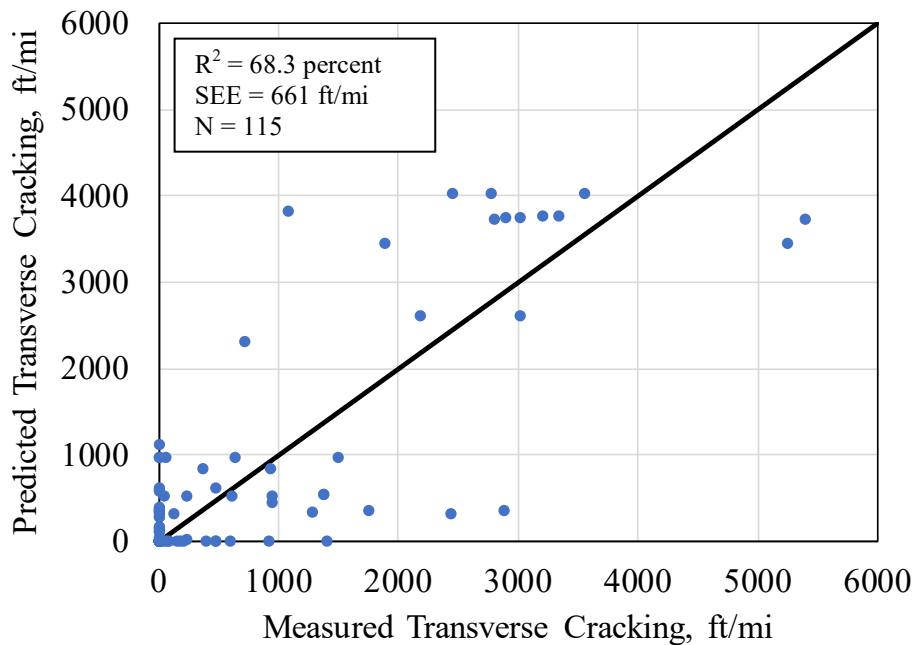


Figure 92. Pavement ME Design local calibration model predicted versus measured transverse cracking

Measured and Pavement ME Design predicted transverse cracking produced with the local calibrated models were analyzed to characterize goodness of fit and identify bias. The results are presented in Table 65 through Table 67 and show the following:

Table 65. Statistical comparison of field measured and Pavement ME Design predicted transverse cracking goodness of fit for New AC, AC over AC, and AC over JPCP

<b>R-Square = 68.32%, RMSE = 661.6 ft/mile, COV = 105.9, N = 115</b>					
Source	DF	Sum of Squares	Mean Square	F Value	Pr > F
Model	1	107646937	107646937	245.90	<0.0001
Error	114	49905759	437770		
Corrected Total	115	157552697			

Table 66. Hypothesis testing for field measured and Pavement ME Design predicted transverse cracking curve slope and intercept for New AC, AC over AC, and AC over JPCP

Variable	DF	Parameter Estimate	Standard Error	t Value	Pr >  t	95% Confidence Limits	
Intercept	1	124.59697	69.22005	1.80	0.0745	-12.52742	261.72136
Slope	1	0.91302	0.04955	18.43	0.0819	0.81486	1.01117

Table 67. Paired t-test results for field measured and Pavement ME Design predicted transverse cracking observations for New AC, AC over AC, and AC over JPCP

N	Mean	Std Dev	Std Err	Minimum	Maximum	t Value	Pr >  t
116	47.9597	675.2	62.6935	-2522.5	2740.2	0.76	0.4458

- Goodness of fit was very good, with an  $R^2 = 68.3$  percent, which implies good relationship between the Pavement ME Design transverse cracking predictions and field-measured/observed transverse cracking.
- The null hypothesis intercept = 0 was accepted as p-value was 0.0745 and thus greater than 0.05 (5 percent significance level). This implies no significant bias for low transverse cracking values.
- The null hypothesis slope = 1.0 was accepted as p-value of 0.0819 was greater than 0.05.
- Paired t-test reported a p-value of 0.04458. The predicted and measured cracking values were thus deemed to belong to the same populations as the null hypothesis was rejected.
- Accepting all three hypotheses was an indication of the absence of significant bias in predicted transverse cracking using the locally calibrated models.

Figure 93 through Figure 96 shows examples of predicted and measured transverse cracking versus age for selected representative projects from the calibration dataset. The plots show reasonable agreement between measured and predicted values of transverse cracking.

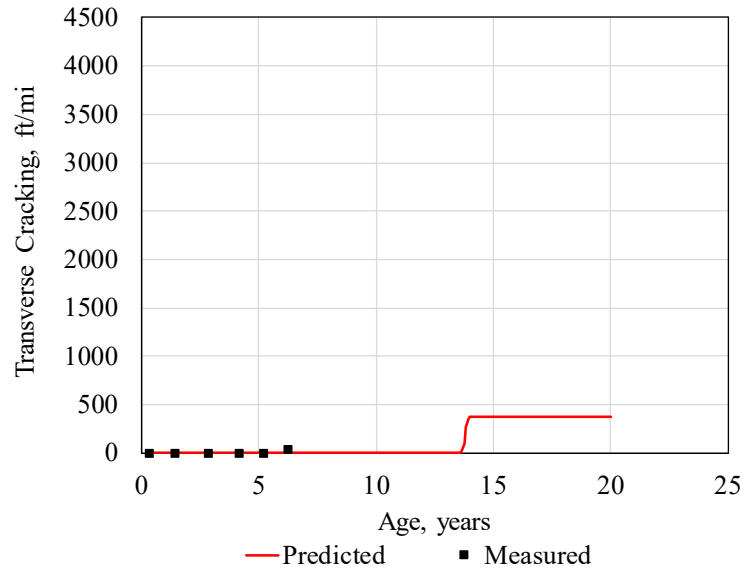


Figure 93. Pavement ME Design local calibration predicted versus measured transverse cracking for LTPP project 0505 (AC over AC)

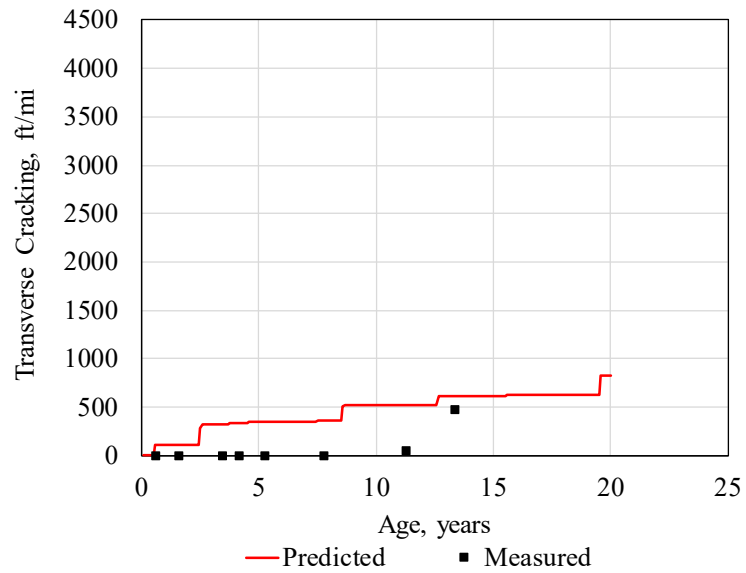


Figure 94. Pavement ME Design local calibration versus measured transverse cracking for LTPP project 0802 (New AC)

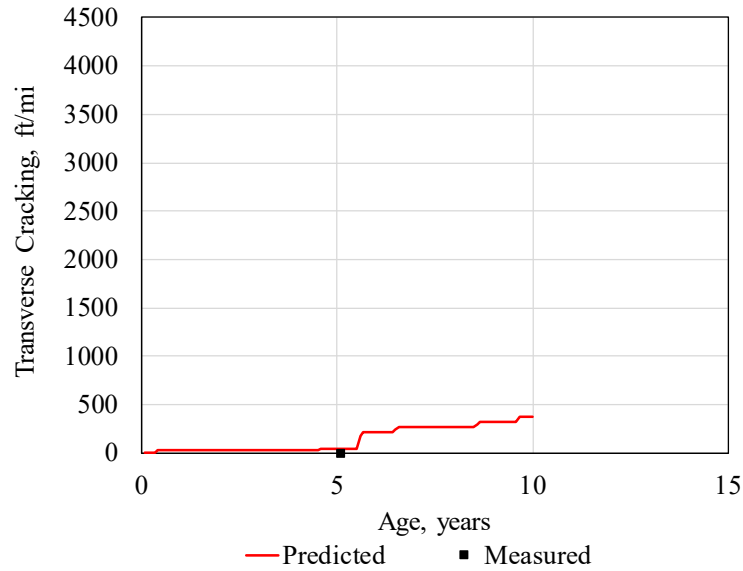


Figure 95. Pavement ME Design local calibration versus measured transverse cracking for MoDOT PMS project AOA2 (AC over AC)

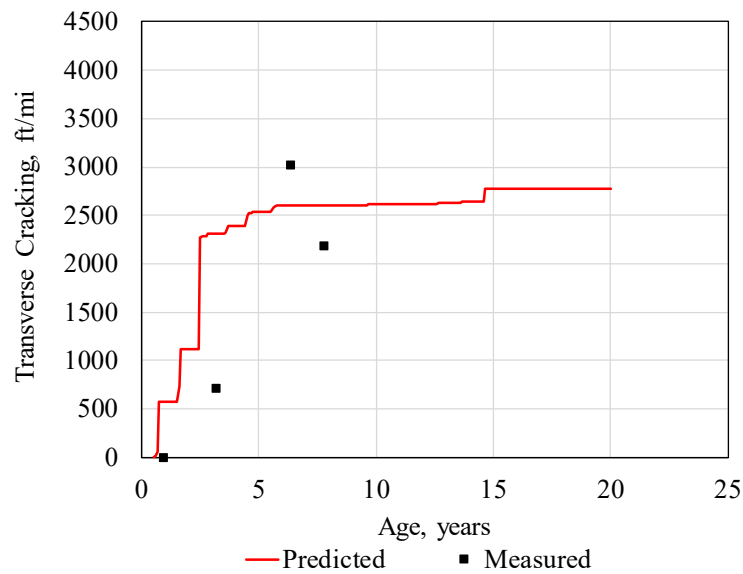


Figure 96. Pavement ME Design local calibration versus measured transverse cracking for LTPP project 0665 (AC over JPCP)

Further validation of the model was done through sensitivity analyses. Specifically impacts of AC thickness, location (ambient temperature), and HMA mix air voids on predicted transverse

cracking (low temperature cracks only) were investigated. The results are presented in Figure 97, Figure 98, and Figure 99.

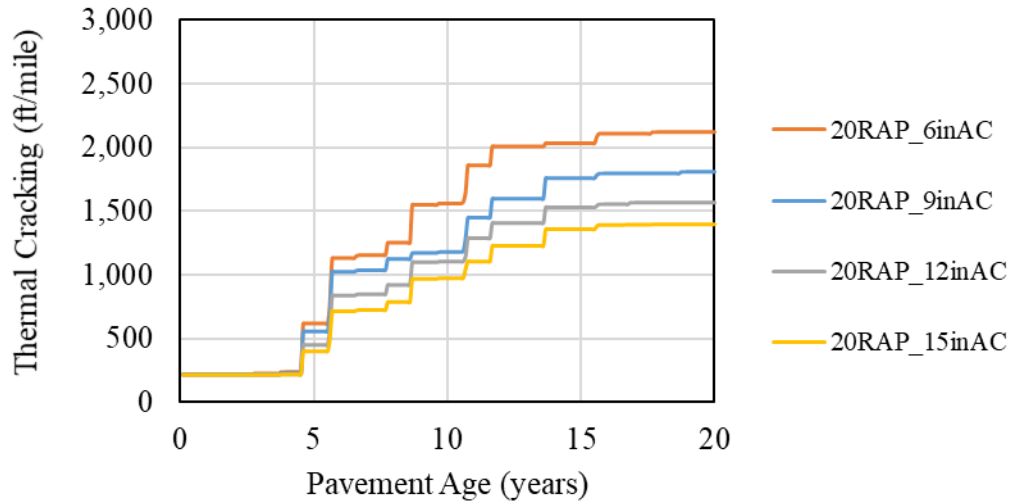


Figure 97. Impact of AC thickness on local calibration predicted thermal transverse cracking for Missouri

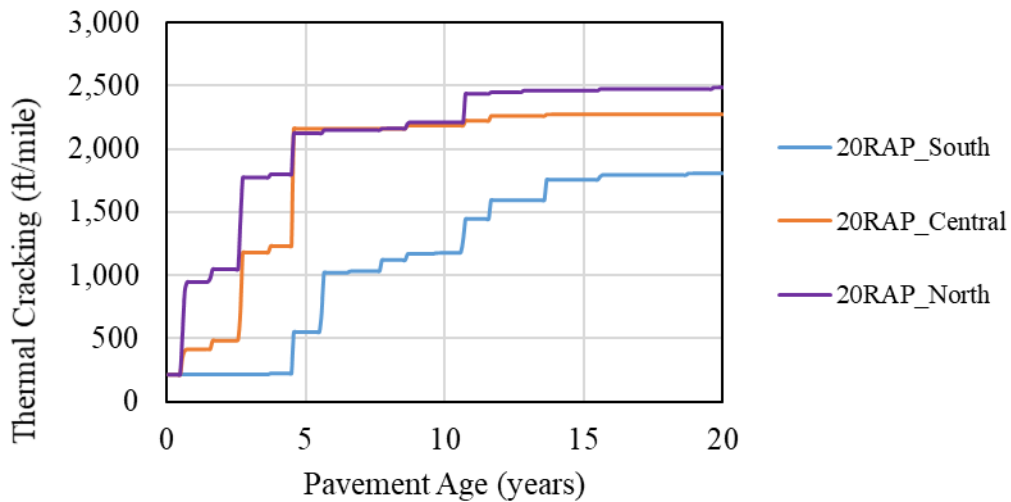


Figure 98. Impact of climate on local calibration predicted thermal transverse cracking for Missouri

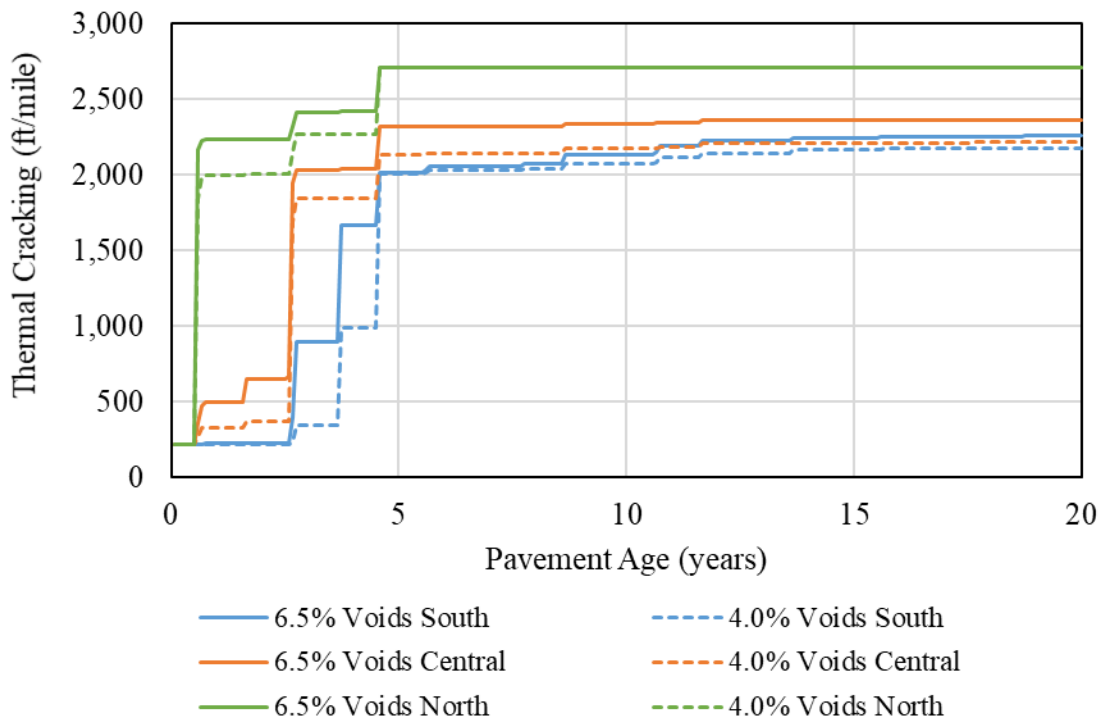


Figure 99. Impact of climate and air voids on local calibration predicted thermal transverse cracking for Missouri

The sensitivity analysis results presented in Figure 97, Figure 98, and Figure 99 show the following:

- Increasing AC thickness significantly reduced low temperature transverse cracking with length of cracking reducing from 2200 ft/mi to 1400 ft/mi with AC thickness increasing from 6 inches to 15 inches (see Figure 97).
- Project location (i.e., ambient temperature and frequency of low temperature cycles) had a considerable impact on predicted cracking as is expected (see Figure 98), although note that transverse cracking is less sensitive to MAAT with the local calibration than with the global calibration model. Predicted cracking for projects located in the southern part of the state was approximately 1800 ft/mi while projects in the colder northern areas had 2500 ft/mi of cracking, which is about 40 percent increase in distress prediction.
- Figure 99 shows impact of HMA air voids (4- and 6.5-percent) and climate on predicted thermal transverse cracking. The HMA mix inputs used for the surface layer for this comparison was one that had the highest difference in indirect tensile strength between 6.5% and 4.0% voids levels. The measured indirect tensile strengths were 775psi at 4% voids, and 510 psi at 6.5% voids. Note that the locations used for the evaluation of the effect of climate had MAAT values of 56F in the southern, 55F in the central, and 51F in the northern region of Missouri. This figure shows that the climate has a greater impact on thermal cracking than material properties, in this case.

- At the next level beyond the effect of climate, this figure also shows HMA mixes with higher air voids (i.e., lower tensile strength and higher creep compliance values) predicted higher thermal cracking as compared to HMA mixes with lower air voids (higher tensile strength and lower creep compliance). This outcome shows that the impact of HMA tensile strength on HMA low temperature cracking is an important factor. Increasing HMA tensile strength may be an approach to mitigate this distress. Similar trends were observed in the sensitivity analyses performed for rehabilitation designs with AC overlays.

In summary the sensitivity analyses results validate the calibration of the transverse thermal and reflection cracking prediction models in New AC, AC over AC, and AC over JPCP designs for Missouri.

### PAVEMENT SMOOTHNESS (IRI) MODELS FOR NEW AC, AC OVER AC, AND AC OVER JPCP

The IRI prediction model in the original MEPDG procedure (ARA, 2004) was fundamentally based on findings from multiple research studies suggesting IRI over time is a function of initial roughness at construction, and structural distress development that contribute to poor ride quality. The IRI model is hence a correlation between IRI at a given age and, the initial IRI and distress development. Overall pavement condition indicator — smoothness — is highly correlated with driver/passenger user comfort, safety, and vehicle operating cost (VOC). Thus, AASHTO Pavement ME design includes a smoothness prediction model that relates distress development with overall pavement condition. The goal is to limit distress to levels that do not adversely impact overall condition. Smoothness (IRI) prediction model for New AC and AC over AC pavements is presented as Equation 30 (AASHTO 2015).

$$IRI = IRI_o + 0.0150(SF) + 0.400(FC_{Total}) + 0.0080(TC) + 40.0(RD) \quad (30)$$

where:

- $IRI_o$  = initial IRI after construction, in/mi
- $SF$  = site factor, refer to equation 31
- $FC_{Total}$  = areal extent of alligator, longitudinal, and reflection cracking in the wheel path reported in terms of percent of total lane area.
- $TC$  = length of transverse cracking (including the reflection of transverse cracks in existing AC pavements), ft/mi.
- $RD$  = average rut depth, in

The site factor is calculated in accordance with the following equation:

$$SF = FROSTH + SWELLP * AGE^{1.5} \quad (31)$$

where:

- FROSTH =  $\text{LN}([\text{PRECIP}+1] * \text{FINES} * [\text{FI}+1])$
- SWELLP =  $\text{LN}([\text{PRECIP}+1] * \text{CLAY} * [\text{PI}+1])$
- FINES = FSAND + SILT
- AGE = pavement age, years
- PI = subgrade soil plasticity index

- PRECIP = mean annual precipitation, in.  
 FI = mean annual freezing index, deg. F Days  
 FSAND = amount of fine sand particles in subgrade (percent of particles between 0.074 and 0.42 mm)  
 SILT = amount of silt particles in subgrade (percent of particles between 0.074 and 0.002 mm)  
 CLAY = amount of clay size particles in subgrade (percent of particles less than 0.002 mm)

For AC over JPCP, smoothness is forecast using the equation below (AASHTO 2015):

$$IRI = IRI_0 + 40.8(RD) - 0.575*(FC_{Total}) - 0.0014(TC) + 0.00825(SF) \quad (32)$$

where all inputs are as already defined.

As the various distress prediction models that provide inputs to the HMA surfaced pavements smoothness models (presented as Equations 30 and 32) were recalibrated, it was logical to recalibrate the smoothness models.

### Calibration of New AC and AC over AC Smoothness Model

Results of New AC and AC over AC smoothness model recalibration are presented in Table 68, Table 69, Table 70, and Table 71. Figure 76 presents a plot of measured versus predicted smoothness.

Table 68. Summary of local coefficients for the New AC and AC over AC smoothness model

Distress Model	Model Coefficient	Local Missouri	Global AASHTOWare Pavement ME Version 2.5.5
Fatigue Cracking <sub>Total</sub>	C1	0.3	0.4
Rut Depth	C2	58.9	40.8
Transverse Cracking	C3	0.0072	0.008
Site Factor	C4	0.0129	0.015

Table 69. Statistical comparison of field measured and Pavement ME Design predicted IRI goodness of fit for New AC and AC over AC pavements

R-Square = 85.6%, RMSE = 6.80 in/mile, COV = 10.3, N = 113					
Source	DF	Sum of Squares	Mean Square	F Value	Pr > F
Model	1	31494	31494	680.24	<.0001
Error	112	5185.36242	46.297		
Corrected Total	113	36679			

Table 70. Hypothesis testing for field measured and Pavement ME Design predicted IRI slope and intercept for New AC and AC over AC pavements

Variable	DF	Parameter Estimate	Standard Error	t Value	Pr >  t	95% Confidence Limits	
Intercept	1	-2.18211	2.69552	-0.81	0.4199	-7.52294	3.15872
Slope	1	0.99431	0.00928	107.15	<.0001	0.97593	1.01270

Table 71. Paired t-test results for field measured and Pavement ME Design predicted IRI observations for New AC and AC over AC pavements

N	Mean	Std Dev	Std Err	Minimum	Maximum	t Value	Pr >  t
114	-0.5010	6.7865	0.6356	-21.1661	20.5846	-0.79	0.4322

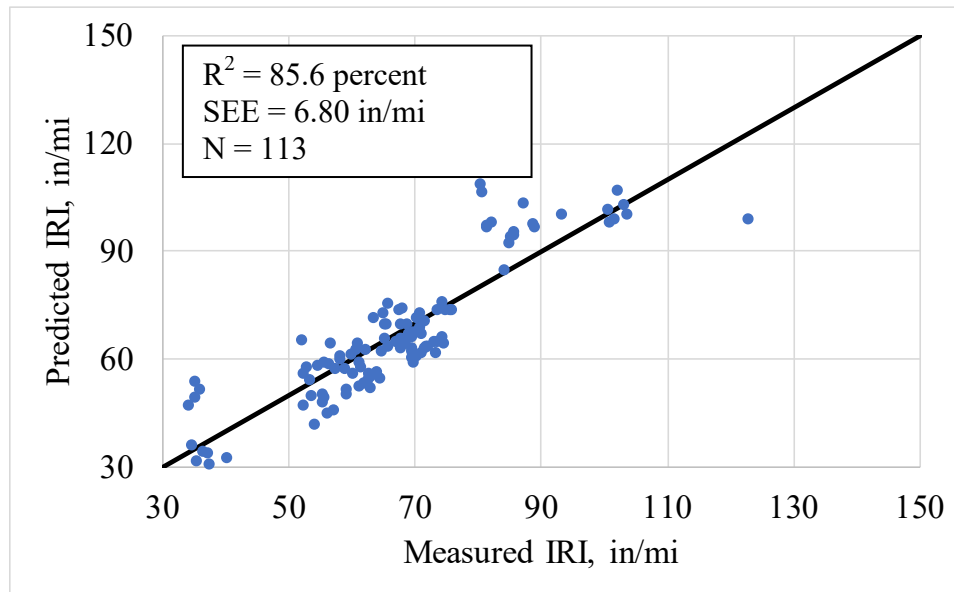


Figure 100. Pavement ME Design local calibration predicted versus field measured IRI for New AC and AC over AC pavements

Data in Table 68 shows the recalibrated New AC and AC over AC IRI model coefficients not very different from the global models' coefficients. Table 69 shows a very good goodness of fit statistic  $R^2$  of 85.6 percent. Table 70 and Table 71 show the results of bias testing for the recalibrated IRI models. The information presented shows no significant bias produced by the locally calibrated IRI model for New AC and AC over AC pavements. All three hypothesis in the statistical tests used to check for bias, were accepted (i.e., intercept of linear model of predicted and measured IRI was 0, slope of the predicted IRI versus measured IRI linear model is equal to 1, and measured and predicted IRI belong to the same populations).

Predicted and field measured IRI versus age comparisons are shown for three projects in Figure 101 to Figure 103. The plots in these figures show reasonable predictions of IRI.

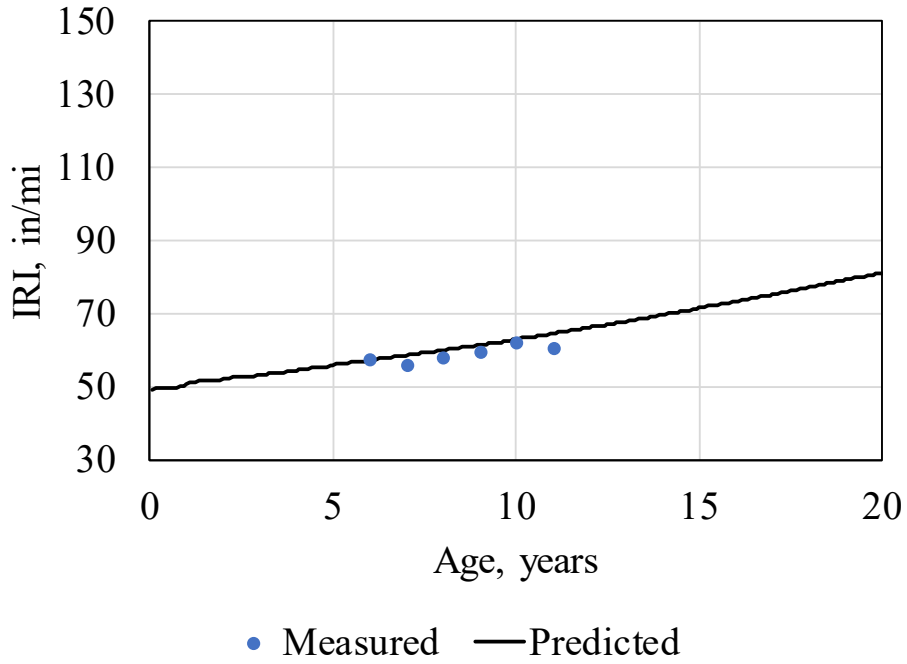


Figure 101. Pavement ME Design predicted versus measured IRI for project FDA2 (New AC)

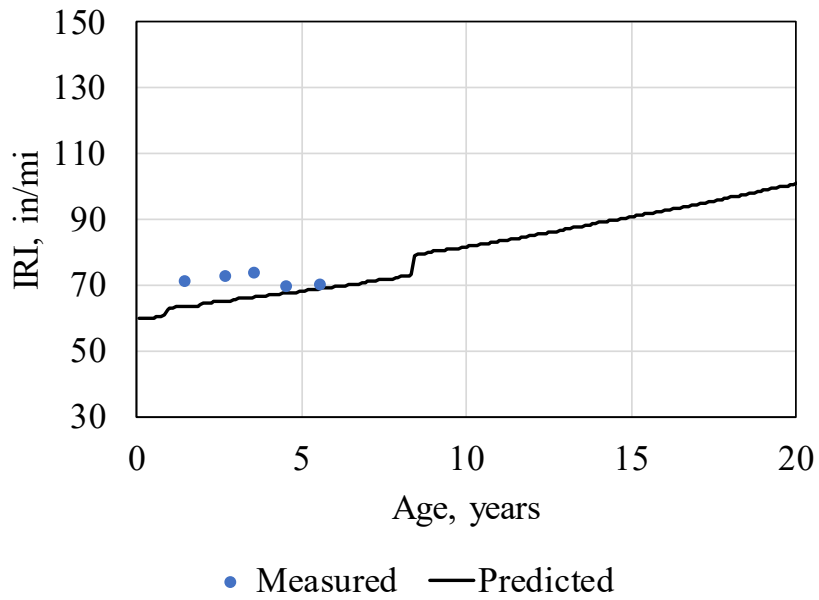


Figure 102. Pavement ME Design local calibration predicted versus measured IRI for LTPP project 0502 (AC over AC)

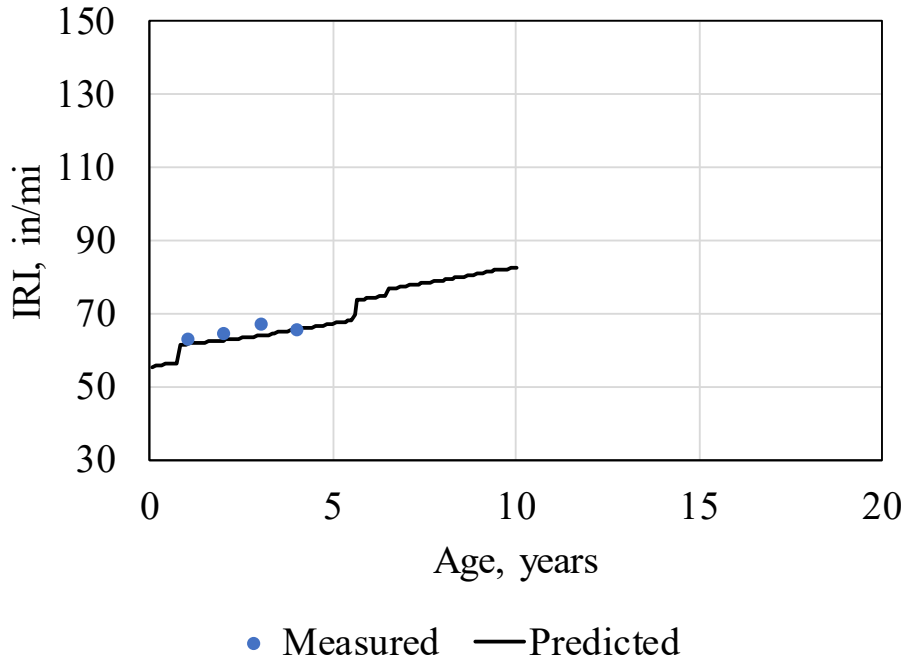


Figure 103. Pavement ME Design local calibration predicted versus measured IRI for project AOA4 (AC over AC)

A sensitivity analysis of the smoothness model was performed using inputs from the recalibrated alligator cracking, transverse cracking, and rutting models. The goal was to assess reasonableness of the locally calibrated New AC and AC over AC IRI model. The verification sensitivity analysis evaluated the impact of AC thickness, climate and HMA air voids on the predicted IRI. The results are presented in Figure 104, Figure 105, and Figure 106.

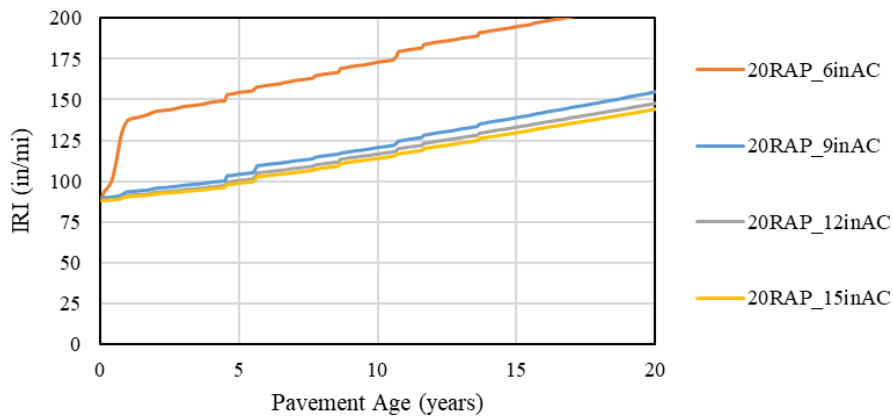


Figure 104. Impact of AC thickness on local calibration model predicted IRI

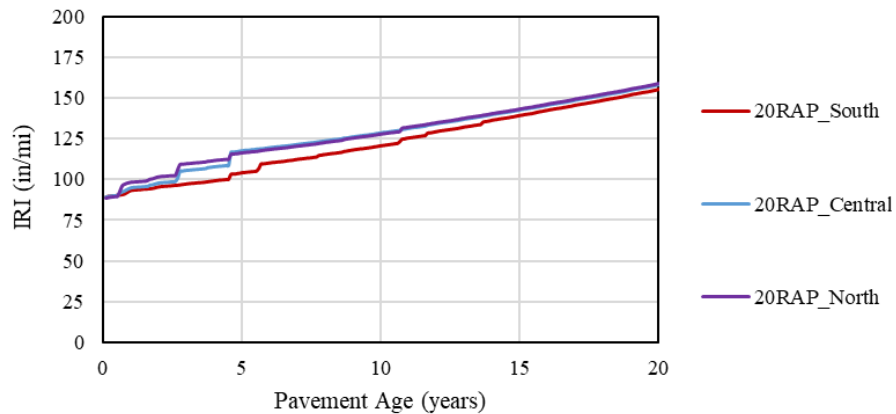


Figure 105. Impact of climate on local calibration predicted IRI

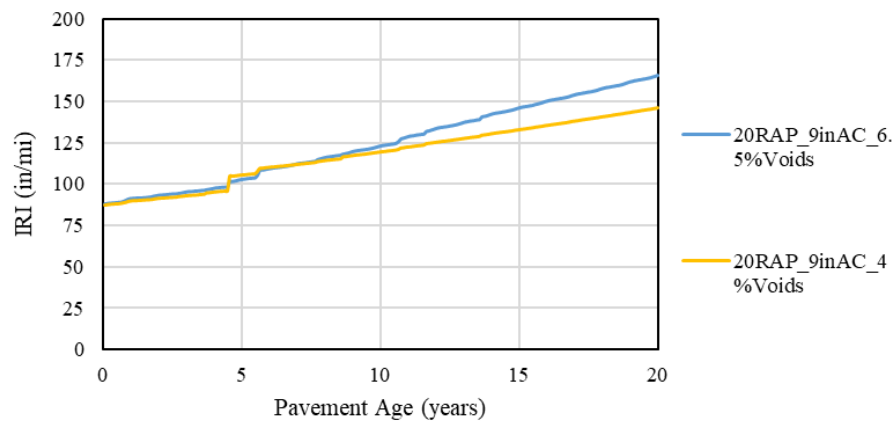


Figure 106. Impact of HMA air voids on local calibration predicted IRI

The sensitivity analysis results presented in Figure 104, Figure 105, and Figure 106 show the following:

- Increasing AC thickness significantly reduced IRI. IRI decreased from 215 in/mi to 147 in/mi with AC thickness increasing from 6 inches to 15 inches. Decrease in IRI was, however, not linear. There was a significantly higher reduction in IRI for AC thickness increasing from 6 to 9 inches when compared to 9 to 15 inches. The major contributor to observed change in IRI was alligator cracking (see Figure 104).
- Project location (i.e., ambient temperature and number of low temperature cycles) had little effect on predicted IRI. Projects located in the northern, central, and southern parts of the state develop different distresses that compensate each other in the loss of smoothness. For example, sections in northern climates undergo higher thermal cracking but lower alligator cracking compared to sections in the southern climates. This results in an overall very similar IRI across all Missouri climates (see Figure 105).

- Figure 106 shows impact of HMA air voids (4- and 6.5-percent) on predicted IRI. The figure shows HMA mixes with higher air voids (i.e., lower tensile strength and higher creep compliance values) predicted slightly higher IRI as compared to HMA mixes with lower air voids (higher tensile strength and lower creep compliance).

### Calibration of AC over JPCP Smoothness Model

Results of AC over JPCP smoothness model recalibration are presented in Table 72, Table 73, Table 74, and Table 75. Figure 107 presents a plot of measured versus predicted smoothness.

Table 72. Summary of local calibration coefficients for the AC over JPCP smoothness model

Model	Model Coefficient	Local Missouri	Global AASHTOWare Pavement ME Version 2.5.5
FC <sub>Total</sub>	C1	0.9	0.4
RD	C2	38.4	40.8
TC	C3	0.00068	0.008
SF	C4	0.013	0.015

Table 73. Statistical comparison of field measured and Pavement ME Design predicted rutting goodness of fit for AC over JPCP

R-Square = 87.9%, RMSE = 3.93 in/mile, COV = 4.73, N = 74					
Source	DF	Sum of Squares	Mean Square	F Value	Pr > F
Model	1	8217.3	8217.3	529.9	< 0.0001
Error	73	1131.8	15.5		
Corrected Total	74	9349.1			

Table 74. Hypothesis testing for field measured and Pavement ME Design predicted rutting curve slope and intercept for AC over JPCP

Variable	DF	Parameter Estimate	Standard Error	t Value	Pr >  t	95% Confidence Limits	
Intercept	1	1.28310	3.58776	0.36	0.7217	-5.86730	8.43350
Slope	1	1.00084	0.00539	185.55	<.0001	0.99009	1.01159

Table 75. Paired t-test results for field measured and Pavement ME Design predicted rutting observations for AC over JPCP

N	Mean	Std Dev	Std Err	Minimum	Maximum	t Value	Pr >  t
74	0.0903	3.9139	0.4519	-11.5442	8.3360	0.20	0.8422

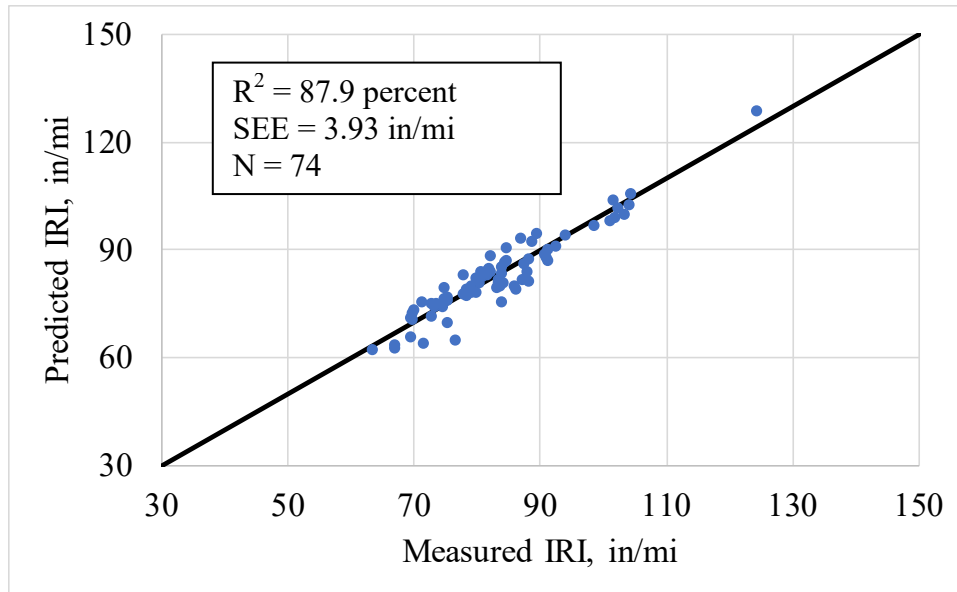


Figure 107. Pavement ME Design local calibration model predicted versus measured IRI for AC over JPCP

Table 72 shows that the recalibrated AC over JPCP IRI model coefficients are significantly different for alligator cracking. For rutting, transverse cracking, and site factors recalibrated models' coefficients were not very different from the global models' coefficients. Table 73 shows a very good goodness of fit statistic  $R^2$  of 87.9 percent. Table 74 and Table 75 show the results of bias testing for the recalibrated rutting models. The information presented shows no significant bias produced by the locally calibrated AC over JPCP IRI model, as all three hypothesis in the statistical tests used to check for bias, were accepted (i.e., intercept of linear model of predicted and measured IRI was 0, slope of the predicted IRI = measured linear model is equal to 1 and measured and predicted rutting belong to the same populations).

Predicted and field measured IRI versus age is shown for several projects in Figure 108 through Figure 110. The plots in these figures shows reasonable predictions of IRI for AC over JPCP.

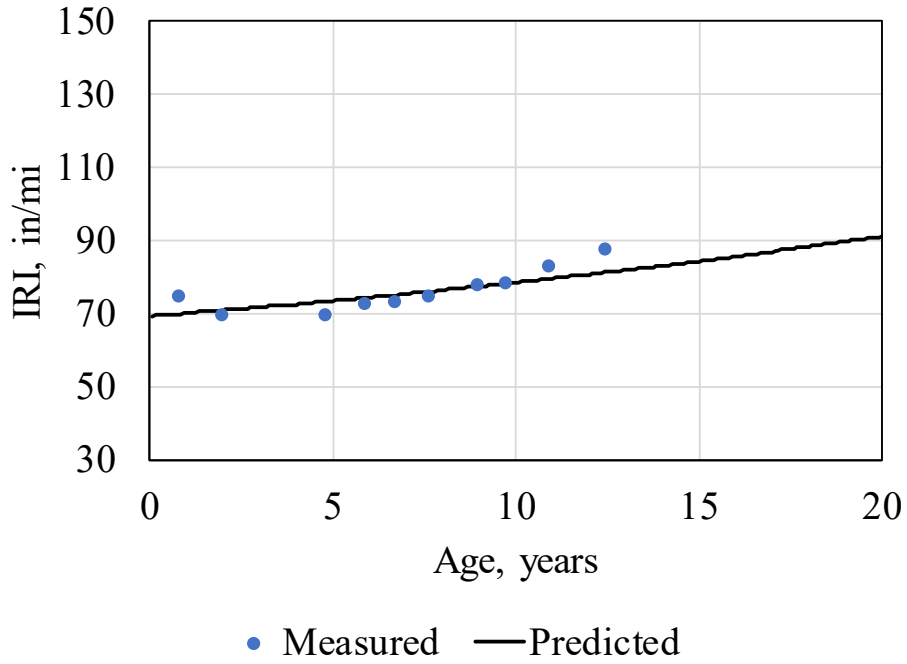


Figure 108. Pavement ME Design local calibration model predicted versus measured IRI for LTPP project 0660

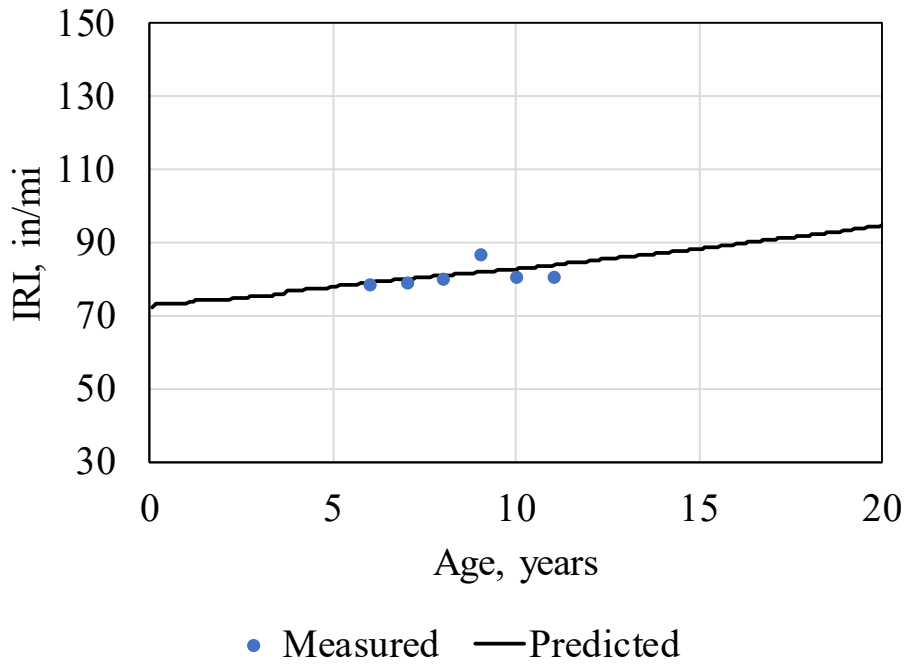


Figure 109. Pavement ME Design local calibration model predicted versus measured IRI for MoDOT PMS project AOC1

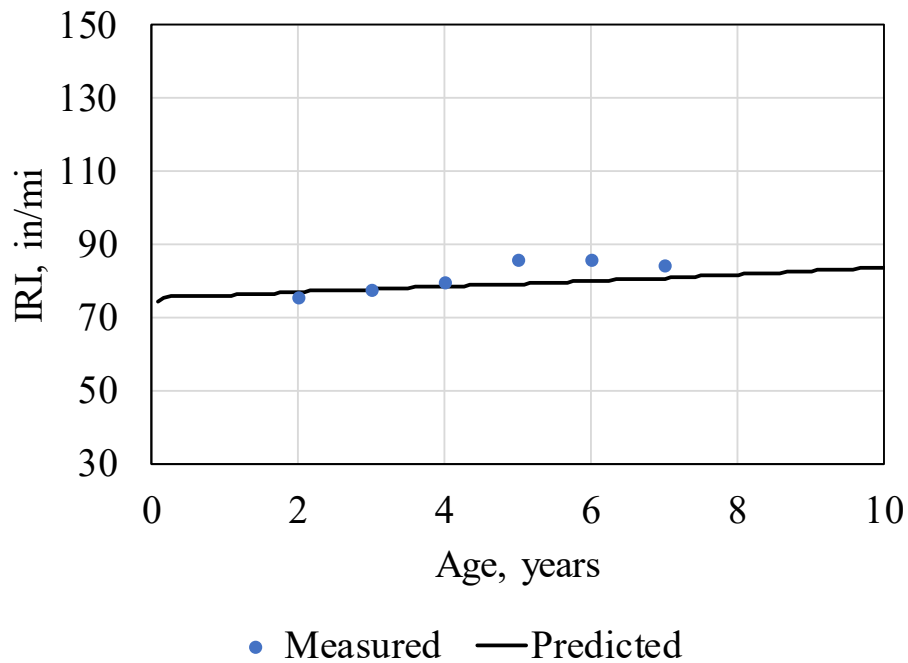


Figure 110. Pavement ME Design local calibration model predicted versus measured IRI for MoDOT PMS project AOC4

#### SUMMARY OF RECALIBRATION FOR AC SURFACED PAVEMENTS

Distress and IRI prediction models were recalibrated for New AC, AC over AC, and AC over JPCP designs under this project. The models were verified statistically and through sensitivity analyses to evaluate the impact of critical input variables. The calibration and verification procedures have been described in detail in this chapter. The analysis resulted in improved locally calibrated distress/IRI models for incorporation into the Pavement ME Design tool for use in flexible pavement design in Missouri. Improvements were reported both in terms of increased  $R^2$  (goodness of fit) and minimizing bias. No changes were made to the reliability prediction models.

## CHAPTER 6. LOCAL CALIBRATION OF *PAVEMENT ME DESIGN* RIGID PAVEMENT DESIGN DISTRESS MODELS

### TRANSVERSE SLAB CRACKING

Pavement ME design considers both bottom-up and top-down modes of transverse slab cracking as there is potential for either mode of cracking under typical truck loading conditions. Pavement ME Design assumes that for a given slab, cracking may be initiated from the bottom-up or top-down, but not both within the same time increment. The procedure, therefore, predicts bottom-up and top-down cracking independently and utilizes a probabilistic relationship to combine the predicted cracking to report total cracking excluding the possibility of both modes of cracking occurring on the same slab. The percentage of slabs with transverse cracks (including all severities) in a given traffic lane is used as the measure of transverse cracking and is predicted using the following globally calibrated equation for both bottom-up and top-down cracking (AASHTO 2015):

$$CRK = \frac{1}{1 + 0.52(DI_F)^{-2.17}} \quad (33)$$

where:

$CRK$  = predicted amount of bottom-up or top-down cracking (fraction)  
 $DI_F$  = fatigue damage calculated using the procedure described in this section

Note that the coefficients, 0.52 and -2.17 are the global calibration constants in version 2.5.5 of the AASHTOWare Pavement ME release. The general expression for fatigue damage in the Pavement ME is an adaptation of Miner's damage hypothesis (Miner 1945) and is expressed as:

$$DI_F = \sum \frac{n_{i,j,k,l,m,n,o}}{N_{i,j,k,l,m,n,o}} \quad (34)$$

where:

$DI_F$  = total fatigue damage (top-down or bottom-up)  
 $n_{i,j,k, \dots}$  = applied number of load applications at condition  $i, j, k, l, m, n$   
 $N_{i,j,k, \dots}$  = allowable number of load applications at condition  $i, j, k, l, m, n$   
 $i$  = age (accounts for change in PCC modulus of rupture and elasticity, slab/base contact friction, traffic loads)  
 $j$  = month (accounts for change in base elastic modulus and effective dynamic modulus of subgrade reaction)  
 $k$  = axle type (single, tandem, and tridem for bottom-up cracking; short, medium, and long wheelbase for top-down cracking)  
 $l$  = load level (incremental load for each axle type)  
 $m$  = equivalent temperature difference between top and bottom PCC surfaces  
 $n$  = traffic offset path  
 $o$  = hourly truck traffic fraction

The applied number of load applications ( $n_{i,j,k,l,m,n}$ ) is the actual number of axle type  $k$  of load level  $l$  that passed through traffic path  $n$  under each condition (age, season, and temperature difference). The allowable number of load applications is the number of load cycles at which fatigue failure is expected on average and is a function of the applied stress and PCC strength. The allowable number of load applications is determined using the following globally calibrated PCC fatigue equation:

$$\log(N_{i,j,k,l,m,n}) = C_1 \cdot \left( \frac{MR_i}{\sigma_{i,j,k,l,m,n}} \right)^{C_2} \quad (35)$$

where:

- $N_{i,j,k,\dots}$  = allowable number of load applications at condition  $i, j, k, l, m, n$ .
- $MR_i$  = PCC modulus of rupture at age  $i$ , psi.
- $\sigma_{i,j,k,\dots}$  = applied stress at condition  $i, j, k, l, m, n$
- $C_1$  = fatigue life calibration constant, 2.0
- $C_2$  = fatigue life calibration constant, 1.22

The fatigue damage calculation is a process of summing damage from each damage increment. Once top-down and bottom-up damage is estimated, the corresponding cracking is computed using equation 31. Equation 36 assumes that a slab may crack from either bottom-up or top-down, but not both.

$$TCRACK = (CRK_{Bottom-up} + CRK_{Top-down} - CRK_{Bottom-up} \cdot CRK_{Top-down}) \cdot 100 \quad (36)$$

where:

- $TCRACK$  = total transverse cracking (percent, all severities)
- $CRK_{Bottom-up}$  = predicted amount of bottom-up transverse cracking (fraction)
- $CRK_{Top-down}$  = predicted amount of top-down transverse cracking (fraction)

For JPCP models calibration, data was assembled mostly from MoDOT PMS projects. The typical project had 12-in thick PCC widened (slab width of 14 ft) slabs and doweled joints. These designs produce pavements that exhibit very little fatigue damage, and as a result, very low fatigue cracking. The doweled joints combined with slab thickness of 12 inches also results in very low joint faulting. Figure 111 presents a distribution of the measured transverse slab cracking data for the MoDOT PMS JPCP projects. The information in Figure 111 shows that approximately 80 percent of all projects report zero (0) percent cracking. The remaining projects except for one reported less than, or equal to, 3 percent cracking. This was also discussed in Chapter 4. The lack of sufficient performance data did not lend a meaningful dataset for full-scale regression-based model calibration. Therefore, a secondary approach, i.e. a classification-based verification procedure was utilized instead.

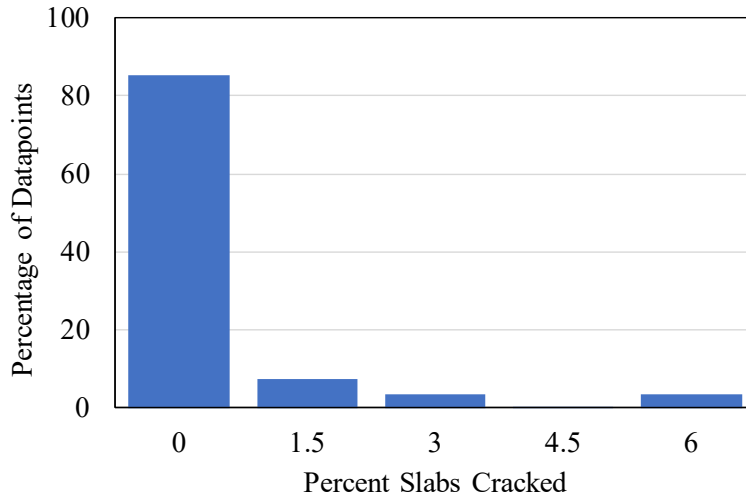


Figure 111. Histogram showing distribution of JPCP transverse cracking for the projects utilized in calibration and validation

### Model Verification

The outcome of model verification is presented in Figure 112. The histogram presented shows the global model prediction is very close to zero cracking values for all projects included in the verification study. Thus, in summary, for the projects verified, cracking predictions matched field measured values.

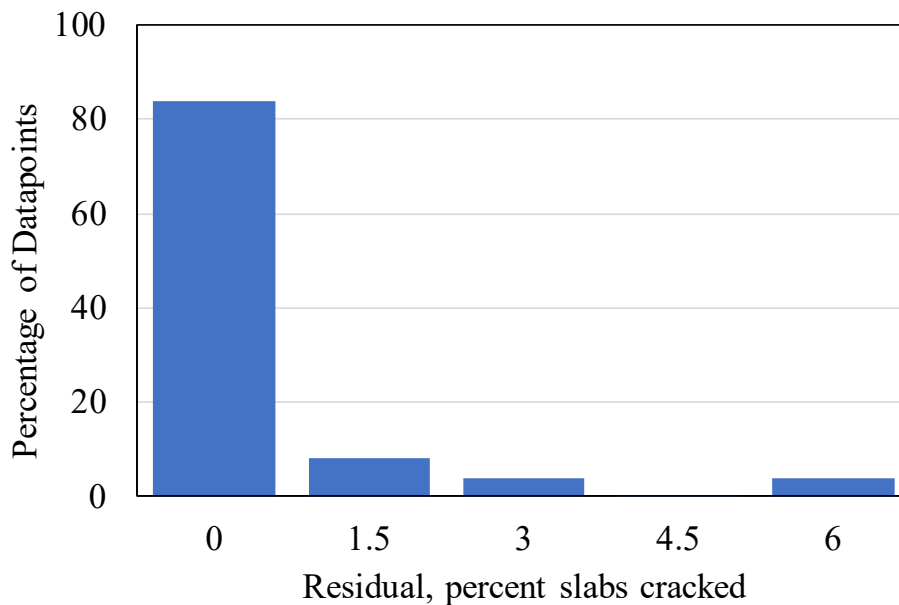


Figure 112. Histogram showing distribution of residual (measured minus predicted transverse cracking) for the projects utilized in calibration and validation

Figure 113 shows plot of predicted and measured cracking versus fatigue damage. The information presented in the plot confirms the earlier observations.

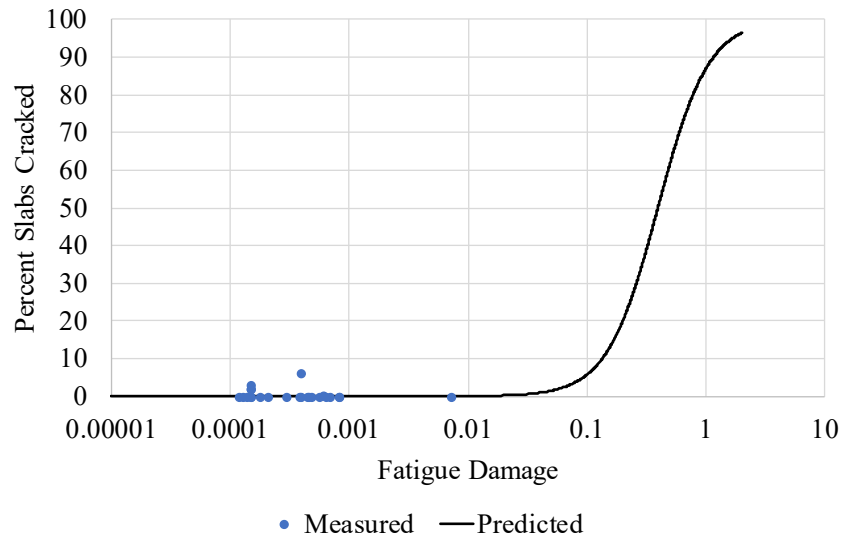


Figure 113. Pavement ME Design global model predicted and measured transverse cracking versus fatigue damage for the projects utilized in calibration and validation

A confusion matrix summarizing prediction results based on classification of measured and predicted transverse slab cracking is presented as Table 76. The confusion matrix forms the basis for estimating model accuracy as follows:

$$Accuracy = \frac{TP+TN}{TP+TN+FP+FN} \quad (37)$$

where:

- TP = true positive, that is observation is greater than or equal to 1 percent and the predicted is also greater than or equal to 1 percent
- FN = false negative, observation is greater than or equal to 1 percent, but is predicted as less than 1 percent
- TN = true negative, observation is less than 1 percent and the predicted is also less than 1 percent
- FP = false positive, observation is less than 1 percent but predicted is greater than or equal to 1 percent

Table 76. Statistical comparison of field measured and Pavement ME Design predicted transverse cracking goodness of fit for new JPCP and unbonded JPCP overlays

Predicted Cracking	Measured Cracking	
	< 1 percent	>= 1 percent
< 1 percent	22	5
>=1	0	0

Using equation 37, a model accuracy of 81.4 percent was estimated. This serves as a starting point to verify the model accuracy. The calibration data available clearly provides the basis to confirm that the global calibration, within the range of fatigue damage data corresponding to less than one percent cracking, is accurate. This is a necessary, but not sufficient, condition to validate the global calibration model. This verification does not substitute, or is not superior to, a comprehensive calibration. A comprehensive calibration and validation is only possible with field measured values corresponding to damage values in the range of 0.01 to 1.0, as was performed in the local calibration efforts of other State DOTs (Darter et al., 2014 and Von Quintus et al., 2015).

In the absence of such data, a verification such as the one using equation 37 performed for MoDOT JPCP designs, was also performed by another state DOT (Mallela et al., 2013) to provide the agency a basis to continue using the global model. Data subgroups created for the verification using MoDOT sections is also a very tight grouping considering over 80 percent of the points have field measured and predicted cracking of zero percent.

A sensitivity analysis was performed to further evaluate suitability of the global transverse cracking model for Missouri. The baseline design used for the sensitivity analyses was a typical JPCP structure in Missouri with typical MoDOT specification inputs. Design life of 30 years was used with a cumulative traffic of over 30 million trucks (considered a very heavy traffic pavement design). The slab width was 12-feet and widened to 13 feet for widened slab analysis. Joint spacing was 15 feet. Doweled joints were used.

The sensitivity analysis results presented in Figure 114 through Figure 118 show the following:

- Increasing PCC thickness significantly reduced transverse slab cracking as shown in Figure 114. This is as expected. Assuming pavement failure at transverse cracking of 15 percent slabs, an 8-in slab fails five years post construction and opening to traffic. Increasing thickness from 8 to 9 inches extends age at failure to approximately 25 years. For PCC thickness greater than 9 inches, the pavements do not fail within the analysis period of 30 years. The trends observed within Missouri conditions are similar to that produced nationally, i.e., significant reduction of cracking for slab thicknesses greater than ten inches.
- Figure 115 shows a significant change in transverse cracking with increasing CTE values. CTE value of 6 microstrain/ °F results in pavement failure (cracking > 15 percent) in approximately 7.5 years. CTE of 5 microstrain/ °F or less results in no failure within the analysis period of 30 years. The observed trends were deemed as reasonable. Coarse aggregate sources in Missouri are mostly limestone and dolomite aggregates, which produce PCC mixes with CTE values in the range of 4.2 to 5.0 microstrain/°F. Designs with PCC inputs in this range generally show good performance over a 30-year design life.
- Figure 116 shows impact of widened slab (from the standard 12 feet to 13 feet) on predicted cracking. The plot shows that for the range of PCC thicknesses shown, slab widening does significantly reduce predicted transverse cracking. The extent of transverse cracking reduction decreases with increased PCC thickness. This trend is in agreement with national observations.

- Figure 117 shows impact of shoulder type (AC shoulder versus tied PCC) on predicted cracking. The plot shows that for the range of PCC thicknesses shown in Figure 84, utilization of tied PCC shoulders does significantly reduce predicted transverse cracking. The extent of transverse cracking reduction decreases with increased PCC thickness. This trend is in agreement with national observations.
- Figure 118 shows impact of PCC flexural strength on predicted cracking. The figure shows a significant reduction in cracking with increasing PCC flexural strength. Pavements constructed with 400 psi flexural strength PCC experience failure within 2 years. Increasing flexural strength to 500 psi increased age at failure to 15 years. Flexural strength of 550 psi produced a design that failed at 22 years (optimal). Flexural strength greater than 550 psi did not produce any failures within the 30-year analysis period.

Note that the results of the sensitivity analyses and findings above are not specifically a result of the current recalibration effort or the result of the verification presented. These results are presented in this chapter because the cases analyzed are specific to Missouri traffic, climate, materials, and designs.

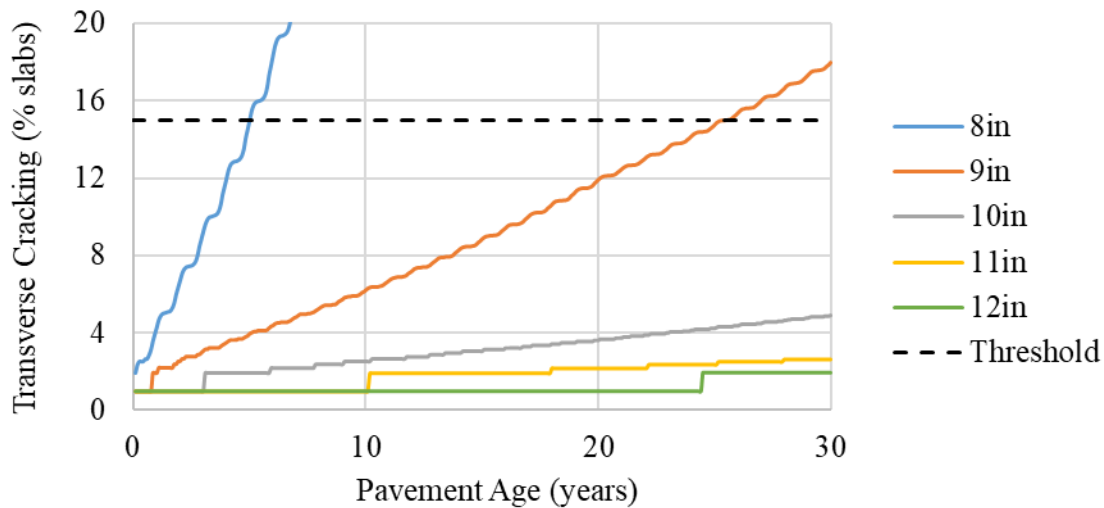


Figure 114. Impact of PCC thickness (8 through 12 inches) on predicted transverse slab cracking for Missouri

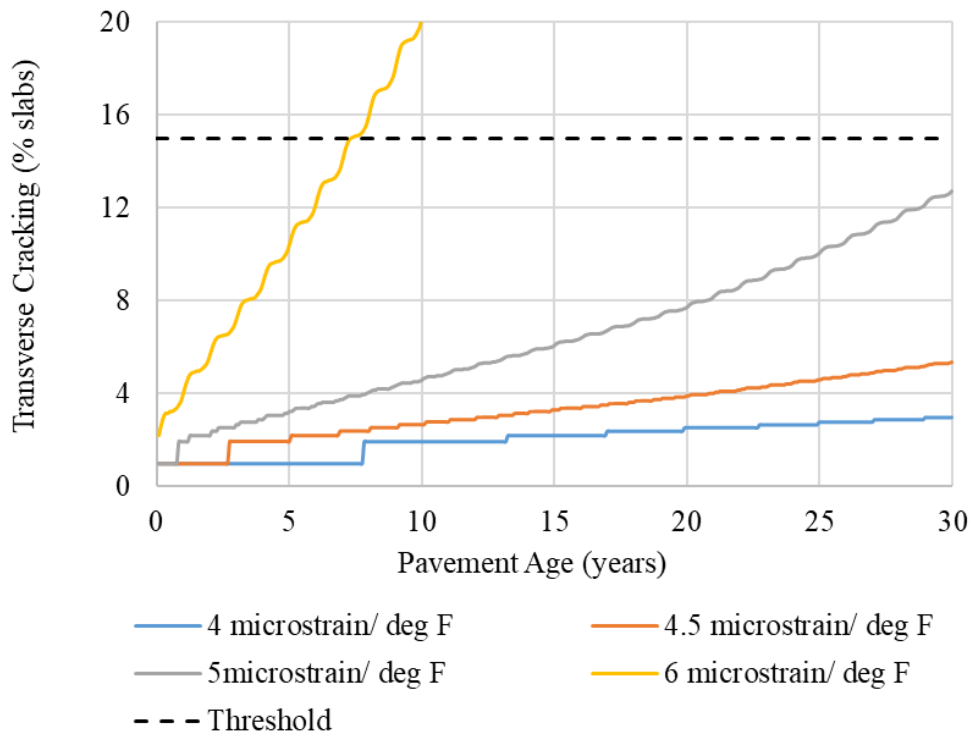


Figure 115. Impact of PCC CTE on predicted transverse slab cracking for Missouri

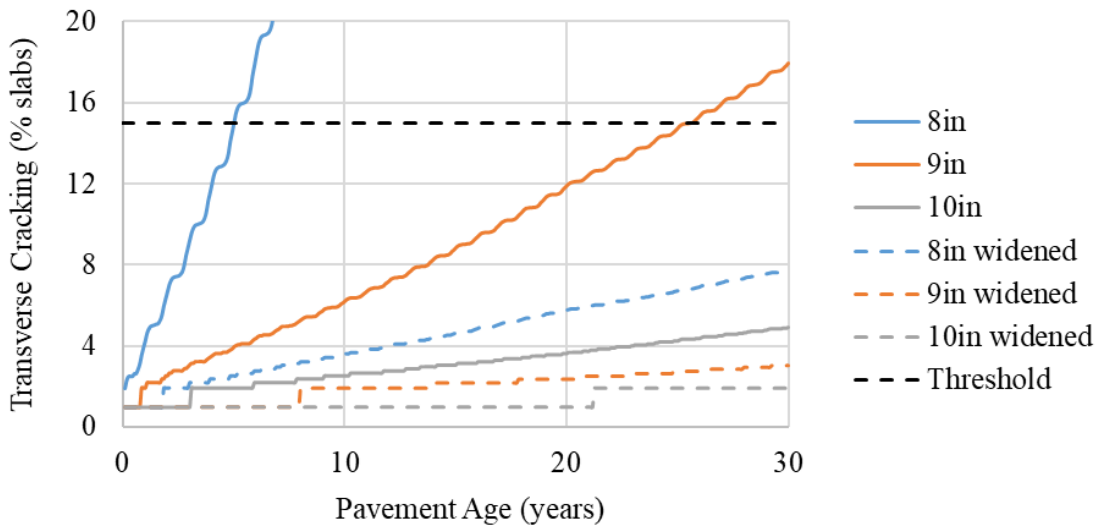


Figure 116. Impact of widened slab and PCC thickness on predicted transverse slab cracking for Missouri

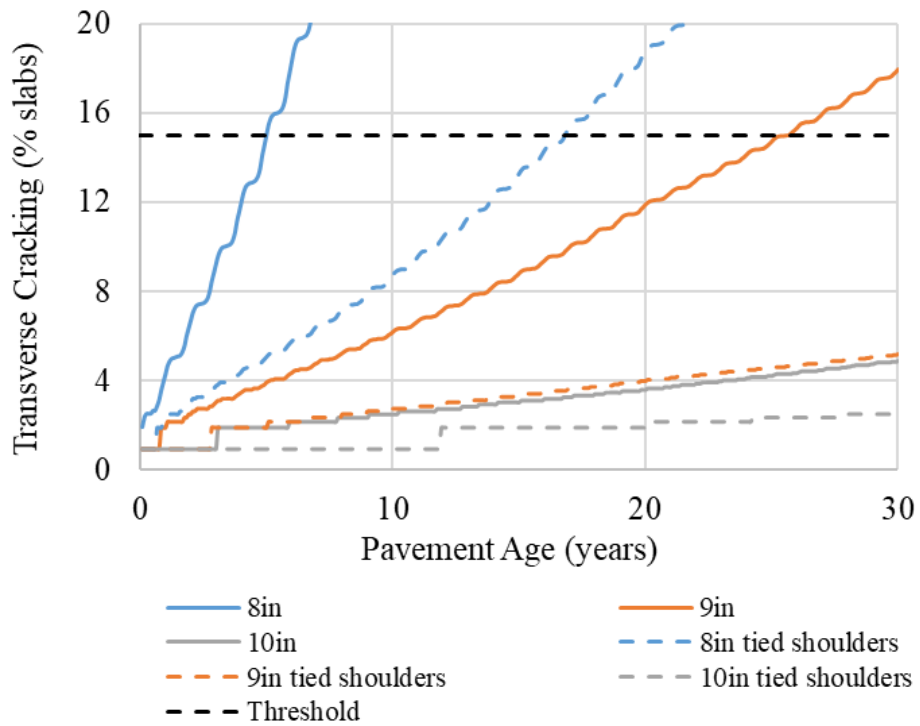


Figure 117. Impact of shoulder type and PCC thickness on predicted slab cracking for Missouri

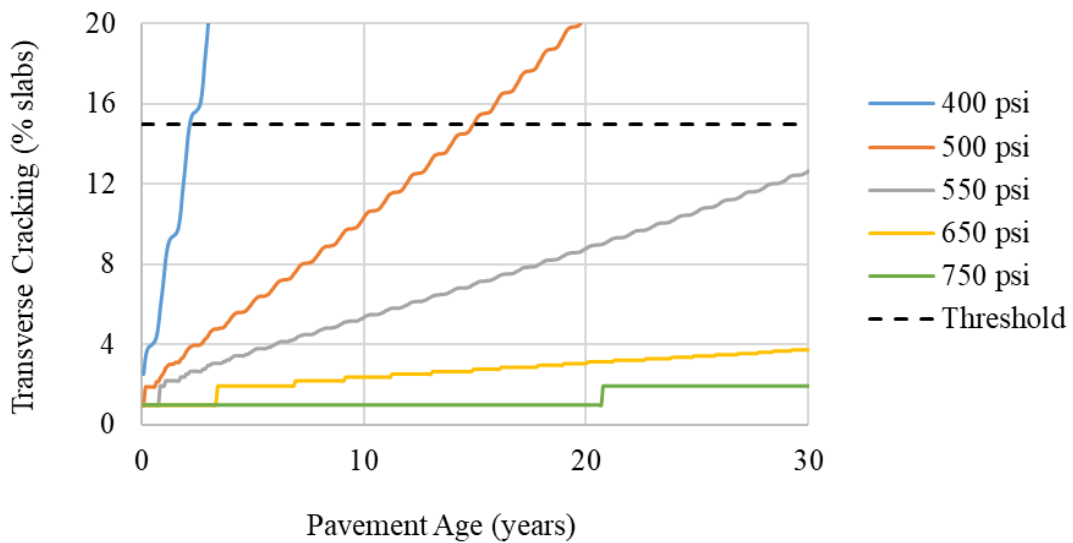


Figure 118. Impact of PCC flexural strength on predicted transverse slab cracking for Missouri

## TRANSVERSE JOINT FAULTING

Pavement ME Design tool predicts faulting incrementally using a series of equations and models. The magnitude of increment is based on current faulting level, the number of axle loads applied, pavement design features, material properties, and climatic conditions. Increments of faulting is reported monthly. Total faulting is determined as a sum of faulting increments from all previous months (i.e., since traffic opening). The equations for predicting joint faulting are presented as follows (AASHTO 2015):

$$Fault_m = \sum_{i=1}^m \Delta Fault_i \quad (38)$$

$$\Delta Fault_i = C_{34} * (FAULTMAX_{i-1} - Fault_{i-1})^2 * DE_i \quad (39)$$

$$FAULTMAX_i = FAULTMAX_0 + C_7 * \sum_{j=1}^m DE_j * \text{Log}(1 + C_5 * 5.0^{EROD})^{C_6} \quad (40)$$

$$FAULTMAX_0 = C_{12} * \delta_{curling} * \left[ \text{Log}(1 + C_5 * 5.0^{EROD}) * \text{Log}\left(\frac{P_{200} * WetDays}{P_s}\right) \right]^{C_6} \quad (41)$$

where

- $Fault_m$  = mean joint faulting at the end of month  $m$ , in.
- $\Delta Fault_m$  = incremental change (monthly) in mean transverse joint faulting during month  $i$ , in
- $FAULTMAX_i$  = maximum mean transverse joint faulting for month  $i$ , in
- $FAULTMAX_0$  = initial maximum mean transverse joint faulting, in
- $EROD$  = base/subbase erodibility factor
- $DE_i$  = differential density of energy of subgrade deformation accumulated during month  $i$
- $\delta_{curling}$  = maximum mean monthly slab corner upward deflection PCC due to temperature curling and moisture warping
- $P_s$  = overburden on subgrade, lb
- $P_{200}$  = percent subgrade material passing No. 200 sieve
- $WetDays$  = average annual number of wet days (greater than 0.1 inch rainfall)
- $C_{1,2,3,4,5,6,7,12,34}$  = global calibration constants

$C_{12}$  and  $C_{34}$  are defined by equations 42 and 43:

$$C_{12} = C_1 + C_2 * FR^{0.25} \quad (42)$$

$$C_{34} = C_3 + C_4 * FR^{0.25} \quad (43)$$

$FR$  = base freezing index defined as percentage of time the top base temperature is below freezing (32 °F) temperature.

The global model coefficients are presented in Table 77.

Table 77. New JPCP and JPCP overlays faulting model coefficients

Calibration Coefficients	Global AASHTOWare Pavement ME Version 2.5.5
C1	0.595
C2	1.636
C3	0.00217
C4	0.00444
C5	250
C6	0.47
C7	7.3

### Model Verification

As noted for transverse cracking, JPCP model’s calibration data was assembled mostly from MoDOT PMS projects with 12-in thick PCC slabs, with a widened lane (slab width of 14 ft), and doweled joints. These designs produce pavements that exhibit very little joint faulting. Thus, transverse joint faulting data used for model verification was mostly zero. Models verification, therefore, was done as previously described for JPCP transverse fatigue cracking. Figure 119 presents a distribution of the transverse joint faulting data used for model verification.

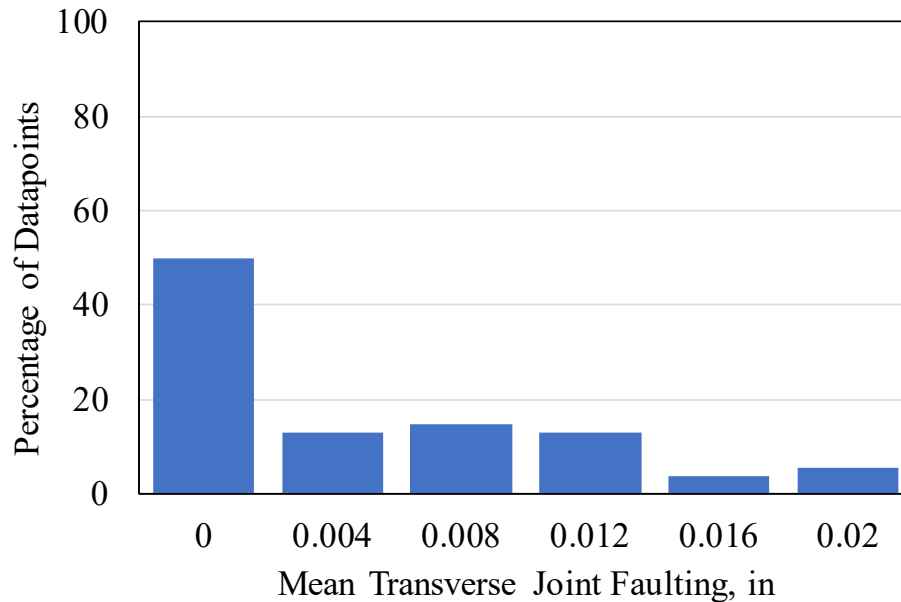


Figure 119. Histogram showing distribution of mean joint faulting for the projects utilized for model verification/calibration

Figure 119 shows that approximately 50 percent of all projects had zero (0) inch joint faulting. The remaining projects reported less than, or equal to, 0.02-inch transverse joint faulting. The outcome of model verification is presented in Figure 120. The histogram presented shows the

global model predicting very close to zero faulting. Residual faulting for all the projects evaluated ranged from -0.009 to 0.021 inch. This is as expected for the projects evaluated and the predictions essentially match field measured faulting values. Table 78 shows confusion matrix table of predicted and measured transverse joint faulting. The information presented in the table confirms the earlier observations, that is 36 out of 54 measured and predicted transverse joint faulting data points closely matched.

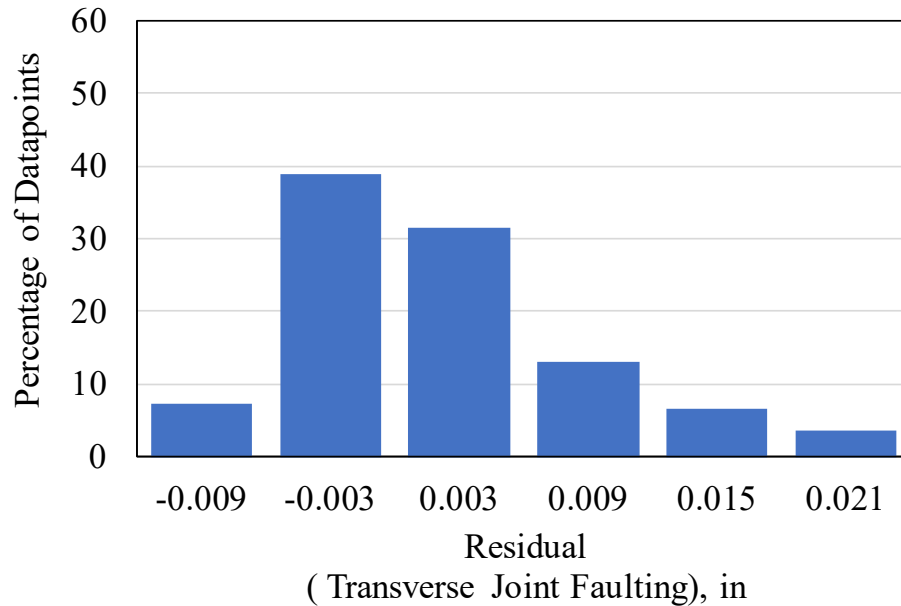


Figure 120. Histogram showing distribution of residual (measured minus predicted transverse joint faulting) for the projects utilized for model verification/calibration

Table 78. Confusion matrix table showing measured versus predicted transverse joint faulting

Frequency Predicted	Measured		Total
	H (Faulting > 0.005)	L (Faulting ≤ 0.005)	
H (faulting > 0.005)	9	5	14
L (faulting ≤ 0.005)	13	27	40
Total	22	32	54

Using equation 37 and the data presented in Table 78, a faulting model accuracy of 66.6 percent was estimated.

A sensitivity analysis was performed to further evaluate suitability of the global transverse joint faulting model for Missouri. Results of the sensitivity analysis, presented in Figure 121 through Figure 123, show the following:

- Increasing PCC thickness reduces transverse joint faulting as shown in Figure 121. The change in faulting, however, is not significant (approximately 0.02 in). This is as expected. Although increasing PCC thickness reduces deflections at the PCC slab corner and thus faulting, the impact overall is not as significant as providing design changes which reduce corner deflections (lower CTE) or improve load transfer (use dowels).
- Figure 122 shows impact of PCC CTE on predicted faulting. The plot shows that for the range of PCC CTE values shown, utilization of mixes with low CTEs can significantly reduce transverse joint faulting. MoDOT coarse aggregates, limestones and dolomites, will result in PCC CTE values below 5.0 in/in/°F, that will enable MoDOT designs to be optimized for faulting.
- Figure 123 shows impact of PCC dowel size on predicted faulting. The figure shows a significant reduction in faulting with increasing dowel size. Pavements constructed with no dowels show 0.7 inches of faulting. Use of a 1-in dowel reduced faulting to 0.43 inches. Dowel size of 1.5 inches reduced faulting to less than 0.15 inches after 30 years in service.

As stated previously, these sensitivity analyses do not represent a recalibration of the JPCP joint faulting model. Rather, these analyses, based on a design with all inputs relevant to Missouri, suggest the national calibration models are suitable for use in Missouri after the preliminary verification performed to the extent possible. They do not validate the accuracy of the faulting model over the entire range of faulting predictions, as would be possible only with data from field JPCP slabs exhibiting faulting values from 0 to >0.2 inches.

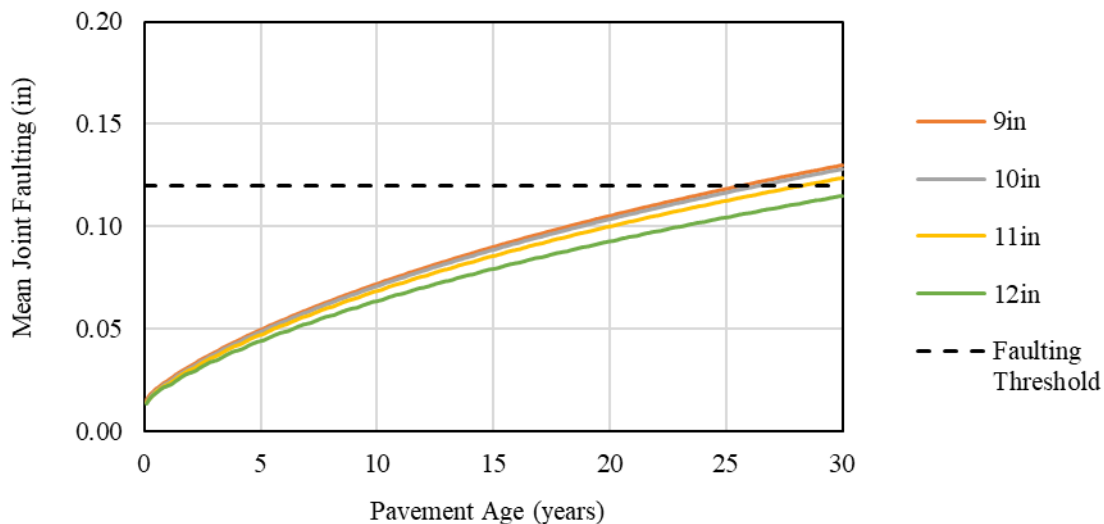


Figure 121. Impact of PCC thickness and widened slab on predicted transverse joint faulting for Missouri

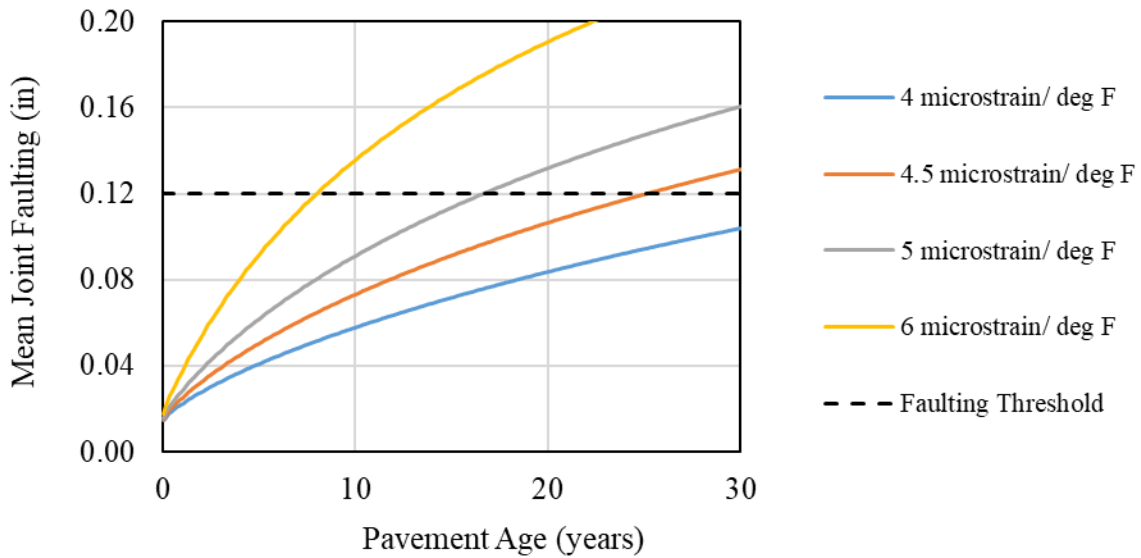


Figure 122. Impact of PCC CTE on predicted transverse joint faulting for Missouri

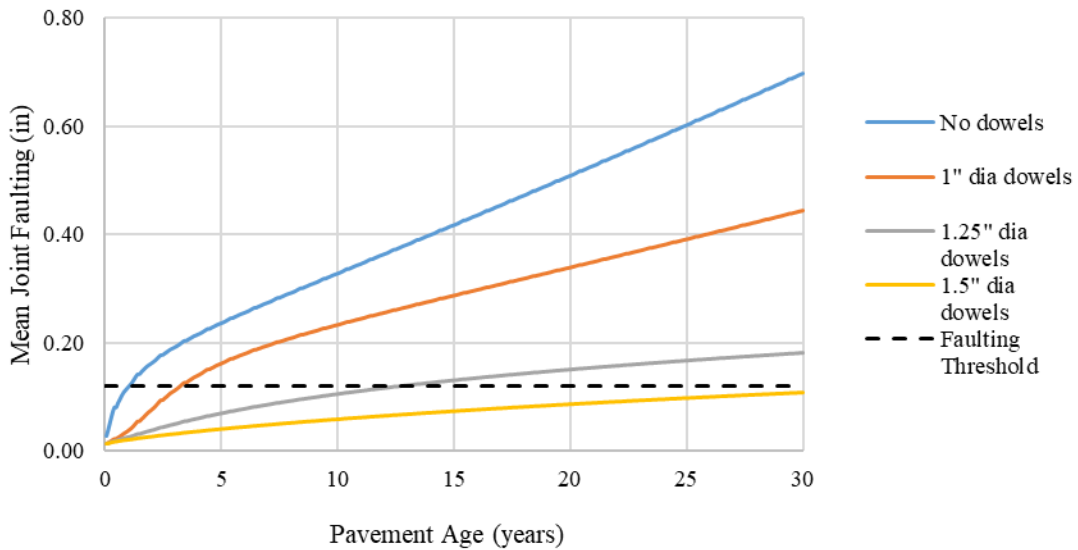


Figure 123. Impact of PCC dowel size on predicted transverse joint faulting for Missouri

### Smoothness (IRI)

AASHTO Pavement ME Design JPCP smoothness prediction model is a linear relationship between initial as-constructed smoothness and change in distress (joint faulting, joint spalling, and transverse cracking) over time and traffic applications. The IRI model was calibrated and validated using LTPP data that represented variety of design, materials, foundations, and climatic

conditions. The following is the globally calibrated model, also included in version 2.5.5 of AASHTOWare Pavement ME:

$$IRI = IRI_I + 0.8203*CRK + 0.4417*SPALL + 1.4929*TFAULT + 25.24*SF \quad (44)$$

where:

- $IRI$  = predicted IRI, in/mi
- $IRI_I$  = initial smoothness measured as IRI, in/mi
- $CRK$  = percent slabs with transverse cracks (all severities)
- $SPALL$  = percentage of joints with spalling (medium and high severities)
- $TFAULT$  = total joint faulting cumulated per mi, in
- $SF$  = site factor

$$SF = AGE (1 + 0.5556*FI) (1 + P_{200}) * 10^{-6} \quad (45)$$

where:

- $AGE$  = pavement age, years
- $FI$  = freezing index, °F-days
- $P_{200}$  = percent subgrade material passing No. 200 sieve

The transverse cracking and faulting predictions are obtained using the cracking and faulting models presented as equations 33 and 38, respectively. The transverse joint spalling is determined using equation 46 below (AASHTO 2015):

$$SPALL = \left[ \frac{AGE}{AGE + 0.01} \right] \left[ \frac{100}{1 + 1.005^{(-12*AGE + SCF)}} \right] \quad (46)$$

where:

- $SPALL$  = percentage joints spalled (medium- and high-severities)
- $AGE$  = pavement age since construction, years
- $SCF$  = scaling factor based on site-, design-, and climate-related variables

$$SCF = -1400 + 350 * AC_{PCC} * (0.5 + PREFORM) + 3.4 f'_c{}^{0.4} - 0.2 (FT_{cycles} * AGE) + 43 H_{PCC} - 536 WC_{PCC} \quad (47)$$

- $AC_{PCC}$  = PCC air content, percent
- $AGE$  = time since construction, years
- $PREFORM$  = 1 if preformed sealant is present; 0 if not
- $f'_c$  = PCC compressive strength, psi
- $FT_{cycles}$  = average annual number of freeze-thaw cycles
- $H_{PCC}$  = PCC slab thickness, in
- $WC_{PCC}$  = PCC water/cement ratio

The Pavement ME Design JPCP IRI model was calibrated using field measured IRI and distress data for over 200 LTPP pavement projects located throughout the U.S. Due to the extensive amount of data used in developing the global smoothness prediction model and relatively limited

smoothness data available for local calibration, a complete recalibration of the smoothness model was not warranted. A verification sensitivity analysis of the smoothness model using inputs from the recalibrated transverse cracking, transverse joint faulting, and transverse joint spalling models was done to assess reasonableness. The sensitivity analysis results presented in Figure 124 through Figure 128 show the following:

- Increasing PCC thickness reduces IRI as shown in Figure 124. The change in IRI is significant for the thinner PCC slabs (< 9 inches). As slab thickness increases beyond 9 inches, the impact of increasing thickness is nonexistent. This observation is in agreement with occurrence of transverse cracking (a contributor to smoothness loss).
- Figure 125 shows a significant change in IRI with increasing CTE values with the change being very pronounced for CTE > 5 microstrain/°F values. This observation aligns with the trends observed for the impact of CTE on transverse cracking, a contributor to IRI.
- Figure 126 shows impact of widened slab (from the standard 12-ft to 13-ft) on predicted IRI. The plot shows that for the range of PCC thicknesses shown in Figure 68, slab widening does significantly reduce predicted IRI. The observed trends in IRI reduction was similar as that presented for joint faulting, a contributor to IRI. The observation was thus deemed as reasonable.
- Figure 127 shows impact of shoulder type (AC shoulder versus tied PCC) on predicted IRI. The plot shows that for the range of PCC thicknesses shown in the figure, utilization of tied PCC shoulders can be more helpful for lower slab thicknesses. The benefit of tied shoulder diminishes as slab thickness increases. This trend is similar to that observed for transverse slab cracking, a contributor to IRI, and thus was deemed reasonable.
- Figure 128 shows impact of PCC flexural strength on predicted IRI. Increasing PCC flexural strength reduces IRI. The change in IRI is very significant for the thinner PCC slabs (< 9 inches). For thicker slabs (> 9 in) the impact of thickness is considerably less. This observation is in agreement with occurrence of transverse cracking (a contributor to smoothness loss).

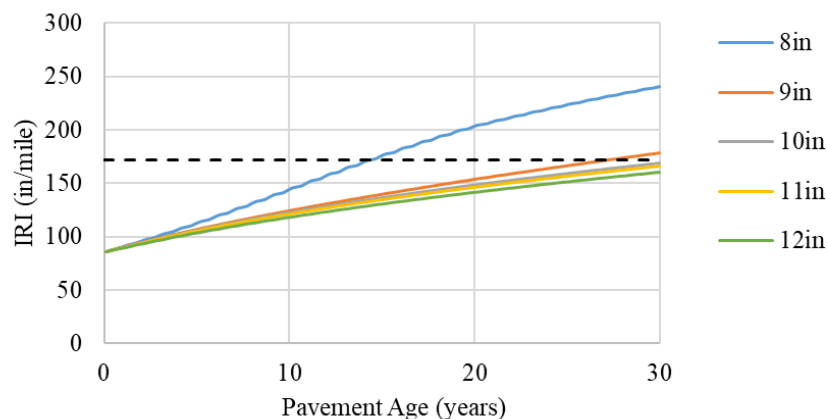


Figure 124. Impact of PCC thickness on predicted IRI for Missouri

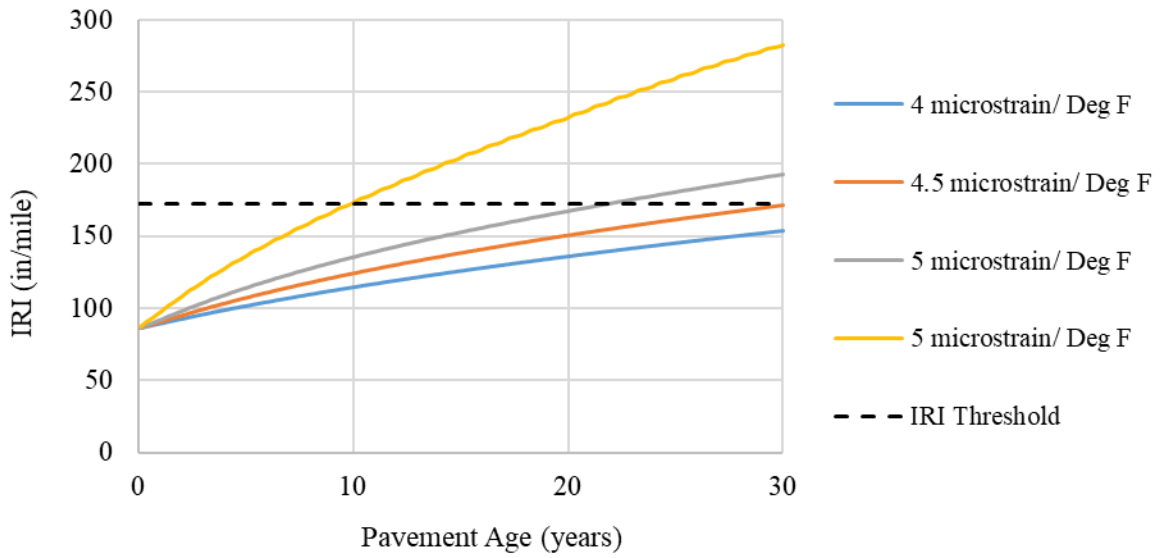


Figure 125. Plot showing impact of PCC CTE on predicted IRI for Missouri

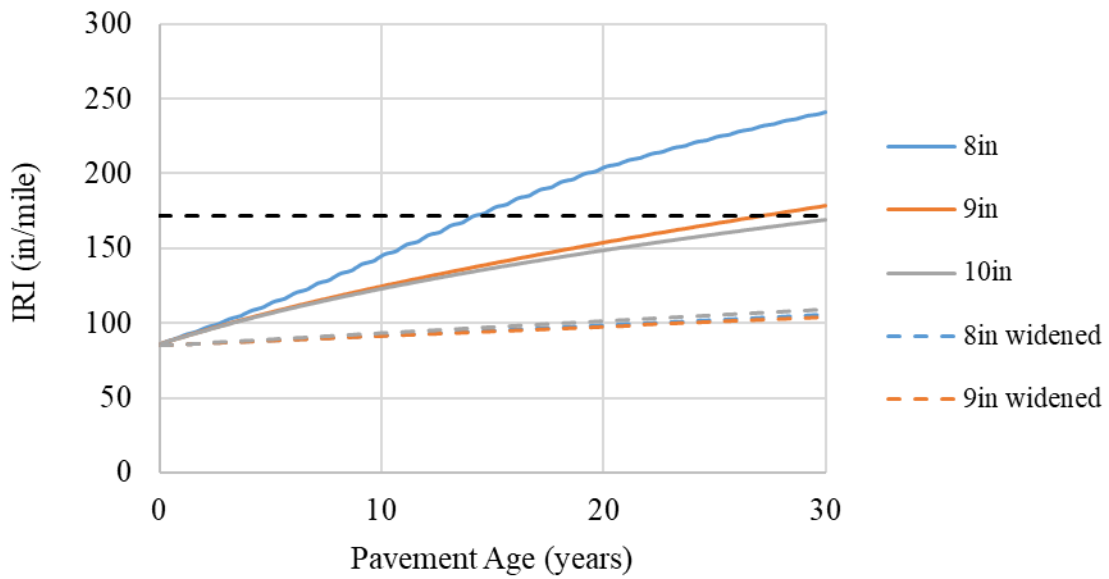


Figure 126. Impact of widened slab and PCC thickness on predicted IRI for Missouri

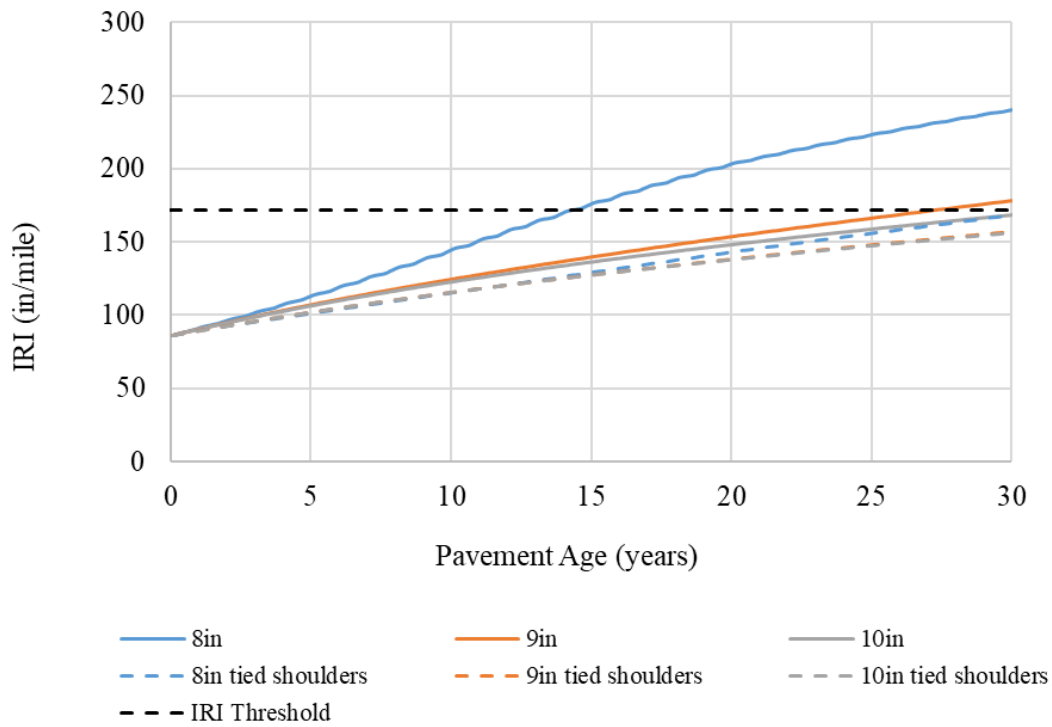


Figure 127. Impact of shoulder type and PCC thickness on predicted IRI for Missouri

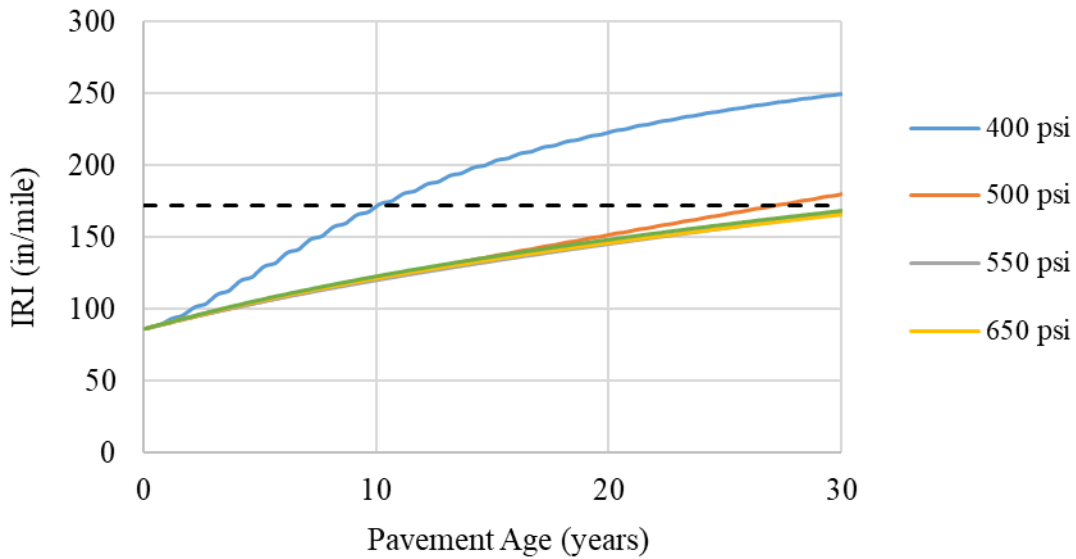


Figure 128. Impact of PCC flexural strength on predicted IRI for Missouri

## SUMMARY

New JPCP and unbonded JPCP overlays distress/IRI prediction models were verified under this project. The verification work has been described in detail in this chapter. Field distress data from the rigid pavement calibration sections did not exhibit transverse cracking or joint faulting to the extent that will allow calibration and validation of the model. Therefore, a limited scale verification was performed to validate the global models within the range of data available. The analysis results showed that the Pavement ME Design global models were suitable for the data range evaluated. A comprehensive sensitivity analysis was performed to further check if the models were suitable for conventional MoDOT JPCP designs i.e., Missouri specific climate, subgrade, material properties, joint spacing, slab thickness and slab width, and other design features such as edge support and doweled joints. The results of these checks were positive.

Recalibration of the JPCP models to improve  $R^2$  (goodness of fit) and minimizing bias will thus be possible when adequate performance data will be available. The global models used for estimating transverse slab cracking, joint faulting, and IRI may be the most suitable models, as significant change in these relationships based on limited number of projects was not warranted.

## CHAPTER 7. CASE STUDIES

This chapter presents two case study examples showing the use of the locally calibrated and verified Pavement ME Design distress models for New AC and AC over AC pavement design.

### NEW AC PAVEMENT CASE STUDY

A case study example of New AC pavement design, borrowed from an actual project in Missouri, is presented in this section.

#### Project Location and Climate

The New AC pavement case study project was located on Taney County. The coordinates of the project location are latitude = 36.5 degrees, longitude = -93.125 degrees. Location specific climate characteristics were as follows:

- Mean annual air temperature (°F): 57.0
- Mean annual precipitation (in): 42.9
- Freezing index (°F - days): 208
- Average annual number of freeze/thaw cycles: 76

Monthly temperature and rainfall averages are presented in Figure 129 and Figure 130.

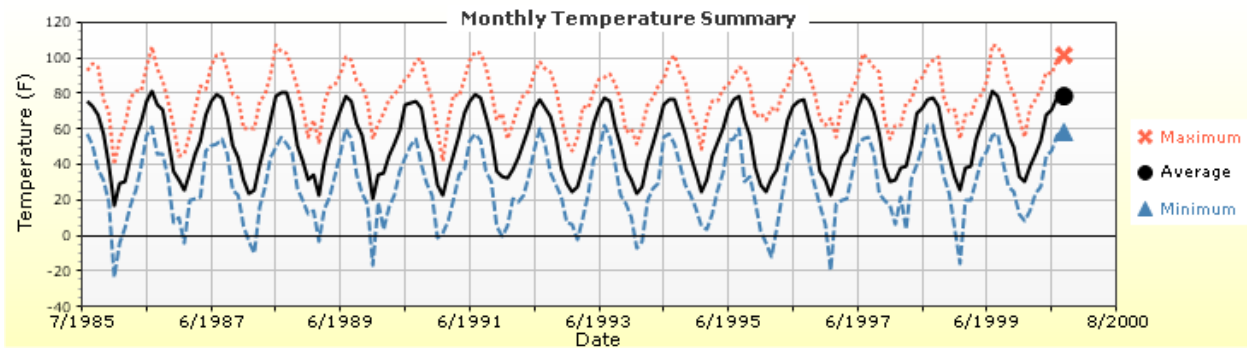


Figure 129. Plot showing distribution of ambient temperature at project site

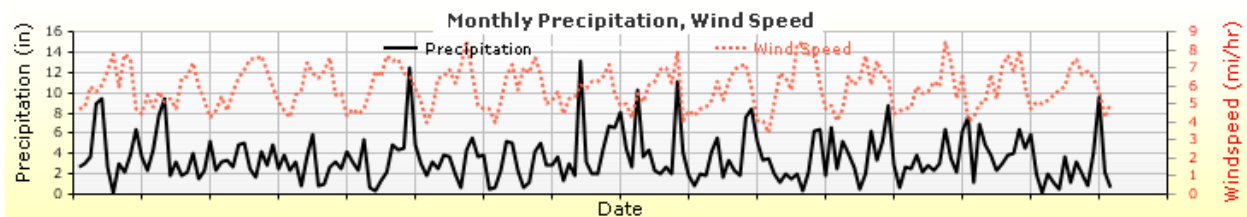


Figure 130. Plot showing distribution of precipitation and windspeed at project site

## Traffic

Future anticipated truck traffic for the selected project site was determined from historical MoDOT traffic volume records and WIM data. Future truck traffic volume estimates are summarized as follows:

- Initial AADTT: 2750 trucks with 0.5% linear growth
- Cumulative truck traffic: ~10 million trucks in 20 years
- Number of lanes in design direction: 2
- Percent of trucks in design direction (%): 50.0
- Percent of trucks in design lane (%): 95.0

The cumulative number of trucks over the 20-year design period was 10 million trucks. Appropriate default vehicle class distribution, hourly truck distribution, and axle load distribution were selected for the case study project based on the project's location and functional class. Selected vehicle class distribution and hourly truck distribution are presented in Figure 131 and Figure 132.

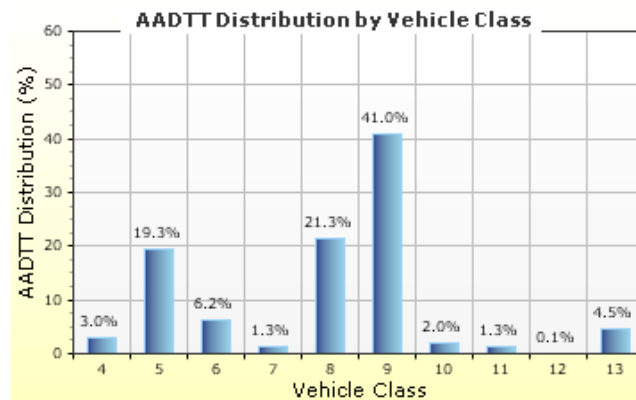


Figure 131. Plot showing vehicle class distribution at project site

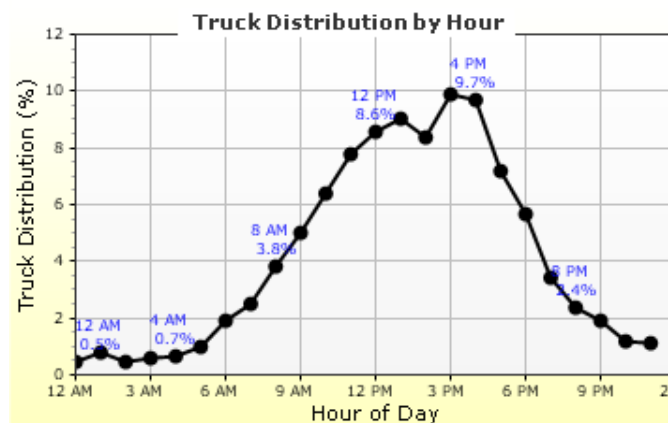


Figure 132. Plot showing truck hourly distribution at project site

## Subgrade Properties

Subgrade material type for the project site was AASHTO soil Class A-6 with an initial subgrade resilient modulus of 14,000 psi.

## Full Depth Asphalt Preliminary/Trial Design

The Pavement ME Design was used to develop an initial trial design using the site conditions as inputs. A design period of 20 years was used for the analysis. Simulation was done beginning with a preliminary trial design that comprised of the layer material types, thicknesses, and properties presented in Table 79. Trial design structure was based on the MoDOT project. The total AC thickness, as noted in Table 79, is 11.7 inches.

Table 79. Trial design for New AC design

Layer #	Layer Type	Mix Design (from MoDOT HMA materials library)	Trial Design Thickness, in
1	Flexible	SP125 15-60, PG 70-22 binder with 11% binder and 6.9% voids	1.7
2	Flexible	SP250 16-68, PG 70-22 binder	6.1
3	Flexible	SP250 16-68, PG 70-22 binder	4.1
4	Non-Stabilized	Crushed stone	5.0
5	Subgrade A-6	A-6 soil	Semi-infinite
<ul style="list-style-type: none"> <li>• Design Life – 20 years</li> <li>• Base construction: June 2019</li> <li>• Pavement construction: July 2019</li> <li>• Traffic opening: August, 2019</li> </ul>			

Using the site properties and trial design inputs presented, Pavement ME Design analyses were performed for the following scenarios:

- Optimize AC layers thicknesses using the new local calibration models.
- Optimize AC layers thicknesses using the global calibration models in version 2.5.5.

Design adequacy was evaluated using performance criteria used by MoDOT for its designs, which are also the distress types with locally calibrated prediction models. Note that the top-down cracking model in the AASHTOWare Pavement ME was not calibrated. The following are the distress types and performance thresholds at 90 percent reliability criteria:

- Alligator cracking: 10 percent lane area.
- Total rutting: 0.50 in.
- AC rutting: 0.25 in.
- Transverse cracking: 2000 ft/mi.
- Smoothness (IRI): 172 in/mi.

## Final Design for the New AC Pavement

One of the objectives of performing the case studies was to evaluate the final design outcomes and to compare feasible design options using the Missouri calibration coefficients and the global calibration. The final optimized designs using the Pavement ME Design program are presented in Table 80. A detailed description is as follows:

- Using global calibration models, AC thickness was optimized to 8 inches to satisfy all the design criteria.
- Using Missouri local calibration models from this study, the 8-inch AC thickness design resulted in higher fatigue cracking predictions based on the criterion of 10 percent allowable cracking, although all other distresses were within the desired criteria. The design thickness was increased for further evaluations.
- AC thickness was increased to 9 and 10 inches in further iterations for design optimization to satisfy the fatigue cracking criterion of 10 percent. Results of these analyses are presented in Table 80. Distress predictions indicate that increasing the thickness to 9 inches results in a bottom-up fatigue cracking of 14.7 percent at the end of 20 year design life. Using a 9-inch thickness reduces the design life by 4 years. The increase of AC thickness to 10 inches was required to produce a pavement design with predicted alligator cracking below the threshold 10 percent. Increasing AC thickness from 9-in to 10-in reduced alligator cracking by approximately 9 percent making the 10-in AC design acceptable.
- As summarized in Table 80, the locally calibrated model for 10-inch thickness predicts higher rutting and lower transverse cracking when compared to the global model with 8-inch thickness. For the same HMA mixes, the locally calibrated models, predicted less transverse cracking. These trends are as expected. Both models predicted transverse cracking levels less than the thresholds for adequate design.
- The locally calibrated model was more sensitive to changes in traffic and site conditions.
- The design thickness using the locally calibrated model is less than the design used on a comparable project in the same location.

Table 80. Summary of New AC design thicknesses and predicted distress/IRI

Distress Type (Units of Measurement)	Criterion	MoDOT Local Calibration				Global Calibration	
		9-inch AC		10-inch AC		8-inch AC	
Terminal IRI, in/mi	172	134.1	✓	129.79	✓	126.1	✓
Total Permanent Deformation, in	0.75	0.37	✓	0.37	✓	0.30	✓
AC bottom-up fatigue cracking, % lane area	10	14.66	×	5.20	✓	1.45	✓
AC thermal cracking, ft/mile	1000	440.6	✓	440.6	✓	528.9	✓
Permanent deformation - AC only, in	0.25	0.22	✓	0.22	✓	0.11	✓

The information presented in Table 80 shows that the locally calibrated model can produce a full depth AC pavement design that is in agreement with MoDOT expectations. The locally calibrated model seemed to be more sensitive to AC fatigue cracking, a frequent cause of early pavement failure.

### AC OVER AC PAVEMENT

A case study example of an AC overlay on existing AC pavement is presented in this section.

#### Project Location and Climate

The AC over AC pavement case study project was located at latitude = 39.0 degrees, longitude = -92.5 degrees (north of the New AC pavement project). Location specific climate characteristics were as follows:

- Mean annual air temperature (°F): 54.1
- Mean annual precipitation (in): 42.9
- Freezing index (°F - days): 452
- Average annual number of freeze/thaw cycles: 86.78

#### AC Overlay Preliminary Design

The Pavement ME Design was used to develop an initial trial design for these site conditions. A design period of 15 years was used for the analysis. Simulation was done beginning with a preliminary trial design that comprised the layer material types, thicknesses, and properties presented in Table 81.

Table 81. Trial AC overlay structure

Layer #	Layer Type	Mix Design (from HMA materials library)	Trial Design Thickness, in	Optimized Thickness, in
1	AC	SP125 16-66, PG 64-22 binder with 7.3% binder and 6.5% voids	1.6	1.5 to 3.0
2	Existing AC	SP 125 default	3.6	N/A
3	Flexible AC	SP250 default	7.1	N/A
4	Non-Stabilized	Crushed stone	4.0	N/A
5	Subgrade A-6	A-6 soil	Semi-infinite	Semi-infinite
Design life: 15 years. Existing construction: July 2007. Pavement construction: July 2019. Traffic opening: August 2019. Location – Northern part of the State. Initial AADTT: 2000 trucks with 0.84% linear growth. Cumulative truck traffic: 5.5 million trucks in 15 years.				

Using the site properties and trial design inputs presented, the Pavement ME Design was used to analyze design feasibility for the following:

- Optimization of AC overlay thickness using the local calibration models.
- Optimization of AC overlay thickness using the version 2.5.5 global calibration models.

Design adequacy was evaluated using the following predicted distress and IRI thresholds (at 90 percent reliability) criteria:

- Alligator cracking: 10 percent lane area.
- Total rutting: 0.50 in.
- AC rutting: 0.25 in.
- Transverse cracking: 2000 ft/mi.
- Smoothness (IRI): 172 in/mi.

Optimum AC overlay thickness was determined using the Pavement ME Design. Results of design optimization are presented in Table 82. This table also shows a comparison of design outcomes.

Table 82. Summary of optimized AC overlay thickness and predicted distress/IRI

Distress Type (Units of Measurement)	Criterion	1.5-inch AC Overlay		2.5-inch AC Overlay		3-inch AC Overlay	
		MoDOT	Global	MoDOT	Global	MoDOT	Global
Terminal IRI (in/mile)	172.00	114.36	126.54	110.6	121.45	104.5	118.76
Total Permanent Deformation (in)	0.75	0.11	0.05	0.07	0.03	0.05	0.03
AC total fatigue cracking: bottom up + reflective (% lane area)	10	12.82 (Fail)	16.64	11.18 (Fail)	14.33	7.88 (Pass)	13.63
AC total transverse cracking: thermal + reflective (ft/mile)	2,500.00	1,600.75	2,371.5	1,304.03	2027.3	1,017.7	1,802.5
Permanent deformation - AC only (in)	0.25	0.11	0.05	0.07	0.03	0.05	0.03
AC thermal cracking (ft/mile)	1,000.00	819.46	1,517.6 (Fail)	587.14	1161.2 (Fail)	376.99	974.84 (Pass)

The following can be concluded from the prediction results:

- The 1.5-in and 2.5-inch AC overlay designs failed in fatigue for the locally calibrated models. For the same overlay thicknesses, the global models indicate failure was from transverse thermal cracking. With the lower MAAT of the project location, the importance of evaluating thermal cracking comes to fore. The mechanism of failure critical for design is different between the two calibrations. As expected, the local calibration models predict higher cracking but lower thermal cracking.
- The 3-in AC overlay design was acceptable for both models. For the locally calibrated models, fatigue cracking controls design thickness while with the global models, thermal cracking-controlled design thickness.
- The local model is more likely to identify early fatigue related failures, especially because it reflects field conditions in Missouri.

In summary, the AC over AC case study showed the sensitivity of the global model to the colder northern climates of the state. The impact of cold climate was, however, significantly less for the locally calibrated model.

## CHAPTER 8. SUMMARY AND CONCLUSIONS

### SUMMARY

Missouri was one of the early adopters of the research grade pavement design procedure and software program developed under NCHRP 1-37A and 1-40D (Mallela, et al., 2009). With ongoing enhancements to the design procedure, calibration models, and the software program, MoDOT recognized the need to reevaluate the applicability of the global calibration models to Missouri's local conditions. Concurrently, MoDOT has been making changes to the HMA materials program, including increasing RAP additions to the HMA and adding advanced testing capabilities to develop Level 1 materials inputs to the Pavement ME Design procedure. MoDOT project 201609 was initiated to recalibrate all Pavement ME Design distress and IRI prediction models. One of the goals of this study was to incorporate current and future materials into the calibration process to ensure the models can be used for future designs. Thus, distress prediction models and the IRI prediction models in the globally calibrated Pavement ME Design were verified and recalibrated to represent Missouri site and pavement design/construction conditions. The verification and local calibration effort involved several major tasks. A summary of key tasks and outcomes are discussed in this chapter.

### Selection of Pavement Design Types of Interest

One of the goals of this study was to include pavement types that are used in current designs and will be used in future MoDOT pavement designs. Based on discussions with MoDOT, pavement types selected were for the verification and calibration of distress models were:

- a. New AC pavement
- b. AC over AC pavement
- c. AC over JPCP
- d. New JPCP
- e. Unbonded JPCP overlay over exiting JPCP

### Project Selection

Calibration projects were selected from two primary databases, the MoDOT PMS and FHWA LTPP. Selection of candidate calibration projects covered all design types, material sources, mix designs, and climate patterns relevant to Missouri pavement design and construction.

The range of parameters included in the MoDOT PMS sections database were as follows:

- For New AC projects, construction was over crushed or large stone base layers on fine subgrades. The HMA wearing surfaces used 9.5 or 12.5 mm nominal aggregate size HMA mix. Intermediate HMA layer mix types considered were nominal aggregate size of 19.0 and 25.0 mm. Binder types included SuperPave Performance Grade (PG) 76-22, 70-22, and 64-22 grades, using virgin aggregates, and RAP contents ranging from about 12 to 24 percent. The projects were constructed over fine-grained soils. Projects were constructed from 2001 to 2010 and were located throughout the state.

- AC over AC projects had HMA overlay thicknesses in the range of 1.5 to 5 inches and were constructed over existing 9 to 12-inch thick HMA layers of AC pavements. AC overlays used 9.5 or 12.55 mm nominal aggregate size HMA mix with varying RAP contents. For some of the projects, the existing HMA layer was milled up to 2 inches prior to HMA overlay placement. The existing pavement base type/subgrade were typical of base materials used by MoDOT for New AC pavements. Existing pavement condition was a mix of good/fair/poor. The existing pavement in several of the AC over AC projects used were considered as New AC pavement projects under the previous calibration effort. HMA overlays were constructed from 2006 to 2013.
- For AC overlay over existing JPCP, the overlay construction was completed in two lifts using 12.5 mm to 19 mm nominal aggregate size HMA layers with a total thickness ranging from 3.7 to 4.2 inches. HMA mixes used 9 to 40 percent RAP contents. PCC materials, base type, and their thicknesses varied, but were typical of MoDOT designs and specifications; subgrades were typical of Missouri soils. Existing pavement condition was a mix of good/fair/poor. The HMA overlays were constructed from 2006 to 2010.
- For new JPCP and unbonded JPCP overlay projects, the majority of projects comprised of PCC thickness greater than 10 inches, widened 14 ft lanes with tied shoulders, and joint spacing of 15 ft. The JPCP projects were doweled and constructed over an aggregate base and fine subgrade.

LTPP sections located in the state of Missouri were included in the calibration database. LTPP experiments included in the calibration and the pavement types therein were:

- SPS-5 – AC overlay on existing AC pavement
- SPS-6 – AC overlay on existing JPCP
- SPS-8 – New AC and JPCP with minimal traffic (SPS-8 was designed to study the effects of environmental factors in the absence of heavy loads)
- SPS-9 – AC overlay on JCP with different AC binder types
- GPS -1 – AC surfaced pavements with unbound granular base
- GPS-6A - Existing AC overlay on AC Pavement
- GPS-6B - AC Overlay with conventional AC on AC Pavement, no milling
- GPS-6S - AC Overlay on AC pavement with milling and/or fabric pretreatment

### **Development of Pavement ME Design Database**

Data from MoDOT and LTPP database were assembled in a format suitable for Pavement ME analyses. MoDOT conducted laboratory and field tests to obtain Level 1 data to the extent possible for use in the calibration as well as in future MoDOT designs.

MERRA Climate data was obtained for all AC surfaced LTPP and MoDOT projects from the LTPP InfoPave Climate tool. For rigid pavements, the Pavement ME uses the NARR climate data that can be accessed directly from the software program interface.

MoDOT Traffic unit is responsible for installation of weigh-in motion sites, traffic data collection, processing, and reporting. Historical traffic records, in weight data format, from 18

installation sites for a 3-year period, 2015, 2016 and 2017 was thus obtained from MoDOT. The historical weight records were then analyzed to develop the following site-specific traffic inputs for the Pavement ME software: Vehicle Class Distribution, Number of Axles Per Truck, Monthly Adjustment Factors, and Axle Load Distribution Profiles. The traffic inputs were then further analyzed to evaluate conformance with generally accepted trends, presence of data clusters, outliers and errors. The outcome of raw WIM traffic data analysis and processing was Missouri specific default traffic inputs for the AASHTO Pavement ME Design tool. Level 1 traffic inputs were used, when available, for the calibration. A MoDOT traffic library was also created for use in future MoDOT designs. Axle load distributions for all axle types for all WIM sites are tabulated in Appendix A.

Layer materials and layer thickness data were assembled from various sources, which primarily included the use of laboratory testing and field testing results. The development of Missouri default Pavement ME data inputs involved the following activities:

- Loose samples of HMA materials and field cores from the AC surfaced PMS sections (New AC, AC over AC and AC over JPCP) were extracted for laboratory testing to develop HMA materials inputs required for design. Laboratory test results were provided for dynamic modulus, low temperature creep compliance, and indirect tensile strength tests. HMA mixes used in these tests used the various MoDOT SP gradations and binder types with RAP contents ranging from 12 to 40 percent. These data were used in calibration and also to develop HMA materials library for MoDOT. HMA materials test data are included in Appendix B.
- Laboratory characterization of PCC materials was conducted under the 2009 calibration effort. No additional PCC tests were performed under this project. Data from previous testing covered all PCC gradations included in the MoDOT specifications. These data were also used to develop PCC materials library for MoDOT.
- Field core data were used to determine layer thicknesses.
- Field FWD test results were used for backcalculating subgrade resilient modulus for local calibration and models verification. FWD tests were performed only on New AC, AC over AC, and AC over JPCP projects.

The final and critical element of the calibration database is performance data. For PMS projects, time-series rutting, faulting, and IRI data were obtained from MoDOT PMS database. Note that, faulting data, was available only for the year 2017. For AC alligator cracking and transverse cracking and JPCP transverse slab cracking, data was obtained by reviewing MoDOT PMS video imaging files and conducting a virtual distress survey as per LTPP distress data collection and reporting protocols. The video imaging data was available only for the year 2017.

The LTPP database was used to assemble all data required for the LTPP sections used in the calibration (<https://infopave.fhwa.dot.gov>, accessed 2017 and 2019).

## Local Calibration of Distress Prediction Models

Local calibration was performed for all AC distress models. For JPCP, the models were verified using a classification type analysis because the calibration sections did not have adequate distress development to develop a meaningful calibration model. Calibration was done to remove bias (consistent over- or under-prediction) and improve accuracy of prediction while verification was done to confirm accuracy and absence of bias. The outcomes of this effort were as follows:

- Significant improvements were made for AC alligator cracking, reflection fatigue cracking, thermal cracking, and transverse reflection cracking prediction models.
- A reasonable improvement in the total rutting model accuracy was achieved. Total rutting data contains considerable amount of variability. Thus, a significant improvement in  $R^2$  was not expected.
- For all the AC models, any significant bias was minimized or eliminated.
- The JPCP models were verified to determine their accuracy and bias for Missouri conditions. Classification methods were applied as field measured distress was nonexistent. The global models were deemed reasonable for MoDOT local conditions within a limited range of field distresses.

## Sensitivity Analysis

Sensitivity studies were done to help establish confidence in the new locally calibrated or verified models. Outcomes were very reasonable, and trends observed were as expected. Summary of sensitivity analysis results is presented as follows:

- Increasing AC thickness reduced AC alligator cracking, rutting, and transverse thermal cracking.
- Increasing air voids in the HMA mixes resulted in increased cracking, rutting, and IRI. Increasing air voids corresponded with decrease in tensile strength and modulus. This resulted in increased alligator cracking and transverse cracking.
- AC pavement located in the warmer parts of the state exhibited considerably more rutting and alligator cracking. The colder regions exhibited more low temperature cracking.
- Increasing PCC thickness, adding edge support, reducing CTE, and increased flexural strength significantly reduced slab cracking. Increasing dowel diameter and reducing CTE significantly reduced joint faulting. Slab widening reduced faulting, transverse cracking, and IRI.

## Case Studies

Case studies were presented for New AC and AC over AC designs. The design inputs and site conditions were specific to Missouri. The case studies compared the results of optimized designs using the newly calibrated Missouri distress prediction models with those resulting from the global models. This was done to highlight how the Missouri calibration models deviate from the global models. In general, the designs showed that the global models predicted lower fatigue cracking and higher transverse cracking.

A higher AC thickness was required with the recalibrated model for a project in the central to southern regions of the state. Optimal AC thickness for New AC pavement design was determined based on fatigue failure criterion. This is key to reducing frequency of early pavement failures from fatigue.

However, for the AC over AC design, which was in a colder northern region of the state, the controlling distress was thermal cracking using the global model while the controlling distress was AC fatigue using the recalibrated model. Both cases resulted in the same thickness, however, the controlling distress changed.

## **CONCLUSIONS AND RECOMMENDATIONS**

The various Pavement ME Design prediction models have been verified, validated, and when adequate data were available, recalibrated using Missouri LTPP and PMS projects. The model verification and calibration efforts were successful. A project database was developed and used in the verification, validation, and recalibration process. This database served as the basis for developing default Level 1 materials and traffic inputs for future pavement design.

Moving forward, the project team provides the following recommendations:

- MoDOT should consider developing a Pavement ME calibration support plan designed to examine the validity of the recalibrated distress models and to enable future adjustments based on field data. This plan is a means to fully realize the efforts and resources invested under this study. The plan should support MoDOT to continue monitoring the performance of the sections used in the current calibration. It should also include guidelines to identify additional sections with adequate design, materials, and construction data so that these sections can be used to supplement and/or validate the models developed under this study. A critical component of this plan is the development of a performance database for the sections identified in the calibration support plan. The goal should be to assemble data collected from routine condition monitoring, so that performance data for these sections can be easily accessed by the Construction and Materials Division of MoDOT.
- For future designs using the calibration models developed under this study, the project team recommends using Level 1 inputs to the extent possible. Note that the calibration was performed using Level 1 data for most PMS sections.
- Changes to the AC fatigue model were necessary to calibrate the bottom-up fatigue cracking model, which was statistically supported to represent field data. The current project did not include the calibration of the top-down fatigue cracking model as MoDOT does not use this distress type as a performance criterion to evaluate trial designs and optimize layer thicknesses. However, changes to the AC fatigue model have changed the top-down fatigue cracking predictions generated from the AASHTOWare Pavement ME analysis. It is recommended that global calibration models be used if top-down fatigue cracking predictions are of interest.

## REFERENCES

1. AASHTO, 2010. *Guide for the Local Calibration of the Mechanistic-Empirical Pavement Design Guide*. American Association of State Highway and Transportation Officials, Washington, D.C.
2. AASHTO, 2015. *Mechanistic-Empirical Pavement Design Guide: A Manual of Practice*, 2nd Edition. (<https://me-design.com/MEDesign/Documents.html> for addendums to the document)
3. AASHTO, 2019a. *AASHTOWare Pavement ME Design Version 2.5.5*. Washington (DC): American Association of State Highway and Transportation Officials.
4. AASHTO, 2019b. *AASHTOWare Pavement ME Design Build 2.5.5 Release Notes (2016 through 2019)*. <https://me-design.com/MEDesign/Documents.html>
5. Applied Research Associates (ARA), 2004. *Development of the 2002 Guide for the Design of New and Rehabilitated Pavement Structures: Phase II, Final Report*, NCHRP Project 1-37A, Transportation Research Board, Washington, D.C.
6. ARA, 2006. *NCHRP Research Results Digest 308: Changes to the Mechanistic-Empirical Pavement Design Guide Software Through Version 0.900*, Transportation Research Board, Washington, D.C.
7. Bonaquist, R., 2010. *Wisconsin Mixture Characterization Using the Asphalt Mixture Performance Tester (AMPT) on Historical Aggregate Structures*, Report No. WHRP 09-03, Wisconsin Department of Transportation, Madison.
8. Bonaquist, R., 2011. *NCHRP Report 702: Precision of the Dynamic Modulus and Flow Number Tests Conducted with the Asphalt Mixture Performance Tester*, Final Report, Phase VI, NCHRP 9-29, Transportation Research Board, Washington, D.C.
9. Darter, M., Titus-Glover, L., Von Quintus, V.L., Bhattacharya, B., and Mallela, J., 2014. *Calibration and Implementation of the AASHTO Mechanistic-Empirical Pavement Design Guide in Arizona*, Report FHWA-AZ-14-606, Project SPR-606, Prepared for Arizona Department of Transportation, AZ.
10. Federal Highway Administration, 2016. *Traffic Monitoring Guide*, US DOT.
11. FHWA, LTPP Database (<https://infopave.fhwa.dot.gov/> accessed 2017; 2019 for HMA in-place air voids data), Turner-Fairbank Highway Research Center, Virginia.
12. Google, N.D., Google Maps, ([google.com/maps](https://google.com/maps)).
13. Lusher, S.M., 2017. *Cold Temperature Creep Compliance and Strength of Missouri Hot Mix Asphalt (HMA) Mixtures Using Indirect Tensile Test*, Final Report MoDOT project # TR201713.
14. Lytton, R. L., Tsai, F.L., Lee, S., Luo, R., Hu, S., Zhou, F., 2010. *Models for Predicting Reflection Cracking of Hot-Mix Asphalt Overlays*, NCHRP 669, Transportation Research Board, Washington, D.C.

15. Mallela, J., Titus-Glover, L., Von Quintus, V.L., Darter, M., Stanley, M., Rao, C., 2009. *Implementing the AASHTO Mechanistic Empirical Pavement Design Guide in Missouri*, Volume I: *Study Findings, Conclusions, and Recommendations*, and Volume II: *MEPDG Model Validation and Calibration*, Report No. CM08.01 for Project RI04-002, Pavement Section Investigation Report.
16. Mallela, J, Titus-Glover, L., Sadasivam, S., Bhattacharya, B., Darter, M., Von Quintus, V.L., 2013. Implementation of AASHTO Mechanistic Empirical Pavement Design Guide for Colorado, Report No. CDOT-2013-4, Colorado Department of Transportation, DTO Applied Research and Innovations Branch, Denver, CO.
17. Miller, J.S., and W.Y. Bellinger, 2014. *Distress Identification Manual for the Long-Term Pavement Performance Program*, Report No. FHWA-HRT-13-092, Federal Highway Administration, McLean, VA.
18. Miner, M. A., 1945. Cumulative Damage in Fatigue, *Journal of Applied Mechanics*, Vol. 12, Transactions of the American Society of Mechanical Engineers.
19. Missouri Department of Transportation, 2018. Missouri Standard Specifications for Highway Construction, Missouri Highways and Transportation Commission.
20. Titus-Glover, L., Bhattacharya, B., Raghunathan, D., Mallela, J., and R. Lytton. 2016. Adaptation of NCHRP project 1-41 reflection cracking models for semirigid pavement design in AASHTOWare pavement ME Design. *Transportation Research Record: Journal of the Transportation Research Board*. 2590. 122-131. 10.3141/2590-14.
21. USDA, 2017. <http://planthardiness.ars.usda.gov/PHZMWeb/> (accessed April 2017).
22. Von Quintus, Harold L.; Mallela, J., Bonaquist, R.; Schwartz, C.W. and Carvalho, R.L., 2012. *Calibration of Rutting Models for Structural and Mix Design*, NCHRP 719, Transportation Research Board, Washington, D.C.

## APPENDIX A: NUMBER OF AXLES PER TRUCK FOR WIM SITES

Table A - 1. Number of axles per truck for MoDOT WIM sites

Site	Vehicle Class	Axle Type				Total Number of Axles
		Single	Tandem	Tridem	Quad	
1881_1_1	4	1.81	0.38	0	0	2.57
1881_1_1	5	2	0	0	0	2
1881_1_1	6	1	1	0	0	3
1881_1_1	7	0.99	0.01	0.99	0	3.98
1881_1_1	8	2.16	0.84	0	0	3.84
1881_1_1	9	1.27	1.86	0	0	5
1881_1_1	10	1.27	1.07	0.85	0.01	6
1881_1_1	11	5	0	0	0	5
1881_1_1	12	4	1	0	0	6
1881_1_1	13	1.35	1.01	0.98	0.22	7.18
1883_5_1	4	1.76	0.38	0	0	2.52
1883_5_1	5	2	0	0	0	2
1883_5_1	6	1	1	0	0	3
1883_5_1	7	1	0.01	0.99	0	3.99
1883_5_1	8	2.16	0.83	0	0	3.82
1883_5_1	9	1.25	1.87	0	0	5
1883_5_1	10	1.5	1.04	0.8	0	6
1883_5_1	11	5	0	0	0	5
1883_5_1	12	4	1	0	0	6
1883_5_1	13	1.22	0.56	1.4	0.18	7.26
2001_1_1	4	1.77	0.23	0	0	2.23
2001_1_1	5	2	0	0	0	2
2001_1_1	6	1	1	0	0	3
2001_1_1	7	1	0	1	0	4
2001_1_1	8	2.27	0.71	0	0	3.7
2001_1_1	9	1.32	1.81	0.01	0	5
2001_1_1	10	1.16	1.06	0.88	0.02	6
2001_1_1	11	5	0	0	0	5
2001_1_1	12	3.2	0.2	0.8	0	6
2001_1_1	13	2.11	1.11	0	0.67	7
2001_1_2	4	1.89	0.15	0	0	2.18
2001_1_2	5	2	0	0	0	2
2001_1_2	6	1	1	0	0	3

Site	Vehicle Class	Axle Type				Total Number of Axles
		Single	Tandem	Tridem	Quad	
2001_1_2	7	1	0	1	0	4
2001_1_2	8	2.27	0.74	0	0	3.75
2001_1_2	9	1.32	1.81	0.01	0	5
2001_1_2	10	1.27	1	0.88	0.02	6
2001_1_2	11	5	0	0	0	5
2001_1_2	12	3.22	0.22	0.78	0	6
2001_1_2	13	1.71	0.51	0.86	0.47	7.21
2003_5_1	4	1.91	0.1	0	0	2.12
2003_5_1	5	2	0	0	0	2
2003_5_1	6	1	1	0	0	3
2003_5_1	7	1	0	1	0	4
2003_5_1	8	2.24	0.77	0	0	3.78
2003_5_1	9	1.36	1.79	0.02	0	5
2003_5_1	10	1.3	0.95	0.93	0.01	6
2003_5_1	11	5	0	0	0	5
2003_5_1	12	3.36	0.36	0.64	0	6
2003_5_1	13	1.35	0.65	1.2	0.25	7.25
2003_5_2	4	1.93	0.09	0	0	2.1
2003_5_2	5	2	0	0	0	2
2003_5_2	6	1	1	0	0	3
2003_5_2	7	1	0	1	0	4
2003_5_2	8	2.26	0.74	0	0	3.74
2003_5_2	9	1.36	1.79	0.02	0	5
2003_5_2	10	1.17	0.99	0.94	0.01	6
2003_5_2	11	5	0	0	0	5
2003_5_2	12	3.57	0.57	0.43	0	6
2003_5_2	13	1.58	0.93	0.93	0.25	7.2
2021_1_1	4	1.85	0.16	0	0	2.17
2021_1_1	5	2	0	0	0	2
2021_1_1	6	1	1	0	0	3
2021_1_1	7	1	0	1	0	4
2021_1_1	8	2.3	0.7	0	0	3.7
2021_1_1	9	1.32	1.82	0.01	0	5
2021_1_1	10	1.17	1.02	0.89	0.03	6
2021_1_1	11	5	0	0	0	5
2021_1_1	12	3.33	0.33	0.67	0	6
2021_1_1	13	1.52	0.52	0.76	0.56	7.08

Site	Vehicle Class	Axle Type				Total Number of Axles
		Single	Tandem	Tridem	Quad	
2021_1_2	4	1.87	0.17	0	0	2.22
2021_1_2	5	2	0	0	0	2
2021_1_2	6	1	1	0	0	3
2021_1_2	7	1	0	1	0	4
2021_1_2	8	2.24	0.76	0	0	3.76
2021_1_2	9	1.32	1.82	0.01	0	5
2021_1_2	10	1.22	1.01	0.88	0.03	6
2021_1_2	11	5	0	0	0	5
2021_1_2	12	3.55	0.55	0.45	0	6
2021_1_2	13	1.48	0.56	0.89	0.49	7.21
2023_5_1	4	1.84	0.18	0	0	2.19
2023_5_1	5	2	0	0	0	2
2023_5_1	6	1	1	0	0	3
2023_5_1	7	1	0	1	0	4
2023_5_1	8	2.3	0.7	0	0	3.7
2023_5_1	9	1.38	1.78	0.02	0	5
2023_5_1	10	1.08	1.08	0.92	0	6
2023_5_1	11	5	0	0	0	5
2023_5_1	12	3.76	0.76	0.24	0	6
2023_5_1	13	1	0.67	1	0.5	7.33
2023_5_2	4	1.89	0.13	0	0	2.14
2023_5_2	5	2	0	0	0	2
2023_5_2	6	1	1	0	0	3
2023_5_2	7	1.02	0.02	0.97	0	4
2023_5_2	8	2.3	0.7	0	0	3.7
2023_5_2	9	1.38	1.78	0.02	0	5
2023_5_2	10	1.14	1.08	0.88	0.02	6
2023_5_2	11	5	0	0	0	5
2023_5_2	12	3.76	0.76	0.24	0	6
2023_5_2	13	1.27	0.83	1.03	0.31	7.27
3021_1_1	4	1.63	0.46	0	0	2.55
3021_1_1	5	2	0	0	0	2
3021_1_1	6	1	1	0	0	3
3021_1_1	7	1	0	1	0	4
3021_1_1	8	2.16	0.86	0	0	3.88
3021_1_1	9	1.03	1.53	0	0	5
3021_1_1	10	1.14	1.05	0.92	0	6

Site	Vehicle Class	Axle Type				Total Number of Axles
		Single	Tandem	Tridem	Quad	
3021_1_1	11	5	0	0	0	5
3021_1_1	12	3.97	0.97	0.03	0	6
3021_1_1	13	1.23	0.41	1.25	0.36	7.24
3023_5_1	4	1.84	0.34	0	0	2.52
3023_5_1	5	2	0	0	0	2
3023_5_1	6	1	1	0	0	3
3023_5_1	7	1	0	1	0	4
3023_5_1	8	2.22	0.8	0	0	3.82
3023_5_1	9	1.26	1.86	0.01	0	5
3023_5_1	10	1.13	1.04	0.93	0	6
3023_5_1	11	5	0	0	0	5
3023_5_1	12	4	1	0	0	6
3023_5_1	13	1.25	0.37	1.42	0.26	7.3
4201_1_1	4	1.85	0.26	0	0	2.37
4201_1_1	5	2	0	0	0	2
4201_1_1	6	1	1	0	0	3
4201_1_1	7	1.01	0.01	0.99	0	4
4201_1_1	8	2.14	0.86	0	0	3.86
4201_1_1	9	1.24	1.87	0.01	0	5
4201_1_1	10	1.15	1.02	0.89	0.03	6
4201_1_1	11	5	0	0	0	5
4201_1_1	12	4	1	0	0	6
4201_1_1	13	1.24	0.49	1.35	0.23	7.2
4413_5_1	4	1.93	0.11	0	0	2.14
4413_5_1	5	2	0	0	0	2
4413_5_1	6	1	1	0	0	3
4413_5_1	7	1	0	1	0	4
4413_5_1	8	2.44	0.54	0	0	3.53
4413_5_1	9	1.27	1.81	0.02	0.02	5
4413_5_1	10	1.22	0.92	0.81	0.13	6
4413_5_1	11	5	0	0	0	5
4413_5_1	12	3.99	0.99	0.01	0	6
4413_5_1	13	1.75	1.01	0.54	0.45	7.19
6101_1_1	4	1.86	0.22	0	0	2.31
6101_1_1	5	2	0	0	0	2
6101_1_1	6	1	1	0	0	3
6101_1_1	7	1.01	0.01	0.99	0	4

Site	Vehicle Class	Axle Type				Total Number of Axles
		Single	Tandem	Tridem	Quad	
6101_1_1	8	2.12	0.88	0	0	3.88
6101_1_1	9	1.24	1.87	0.01	0	5
6101_1_1	10	1.47	0.94	0.86	0.02	6
6101_1_1	11	5	0	0	0	5
6101_1_1	12	4	1	0	0	6
6101_1_1	13	1.24	0.24	1.56	0.22	7.28
6103_5_1	4	1.86	0.23	0	0	2.31
6103_5_1	5	2	0	0	0	2
6103_5_1	6	1	1	0	0	3
6103_5_1	7	1	0	1	0	4
6103_5_1	8	2.09	0.91	0	0	3.92
6103_5_1	9	1.27	1.86	0.01	0	5
6103_5_1	10	1.11	1.04	0.93	0.01	6
6103_5_1	11	5	0	0	0	5
6103_5_1	12	4	1	0	0	6
6103_5_1	13	1.25	0.54	1.32	0.23	7.21
7401_1_1	4	1.83	0.31	0	0	2.45
7401_1_1	5	2	0	0	0	2
7401_1_1	6	1	1	0	0	3
7401_1_1	7	1	0	1	0	4
7401_1_1	8	2.15	0.85	0	0	3.86
7401_1_1	9	1.22	1.88	0.01	0	5
7401_1_1	10	1.19	0.96	0.85	0.09	6
7401_1_1	11	5	0	0	0	5
7401_1_1	12	4	1	0	0	6
7401_1_1	13	1.22	1.05	0.64	0.48	7.15
7403_5_1	4	1.74	0.36	0	0	2.47
7403_5_1	5	2	0	0	0	2
7403_5_1	6	1	1	0	0	3
7403_5_1	7	1	0	1	0	4
7403_5_1	8	2.06	0.92	0	0	3.91
7403_5_1	9	1.2	1.89	0.01	0	5
7403_5_1	10	1.04	1	0.97	0.01	6
7403_5_1	11	5	0	0	0	5
7403_5_1	12	4	1	0	0	6
7403_5_1	13	1.19	0.63	1.13	0.34	7.22
7602_3_1	4	1.9	0.15	0	0	2.2

Site	Vehicle Class	Axle Type				Total Number of Axles
		Single	Tandem	Tridem	Quad	
7602_3_1	5	2	0	0	0	2
7602_3_1	6	1	1	0	0	3
7602_3_1	7	1.14	0.05	0.92	0	4
7602_3_1	8	2.47	0.68	0	0	3.83
7602_3_1	9	1.19	1.9	0	0	5
7602_3_1	10	1.61	1.11	0.71	0.01	6.01
7602_3_1	11	5	0	0	0	5
7602_3_1	12	4	1	0	0	6
7602_3_1	13	1.5	2.25	0.23	0.09	7.03
9202_3_1	4	1.92	0.16	0	0	2.24
9202_3_1	5	2	0	0	0	2
9202_3_1	6	1	1	0	0	3
9202_3_1	7	1	0	1	0	4
9202_3_1	8	2.27	0.69	0.01	0	3.68
9202_3_1	9	1.41	1.77	0.01	0	5
9202_3_1	10	1.14	1.06	0.89	0.01	6
9202_3_1	11	5	0	0	0	5
9202_3_1	12	4	1	0	0	6
9202_3_1	13	1.21	0.51	1.26	0.31	7.26
9204_7_1	4	1.92	0.22	0	0	2.37
9204_7_1	5	2	0	0	0	2
9204_7_1	6	1	1	0	0	3
9204_7_1	7	1	0	1	0	4
9204_7_1	8	2.27	0.72	0	0	3.72
9204_7_1	9	1.4	1.78	0.01	0	5
9204_7_1	10	1.14	1.02	0.9	0.03	6
9204_7_1	11	5	0	0	0	5
9204_7_1	12	3.98	0.98	0.02	0	6
9204_7_1	13	1.29	0.73	0.89	0.47	7.28
9302_3_1	4	1.93	0.22	0	0	2.37
9302_3_1	5	2	0	0	0	2
9302_3_1	6	1	1	0	0	3
9302_3_1	7	1	0	1	0	4
9302_3_1	8	2.29	0.71	0	0	3.72
9302_3_1	9	1.18	1.9	0	0	5
9302_3_1	10	1.45	1.07	0.78	0.02	6
9302_3_1	11	5	0	0	0	5

Site	Vehicle Class	Axle Type				Total Number of Axles
		Single	Tandem	Tridem	Quad	
9302_3_1	12	4	1	0	0	6
9302_3_1	13	1.32	1.42	0.62	0.29	7.16

## APPENDIX B: LEVEL 1 HMA MATERIALS TEST RESULTS

This appendix presents Level 1 HMA materials test data for Pavement ME inputs. Table B - 1, Table B - 2, and Table B - 3 summarize dynamic modulus, indirect tensile strength and creep compliance values respectively. These data were also utilized in the calibration of the New AC, AC over AC, and AC over PCC distress prediction models.

Table B - 1. Dynamic modulus inputs for MoDOT HMA mixes, psi

Mix Designation	Air Voids	Test Temperature (°F)	Test Frequency (Hz)			
			0.1	1	10	25
SP190 15-27	4.00%	14	2771403	3024705	3188720	3235415
		40	1916194	2401212	2769571	2883157
		70	809222	1323668	1878794	2086480
		100	236657	478408	880311	1080167
		130	75881	147285	302348	400240
SP190 15-27	6.50%	14	2504551	2805685	3009146	3068481
		40	1627351	2125200	2529715	2659413
		70	660608	1109759	1632571	1838461
		100	208476	408036	749959	925884
		130	77095	140390	274106	358119
SP190 15-48	4.00%	14	2731366	3002663	3177609	3227159
		40	1867443	2371851	2755431	2873360
		70	781270	1305264	1874467	2087181
		100	227356	473995	889346	1096073
		130	71777	145163	308718	412904
SP190 15-48	6.50%	14	2463948	2748956	2951749	3013437
		40	1646002	2096441	2470410	2593853
		70	719143	1147437	1625289	1812110
		100	232277	447759	787547	954326
		130	75976	149330	296621	384825
SP190 15-57	4.00%	14	2616082	2926111	3129390	3187432
		40	1689799	2228124	2652634	2785565
		70	637925	1135526	1712420	1935956
		100	167077	372970	748379	944819
		130	49106	104626	237195	325898
SP190 15-57	6.50%	14	2328973	2667627	2907584	2979811
		40	1405610	1910186	2345957	2491482
		70	504238	900543	1395959	1600998
		100	136406	289567	571639	724339
		130	42870	85632	182356	246059

Mix Designation	Air Voids	Test Temperature (°F)	Test Frequency (Hz)			
			0.1	1	10	25
SP250 16-68	4.00%	14	2509491	2860320	3098437	3167823
		40	1543094	2095846	2555740	2704459
		70	562050	1015499	1573931	1799837
		100	155864	333967	665841	844814
		130	51870	102234	218422	295714
SP250 16-68	6.50%	14	2221141	2605137	2880545	2963585
		40	1255924	1784669	2261278	2423411
		70	418699	782714	1272572	1484046
		100	115380	243225	492920	634501
		130	40615	76320	157812	212629
SP125 16-44	4.00%	14	2489622	2824717	3048411	3112843
		40	1544436	2088994	2534731	2677090
		70	562872	1018816	1575978	1799336
		100	155276	333788	667994	848139
		130	52054	101980	218045	295647
SP125 16-44	6.50%	14	2636151	2916695	3087713	3134000
		40	1695180	2247211	2660408	2783810
		70	587235	1095687	1700699	1933378
		100	144651	325087	685102	883493
		130	48064	91627	200316	277012
SP125 16-55	4.00%	14	2329087	2685039	2938169	3014462
		40	1406785	1925475	2374154	2523994
		70	512100	923082	1433970	1644211
		100	139064	303501	605419	767407
		130	42133	88923	196804	267980
SP125 16-55	6.50%	14	2152272	2533300	2808611	2892061
		40	1213277	1730587	2198975	2358927
		70	402704	759099	1238314	1445120
		100	108066	233795	480234	619782
		130	36078	70737	151267	205778
SP125 16-66	4.00%	14	2491473	2815105	3035006	3099307
		40	1581224	2102154	2529773	2667538
		70	610389	1064751	1603855	1817959
		100	176546	369163	711613	890764
		130	58537	115678	243420	326144
SP125 16-66	6.50%	14	2322606	2676459	2918351	2988971
		40	1375714	1912487	2370090	2519729

Mix Designation	Air Voids	Test Temperature (°F)	Test Frequency (Hz)			
			0.1	1	10	25
		70	475476	882455	1406706	1624462
		100	130914	279654	567743	728039
		130	45820	87080	182957	247744
		14	2404661	2739073	2967362	3034181
SP190 14-18	6.50%	40	1457725	1983927	2426696	2571018
		70	515063	931503	1454801	1669827
		100	141112	296439	589791	750741
		130	48314	91163	188805	253942
		14	2672728	2973223	3165221	3218976
SP190 14-18	4.00%	40	1745536	2287844	2708116	2837585
		70	676471	1181759	1767761	1993759
		100	197328	407626	787975	987349
		130	71024	131763	269279	359601
		14	2623002	2962453	3163308	3215991
SP125 14-3	4.00%	40	1685947	2301158	2755530	2887740
		70	642333	1208596	1871686	2119142
		100	195031	429892	883071	1122162
		130	77277	146898	319040	436937
		14	1935431	2359386	2679335	2778939
SP125 14-3	6.50%	40	1070144	1588175	2072848	2241924
		70	357827	714495	1195637	1402906
		100	89432	224411	493649	643999
		130	23438	60404	156138	222665
		14	1953796	2398374	2718903	2814992
SP125 16-9	4.00%	40	1039714	1602386	2118920	2294177
		70	308037	677874	1199756	1425455
		100	65285	186817	459149	619229
		130	15287	43489	127723	191474
		14	1720859	2167240	2511478	2619642
SP125 16-9	6.50%	40	850069	1354786	1854105	2033087
		70	228751	519270	958072	1158917
		100	43973	129300	329307	452194
		130	9243	27339	82768	125801
		14	2653555	2930740	3112619	3164772
SP125 15-60	4.00%	40	1779546	2280570	2669337	2790608
		70	716952	1216657	1771657	1982598
		100	197247	421538	807785	1003350
		130	58230	121669	266191	359712

Mix Designation	Air Voids	Test Temperature (°F)	Test Frequency (Hz)			
			0.1	1	10	25
SP125 15-60	6.50%	14	2407968	2735750	2956398	3020387
		40	1455136	1986847	2427769	2569938
		70	490396	915071	1449258	1667482
		100	119901	270030	564458	728210
		130	36151	73608	164599	227511
SP125 16-39	4.00%	14	2709912	2952665	3116204	3164234
		40	1911624	2355790	2700308	2809082
		70	867137	1353733	1863814	2054138
		100	271086	528035	924464	1113931
		130	83280	166850	337859	440671
SP125 16-39	6.50%	14	2405271	2703444	2914570	2978403
		40	1565565	2029805	2418684	2547161
		70	653238	1072019	1554136	1745425
		100	205597	402425	725897	888915
		130	69184	133645	266413	347788
SP095 16-13	6.50%	14	1931146	2349779	2663885	2761268
		40	1070643	1586835	2067298	2234218
		70	357946	715231	1196144	1402745
		100	89313	224380	494182	644814
		130	23465	60345	156077	222703
SP095 16-13	4.00%	14	2338845	2724184	2964600	3029664
		40	1276077	1898971	2417453	2578855
		70	359222	762383	1348725	1600839
		100	91895	203491	463086	625099
		130	37886	64713	133707	185103
SP095 16-13	6.50%	14	2045046	2460569	2748971	2833007
		40	1068581	1624409	2133826	2305098
		70	311399	645643	1140400	1361911
		100	81363	181391	402578	537780
		130	30699	56556	120798	167102
BP2_1587	3.50%	14	2490976	2848029	3079909	3145083
		40	1488572	2072214	2550157	2700949
		70	503104	955437	1538380	1776674
		100	137356	295902	614397	794251
		130	50906	93422	195180	265617
BP2_1587	6.50%	14	1757876	2234466	2604230	2719902
		40	864264	1375727	1900484	2091600
		70	265360	542734	972934	1175824

Mix Designation	Air Voids	Test Temperature (°F)	Test Frequency (Hz)			
			0.1	1	10	25
		100	78360	168784	361872	479147
		130	31135	57934	121365	165526
BP1_1661	3.50%	14	2616162	2916698	3119403	3178613
		40	1684202	2199283	2614766	2747745
		70	633306	1100860	1647039	1862288
		100	164930	355120	696367	875640
		130	47968	98724	215510	292545
BP1_1661	6.50%	14	2188570	2552376	2820325	2902948
		40	1266943	1759581	2207480	2362157
		70	449520	800475	1259045	1455852
		100	131268	264235	509055	643685
		130	46621	86221	171689	226981

Table B - 2. Indirect tensile strength inputs for MoDOT HMA mix designs

Mix Design ID	Mix with Lower Voids		Mix with Higher Voids	
	% AC Voids	Indirect Tensile Strength, psi	% AC Voids	Indirect Tensile Strength, psi
SP250 16-68	4.0	579	6.5	450
SP190 15-57	4.0	626	6.5	514
SP190 15-48	4.0	612	6.5	479
SP190 15-27	4.0	610	6.5	508
SP190 14-18	4.0	606	6.5	520
SP125 16-99	4.0	718	6.5	590
SP125 16-98	4.0	654	6.5	597
SP125 16-95	4.0	577	6.5	492
SP125 16-94	4.0	774	6.5	509
SP125 16-93	4.0	614	6.5	497
SP125 16-91	4.0	575	6.5	499
SP125 16-9 SMA	4.0	551	6.5	505
SP125 16-89	4.0	585	6.5	521
SP125 16-84	4.0	745	6.5	614
SP125 16-83	4.0	723	6.5	605
SP125 16-80	4.0	671	6.5	576
SP125 16-66	4.0	587	6.5	509
SP125 16-44	4.0	636	6.5	535
SP125 16-39	4.0	623	6.5	525
SP125 16-100	4.0	643	6.5	561
SP125 15-60	4.0	617	6.5	524
SP125 14-3	4.0	581	6.5	492
SP095 16-63	4.0	560	6.5	500
SP095 16-13	4.0	606	6.5	509
BP2 15-87	3.5	671	6.5	527
BP1 16-61	3.5	617	6.5	483

Table B - 3. Creep compliance inputs for MoDOT HMA mix designs, D(t) 1/psi

Mix #	BP2 15-87				BP2 15-87			
Lab ID	16PJ5B001				16PJ5B001			
Test ID	SS001-3.5				SS001-6.5			
Specimen Type	Sawn				Sawn			
Target Voids (%)	3.5				6.5			
Test Date	6/16/17				6/17/17			
Gmm	2.510				2.510			
Lab ID	16PJ5B001				16PJ5B001			
Average Air Voids	3.41				6.53			
Std Dev., Percent	0.03				0.16			
Time, Sec	Level 1 Creep Compliance D(t), 1/psi				Level 1 Creep Compliance D(t), 1/psi			
	At -20C	At -10C	At 0C	Indirect Tensile Strength, psi	At -20C	At -10C	At 0C	Indirect Tensile Strength, psi
1	2.08572E-07	2.62693E-07	3.30825E-07	671	2.97388E-07	3.69799E-07	4.92848E-07	527
2	2.18506E-07	2.81914E-07	3.72401E-07		3.08493E-07	3.98773E-07	5.39567E-07	
5	2.23730E-07	3.06339E-07	4.25221E-07		3.24042E-07	4.30775E-07	6.41144E-07	
10	2.33538E-07	3.28258E-07	4.77794E-07		3.37076E-07	4.64951E-07	7.23338E-07	
20	2.41784E-07	3.53107E-07	5.48170E-07		3.51902E-07	5.01021E-07	8.37728E-07	
50	2.60507E-07	3.94720E-07	6.58999E-07		3.78185E-07	5.58484E-07	1.05705E-06	
100	2.77079E-07	4.36936E-07	7.72416E-07		4.03115E-07	6.31880E-07	1.27841E-06	

Table B - 3. Creep compliance inputs for MoDOT HMA mix designs, D(t) 1/psi, Continued

Mix #	SP190 15-27				SP190 15-27			
Lab ID	16PJ5B002				16PJ5B002			
Test ID	SS002-4.0				SS002-6.5			
Specimen Type	Sawn				Sawn			
Target Voids (%)	4.0				6.5			
Test Date	8/21/17				8/22/17			
Gmm	2.474				2.474			
Lab ID	16PJ5B002				16PJ5B002			
Average Air Voids	6.28				6.28			
Std Dev., Percent	0.03				0.03			
Time, Sec	Level 1 Creep Compliance D(t), 1/psi				Level 1 Creep Compliance D(t), 1/psi			
	At -20C	At -10C	At 0C	Indirect Tensile Strength, psi	At -20C	At -10C	At 0C	Indirect Tensile Strength, psi
1	2.71550E-07	2.57288E-07	3.55629E-07	610	1.99656E-07	2.33596E-07	3.19361E-07	508
2	2.82088E-07	2.75128E-07	3.82556E-07		2.02733E-07	2.49248E-07	3.38600E-07	
5	2.90850E-07	2.83576E-07	4.29406E-07		2.14942E-07	2.60985E-07	3.94327E-07	
10	2.99852E-07	3.01311E-07	4.65950E-07		2.22272E-07	2.79207E-07	4.31664E-07	
20	3.05039E-07	3.24320E-07	5.18677E-07		2.28875E-07	2.94197E-07	4.72163E-07	
50	3.22474E-07	3.42522E-07	5.84853E-07		2.43504E-07	3.23693E-07	5.71314E-07	
100	3.37450E-07	3.63504E-07	6.80109E-07		2.52767E-07	3.50352E-07	6.60749E-07	

Table B - 3. Creep compliance inputs for MoDOT HMA mix designs, D(t) 1/psi, Continued

Mix #	SP095 16-13				SP095 16-13			
Lab ID	16PJ5B003				16PJ5B003			
Test ID	SS003-4.0				SS003-6.5			
Specimen Type	Sawn				Sawn			
Target Voids (%)	4.0				6.5			
Test Date	6/2/17				6/7/17			
Gmm	2.425				2.425			
Lab ID	16PJ5B003				16PJ5B003			
Average Air Voids	6.28				6.28			
Std Dev., Percent	0.03				0.03			
Time, Sec	Level 1 Creep Compliance D(t), 1/psi				Level 1 Creep Compliance D(t), 1/psi			
	At -20C	At -10C	At 0C	Indirect Tensile Strength, psi	At -20C	At -10C	At 0C	Indirect Tensile Strength, psi
1	2.79057E-07	3.37317E-07	4.86958E-07	606	2.97859E-07	3.74064E-07	5.02436E-07	509
2	2.86953E-07	3.62172E-07	5.55711E-07		3.08363E-07	3.98593E-07	5.69424E-07	
5	3.00779E-07	3.80444E-07	6.37178E-07		3.23432E-07	4.30589E-07	6.76106E-07	
10	3.08681E-07	4.12759E-07	7.35616E-07		3.37107E-07	4.68503E-07	7.92318E-07	
20	3.14914E-07	4.35959E-07	8.77993E-07		3.41350E-07	5.02971E-07	9.16990E-07	
50	3.39625E-07	4.93780E-07	1.11378E-06		3.74694E-07	5.75049E-07	1.21002E-06	
100	3.54628E-07	5.55501E-07	1.37616E-06		3.85385E-07	6.45998E-07	1.52007E-06	

Table B - 3. Creep compliance inputs for MoDOT HMA mix designs, D(t) 1/psi, Continued

Mix #	SP125 14-3				SP125 14-3			
Lab ID	16PJ5B004				16PJ5B004			
Test ID	SS004-4.0				SS004-6.5			
Specimen Type	Sawn				Sawn			
Target Voids (%)	4.0				6.5			
Test Date	6/10/17				6/14/17			
Gmm	2.451				2.451			
Lab ID	16PJ5B004				16PJ5B004			
Average Air Voids	3.83				6.50			
Std Dev., Percent	0.25				0.31			
Time, Sec	Level 1 Creep Compliance D(t), 1/psi				Level 1 Creep Compliance D(t), 1/psi			
	At -20C	At -10C	At 0C	Indirect Tensile Strength, psi	At -20C	At -10C	At 0C	Indirect Tensile Strength, psi
1	2.74926E-07	3.14139E-07	4.09406E-07	581	3.16303E-07	3.35397E-07	4.46754E-07	492
2	2.81525E-07	3.27496E-07	4.48284E-07		3.18668E-07	3.54431E-07	4.92698E-07	
5	2.89991E-07	3.53756E-07	5.03498E-07		3.34405E-07	3.75586E-07	5.56926E-07	
10	2.97979E-07	3.74913E-07	5.61502E-07		3.44370E-07	3.97449E-07	6.28092E-07	
20	3.10580E-07	3.91676E-07	6.42980E-07		3.40025E-07	4.22382E-07	7.26583E-07	
50	3.17640E-07	4.26140E-07	7.73006E-07		3.63430E-07	4.63453E-07	8.64242E-07	
100	3.36257E-07	4.71306E-07	9.15262E-07		3.80523E-07	4.99477E-07	1.04792E-06	

Table B - 3. Creep compliance inputs for MoDOT HMA mix designs, D(t) 1/psi, Continued

Mix #	BP1 16-61				BP1 16-61			
Lab ID	16PJ5B005				16PJ5B005			
Test ID	SS005-3.5				SS005-6.5			
Specimen Type	Sawn				Sawn			
Target Voids (%)	3.5				6.5			
Test Date	7/9/17				7/6/17			
Gmm	2.455				2.455			
Lab ID	16PJ5B005				16PJ5B005			
Average Air Voids	3.46				6.32			
Std Dev., Percent	0.20				0.06			
Time, Sec	Level 1 Creep Compliance D(t), 1/psi				Level 1 Creep Compliance D(t), 1/psi			
	At -20C	At -10C	At 0C	Indirect Tensile Strength, psi	At -20C	At -10C	At 0C	Indirect Tensile Strength, psi
1	2.87796E-07	3.37362E-07	4.37713E-07	617	3.27470E-07	4.06388E-07	5.42096E-07	483
2	2.88703E-07	3.53517E-07	4.76022E-07		3.29771E-07	4.26965E-07	5.67731E-07	
5	3.10149E-07	3.80489E-07	5.28492E-07		3.53017E-07	4.58889E-07	6.72991E-07	
10	3.12176E-07	3.94645E-07	5.85280E-07		3.60156E-07	4.91740E-07	7.50542E-07	
20	3.28023E-07	4.25134E-07	6.48079E-07		3.73608E-07	5.18094E-07	8.23553E-07	
50	3.44382E-07	4.64604E-07	7.74572E-07		4.00042E-07	5.75103E-07	1.00984E-06	
100	3.64895E-07	4.98765E-07	8.95416E-07		4.17551E-07	6.30114E-07	1.16798E-06	

Table B - 3. Creep compliance inputs for MoDOT HMA mix designs, D(t) 1/psi, Continued

Mix #	SP125 16-9 SMA				SP125 16-9 SMA			
Lab ID	16PJ5B006				16PJ5B006			
Test ID	SS006-4.0				SS006-6.5			
Specimen Type	Sawn				Sawn			
Target Voids (%)	4.0				6.5			
Test Date	5/31/17				5/25/17			
Gmm	2.378				2.378			
Lab ID	16PJ5B006				16PJ5B006			
Average Air Voids	3.77				6.39			
Std Dev., Percent	0.24				0.38			
Time, Sec	Level 1 Creep Compliance D(t), 1/psi				Level 1 Creep Compliance D(t), 1/psi			
	At -20C	At -10C	At 0C	Indirect Tensile Strength, psi	At -20C	At -10C	At 0C	Indirect Tensile Strength, psi
1	2.72648E-07	3.43963E-07	5.23700E-07	551	3.31927E-07	3.96480E-07	5.44762E-07	505
2	2.87062E-07	3.73479E-07	6.02795E-07		3.42134E-07	4.19583E-07	6.15970E-07	
5	2.98243E-07	4.06034E-07	7.22674E-07		3.61385E-07	4.69881E-07	7.62359E-07	
10	3.13224E-07	4.37429E-07	8.44565E-07		3.77659E-07	5.07179E-07	9.01003E-07	
20	3.35669E-07	4.86570E-07	1.00650E-06		3.91131E-07	5.58729E-07	1.07407E-06	
50	3.56341E-07	5.52965E-07	1.30967E-06		4.12447E-07	6.32023E-07	1.44923E-06	
100	3.79143E-07	6.18153E-07	1.64159E-06		4.48544E-07	7.36177E-07	1.84051E-06	

Table B - 3. Creep compliance inputs for MoDOT HMA mix designs, D(t) 1/psi, Continued

Mix #	SP095 16-63				SP095 16-63				
Lab ID	16PJ5B007				16PJ5B007				
Test ID	SS007-4.0				SS007-6.5				
Specimen Type	Sawn				Sawn				
Target Voids (%)	4.0				6.5				
Test Date	1/0/00				6/6/17				
Gmm	2.476				2.476				
Lab ID	16PJ5B007				16PJ5B007				
Average Air Voids	3.80				6.45				
Std Dev., Percent	0.17				0.15				
Time, Sec	Level 1 Creep Compliance D(t), 1/psi				Indirect Tensile Strength, psi	Level 1 Creep Compliance D(t), 1/psi			Indirect Tensile Strength, psi
	At -20C	At -10C	At 0C	At -20C		At -10C	At 0C		
1	2.76225E-07	3.42541E-07	4.54500E-07	560	3.18854E-07	3.87821E-07	5.37895E-07	500	
2	2.88200E-07	3.60715E-07	4.93022E-07		3.30674E-07	4.16117E-07	5.99240E-07		
5	2.98607E-07	3.93447E-07	5.76390E-07		3.50155E-07	4.45320E-07	7.00437E-07		
10	3.15538E-07	4.18810E-07	6.46817E-07		3.61246E-07	4.79279E-07	7.88112E-07		
20	3.13183E-07	4.45136E-07	7.31495E-07		3.78353E-07	5.15112E-07	9.00049E-07		
50	3.40674E-07	5.04738E-07	9.03105E-07		4.04619E-07	5.76346E-07	1.10189E-06		
100	3.57425E-07	5.51080E-07	1.06483E-06		4.30570E-07	6.31979E-07	1.32530E-06		

Table B - 3. Creep compliance inputs for MoDOT HMA mix designs, D(t) 1/psi, Continued

Mix #	SP190 14-18				SP190 14-18			
Lab ID	16PJ5B008				16PJ5B008			
Test ID	SS008-4.0				SS008-6.5			
Specimen Type	Sawn				Sawn			
Target Voids (%)	4.0				6.5			
Test Date	1/0/00				8/15/17			
Gmm	2.495				2.495			
Lab ID	16PJ5B008				16PJ5B008			
Average Air Voids	3.86				6.48			
Std Dev., Percent	0.18				0.06			
Time, Sec	Level 1 Creep Compliance D(t), 1/psi			Indirect Tensile Strength, psi	Level 1 Creep Compliance D(t), 1/psi			Indirect Tensile Strength, psi
	At -20C	At -10C	At 0C		At -20C	At -10C	At 0C	
1	2.66824E-07	3.17870E-07	3.52933E-07	606	3.44433E-07	3.98623E-07	4.95670E-07	520
2	2.76492E-07	3.33456E-07	3.95494E-07		3.54138E-07	4.16517E-07	5.36816E-07	
5	2.85458E-07	3.54618E-07	4.29293E-07		3.70922E-07	4.53456E-07	6.26841E-07	
10	2.98193E-07	3.74941E-07	4.82585E-07		3.83867E-07	4.77579E-07	6.92641E-07	
20	3.10762E-07	4.03060E-07	5.19098E-07		4.05819E-07	5.14695E-07	8.02634E-07	
50	3.28763E-07	4.36793E-07	6.23969E-07		4.23461E-07	5.61603E-07	9.78884E-07	
100	3.42223E-07	4.67848E-07	7.09682E-07		4.51888E-07	6.18199E-07	1.17608E-06	

Table B - 3. Creep compliance inputs for MoDOT HMA mix designs, D(t) 1/psi, Continued

Mix #	SP125 16-39				SP125 16-39			
Lab ID	16PJ5B009				16PJ5B009			
Test ID	SS009-4.0				SS009-6.5			
Specimen Type	Sawn				Sawn			
Target Voids (%)	4.0				6.5			
Test Date	6/15/17				5/2/17			
Gmm	2.454				2.454			
Lab ID	16PJ5B009				16PJ5B009			
Average Air Voids	3.78				5.92			
Std Dev., Percent	0.07				0.10			
Time, Sec	Level 1 Creep Compliance D(t), 1/psi			Indirect Tensile Strength, psi	Level 1 Creep Compliance D(t), 1/psi			Indirect Tensile Strength, psi
	At -20C	At -10C	At 0C		At -20C	At -10C	At 0C	
1	2.58140E-07	2.92533E-07	3.63345E-07	623	3.32364E-07	3.85465E-07	5.15002E-07	525
2	2.67260E-07	3.02398E-07	3.84660E-07		3.36706E-07	4.10681E-07	5.45298E-07	
5	2.71981E-07	3.23608E-07	4.28117E-07		3.53907E-07	4.30320E-07	6.10817E-07	
10	2.79952E-07	3.36634E-07	4.61930E-07		3.63273E-07	4.44764E-07	6.60628E-07	
20	2.87826E-07	3.58891E-07	5.04430E-07		3.58787E-07	4.83341E-07	7.25284E-07	
50	3.03137E-07	3.86037E-07	5.79979E-07		3.81207E-07	5.13334E-07	8.20005E-07	
100	3.13641E-07	4.14859E-07	6.40049E-07		4.00915E-07	5.52500E-07	9.22673E-07	

Table B - 3. Creep compliance inputs for MoDOT HMA mix designs, D(t) 1/psi, Continued

Mix #	SP190 15-48				SP190 15-48			
Lab ID	16PJ5B010				16PJ5B010			
Test ID	SS010-4.0				SS010-6.5			
Specimen Type	Sawn				Sawn			
Target Voids (%)	4.0				6.5			
Test Date	8/11/07				8/12/17			
Gmm	2.443				2.443			
Lab ID	16PJ5B010				16PJ5B010			
Average Air Voids	3.93				6.35			
Std Dev., Percent	0.14				0.35			
Time, Sec	Level 1 Creep Compliance D(t), 1/psi				Level 1 Creep Compliance D(t), 1/psi			
	At -20C	At -10C	At 0C	Indirect Tensile Strength, psi	At -20C	At -10C	At 0C	Indirect Tensile Strength, psi
1	2.69401E-07	2.95435E-07	3.94131E-07	612	3.22646E-07	3.69335E-07	4.43808E-07	479
2	2.75785E-07	3.17199E-07	4.12367E-07		3.36641E-07	3.85628E-07	4.73206E-07	
5	2.87010E-07	3.25414E-07	4.72717E-07		3.47823E-07	4.06569E-07	5.18984E-07	
10	2.96965E-07	3.39746E-07	4.93813E-07		3.57860E-07	4.27087E-07	5.66513E-07	
20	3.05522E-07	3.59590E-07	5.38651E-07		3.78669E-07	4.46913E-07	6.29280E-07	
50	3.19207E-07	3.85885E-07	6.11776E-07		3.98041E-07	4.84997E-07	7.18613E-07	
100	3.34231E-07	4.11965E-07	6.79373E-07		4.21233E-07	5.21789E-07	8.13935E-07	

Table B - 3. Creep compliance inputs for MoDOT HMA mix designs, D(t) 1/psi, Continued

Mix #	SP125 15-60				SP125 15-60			
Lab ID	16PJ5B011				16PJ5B011			
Test ID	SS011-4.0				SS011-6.5			
Specimen Type	Sawn				Sawn			
Target Voids (%)	4.0				6.5			
Test Date	7/9/17				7/10/17			
Gmm	2.430				2.430			
Lab ID	16PJ5B011				16PJ5B011			
Average Air Voids	3.96				6.46			
Std Dev., Percent	0.16				0.15			
Time, Sec	Level 1 Creep Compliance D(t), 1/psi				Level 1 Creep Compliance D(t), 1/psi			
	At -20C	At -10C	At 0C	Indirect Tensile Strength, psi	At -20C	At -10C	At 0C	Indirect Tensile Strength, psi
1	2.61266E-07	2.88580E-07	3.76862E-07	617	2.85638E-07	3.10444E-07	4.00227E-07	524
2	2.79363E-07	3.06260E-07	4.07918E-07		2.97928E-07	3.28592E-07	4.35169E-07	
5	2.81449E-07	3.22498E-07	4.61834E-07		3.07213E-07	3.50681E-07	4.92524E-07	
10	2.97926E-07	3.41159E-07	5.02907E-07		3.20529E-07	3.71555E-07	5.38345E-07	
20	3.06534E-07	3.66147E-07	5.61763E-07		3.26444E-07	3.94543E-07	6.09746E-07	
50	3.27080E-07	3.98857E-07	6.63044E-07		3.45587E-07	4.35082E-07	7.20031E-07	
100	3.38218E-07	4.29325E-07	7.56880E-07		3.66013E-07	4.74322E-07	8.31697E-07	

Table B - 3. Creep compliance inputs for MoDOT HMA mix designs, D(t) 1/psi, Continued

Mix #	SP190 15-57				SP190 15-57			
Lab ID	16PJ5B012				16PJ5B012			
Test ID	SS012-4.0				SS012-6.5			
Specimen Type	Sawn				Sawn			
Target Voids (%)	4.0				6.5			
Test Date	8/24/17				8/25/17			
Gmm	2.438				2.438			
Lab ID	16PJ5B012				16PJ5B012			
Average Air Voids	3.79				6.45			
Std Dev., Percent	0.10				0.00			
Time, Sec	Level 1 Creep Compliance D(t), 1/psi				Level 1 Creep Compliance D(t), 1/psi			
	At -20C	At -10C	At 0C	Indirect Tensile Strength, psi	At -20C	At -10C	At 0C	Indirect Tensile Strength, psi
1	2.00613E-07	2.39105E-07	3.09811E-07	626	2.26714E-07	2.53241E-07	2.93107E-07	514
2	2.06984E-07	2.43322E-07	3.30739E-07		2.34768E-07	2.71157E-07	3.25772E-07	
5	2.17226E-07	2.66022E-07	3.79261E-07		2.46191E-07	2.83138E-07	3.61153E-07	
10	2.23744E-07	2.73478E-07	4.16247E-07		2.53952E-07	3.02325E-07	3.98140E-07	
20	2.30671E-07	2.95636E-07	4.55021E-07		2.65932E-07	3.22292E-07	4.53479E-07	
50	2.41302E-07	3.16646E-07	5.35750E-07		2.80980E-07	3.54309E-07	5.33476E-07	
100	2.49936E-07	3.36381E-07	6.24788E-07		2.99720E-07	3.76622E-07	6.19355E-07	

Table B - 3. Creep compliance inputs for MoDOT HMA mix designs, D(t) 1/psi, Continued

Mix #	SP250 16-68				SP250 16-68			
Lab ID	16PJ5B013				16PJ5B013			
Test ID	SS013-4.0				SS013-6.5			
Specimen Type	Sawn				Sawn			
Target Voids (%)	4.0				6.5			
Test Date	8/17/17				8/18/17			
Gmm	2.495				2.495			
Lab ID	16PJ5B013				16PJ5B013			
Average Air Voids	4.08				6.36			
Std Dev., Percent	0.30				0.06			
Time, Sec	Level 1 Creep Compliance D(t), 1/psi				Level 1 Creep Compliance D(t), 1/psi			
	At -20C	At -10C	At 0C	Indirect Tensile Strength, psi	At -20C	At -10C	At 0C	Indirect Tensile Strength, psi
1	2.58369E-07	3.36543E-07	4.49143E-07	579	3.16044E-07	3.71812E-07	5.68509E-07	450
2	2.69921E-07	3.49637E-07	4.84536E-07		3.26945E-07	3.92363E-07	6.32730E-07	
5	2.74277E-07	3.76200E-07	5.52328E-07		3.42580E-07	4.22302E-07	7.24953E-07	
10	2.85731E-07	3.94397E-07	6.14301E-07		3.52780E-07	4.47175E-07	8.19321E-07	
20	2.98392E-07	4.15551E-07	6.82423E-07		3.68121E-07	4.75898E-07	9.63126E-07	
50	3.16494E-07	4.60778E-07	8.25254E-07		3.92044E-07	5.30325E-07	1.17988E-06	
100	3.27494E-07	4.95552E-07	9.70653E-07		4.12324E-07	5.80228E-07	1.42504E-06	

Table B - 3. Creep compliance inputs for MoDOT HMA mix designs, D(t) 1/psi, Continued

Mix #	SP125 16-66				SP125 16-66				
Lab ID	16PJ5B014				16PJ5B014				
Test ID	SS014-4.0				SS014-6.5				
Specimen Type	Sawn				Sawn				
Target Voids (%)	4.0				6.5				
Test Date	6/29/17				7/5/17				
Gmm	2.442				2.442				
Lab ID	16PJ5B014				16PJ5B014				
Average Air Voids	4.00				6.13				
Std Dev., Percent	0.61				0.12				
Time, Sec	Level 1 Creep Compliance D(t), 1/psi				Indirect Tensile Strength, psi	Level 1 Creep Compliance D(t), 1/psi			
	At -20C	At -10C	At 0C	At -20C		At -10C	At 0C	Indirect Tensile Strength, psi	
1	2.68793E-07	3.03252E-07	3.92380E-07	587	3.10341E-07	3.56661E-07	4.54734E-07	509	
2	2.85279E-07	3.25256E-07	4.30375E-07		3.11609E-07	3.68976E-07	4.97822E-07		
5	2.90124E-07	3.48091E-07	4.87949E-07		3.34923E-07	4.04977E-07	5.67391E-07		
10	3.06050E-07	3.68524E-07	5.42648E-07		3.37866E-07	4.23930E-07	6.46556E-07		
20	3.19086E-07	3.99098E-07	6.07736E-07		3.62725E-07	4.52062E-07	6.98663E-07		
50	3.30171E-07	4.47997E-07	7.36442E-07		3.74626E-07	4.97681E-07	8.58984E-07		
100	3.52864E-07	4.78087E-07	8.38283E-07		3.99371E-07	5.48435E-07	1.00302E-06		

Table B - 3. Creep compliance inputs for MoDOT HMA mix designs, D(t) 1/psi, Continued

Mix #	SP125 16-44				SP125 16-44			
Lab ID	16PJ5B016				16PJ5B016			
Test ID	SS016-4.0				SS016-6.5			
Specimen Type	Sawn				Sawn			
Target Voids (%)	4.0				6.5			
Test Date	6/24/17				6/27/17			
Gmm	2.537				2.537			
Lab ID	16PJ5B016				16PJ5B016			
Average Air Voids	3.66				5.98			
Std Dev., Percent	0.22				0.03			
Time, Sec	Level 1 Creep Compliance D(t), 1/psi				Level 1 Creep Compliance D(t), 1/psi			
	At -20C	At -10C	At 0C	Indirect Tensile Strength, psi	At -20C	At -10C	At 0C	Indirect Tensile Strength, psi
1	2.23424E-07	2.38932E-07	2.91874E-07	636	2.80987E-07	3.38244E-07	4.36928E-07	535
2	2.29084E-07	2.55444E-07	3.20089E-07		2.87938E-07	3.54319E-07	4.85509E-07	
5	2.38544E-07	2.69640E-07	3.64574E-07		3.04106E-07	3.89252E-07	5.40812E-07	
10	2.45440E-07	2.89010E-07	4.05626E-07		3.12292E-07	4.08762E-07	6.12605E-07	
20	2.49274E-07	3.08870E-07	4.56157E-07		3.29049E-07	4.44905E-07	6.84174E-07	
50	2.63601E-07	3.35100E-07	5.55461E-07		3.42181E-07	4.84467E-07	8.33246E-07	
100	2.75679E-07	3.68656E-07	6.50175E-07		3.66728E-07	5.47009E-07	9.75783E-07	

Table B - 3. Creep compliance inputs for MoDOT HMA mix designs, D(t) 1/psi, Continued

Mix #	SP125 16-80				SP125 16-80			
Lab ID	16PJ5B017				16PJ5B017			
Test ID	SS017-4.0				SS017-6.5			
Specimen Type	Sawn				Sawn			
Target Voids (%)	4.0				6.5			
Test Date	8/26-27/17				8/26-27/17			
Gmm	2.470				2.470			
Lab ID	16PJ5B017				16PJ5B017			
Average Air Voids	4.15				6.41			
Std Dev., Percent	0.17				0.06			
Time, Sec	Level 1 Creep Compliance D(t), 1/psi				Level 1 Creep Compliance D(t), 1/psi			
	At -20C	At -10C	At 0C	Indirect Tensile Strength, psi	At -20C	At -10C	At 0C	Indirect Tensile Strength, psi
1	1.53861E-07	1.99721E-07	2.51261E-07	671	2.11066E-07	2.23236E-07	2.96787E-07	576
2	1.60538E-07	2.05753E-07	2.83478E-07		2.16677E-07	2.38519E-07	3.33940E-07	
5	1.66612E-07	2.26453E-07	3.07557E-07		2.29382E-07	2.56084E-07	3.78735E-07	
10	1.71915E-07	2.37747E-07	3.45627E-07		2.36702E-07	2.76043E-07	4.24830E-07	
20	1.82065E-07	2.52961E-07	3.96287E-07		2.46174E-07	2.98021E-07	4.95750E-07	
50	1.94676E-07	2.80127E-07	4.75837E-07		2.61388E-07	3.31696E-07	5.96245E-07	
100	2.00429E-07	3.06727E-07	5.50943E-07		2.75143E-07	3.61358E-07	7.18075E-07	

Table B - 3. Creep compliance inputs for MoDOT HMA mix designs, D(t) 1/psi, Continued

Mix #	SP125 16-83				SP125 16-83				
Lab ID	16CDCJB013				16CDCJB013				
Test ID	SSCDC013-4.0				SSCDC013-6.5				
Specimen Type	Sawn				Sawn				
Target Voids (%)	4.0				6.5				
Test Date	6/19/17				6/20/17				
Gmm	2.474				2.474				
Lab ID	16CDCJB013				16CDCJB013				
Average Air Voids	3.77				6.46				
Std Dev., Percent	0.19				0.43				
Time, Sec	Level 1 Creep Compliance D(t), 1/psi				Indirect Tensile Strength, psi	Level 1 Creep Compliance D(t), 1/psi			Indirect Tensile Strength, psi
	At -20C	At -10C	At 0C	At -20C		At -10C	At 0C		
1	2.25296E-07	2.52376E-07	3.30009E-07	723	2.83510E-07	3.05048E-07	4.65324E-07	605	
2	2.33152E-07	2.71469E-07	3.65305E-07		2.98135E-07	3.20421E-07	5.03033E-07		
5	2.43307E-07	2.89157E-07	4.02898E-07		3.06571E-07	3.50519E-07	5.89230E-07		
10	2.54015E-07	3.11123E-07	4.53662E-07		3.22553E-07	3.80091E-07	6.54675E-07		
20	2.56924E-07	3.24950E-07	5.08814E-07		3.36061E-07	3.96747E-07	7.40856E-07		
50	2.75643E-07	3.67881E-07	6.13866E-07		3.49356E-07	4.49537E-07	9.11941E-07		
100	2.95442E-07	4.00881E-07	7.04101E-07		3.67349E-07	4.98823E-07	1.09676E-06		

Table B - 3. Creep compliance inputs for MoDOT HMA mix designs, D(t) 1/psi, Continued

Mix #	SP125 16-100				SP125 16-100				
Lab ID	16CDCJB014				16CDCJB014				
Test ID	SSCDC014-4.0				SSCDC014-6.5				
Specimen Type	Sawn				Sawn				
Target Voids (%)	4.0				6.5				
Test Date	7/30/17				7/30/17				
Gmm	2.491				2.491				
Lab ID	16CDCJB014				16CDCJB014				
Average Air Voids	3.81				6.31				
Std Dev., Percent	0.44				0.14				
Time, Sec	Level 1 Creep Compliance D(t), 1/psi				Indirect Tensile Strength, psi	Level 1 Creep Compliance D(t), 1/psi			Indirect Tensile Strength, psi
	At -20C	At -10C	At 0C	At -20C		At -10C	At 0C		
1	2.55306E-07	2.91673E-07	4.23134E-07	643	2.87079E-07	3.09898E-07	4.77703E-07	561	
2	2.59048E-07	3.12881E-07	4.61250E-07		2.97848E-07	3.34058E-07	5.37004E-07		
5	2.77292E-07	3.33391E-07	5.51899E-07		3.10914E-07	3.60934E-07	6.28663E-07		
10	2.83446E-07	3.55285E-07	6.17399E-07		3.26639E-07	3.87524E-07	7.14276E-07		
20	2.96159E-07	3.82942E-07	6.91862E-07		3.34594E-07	4.27422E-07	8.33046E-07		
50	3.16551E-07	4.27688E-07	8.54703E-07		3.57719E-07	4.81706E-07	1.05328E-06		
100	3.38233E-07	4.68493E-07	1.03859E-06		3.82783E-07	5.28042E-07	1.30062E-06		

Table B - 3. Creep compliance inputs for MoDOT HMA mix designs, D(t) 1/psi, Continued

Mix #	SP125 16-93				SP125 16-93			
Lab ID	16CDCJB015				16CDCJB015			
Test ID	SSCDC015-4.0				SSCDC015-6.5			
Specimen Type	Sawn				Sawn			
Target Voids (%)	4.0				6.5			
Test Date	7/14/17				7/10/17			
Gmm	2.489				2.489			
Lab ID	16CDCJB015				16CDCJB015			
Average Air Voids	3.84				6.42			
Std Dev., Percent	0.25				0.29			
Time, Sec	Level 1 Creep Compliance D(t), 1/psi				Level 1 Creep Compliance D(t), 1/psi			
	At -20C	At -10C	At 0C	Indirect Tensile Strength, psi	At -20C	At -10C	At 0C	Indirect Tensile Strength, psi
1	2.77162E-07	3.01133E-07	4.60367E-07	614	2.95976E-07	3.60276E-07	5.03305E-07	497
2	2.85151E-07	3.21544E-07	5.07741E-07		3.01281E-07	3.76294E-07	5.64130E-07	
5	3.00957E-07	3.46147E-07	6.02277E-07		3.20562E-07	4.09218E-07	6.75336E-07	
10	3.15007E-07	3.71636E-07	6.86177E-07		3.34631E-07	4.36428E-07	7.75324E-07	
20	3.27300E-07	4.00317E-07	8.00993E-07		3.44901E-07	4.76573E-07	8.98864E-07	
50	3.44853E-07	4.48436E-07	9.66494E-07		3.75187E-07	5.45342E-07	1.16458E-06	
100	3.74439E-07	4.91216E-07	1.19779E-06		3.95095E-07	6.10624E-07	1.45777E-06	

Table B - 3. Creep compliance inputs for MoDOT HMA mix designs, D(t) 1/psi, Continued

Mix #	SP125 16-84				SP125 16-84			
Lab ID	16CDCJB016				16CDCJB016			
Test ID	SSCDC016-4.0				SSCDC016-6.5			
Specimen Type	Sawn				Sawn			
Target Voids (%)	4.0				6.5			
Test Date	7/26/17				7/27/17			
Gmm	2.517				2.517			
Lab ID	16CDCJB016				16CDCJB016			
Average Air Voids	3.71				6.21			
Std Dev., Percent	0.13				0.11			
Time, Sec	Level 1 Creep Compliance D(t), 1/psi				Level 1 Creep Compliance D(t), 1/psi			
	At -20C	At -10C	At 0C	Indirect Tensile Strength, psi	At -20C	At -10C	At 0C	Indirect Tensile Strength, psi
1	2.33138E-07	2.71443E-07	3.62972E-07	745	2.84968E-07	3.52894E-07	5.01742E-07	614
2	2.40658E-07	2.80729E-07	4.02590E-07		2.97893E-07	3.78337E-07	5.44913E-07	
5	2.52604E-07	3.13046E-07	4.73409E-07		3.13336E-07	4.01838E-07	6.60599E-07	
10	2.62081E-07	3.30944E-07	5.38924E-07		3.26030E-07	4.39324E-07	7.38953E-07	
20	2.70145E-07	3.54916E-07	6.10908E-07		3.39729E-07	4.80307E-07	8.48218E-07	
50	2.88774E-07	3.94846E-07	7.74864E-07		3.60778E-07	5.40544E-07	1.07767E-06	
100	3.07034E-07	4.29528E-07	9.36442E-07		3.88558E-07	5.95936E-07	1.31794E-06	

Table B - 3. Creep compliance inputs for MoDOT HMA mix designs, D(t) 1/psi, Continued

Mix #	SP125 16-99				SP125 16-99				
Lab ID	16CDCJB017				16CDCJB017				
Test ID	SSCDC017-4.0				SSCDC017-6.5				
Specimen Type	Sawn				Sawn				
Target Voids (%)	4.0				6.5				
Test Date	7/23/17				7/25/17				
Gmm	2.484				2.484				
Lab ID	16CDCJB017				16CDCJB017				
Average Air Voids	3.90				6.33				
Std Dev., Percent	0.20				0.35				
Time, Sec	Level 1 Creep Compliance D(t), 1/psi				Indirect Tensile Strength, psi	Level 1 Creep Compliance D(t), 1/psi			Indirect Tensile Strength, psi
	At -20C	At -10C	At 0C	At -20C		At -10C	At 0C		
1	2.32632E-07	2.63465E-07	3.18603E-07	718	2.66020E-07	3.04460E-07	3.52414E-07	590	
2	2.29782E-07	2.70377E-07	3.51613E-07		2.80232E-07	3.15313E-07	3.72996E-07		
5	2.48317E-07	2.90240E-07	3.75550E-07		2.80448E-07	3.35858E-07	4.16472E-07		
10	2.52685E-07	3.01856E-07	4.08086E-07		2.90165E-07	3.56152E-07	4.52074E-07		
20	2.53596E-07	3.21608E-07	4.47978E-07		3.01507E-07	3.67991E-07	4.84241E-07		
50	2.74092E-07	3.33287E-07	5.01185E-07		3.11650E-07	4.00558E-07	5.65580E-07		
100	2.83576E-07	3.66480E-07	5.70877E-07		3.22580E-07	4.25612E-07	6.46072E-07		

Table B - 3. Creep compliance inputs for MoDOT HMA mix designs, D(t) 1/psi, Continued

Mix #	SP125 16-91				SP125 16-91			
Lab ID	16CDCJB018				16CDCJB018			
Test ID	SSCDC018-4.0				SSCDC018-6.5			
Specimen Type	Sawn				Sawn			
Target Voids (%)	4.0				6.5			
Test Date	1/0/00				7/21/17			
Gmm	2.498				2.498			
Lab ID	16CDCJB018				16CDCJB018			
Average Air Voids	3.94				6.36			
Std Dev., Percent	0.22				0.09			
Time, Sec	Level 1 Creep Compliance D(t), 1/psi				Level 1 Creep Compliance D(t), 1/psi			
	At -20C	At -10C	At 0C	Indirect Tensile Strength, psi	At -20C	At -10C	At 0C	Indirect Tensile Strength, psi
1	2.51531E-07	3.00429E-07	4.14446E-07	575	2.77359E-07	3.34586E-07	5.26408E-07	499
2	2.65634E-07	3.18103E-07	4.56329E-07		2.87460E-07	3.63673E-07	5.76808E-07	
5	2.82113E-07	3.59430E-07	5.57146E-07		3.05312E-07	3.98262E-07	7.17068E-07	
10	2.95380E-07	3.87103E-07	6.23739E-07		3.22132E-07	4.33074E-07	8.10207E-07	
20	3.12243E-07	4.25586E-07	7.45636E-07		3.34415E-07	4.74628E-07	9.48129E-07	
50	3.36310E-07	4.86812E-07	9.50134E-07		3.66889E-07	5.43855E-07	1.23439E-06	
100	3.64922E-07	5.51379E-07	1.15641E-06		3.88006E-07	6.20996E-07	1.53744E-06	

Table B - 3. Creep compliance inputs for MoDOT HMA mix designs, D(t) 1/psi, Continued

Mix #	SP125 16-89				SP125 16-89				
Lab ID	16CDCJB019				16CDCJB019				
Test ID	SSCDC019-4.0				SSCDC019-6.5				
Specimen Type	Sawn				Sawn				
Target Voids (%)	4.0				6.5				
Test Date	8/3/17				8/3/17				
Gmm	2.476				2.476				
Lab ID	16CDCJB019				16CDCJB019				
Average Air Voids	3.98				6.49				
Std Dev., Percent	0.19				0.07				
Time, Sec	Level 1 Creep Compliance D(t), 1/psi				Indirect Tensile Strength, psi	Level 1 Creep Compliance D(t), 1/psi			
	At -20C	At -10C	At 0C	Indirect Tensile Strength, psi		At -20C	At -10C	At 0C	Indirect Tensile Strength, psi
1	2.46795E-07	2.85561E-07	3.51668E-07	585	2.89203E-07	3.59137E-07	4.52138E-07	521	
2	2.56371E-07	3.03860E-07	3.96675E-07		2.93485E-07	3.78718E-07	5.05841E-07		
5	2.67768E-07	3.24487E-07	4.35357E-07		3.16669E-07	4.09529E-07	5.66369E-07		
10	2.84493E-07	3.46472E-07	4.87968E-07		3.28315E-07	4.41849E-07	6.37909E-07		
20	2.87892E-07	3.61926E-07	5.52027E-07		3.38969E-07	4.72125E-07	7.26437E-07		
50	3.09530E-07	4.07187E-07	6.46013E-07		3.64137E-07	5.28050E-07	8.75224E-07		
100	3.29266E-07	4.39094E-07	7.46426E-07		3.84655E-07	5.74860E-07	1.02674E-06		

Table B - 3. Creep compliance inputs for MoDOT HMA mix designs, D(t) 1/psi, Continued

Mix #	SP125 16-98				SP125 16-98			
Lab ID	16CDCJB020				16CDCJB020			
Test ID	SSCDC020-4.0				SSCDC020-6.5			
Specimen Type	Sawn				Sawn			
Target Voids (%)	4.0				6.5			
Test Date	8/5/17				8/5/17			
Gmm	2.461				2.461			
Lab ID	16CDCJB020				16CDCJB020			
Average Air Voids	4.09				6.47			
Std Dev., Percent	0.14				0.28			
Time, Sec	Level 1 Creep Compliance D(t), 1/psi				Level 1 Creep Compliance D(t), 1/psi			
	At -20C	At -10C	At 0C	Indirect Tensile Strength, psi	At -20C	At -10C	At 0C	Indirect Tensile Strength, psi
1	2.47653E-07	2.74349E-07	4.05678E-07	654	2.70819E-07	3.11942E-07	4.57190E-07	597
2	2.62177E-07	2.95703E-07	4.52741E-07		2.71859E-07	3.25010E-07	4.96729E-07	
5	2.67728E-07	3.08666E-07	5.07557E-07		2.92110E-07	3.58444E-07	5.87647E-07	
10	2.79616E-07	3.36839E-07	5.77133E-07		2.98648E-07	3.77331E-07	6.58143E-07	
20	2.95257E-07	3.66572E-07	6.34299E-07		3.07239E-07	4.04787E-07	7.35808E-07	
50	3.15489E-07	4.07939E-07	7.80661E-07		3.33167E-07	4.55881E-07	9.10697E-07	
100	3.23212E-07	4.42775E-07	9.19786E-07		3.56869E-07	5.03454E-07	1.08879E-06	

Table B - 3. Creep compliance inputs for MoDOT HMA mix designs, D(t) 1/psi, Continued

Mix #	SP125 16-95				SP125 16-95				
Lab ID	16CDCJB021				16CDCJB021				
Test ID	SSCDC021-4.0				SSCDC021-6.5				
Specimen Type	Sawn				Sawn				
Target Voids (%)	4.0				6.5				
Test Date	7/17/17				7/18/17				
Gmm	2.449				2.449				
Lab ID	16CDCJB021				16CDCJB021				
Average Air Voids	4.08				6.43				
Std Dev., Percent	0.27				0.12				
Time, Sec	Level 1 Creep Compliance D(t), 1/psi				Indirect Tensile Strength, psi	Level 1 Creep Compliance D(t), 1/psi			Indirect Tensile Strength, psi
	At -20C	At -10C	At 0C	At -20C		At -10C	At 0C		
1	2.49693E-07	3.11477E-07	4.13172E-07	577	3.18290E-07	3.73267E-07	5.21991E-07	492	
2	2.61108E-07	3.24756E-07	4.71837E-07		3.31490E-07	3.99984E-07	5.91395E-07		
5	2.69695E-07	3.62575E-07	5.15803E-07		3.50912E-07	4.39433E-07	6.64861E-07		
10	2.82924E-07	3.84241E-07	5.87183E-07		3.64999E-07	4.73124E-07	7.52251E-07		
20	2.93931E-07	4.08677E-07	6.74225E-07		3.83556E-07	5.25607E-07	8.54658E-07		
50	3.16464E-07	4.58334E-07	7.93340E-07		4.09255E-07	5.89583E-07	1.03437E-06		
100	3.36848E-07	5.13319E-07	9.17381E-07		4.36132E-07	6.54371E-07	1.22105E-06		

Table B - 3. Creep compliance inputs for MoDOT HMA mix designs, D(t) 1/psi, Continued

Mix #	SP125 16-94				SP125 16-94			
Lab ID	16CDCJB022				16CDCJB022			
Test ID	SSCDC022-4.0				SSCDC022-6.5			
Specimen Type	Sawn				Sawn			
Target Voids (%)	4.0				6.5			
Test Date	8/8/17				8/8/17			
Gmm	2.476				2.476			
Lab ID	16CDCJB022				16CDCJB022			
Average Air Voids	3.99				6.37			
Std Dev., Percent	0.14				0.24			
Time, Sec	Level 1 Creep Compliance D(t), 1/psi				Level 1 Creep Compliance D(t), 1/psi			
	At -20C	At -10C	At 0C	Indirect Tensile Strength, psi	At -20C	At -10C	At 0C	Indirect Tensile Strength, psi
1	2.33883E-07	2.81330E-07	3.73098E-07	774	2.83213E-07	3.45068E-07	4.80020E-07	509
2	2.44235E-07	3.03229E-07	3.97633E-07		2.94030E-07	3.61097E-07	5.11619E-07	
5	2.54435E-07	3.21442E-07	4.72923E-07		3.10939E-07	3.93743E-07	6.00671E-07	
10	2.67410E-07	3.48256E-07	5.15252E-07		3.21193E-07	4.20503E-07	6.55545E-07	
20	2.74499E-07	3.67300E-07	5.69396E-07		3.36295E-07	4.48868E-07	7.44310E-07	
50	2.91027E-07	4.09496E-07	6.88307E-07		3.63066E-07	5.04945E-07	8.68137E-07	
100	3.12096E-07	4.47667E-07	7.79828E-07		3.89055E-07	5.53116E-07	1.01552E-06	

Table B - 3. Creep compliance inputs for MoDOT HMA mix designs, D(t) 1/psi, Continued

Creep Compliance D(t), 1/psi

Test ID	TL311	Time, Sec	At -20C	At -10C	At 0C	Indirect Tensile Strength, psi
Specimen Type	Top-lift cores	1	2.62818E-07	3.13647E-07	4.94632E-07	512
Lab ID	16PJ5B311	2	2.70805E-07	3.3203E-07	5.46758E-07	
Material	0403SP125C	5	2.84073E-07	3.66121E-07	6.38589E-07	
Mix Type	SP125C	Section 10	2.91691E-07	3.88553E-07	7.11348E-07	
Mix #	SP125 07-35	20	3.05042E-07	4.14408E-07	8.04297E-07	
P/S	Magruder Paving	50	3.23767E-07	4.76521E-07	9.84758E-07	
Notes:	MO 5, Camden, J5P0590,	100	3.39757E-07	5.26528E-07	1.18018E-06	
Test Date:	1/23/2017					

FDA1-1

Lab ID 16PJ5B311  
 Average Air Voids 4.91  
 Air Voids StdDev 0.57

Test ID	TL315	Time, Sec	At -20C	At -10C	At 0C	Indirect Tensile Strength, psi
Specimen Type	Top-lift cores	1	2.12228E-07	2.63957E-07	4.24555E-07	697
Lab ID	16PJ5B315	2	2.2217E-07	2.86624E-07	4.82069E-07	
Material	0403SP125C	5	2.33179E-07	3.10288E-07	5.91015E-07	
Mix Type	SP125C	Section 10	2.43181E-07	3.41174E-07	6.96285E-07	
Mix #	SP125 08-18	20	2.64663E-07	3.77463E-07	8.28648E-07	
P/S	Magruder Paving	50	2.77543E-07	4.30776E-07	1.07837E-06	
Notes:	MO 5, Camden, J5P0590,	100	2.9985E-07	4.78718E-07	1.35001E-06	
Test Date:	1/23/2017					

FDA1-2

Lab ID 16PJ5B315  
 Average Air Voids 2.03  
 Air Voids StdDev 0.93

Table B - 3. Creep compliance inputs for MoDOT HMA mix designs, D(t) 1/psi, Continued

Test ID	TL348	Time, Sec	At -20C	At -10C	At 0C	Indirect Tensile Strength, psi
Specimen Type	Top-lift cores	1	3.58192E-07	4.66629E-07	7.69005E-07	539
Lab ID	16PJ5B348	2	3.72834E-07	4.95946E-07	8.87921E-07	
Material	0403SP095BSMR	5	3.93986E-07	5.63003E-07	1.06023E-06	
Mix Type	SP095BSMR	10	4.14206E-07	6.1036E-07	1.2339E-06	
Mix #	SP095 10-116	20	4.31321E-07	6.66482E-07	1.45685E-06	
P/S	Bross Construction	50	4.68733E-07	7.7328E-07	1.84686E-06	
Notes:	Rte 66 [US 66], Jasper, J7	100	4.96216E-07	8.65331E-07	2.2708E-06	
Test Date:	1/30/2017					

FDA3  
 Lab ID 16PJ5B348  
 Average Air Voids 5.02  
 Air Voids StdDev 0.28

Test ID	TL363	Time, Sec	At -20C	At -10C	At 0C	Indirect Tensile Strength, psi
Specimen Type	Top-lift cores	1	3.32619E-07	4.01272E-07	8.20586E-07	371
Lab ID	16PJ5B363	2	3.4399E-07	4.39836E-07	9.26174E-07	
Material	0403SP125C	5	3.69091E-07	4.8874E-07	1.07158E-06	
Mix Type	SP125C	10	3.85615E-07	5.3253E-07	1.2179E-06	
Mix #	SP125 ?	20	4.02908E-07	5.77966E-07	1.39305E-06	
P/S	Bross Construction	50	4.40511E-07	6.55707E-07	1.70459E-06	
Notes:	Rt 266, Greene, J8P0851	100	4.70344E-07	7.39319E-07	2.03207E-06	
Test Date:	2/12/2017					

FDA4  
 Lab ID 16PJ5B363  
 Average Air Voids 7.45  
 Air Voids StdDev 0.25

Table B - 3. Creep compliance inputs for MoDOT HMA mix designs, D(t) 1/psi, Continued

Test ID	TL326	Time, Sec	At -20C	At -10C	At 0C	Indirect Tensile Strength, psi
Specimen Type	Top-lift cores	1	3.47347E-07	4.73424E-07	7.89744E-07	371
Lab ID	16PJ5B326	2	3.6061E-07	4.90611E-07	8.49668E-07	
Material	0403SP125C	5	3.73328E-07	5.31603E-07	9.3901E-07	
Mix Type	SP125C	10	3.8558E-07	5.56583E-07	1.02991E-06	
Mix #	SP125 01-48	20	3.90952E-07	6.04388E-07	1.14206E-06	
P/S	Superior-Bowen	50	4.12982E-07	6.55256E-07	1.32829E-06	
Notes:	MO 7, Jackson, J4S0915	100	4.23551E-07	7.04354E-07	1.56064E-06	
Test Date:	1/25/2017					

FDA5

Lab ID 16PJ5B326  
 Average Air Voids 5.37  
 Air Voids StdDev 0.36

Test ID	TL339	Time, Sec	At -20C	At -10C	At 0C	Indirect Tensile Strength, psi
Specimen Type	Top-lift cores	1	4.65452E-07	4.23409E-07	7.03673E-07	374
Lab ID	16PJ5B339	2	4.83786E-07	4.53928E-07	7.57064E-07	
Material	0403SP125C	5	5.13626E-07	4.97159E-07	8.74215E-07	
Mix Type	SP125C	10	5.33768E-07	5.29602E-07	9.41324E-07	
Mix #	SP125 16-139	20	5.50749E-07	5.72241E-07	1.04714E-06	
P/S	Journagan Asphalt	50	5.8303E-07	6.34958E-07	1.19457E-06	
Notes:	US 65, Taney, J8P0609B?	100	6.08305E-07	6.96841E-07	1.34831E-06	
Test Date:	2/15/2017					

FDA6

Lab ID 16PJ5B339  
 Average Air Voids 6.82  
 Air Voids StdDev 0.99

Table B - 3. Creep compliance inputs for MoDOT HMA mix designs, D(t) 1/psi, Continued

Test ID	TL300	Time, Sec	At -20C	At -10C	At 0C	Indirect Tensile Strength, psi
Specimen Type	Top-lift cores	1	3.50767E-07	4.47483E-07	7.21196E-07	476
Lab ID	16PJ5B300	2	3.65928E-07	4.87939E-07	8.08303E-07	
Material	0403SP125BSM	5	3.778E-07	5.23023E-07	9.60779E-07	
Mix Type	SP125BSM	10	3.97475E-07	5.72399E-07	1.09571E-06	
Mix #	SP125 06-45	20	4.19433E-07	6.25786E-07	1.27937E-06	
P/S	APAC - Asphalt Plants	50	4.42024E-07	7.04623E-07	1.63449E-06	
Notes:	I-35, Clinton, J1D0600J	100	4.63944E-07	7.87922E-07	2.00093E-06	
Test Date:	1/10/2017					

AOC1  
 Lab ID 16PJ5B300  
 Average Air Voids 3.71  
 Air Voids StdDev 0.33

Test ID	TL319	Time, Sec	At -20C	At -10C	At 0C	Indirect Tensile Strength, psi
Specimen Type	Top-lift cores	1	2.41326E-07	2.8619E-07	3.61821E-07	555
Lab ID	16PJ5B319	2	2.48445E-07	3.03812E-07	4.02227E-07	
Material	0403SP125BSM	5	2.62995E-07	3.17413E-07	4.45086E-07	
Mix Type	SP125BSM	10	2.69133E-07	3.40774E-07	4.94304E-07	
Mix #	SP125 05-143	20	2.73982E-07	3.57565E-07	5.48002E-07	
P/S	APAC - Asphalt Plants	50	2.8521E-07	3.9487E-07	6.45962E-07	
Notes:	MO 100, St. Louis, J6D0600J	100	3.04529E-07	4.29365E-07	7.51361E-07	
Test Date:	1/11/2017					

AOC2  
 Lab ID 16PJ5B319  
 Average Air Voids 3.82  
 Air Voids StdDev 1.25

Table B - 3. Creep compliance inputs for MoDOT HMA mix designs, D(t) 1/psi, Continued

Test ID	TL322	Time, Sec	At -20C	At -10C	At 0C	Indirect Tensile Strength, psi
Specimen Type	Top-lift cores	1	2.85773E-07	4.0397E-07	6.69158E-07	366
Lab ID	16PJ5B322	2	3.00015E-07	4.28771E-07	7.42795E-07	
Material	0403SP125C	5	3.21835E-07	4.7295E-07	8.3559E-07	
Mix Type	SP125C	10	3.41195E-07	5.07196E-07	9.31747E-07	
Mix #	SP125 08-24	20	3.60022E-07	5.46807E-07	1.03685E-06	
P/S	Bross Construction	50	4.0101E-07	6.16719E-07	1.2245E-06	
Notes:	US 63, Macon, J2P0773	100	4.28833E-07	6.88305E-07	1.41964E-06	
Test Date:	2/14/2017					

AOC3  
 Lab ID 16PJ5B322  
 Average Air Voids 5.93  
 Air Voids StdDev 0.82

Test ID	TL356	Time, Sec	At -20C	At -10C	At 0C	Indirect Tensile Strength, psi
Specimen Type	Top-lift cores	1	3.28178E-07	3.99164E-07	8.06942E-07	381
Lab ID	16PJ5B356	2	3.44689E-07	4.30495E-07	8.94197E-07	
Material	0403SP125C	5	3.59971E-07	4.83302E-07	1.03307E-06	
Mix Type	SP125C	10	3.79734E-07	5.2344E-07	1.15922E-06	
Mix #	SP125 ?	20	4.01596E-07	5.71809E-07	1.31891E-06	
P/S	Bross Construction	50	4.35408E-07	6.49406E-07	1.59867E-06	
Notes:	US 60, Shannon, J9P0596	100	4.6684E-07	7.26951E-07	1.89411E-06	
Test Date:	2/10/2017					

AOC4  
 Lab ID 16PJ5B356  
 Average Air Voids 8.86  
 Air Voids StdDev 1.19

Table B - 3. Creep compliance inputs for MoDOT HMA mix designs, D(t) 1/psi, Continued

Test ID	TL352	Time, Sec	At -20C	At -10C	At 0C	Indirect Tensile Strength, psi
Specimen Type	Top-lift cores	1	3.80099E-07	4.57937E-07	5.21276E-07	321
Lab ID	16PJ5B352	2	3.93543E-07	4.74262E-07	5.47402E-07	
Material	0403SP125C	5	4.08709E-07	4.96058E-07	5.9412E-07	
Mix Type	SP125C	10	4.20785E-07	5.09627E-07	6.20996E-07	
Mix #	SP125 06-150	20	4.35068E-07	5.32073E-07	6.57233E-07	
P/S	Bross Construction	50	4.50094E-07	5.514E-07	7.21983E-07	
Notes:	US 61, Lincoln, J3D0600A	100	4.6427E-07	5.84511E-07	7.86344E-07	
Test Date:	2/6/2017					

AOC5  
 Lab ID 16PJ5B352  
 Average Air Voids 6.89  
 Air Voids StdDev 0.28

Test ID	TL346	Time, Sec	At -20C	At -10C	At 0C	Indirect Tensile Strength, psi
Specimen Type	Top-lift cores	1	4.07677E-07	5.05564E-07	6.63167E-07	334
Lab ID	16PJ5B346	2	4.24124E-07	5.27331E-07	7.38643E-07	
Material	0403SP125C	5	4.39391E-07	5.7493E-07	8.45006E-07	
Mix Type	SP125C	10	4.56546E-07	6.10408E-07	9.4733E-07	
Mix #	SP125 12-48	20	4.75628E-07	6.50069E-07	1.07722E-06	
P/S	Journagan Asphalt	50	5.03912E-07	7.13974E-07	1.28222E-06	
Notes:	US 65, Christian, J8P2268	100	5.20964E-07	7.79767E-07	1.50811E-06	
Test Date:	2/3/2017					

AOA2  
 Lab ID 16PJ5B346  
 Average Air Voids 9.12  
 Air Voids StdDev 0.35

Table B - 3. Creep compliance inputs for MoDOT HMA mix designs, D(t) 1/psi, Continued

Test ID	TL330	Time, Sec	At -20C	At -10C	At 0C	Indirect Tensile Strength, psi
Specimen Type	Top-lift cores	1	4.06011E-07	5.64765E-07	4.58291E-07	347
Lab ID	16PJ5B330	2	4.2613E-07	6.11451E-07	5.0207E-07	
Material	0403SP125C Counties	5	4.40021E-07	6.62767E-07	6.05267E-07	
Mix Type	SP125C	10	4.6185E-07	7.21814E-07	6.79127E-07	
Mix #	?	20	4.77335E-07	7.82308E-07	7.88752E-07	
P/S	Superior Bowen Asphalt	50	5.20519E-07	8.92497E-07	9.88946E-07	
Notes:	MO 21, Washington/Iron	100	5.54551E-07	9.94638E-07	1.21094E-06	
Test Date:	12/11/2016					

AOA3  
 Lab ID 16PJ5B330  
 Average Air Voids 9.01  
 Air Voids StdDev 2.04

Test ID	TL305	Time, Sec	At -20C	At -10C	At 0C	Indirect Tensile Strength, psi
Specimen Type	Top-lift cores	1	3.27368E-07	4.11142E-07	6.8544E-07	417
Lab ID	16PJ5B305	2	3.32913E-07	4.38762E-07	7.36033E-07	
Material	0403SP125CLG	5	3.55657E-07	4.66301E-07	8.43765E-07	
Mix Type	SP125CLG DesC 80 gyros	10	3.68983E-07	4.98739E-07	9.29978E-07	
Mix #	SP125 13-86	20	3.84921E-07	5.27938E-07	1.04651E-06	
P/S	Bross Construction	50	4.17982E-07	5.84002E-07	1.24141E-06	
Notes:	US 63, Boone, J5P0964	100	4.39784E-07	6.32855E-07	1.44337E-06	
Test Date:	42753.00					

AOA4  
 Lab ID 16PJ5B305  
 Average Air Voids 6.10  
 Air Voids StdDev 0.35

Table B - 3. Creep compliance inputs for MoDOT HMA mix designs, D(t) 1/psi, Continued

Test ID	TL308	Time, Sec	At -20C	At -10C	At 0C	Indirect Tensile Strength, psi
Specimen Type	Top-lift cores	1	3.79787E-07	4.23398E-07	7.61013E-07	403
Lab ID	16PJ5B308	2	3.89176E-07	4.44751E-07	8.42213E-07	
Material	0403SP125C	5	4.10863E-07	4.75585E-07	9.28563E-07	
Mix Type	SP125C	10	4.25828E-07	5.0858E-07	1.02767E-06	
Mix #	SP125 06-125	20	4.31933E-07	5.30073E-07	1.14066E-06	
P/S	Superior Bowen Asphalt	50	4.54866E-07	5.75822E-07	1.32517E-06	
Notes:	MO 210, Ray, J451737	100	4.68013E-07	6.11907E-07	1.52496E-06	
Test Date:	12/15/2016					

AOA5

Lab ID

16PJ5B308

Average Air Voids

6.60

Air Voids StdDev

0.71